INVESTIGATING MECHANISMS OF HEPATITIS C VIRUS ENDOCYTOSIS

by

JENNIFER THORLEY

A thesis submitted to
The University of Birmingham
for the degree of
DOCTOR OF PHILOSOPHY

School of Biosciences
The University of Birmingham
May 2014

ABSTRACT

This abstract was written J. A. Thorley and also appears on the Rappoport laboratory website. This statement is confirmed by supervisor J. Z. Rappoport.

Joshua Z. Rappoport PhD

Director of the Center for Advanced Microscopy and the Nikon Imaging Center at Northwestern University
Northwestern University Feinberg School of Medicine
303 E. Chicago Avenue
Chicago, IL 60611

Many viruses exploit and in some cases, promote host cell endocytic pathways for infection. These pathways include caveolar and clathrin-mediated endocytosis, as well as caveolin- and clathrin-independent pathways, such as macropinocytosis. The entry mechanisms of many viruses are not clear cut, with more than one pathway implicated in some cases. Hepatitis C virus (HCV) is a hepatotropic virus associated with liver disease, fibrosis, cirrhosis and hepatocellular carcinoma. There are four well-established co-receptors or “entry factors” for HCV, namely, the tetraspanin CD81, scavenger receptor BI (SR-BI) (which have been shown to directly bind the virus) and the tight junction proteins Claudin 1 (CLDN1) and Occludin (internalisation of which is required for viral entry). Clathrin-dependent endocytosis of HCV has been demonstrated in hepatoma cell lines and has also been shown to be the route of entry for co-receptor CD81.

However, clathrin-dependent endocytosis of HCV has been demonstrated in hepatoma cell lines, which do not express detectable levels of caveolin 1, a protein required for caveolar endocytosis. Due to this fact, the potential role of caveolae in HCV entry has largely been ignored, despite the fact that hepatocytes in the liver have been shown to express caveolin 1. Data in this thesis demonstrate that SkHep1 (SRBI+ CLDN1) cells offer a model cell line for HCV entry studies as they express caveolin 1, take up the caveolar cargo cholera toxin B, and can be infected with pseudotype virus. Using Dynasore, a small molecule inhibitor of dynamin, we have demonstrated that HCV entry shows a marked dependence on dynamin in these cells. In addition, using siRNA knockdown of caveolin 1 and adaptor protein 2 complex (AP2), we have demonstrated a strong dependency on AP2. However, knockdown of caveolin 1 had no significant effect on viral entry.

Recently it has become apparent that the epidermal growth factor receptor (EGFR) is required for viral entry into hepatoma cells and that stimulation with EGF results in increased entry and infection. We demonstrate that EGF stimulation of hepatoma cell lines results in the ruffling and blebbing of the plasma membrane typical of macropinocytosis, an increase in the uptake of fluid phase markers and loss of EGFR from the cell surface when compared with unstimulated cells. EGF stimulation also promoted filopodia formation and elongation, offering another potential mechanism for the role of EGFR in HCV entry. However, TIRF microscopy revealed that the formation of clathrin-coated pits is also upregulated in response to EGF treatment, and a proportion of overexpressed EGFR-GFP relocalises to clathrin punctae on the cell surface, suggesting that both pathways could contribute to the EGF-induced promotion of viral entry. Knockdown of PAK1 and AP2 has been

achieved and will allow for the contribution of each pathway to this effect to be determined in future work.

Localisation and trafficking of EGFR and the HCV co-receptor CD81 were assayed by live-cell confocal microscopy, revealing that internalisation and degradation of both receptors was promoted by EGF stimulation. Furthermore, the two proteins colocalise on the cell surface at early timepoints following EGF stimulation, suggesting that they internalise together. This is the first evidence of an association between CD81 and EGFR on the cell surface. Super-resolution imaging of CD81 by structured illumination microscopy (SIM) showed fewer clusters of CD81 in the plasma membrane after EGF stimulation, corroborating the rapid internalisation and degradation of the CD81 in response to EGF treatment.

TABLE OF CONTENTS

LIST OF FIGURES AND TABLES

LIST OF ABBREVIATIONS

Adaptor protein 2 complex	**AP2**
Ammonium persulphate	**APS**
Bovine serum albumin	**BSA**
Cell imaging media	**CIM**
Clathrin-coated pit	**CCP**
Clathrin-mediated endocytosis	**CME**
Cholera toxin B subunit	**CTB**
Claudin 1	**CLDN1**
CTB- Alexafluor555	**CTB-555**
Dulbecco's modified eagle medium	**DMEM**
Dulbecco's phosphate buffered saline	**DPBS**
Epidermal growth factor	**EGF**
Epidermal growth factor receptor	**EGFR**
Epidermal growth factor receptor substrate 15	**Eps15**
Foetal calf serum	**FCS**
Fluorescence resonance energy transfer	**FRET**
Green fluorescent protein	**GFP**
Hepatitis C virus	**HCV**
Hepatitis C virus pseudoparticles	**HCVpp**
Immunocytochemistry	**IC**
Immunoprecipitation	**IP**
Low density lipoprotein	**LDL**
Luria Broth	**LB**
Mitogen activated protein kinase	**MAPK**
Murine leukaemia virus	**MLV**
Paraformaldehyde	**PFA**
Primary human hepatocytes	**PHH**

Region of interest	**ROI**
Scavenger receptor B1	**SRBI**
Serum-free medium	**SFM**
Small interfering RNA	**siRNA**
Sodium dodecyl sulphate	**SDS**
Structured illumination microscopy	**SIM**
Stochastic optical reconstruction microscopy	**STORM**
Tetraspanin-enriched microdomain	**TEM**
Total internal reflection fluorescence	**TIRF**
Transferrin	**Tf**
Transferrin receptor	**TfR**
Vesicular stomatitis virus	**VSV**
Western blot	**WB**

CHAPTER 1

INTRODUCTION

Sections in this chapter resulted in publications in which the student, J.A. Thorley, is the first author (Thorley et al 2010, Thorley et al 2014; see reference list), although these publications were written in collaboration with the supervisor and all the other authors.

This statement is counter-signed by the supervisor, J.Z. Rappoport, to acknowledge that the supervisor's contribution to the text was not substantial:

Joshua Z. Rappoport PhD

Director of the Center for Advanced Microscopy and the Nikon Imaging Center at Northwestern University
Northwestern University Feinberg School of Medicine
303 E. Chicago Avenue
Chicago, IL 60611

1.1 Hepatitis C virus (HCV)

1.1.1 Historical and clinical perspectives

HCV is a hepatotropic virus associated with chronic liver disease, fibrosis, cirrhosis and hepatocellular carcinoma (HCC). HCV has a narrow host range, infecting only humans and chimpanzees (Kolykhalov et al 1997, Yanagi et al 1997). Although primarily leading to liver disease, hepatitis C has been shown to affect several other areas of the body, including the digestive tract, the immune system and the brain (Lauer and Walker 2001). Recent evidence suggests the virus is able to infect B-lymphocytes, dendritic cells and endothelial cells (Fletcher et al 2012).

It is estimated that around 180 million individuals are infected worldwide (WHO epidemiological record 2009), making the virus a global health concern. The prevalence varies widely from country to country, and is highest in South America, Africa and Asia (Shepard et al 2006, WHO epidemiological record 2009). HCV infection remains the leading cause of liver transplant in the USA and Europe (Adam et al 2003, Wiesner et al 2003).

HCV was first discovered in the 1975, when it became clear that a virus other than Hepatitis A and B was causing liver disease (Feinstone et al 1975). This aetiological agent became known as non-A non-B hepatitis (NANBH), but was not identified for over a decade later due to its inability to propagate efficiently in cell culture. Hepatitis C virus was identified as the aetiological agent of NANBH in 1989 (Choo et al 1989, Kuo et al 1989) and was first viewed by electron microscopy in 1995 (Li et al 1995). This makes HCV a relatively newly identified virus and thus many aspects of infection and the viral life cycle are still poorly understood.

The virus is blood-borne and as such is transmitted from person to person by the use of unscreened blood products (the primary route of transmission in the developing world), the sharing of needles between intravenous drug users (the primary route of transmission in developed countries), sexual exposure and vertical transmission from mother to child. There are seven genetically heterogeneous major genotypes of HCV (differing by around 35% in their nucleotide sequence), numbered 1-7, which predominate in different areas of the world (Kuiken et al 2009).

HCV infection is typically initially asymptomatic, with around 85% of cases failing to clear the virus without clinical intervention (Rustgi 2007, WHO epidemiological record 2009). Persistent infection frequently leads to chronic hepatitis which can result in fibrosis, cirrhosis and HCC. Liver inflammation in response to infection is thought to be the leading cause of HCV-induced liver damage, however, there is evidence that some viral proteins additionally contribute directly to the oncogenic transformation of hepatocytes (Koike et al 2007).

The standard therapy regime for HCV has traditionally consisted of the non-specific antivirals, PEGylated interferon-α and ribavirin taken in combination. This treatment has had limited success and is effective in only around 55% of patients (Zeuzem et al 2004), depending on viral genotype (around 50% for genotype 1 and 80% for genotypes 2 and 3). The current standard of care for genotype 1-infected patients comprises the new protease inhibitors Telaprevir and Boceprevir (Kiser et al 2012). There is currently no vaccine or preventative treatment for HCV.

A better understanding of key steps in the viral life cycle would help to identify better antiviral targets and aid in the development of potential treatments for HCV.

1.1.2 The HCV virion

Hepatitis C virus (HCV) is an enveloped, single-stranded RNA virus of the *flaviviridae* family (Choo et al 1989). The HCV particle comprises a single stranded positive-sense RNA, which is surrounded by a capsid (formed from the core protein) and an envelope that is derived from the host cell lipid bilayer and contains the viral glycoproteins E1 and E2 (Bartosch and Cosset 2006), shown in **Figure 1.1**. HCV virions are 50-60 nm in diameter (Li et al 1995).

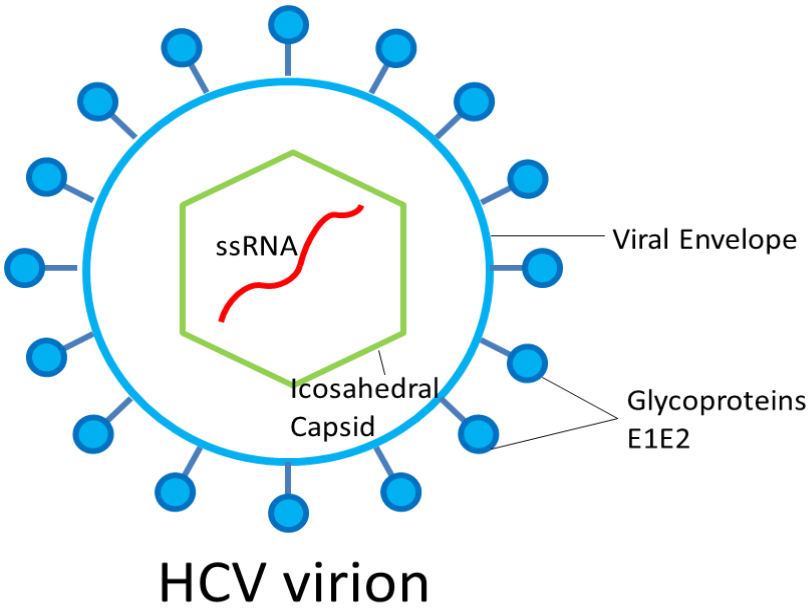

Figure 1.1: The HCV virion. The HCV virion consists of a single-stranded RNA genome of positive polarity (+ssRNA) surrounded by an icosahedral capsid and viral envelope from which protrude the viral glycoproteins E1 and E2.

The HCV genome encodes a large polyprotein of around 3000 amino acid residues in length. Following translation, the polyprotein is processed by both viral and host cell proteases to generate the viral structural and non-structural proteins as well as a small ion channel, p7. Although p7 is not involved in viral replication, it is required for

the production of infectious HCV particles, which suggests that it may be involved in the assembly or release of nascent virions (Sakai et al 2004, Jones et al 2007, Steinman et al 2007).

Three N-terminal structural proteins (Core, E1 and E2) are generated. Core makes up the viral capsid and E1 and E2 are envelope glycoproteins which play critical roles in receptor binding and membrane fusion (Keck et al 2004, Op De Beeck et al 2004, Helle et al 2008). The six C-terminal non-structural proteins generated are known as NS2, NS3, NS4A, NS4B, NS5A and NS5B. NS3-5B make up the viral replication complex and were shown to be required and sufficient for viral RNA replication (Bartenschlager et al 2000, Bartenschlager et al 2003).

1.1.3 The viral life cycle

HCV particles circulate in the blood along with very low- and/or low-density lipoproteins (VLDLs and LDLs) which are carriers of cholesterol and trigylcerides (Andre et al 2002, Nielsen et al 2008). The first step in the viral life cycle is attachment to the hepatocyte cell surface. This is thought to be mediated by attachment molecules such as the glycosaminoglycan heparin sulphate and the low density lipoprotein receptor (LDLR) (Barth et al 2003, Koutsoudakis et al 2006, Agnello et al 1999, Monazahian et al 1999, Wunschmann et al 2000, Molina et al 2007).

Following attachment, HCV is brought into contact with multiple host cell co-receptors (which will be discussed in more detail in **section 1.4**) via the envelope glycoproteins E1 and E2, followed by endocytosis of viral particles in a receptor-mediated manner (Blanchard et al 2006). Following endocytosis, it is thought that

endosomal acidification results in fusion of the viral and endosomal membranes, uncoating and release of viral RNA (Tscherne et al 2006, Lavillette et al 2006, Sharma et al 2011).

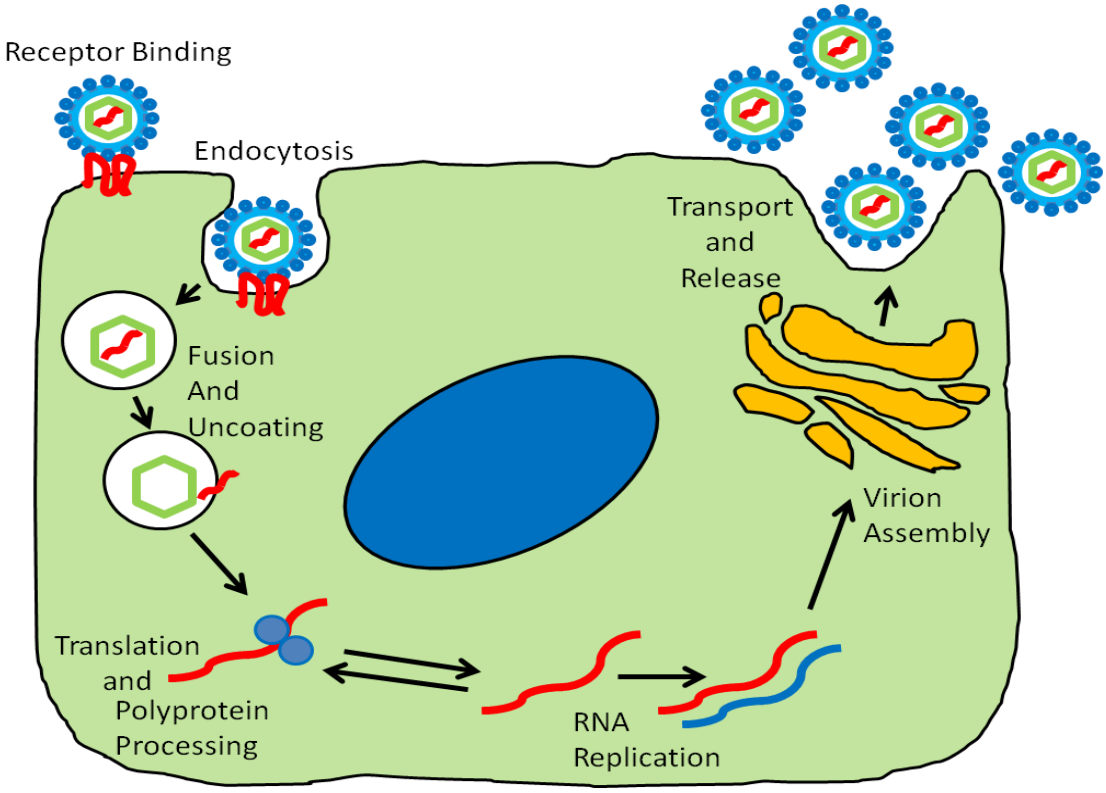

Figure 1.2: The HCV life cycle. Following attachment, virus particles interact with host cell receptors, resulting in endocytosis and cellular entry. Uncoating and release of the viral RNA results in translation of the viral polyprotein and RNA replication to produce new virions. The polyprotein is processed by both viral and cellular proteins and new virions are assembled on the endoplasmic reticulum and lipid droplets before release.

The single strand of viral RNA enclosed within the nucleocapsid acts as both mRNA for translation and as a template for RNA replication, as shown in **Figure 1.2**. Once translated, the non-structural proteins induce membrane alterations known as 'membranous webs' and form a membrane-bound replication complex. . The polyprotein containing the structural proteins is cleaved by host cell signal peptidases. New viral particles are then assembled from the matured structural

proteins, and are released from the cell via the host cell secretory pathway (reviewed in Ashfaq et al 2011).. Assembly of nascent viral particles is thought to take place within the endoplasmic reticulum and on lipid droplets (Miyanari et al 2007), although the exact mechanism of viral egress is not well understood. The key steps in the viral life-cycle are shown schematically in **Figure 1.2**.

1.1.4 HCV in cell culture

Identification of HCV as the causative agent of non-A non-B hepatitis was severely impaired by the inability of the virus to propagate in cell culture. The HCV pseudoparticle (HCVpp) system was first reported in 2003 and this has enabled the study of critical steps in the viral entry process, including binding, attachment and internalisation (Bartosch et al 2003, Bartosch et al 2009). HCVpp can be assembled by displaying functional HCV E1/E2 heterodimers on retroviral and lentiviral particles, as shown in **Figure 1.3**. A reporter gene, for example, encoding green fluorescent protein (GFP) or luciferase allows the detection of infected cells. HCVpp are an ideal system for studying viral

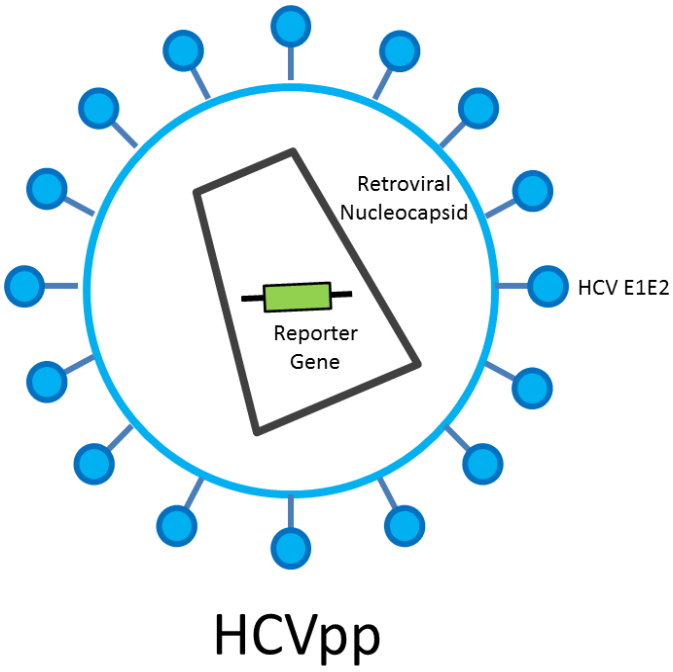

Figure 1.3: **HCV pseudoparticles (HCVpp)**. HCVpp are generated by displaying HCV glycoproteins E1 and E2 on retroviral core particles, which include a reporter gene, allowing infected cells to be detected.

entry in isolation from other aspects of the viral life cycle. This system has enabled the identification of several HCV co-receptors and entry factors such as Claudin1 and Occludin (Evans et al 2007, Bartosch et al 2009).

Additionally, in 2005, three independent groups reported the production of authentic HCV particles in cell culture, known as HCVcc (Lindenbach et al 2005, Wakita et al 2005, Zhong et al 2005). These reports were based on a genotype 2a isolated JFH1, that was obtained from a patient in Japan with fulminant hepatitis. HCVcc has enabled the study of the entire HCV life cycle *in vitro*. JFH1 infection of human hepatoma cells resulted in release of progeny virus particles which are capable of infecting naïve cells and are also infectious in chimpanzees and in a humanized mouse model system (Lindenbach et al 2006). Following this, infectious genotype 1a particles have also been generated (Yi et al 2006).

1.2 Endocytosis and intracellular trafficking

1.2.1 Endocytosis

Cellular membranes compartmentalise cellular processes and provide an important barrier to extracellular pathogens such as viruses. The plasma membrane is the surface through which the cell communicates with the extracellular environment, and for this communication to function optimally, the contents of the membrane must be tightly regulated. Endocytosis is involved in regulating the contents of the plasma membrane by internalising membrane lipids and integral membrane proteins along with bound ligands.

Endocytosis plays a key role in a variety of apparently disparate cellular processes, including mitosis (Tacheva-Grigorova et al 2013), antigen presentation (Burgdorf and Kurts 2008) and cell migration (Fletcher and Rappoport 2009), as well as the regulation of intracellular signalling pathways (Wiedłocha and Sørensen 2004). Importantly, many pathogens including numerous viruses have been shown to exploit endogenous host cell endocytic pathways to enter the cell (reviewed in Thorley et al 2010).

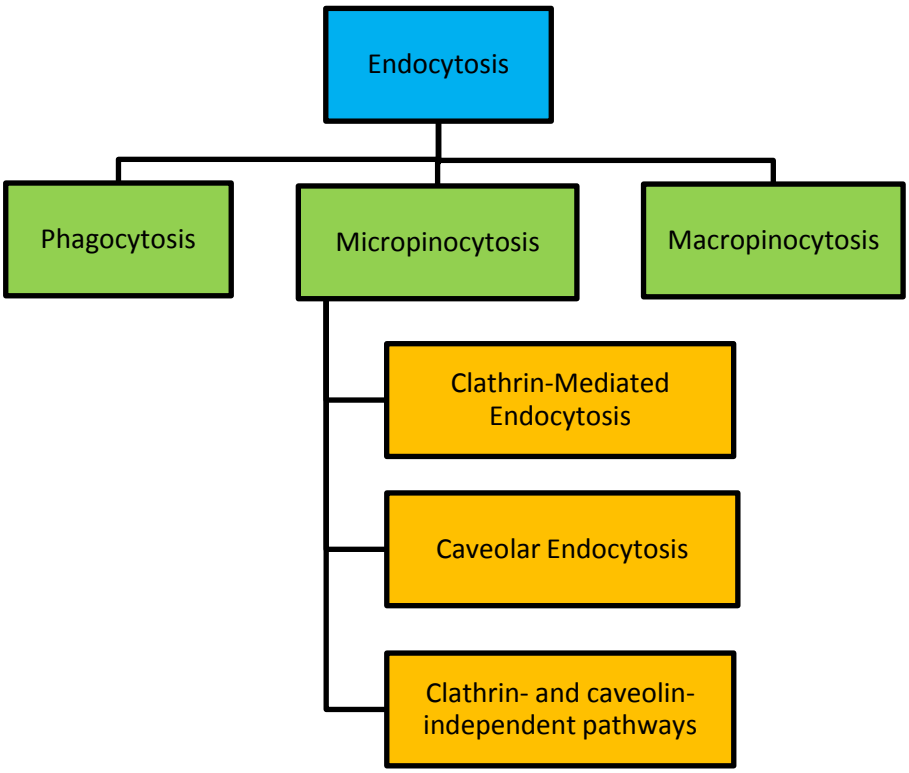

Figure 1.4: Endocytic Pathways. Internalisation pathways covered under the term 'endocytosis' include phagocytosis, macropinocytosis and the receptor-mediated pathways. Micropinocytic pathways include the well-studied clathrin-mediated route and caveolar endocytosis, as well as clathrin- and caveolin-independent pathways.

The term ‘endocytosis’ encompasses a variety of pathways (outlined in **Figure 1.4**) including macropinocytosis, phagocytosis and micropinocytosis. Macropinocytosis is often termed ‘cell drinking’, and generally refers to non-specific uptake of extracellular fluid, although there is some evidence that the pathway is more specific and tightly regulated than generally assumed (Schmees et al 2012). Phagocytosis is often termed ‘cell eating’ and involves the engulfing of solid particles by specialised phagocytic cells.

Micropinocytosis involves formation of small (50-150 nm) diameter vesicles usually containing extracellular ligands bound to their cognate cellular receptors, and encompasses the well-described clathrin-mediated pathway, the caveolar pathway and more recently described pathways acting independently of both clathrin and caveolin 1 (Sandvig et al 2011). Micropinocytic pathways are generally considered the most important when studying viral entry, as viruses often form specific interactions with host cell receptors, mimicking extracellular ligands and often inducing their own endocytosis as a result (Grove and Marsh 2011).

1.2.1.1 Clathrin-mediated endocytosis

Clathrin mediated endocytosis is the most well studied endocytic pathway, and the mechanisms by which endocytic cargo is recruited into clathrin-coated pits as well as those by which clathrin-coated vesicles are formed are comparatively well understood (McMahon and Boucrot et al 2011). During clathrin-mediated endocytosis, adaptor and accessory proteins help to package transmembrane

receptors and their bound ligands into clathrin-coated vesicles. In addition to endocytosis, clathrin-coated vesicles also function in other intracellular trafficking process, which is mediated by different adaptor proteins. These adaptor and accessory proteins mediate the formation of a curved clathrin lattice at the site of the membrane to be internalised, leading to the stabilised deformation of the membrane (reviewed in Doherty and McMahon 2009).

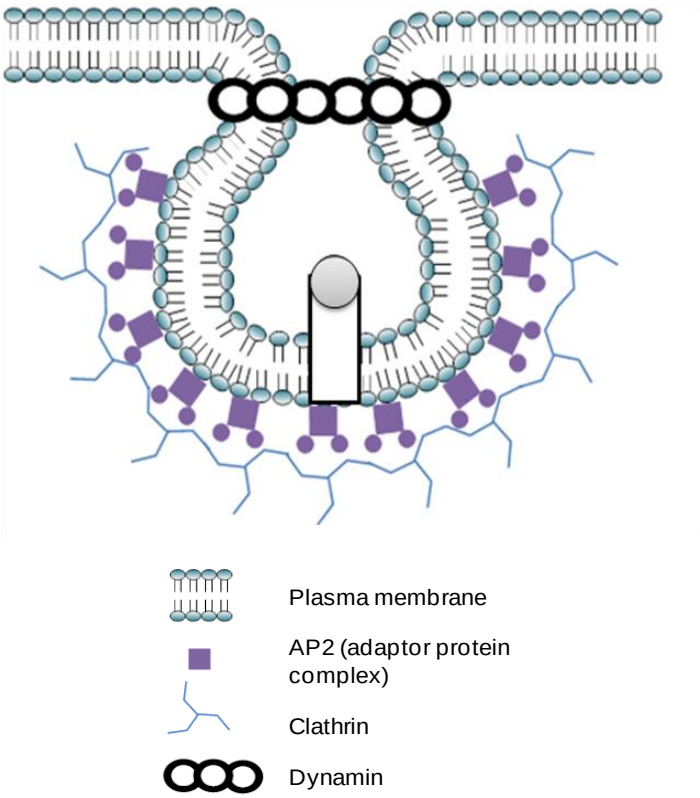

Figure 1.5: Clathrin-mediated endocytosis. A clathrin lattice is formed on the internal side of the plasma membrane, linked to membrane phospholipids via the adaptor protein 2 (AP2) complex and accessory proteins. Budding of the vesicle is mediated by the large GTPase dynamin.

During clathrin-mediated endocytosis, the clathrin lattice is linked to PI(4,5)P_2 in the plasma membrane by the adaptor protein 2 complex (AP2) and accessory proteins including Epsins and Eps15 (epidermal growth factor receptor phosphorylation substrate 15) (Smythe et al 1992, Chang et al 1993). The Epsin family of proteins also help to drive membrane deformation through the insertion of an amphipathic helix into the plasma membrane (Ford et al 2002). Eps15 acts as a scaffolding protein, helping to cluster AP2 complexes (Schmid et al 2006). In order for vesiculation of the membrane to be completed, the large GTPase dynamin forms a helical polymer around the vesicle neck, mediating vesicle fission upon GTP

hydrolysis (Hinshaw and Schmid 1995). The proteins involved in clathrin-mediated endocytosis are depicted in **Figure 1.5.** Following uncoating, the nascent vesicle then undergoes intracellular trafficking through the endosomal system (described in **section 1.2.2.1**).

Many of the proteins involved in the formation of clathrin-coated pits and vesicles have been identified, allowing researchers to make use of both specific markers and specific inhibitors of the pathway. Transferrin (Tf) is internalised exclusively and constitutively via the clathrin-mediated pathway and as such, fluorescent-labelled Tf is often used as a marker for this pathway in cells. Specific means of inhibiting clathrin-mediated endocytosis include dominant negative constructs such as EH29-GFP, a GFP-tagged trans-dominant mutant of Eps15 (Benmerah et al 1999). Small interfering RNAs (siRNA) targeting clathrin heavy chain or components of the AP2 complex such as α-adaptin are also commercially available, although both proteins are very stable and multiple rounds of transfection are generally required to deplete the cell of these proteins. Knockdown of AP2 components is preferable, as this complex is only involved in clathrin-mediated endocytosis, whereas clathrin is known to play a role in other membrane trafficking events (Hinners and Tooze 2003). Less specific chemical inhibitors of clathrin-mediated endocytosis such as the cationic amphipathic drug chlorpromazine (CPZ) are also frequently used throughout the literature (Wang et al 1993); however, pharmacological inhibitors are known to exhibit off-target effects and should be used with careful controls and/or in conjunction with more specific inhibitory strategies.

While traditionally, clathrin-mediated endocytosis is thought to rely on the adaptor protein 2 complex (AP2) and accessory proteins such as Eps15, which link the clathrin lattice to the plasma membrane/receptor cytosolic tails and cause coated pit

formation, there is some, albeit, limited evidence for clathrin-mediated pathways which can act independently of AP2 and Eps15. For example, two studies have demonstrated a clathrin-mediated but AP2-independent EGFR uptake pathway in HeLa cells (Motley et al 2003, Hinrichsen et al 2003) and mouse hepatitis virus has also been shown to be dependent on clathrin but not on Eps15 for its entry into cells (Pu and Zhang 2008). It is thought that these clathrin-mediated pathways rely on other adaptor and accessory proteins, but it is unclear which proteins are involved and how this pathway differs from the canonical clathrin-mediated endocytic pathway.

1.2.1.2 Clathrin-independent endocytosis

Although clathrin-mediated endocytosis is an extremely important ubiquitous endocytic pathway and accounts for a significant proportion of endocytic events, there are an ever increasing number of molecules and receptors shown to undergo endocytosis independently of clathrin and its accessory proteins (Kirkham et al 2005, Kirkham and Parton 2005, Mayor and Pagano 2007). These clathrin-independent mechanisms can be divided into distinct endocytic pathways on the basis of their reliance on different proteins, their sensitivity to inhibitory drugs and their ability to internalise different ligand markers. Clathrin-independent endocytic pathways include caveolar endocytosis (Pelkmans and Helenius 2002), flotillin-dependent endocytosis (Glebov et al 2006, Frick et al 2007) and Arf6-dependent endocytosis (D'Souza-Schorey and Chavrier 2006).

1.2.1.2.1 Caveolar endocytosis

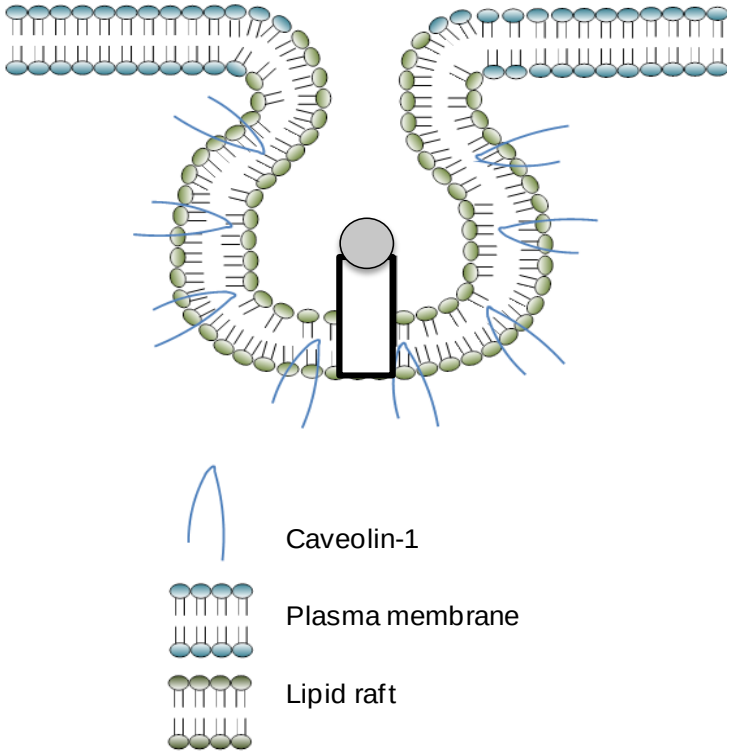

Figure 1.6: Caveolar Endocytosis. Caveolae involve lipid rafts enriched in cholesterol and glycosphingolipids. The protein caveolin1 inserts into the lipid raft with intracellular N- and C-termini.

Caveolar endocytosis is the most well-described clathrin-independent pathway and involves areas of the membrane which are enriched in cholesterol and glycosphingolipids, known as lipid rafts. Caveolin proteins insert into the lipid rafts stabilising them in the membrane (Phuong et al 2001). There are three mammalian caveolin proteins, caveolins -1, -2, and -3. Caveolin 3 is muscle specific, while caveolins -1 and -2 are found widely in non-muscle cells. Caveolin 1 is enriched in caveolae and cells which do not express this protein are devoid of caveolae even in the presence of caveolin 2 (Li et al 1996). Overexpression of caveolin 1 in caveolin 1-deficient cells leads to formation of morphologically evident caveolae, suggesting that caveolin 1 is both necessary and sufficient for caveolae formation (Rothberg et al 1992, Li et al 1996, Lipardi et al 1998, Pelkmans and Zerial 2005). However, more recently there is evidence that adaptor proteins known as cavins are also involved in caveolar endocytosis (Liu and Pilch 2008, Aboulaich et al 2004, Liu et al 2008). These

proteins are thought to be involved in regulation of caveolae and promote membrane remodelling as well as exercising their own activity independently of caveolae. As such, the relationship between caveolins and cavins is complex and remains poorly understood. The importance of cavins in caveolar endocytosis and whether they are essential to caveolae function is yet to be fully elucidated.

Phosphorylation of tyrosine14 of caveolin 1 is critical for caveolar endocytosis and is thought to lead to the vesiculation of caveolae (Orlichenko et al 2005). Budding of caveolae from the plasma membrane is believed to be mediated by the large GTPase dynamin (Henley et al 1998, Oh et al 1998), although some evidence suggests that caveolae are able to bud in the absence of dynamin (Liu et al 2008). A schematic of caveolar endocytosis is shown in **Figure 1.6.**

Ligands such as cholera toxin B subunit (CTB) (Orlandi and Fishman 1998, Wolf et al 1998) and Simian Virus 40 (SV40) (Pelkmans et al 2001, Pelkmans et al 2002) have been described to enter cells via caveolar endocytosis and as such, fluorescent- labelled CTB and SV40 are frequently experimentally used as markers for the pathway. Inhibitors of the caveolar pathway include drugs such as nystatin, fillipin, methyl- beta cyclodextrin, and indomethacin, all of which complex membrane cholesterol, leading to changes in the membrane composition, and subsequent flattening of caveolae (Lajoie and Nabi 2010). However, extraction of membrane cholesterol can also inhibit other forms of endocytosis (Rodal et al 1999), and both CTB (Torgersen et al 2001) and SV40 (Damm et al 2005) have been shown to enter cells independently of caveolae in some circumstances. As the involvement of a specific set of proteins in caveolar endocytosis is less clear cut, inhibition or knockdown of caveolin 1 is currently the most dependable means of inhibiting the pathway without eliciting undesired off-target effects. Therefore, the most specific

mechanisms of inhibition include overexpression of dominant negative caveolin 1 constructs such as Cav1Y14F-GFP (Orlichenko et al 2005), and siRNA targeted against caveolin 1 (Sottile and Chandler 2004, Moriyama et al 2007).

While the clathrin-mediated pathway is ubiquitous, caveolae have only been demonstrated in a limited number of cell types (Parton and Simons 2007). Most notably, neurons and leukocytes do not have caveolae. Nevertheless, caveolar entry pathways have been described for a selected number of viruses including SV40 and human coronavirus 229E (Anderson et al 1996, Nomura at al 2004, Kawase et al 2009), highlighting the physiological importance of the pathway. Finally, while some integral membrane proteins such as certain integrins have been shown to undergo caveolar endocytosis (Caswell and Norman 2006), to date no endogenous receptor-ligand complexes have been shown to enter cells via this pathway.

1.2.1.3 Macropinocytosis

Macropinocytosis is an archaic form of endocytic pathway by which cells are able to indiscriminately internalise large volumes of extracellular fluid into endocytic vacuoles known as macropinosomes. Macropinosomes were first described by Lewis in 1931 (Lewis 1931) as large, heterogeneous organelles of over 2 μm in diameter, which form from dynamic extensions of the plasma membrane known as ruffles. As such, the process is associated with cell-wide plasma membrane reorganisation, which is induced by activation of membrane-associated actin. The resulting plasma membrane ruffles can be categorised as planar folds (known as lamellipodia), circular ruffles or large plasma membrane extrusions (known as blebs), which are shown in **Figure 1.7**. As with the micropinocytotic pathways, it is unclear

whether these differences represent variations on a theme or distinct processes. It is interesting to speculate that this variation results from the different roles of macropinocytosis in different cell types and tissues. For example, specialised cell types, such as immunological and renal cells may require macropinocytosis for degradation, whereas growth-factor stimulated cells may require macropinocytosis for the downregulation of signalling and reorganisation of the the plasma membrane following the activation of receptor tyrosine kinases.

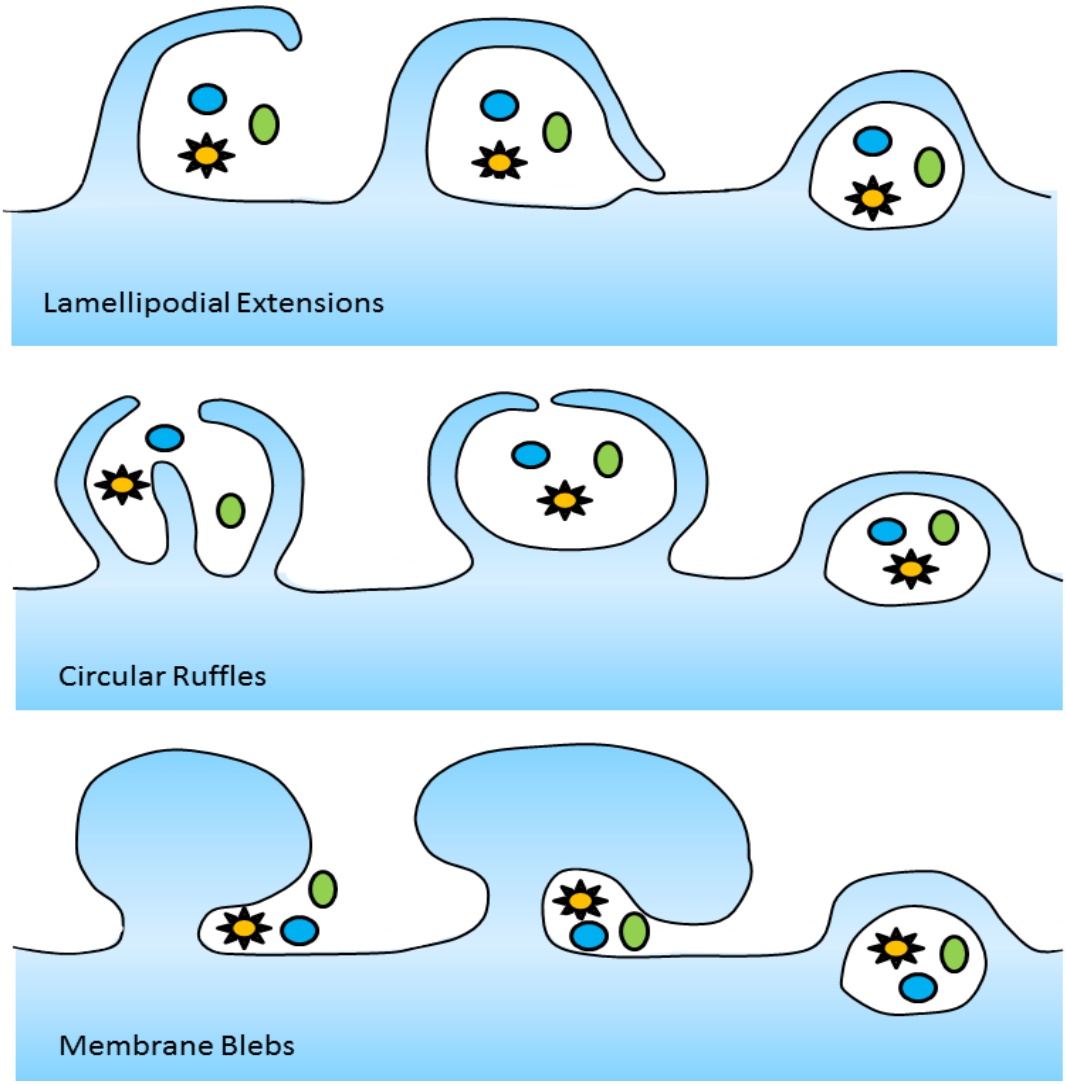

Figure 1.7: Macropinocytosis. Macropinosomes can be formed by lamellipodial extensions, filopodia or membrane blebs folding back and fusing with the plasma membrane, resulting in uptake of the extracellular fluid, solutes and substances suspended within.

During macropinocytosis, the ruffles and blebs that are formed are able to provide both the energy and the membrane that are required for the formation of macropinosomes. Although most of these ruffles seamlessly rejoin the plasma membrane, a few fold back to form fluid-filled cavities that undergo membrane fission and form macropinosomes, as shown in **Figure 1.7**.

Macropinocytosis is typically stimulated by growth factors, which results in the activation of cell-surface receptors, such as receptor tyrosine kinases (Mercer and Helenius 2009). The resulting signalling cascade triggers actin polymerisation and ruffling of the plasma membrane (Bar-Sagi et al 1986, Ridley et al 1992, Lanzetti et al 2004).

Macropinocytosis has many important physiological roles; for example, macrophages and dendritic cells primarily monitor their external environment for circulating antigens by constitutively macropinocytosing the extracellular solute (Sallusto et al 1995). As these cells are constitutively macropinocytic, they are able to internalise up to 100% of their membrane within 30 minutes (Steinman et al 1976). Macropinocytosis is also involved in the chemotaxis of neutrophils and macrophages (Carpentier et al 1991). In addition to these crucial roles in specialised cell types, macropinocytosis is also involved in the downregulation of signalling and reorganisation of the plasma membrane in cells that are not constitutively macropinocytic (Owen and Evans 1998). This is corroborated by the observation of Src family kinases within macropinosomes (Kasahara et al 2007). As large areas of the plasma membrane are internalised within macropinosomes, considerable reorganisation of the membrane is likely to occur. Moreover, because of the inherent dependence on membrane ruffling and lamellipodia formation, macropinocytosis is also thought to have a role in cell migration (Swanson and Watts 1995), and

consequently in tumour progression and metastasis (Platek et al 2004, Platek et al 2007).

As with the micropinocytotic processes, macropinocytosis can be hijacked by bacteria and viruses, which are able to induce macropinocytosis independently of growth factor activation, resulting in their internalisation within the macropinosome. Examples of pathogens that utilise macropinocytosis for cellular entry include salmonella and shigella (Alpuche-Aranda et al 1994, Schroeder and Hilbi 2008, Francis et al 1993), in addition to ebola Zaire virus (Nanbo et al 2010, Saeed et al 2010).

Macropinocytosis is often defined by inhibition with amiloride and its derivative EIPA (West et al 1989). These inhibit Na+/H+ exchangers; however, it is unclear how they inhibit macropinocytosis (Dowrick et al 1993). As with other pharmacological inhibitors, cell-specific effects involving non-macropinocytic endocytic pathways have been observed and it is not advisable to rely solely on amiloride inhibition to classify a process as macropinocytic (Ivanov 2008).

Members of the Rho GTPase family (such as Rho, Cdc42 and Rac) (together with phosphoinositide 4,5-bisphosphate $PI(4,5)P_2$) initiate the actin polymerisation that is required for macropinocytosis, and also activate WASP proteins, which coordinate the assembly of the Arp2/3 complex on actin filaments. Ruffles and blebs are enriched in proteins that are involved in actin polymerisation, such as WAVE and the Arp2/3 complex (Lavoie et al 1993, Bretscher et al 1997, Holt and Koffer 2001, Buccione et al 2004, Charras et al 2006, Takenawa et al 2007) and the process is thought to be highly actin-dependent.

In addition, p21-activated kinases (PAKs) have been shown to be directly involved in macropinocytosis; for example, PAK1 associates with both membrane ruffles and macropinosomes in fibroblasts (Kerr et al 2009). PAK1 is activated by Rac1 and Cdc42 and regulates cytoskeleton dynamics as well as CtBP1/BARS, which is required for macropinosomes closure. As such, PAK1 is required throughout macropinocytosis, from macropinosome formation to closure (Dharmawardhane et al 2000, Parrini et al 2005, Liberali et al 2008, Bar-Sagi et al 1987, Galisteo et al 1996, Puto et al 2003, Liberali et al 2008). is required for scission of macropinosomes (). The role that PAK1 plays in various stages of macropinocytosis is summarised in **Figure 1.8**.

Protein kinase C (PKC) is also involved in macropinocytosis. Following activation by receptor tyrosine kinases or PI3K, PKC associates with the plasma membrane, where it plays a role in the formation of macropinosomes (Miyata et al 1989, Amyere et al 2000). Phorbol esters (e.g. PMA), which are able to activate PKC, can induce macropinocytosis in the absence of growth factors (Keller et al 1990, Ridley et al 1992).

In addition to these factors, c-src, which is a non-receptor tyrosine src-family kinase, has also been implicated in macropinocytosis (Kasahara et al 2007), in which it is thought to enhance the activity of the activated receptor tyrosine kinases (Sandilands et al 2004, Donepudi et al 2008), as well as activating Arp2/3 and PI3K (Amyere et al 2000).

Different factors are required for the closure of macropinosomes than those that are involved in macropinosome formation; these factors include myosins and GTPases (Sun et al 2003). Dynamin seems to be required in some cases, and inhibition of

dynamin prevents Rac1 from localising to ruffles (Schlunck et al 2004, Liu et al 2008). Bleb closure in particular is thought to be dynamin-independent, although the exact mechanism remains unlear (Mercer and Helenius 2008).

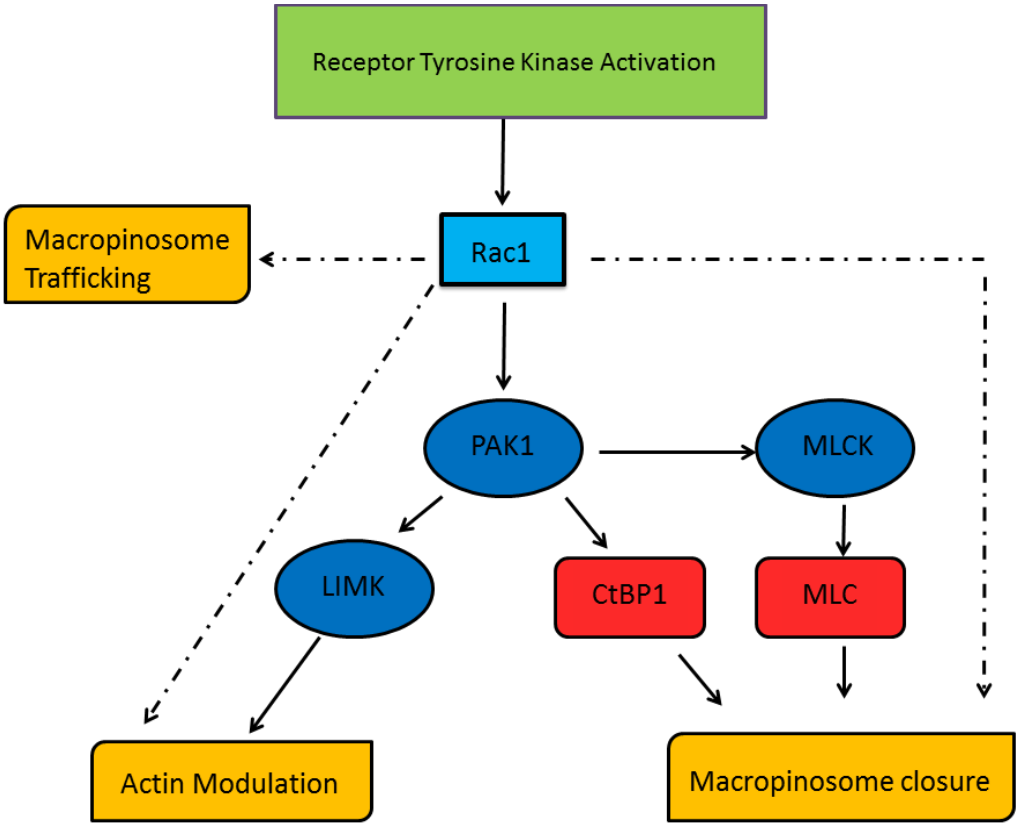

Figure 1.8: Growth factor receptor signalling regulates macropinocytosis. Activation of receptor tyrosine kinases results in activation of Rac1, a protein involved in actin modulation. In turn PAK1 is activated and downstream signalling results in actin modulation and macropinosome closure.

Although it is traditionally thought that membrane proteins are internalised by macropinocytosis as a result of bulk plasma membrane uptake, there is some evidence of a sorting function in macropinocytosis. This is consistent with the fact that the process is often stimulated by growth factor stimulation and supported by the fact that simultaneous stimulation with platelet-derived growth factor (PDGF) and EGF results in macropinocytosis of EGFR in fibroblasts, whereas stimulation with

either ligand alone does not (Schmees et al 2012). This suggests that activated receptor tyrosine kinases are selectively sorted into macropinosomes, rather than simply being internalised as a result of uniform membrane uptake.

1.2.3 Intracellular trafficking

1.2.3.1 The endosomal pathway

The endosomal pathway involves trafficking of internalised endocytic vesicles, either through compartments of increasing acidity (early and late endosomes), resulting in degradation by the lysosome or recycling back to the plasma membrane. Many viruses are able to uncoat and fuse with the endosomal membrane under the acidic conditions of early and late endosomes, releasing their genetic material and escaping lysosomal degradation (Gruenberg and Van der Goot 2006, Körner et al 2006).

There are three different types of endocytic compartments: early endosomes, late endosomes and recycling endosomes (Mellman 1996). Early endosomes provide an environment for the sorting of internalised endocytic cargo before it ultimately reaches the degradative lysosome or is recycled back to the cell surface, and are therefore often referred to as sorting endosomes (Jovic et al 2010) . The different endocytic compartments are distinguished by markers such as Rab proteins, which regulate vesicle formation, vesicle movement along microtubules and membrane fusion (Stenmark and Olkkhonen 2001). Once vesicles have uncoated following endocytosis, they fuse with early endosomes, which mature into late endosomes in a Rab5-dependent process (Huotari and Helenius 2011). Activity of the vacuolar

membrane proton pump, v-ATPase (vacuolar ATPase), leads to increased acidity and maturation of the endosome (Kane 2006, Forgac 2007). Early endosomes increase in size during maturation due to homotypic fusion with other early endosomes. Molecules within endosomes may become sorted into smaller vesicles that bud into the endosomal lumen, resulting in a multi-vesicular appearance which has led to late endosomes often being called multivesicular bodies (MVBs).

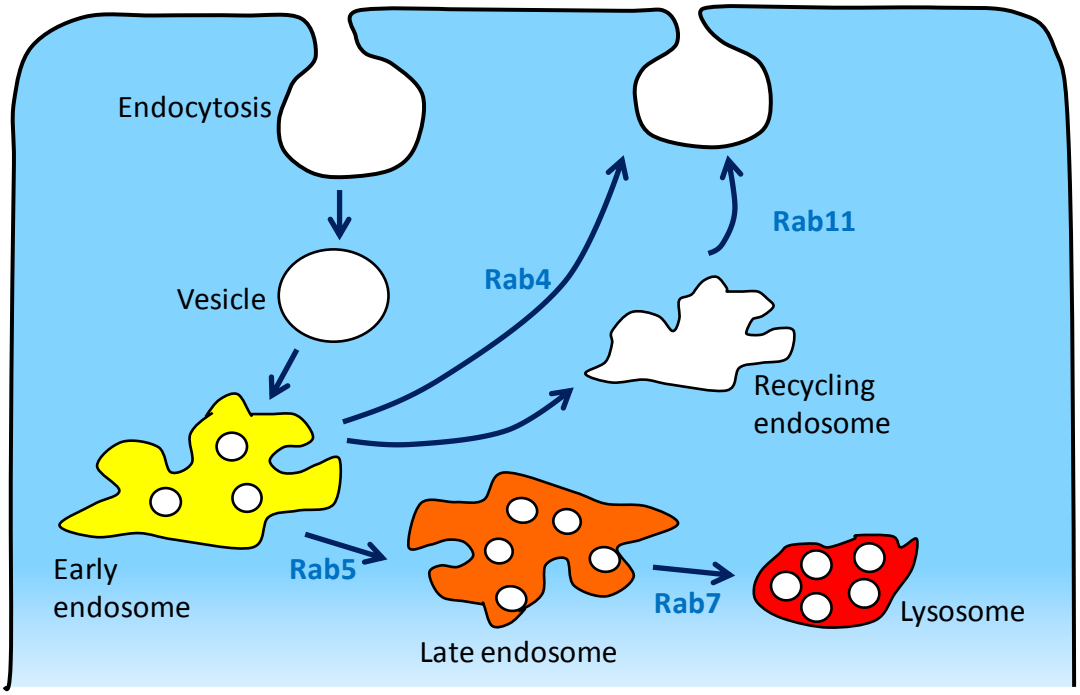

Figure 1.9: **The endosomal system.** Internalised endocytic vesicles fuse with the early endosome where their contents may recycle back to the plasma membrane in Rab4 and Rab11- dependent processes, or traffic through compartments of increasing acidity to the lysosome for degradation.

Finally, early endosomes lose Rab5 and gain Rab7, allowing them to fuse with lysosomes as shown in **Figure 1.9**. Some pathogens can subvert the endosomal maturation process, for example, by preventing acquisition of Rab7 by the late

endosome, allowing escape from lysosomal degradation (Körner et al 2006, Gruenberg and Van der Goot 2006).

Phagosomes and macropinosomes are thought to mature in a similar manner and often fuse with compartments of the endosomal system (Racoosin and Swanson 1993). Thus, it can be difficult to clearly delineate all aspects of phagosome, macropinosome and endosomal trafficking.

1.2.3.2 Maturation and trafficking of macropinosomes

Internalised macropinosomes have been shown to mature in a similar manner to endosomes, undergoing acidification and fusion with endosomal compartments (West et al 1989, Hewlett et al 1994). Macropinosomes have been shown to rapidly acquire the endosomal marker Rab7 before ultimately fusing with the lysosomal compartment (Racoosin and Swanson 1993, Kerr et al 2006, Lim et al 2008), indicating that macropinosomes traffic down the endosomal pathway towards lysosomal degradation, with their cargo meeting a similar fate to that internalised by micropinocytosis. However exchange of constituents with the endolysosomal system and lack of molecular markers have hampered the definitive molecular dissection of macropinosome maturation. Transferrin receptor, which typically traffics to the early endosome, has been shown to be lost from macropinosomes as they mature; this suggests that sorting of cargo occurs during macropinosome trafficking (Racoosin and Swanson 1993).

Furthermore, the ultimate fate of the macropinosome seems to be cell-type dependent. In macrophages and kidney cells, macropinosomes are thought to fuse with the endolysosomal system (Racoosin and Swanson et al 1993); however,

macropinosomes in human A431 and NIH-3t3 cells seem to be independent of endosomal trafficking and ultimately fuse back with the plasma membrane (Hewlett et al 1994, Schnatwinkel et al 2004), although they do gain some early endosomal markers for fusion with other macropinosomes (Roberts et al 2000, Hamasaki et al 2004). Thus, there is no real consensus on the trafficking pathway that is followed by internalised macropinosomes, and the process seems to be remarkably cell-type- and context-dependent.

1.3 Viral Entry

Viruses are obligate intracellular pathogens and entry into the host cell is a critical step in the viral life cycle. Cellular membranes present a barrier between the viral particle and intracellular site(s) of replication in the cytosol or nucleus. Viral entry mechanisms thus present a good therapeutic target, and several viral entry inhibitors have been successfully developed or are undergoing clinical trials, most notably inhibitors of HIV-1 entry (Lalezari et al 2003, Lin et al 2003, Guo et al 2003, Kuritzkes et al 2004, Hicks et al 2005, Clotet et al 2007) and Influenza virus A entry (Voss et al 2008, Song et al 2009, Yamaya et al 2010).

Viruses have a proteinaceous capsid that encapsulates their genetic material; in enveloped viruses, this is surrounded by a lipid bilayer. Both enveloped viruses and non-enveloped viruses have evolved complex and often poorly defined mechanisms to enter cells. Identification of host cell receptors and their trafficking pathways provide tools to study viral entry. Although this generally involves the endocytic processes of the host cell, the exact entry mechanisms of many medically important viruses, including HCV, have yet to be fully elucidated.

The entry of both enveloped and non-enveloped viral particles requires specific interactions between host cell molecules, or receptors, and virus-encoded envelope or capsid proteins. One key result of this is to bring the virus into close contact with the plasma membrane and in some documented cases, to initiate a cascade of signalling events important to the viral life cycle (Dangoria et al 1996). In addition to primary receptors critical for virus attachment to the cell surface (e.g. CD4 for HIV), important co-receptors have been identified (e.g. chemokine receptors CXCR4 or CCR5 for HIV). It is now becoming apparent that a wide variety of host cell molecules are important for virus internalisation in the absence of any direct association with the virus particle. This has led to the notion of "entry factors", for example the tight junction protein occludin appears to play an indirect role in Coxsackie B group virus entry (Bergelson et al 1997, Patel et al 2009), while both claudin-1 and occludin appear to play an indirect role in HCV entry (Benedictio et al 2009, Ploss et al 2009).

Following attachment to the host cell surface, direct virus entry at the plasma membrane has been described for many viruses such as HIV and polio virus (Stein et al 1987, Dunnebacke et al 1969). Some enveloped viruses can fuse with the plasma membrane, releasing the capsid directly into the cytosol. However, in contrast to fusion at the plasma membrane, many viruses (such as SV40 and Influenza A) utilise intracellular trafficking pathways and fuse with internal membranes to release their genomic material into the cytosol (Anderson et al 1996, Lakadamyali et al 2004).

Host cells offer a variety of internalisation mechanisms for virus entry, as described in **Section 1.2**. Receptor trafficking pathways often define particle internalisation routes and viruses typically infect the cell by a single defined pathway, although

examples have been reported where viruses utilise multiple pathways in diverse cell types (Meier et al 2002, Damm et al 2005, Patel et al 2009). It is clear that viral entry is not a simple process and that a more complete understanding of cellular endocytic pathways will provide us with a better perspective regarding viral entry mechanisms. Moreover, the study of viral entry has historically, and continues to be, key to our understanding of endocytosis and trafficking pathways within the host cell, for example, the study of SV40 endocytosis has provided much of the current knowledge regarding caveolar endocytosis (Anderson et al 1996).

While classical understanding of viral entry is that a virus will enter via one defined pathway determined by receptor binding, recent studies indicate that many viruses are capable of utilising more than one entry mechanism to cause infection. It has long been thought that productive entry of HIV occurs via direct fusion of the viral envelope with the host cell plasma membrane. One key piece of evidence for an endocytosis-independent mode of entry is the observation that infection is insensitive to neutralisation of endosomal pH (Stein et al 1987). Despite this long-standing belief, studies employing EM have shown internalised virions in membrane-bound vesicles (Grewe et al 1990). Whilst the clathrin-mediated entry pathway for HIV has been documented for almost as long as the classical plasma membrane entry mechanism, it has only recently been confirmed that this route may offer a productive entry pathway for infectious viral particles (Daecke et al 2005).

In addition, SV40, the first virus to be described to enter via the caveolar pathway (Pelkmans et al 2001, Pelkmans et al 2002) has recently been shown enter cells lacking detectable caveolae, suggesting that it is capable of entering the cell via alternative pathways (Damm et al 2005). SV40 entry via a caveolin-independent pathway was also observed in wild-type embryonic fibroblasts with an active

caveolar pathway (Damm et al 2005). In all of the aforementioned cells, viruses were seen to internalise in small, tight-fitting vesicles similar to those seen in the first EM images of SV40 infection. The virus was subsequently transported to pH-neutral organelles, which resembled “caveosomes” despite being devoid of both caveolin 1 and caveolin 2 (Damm et al 2005). Furthermore, expression of SV40 T-antigen following viral entry in these cells suggested that this pathway supported productive infection. The fact that this entry mechanism was observed in cells with detectable caveolin 1 indicates that this alternative pathway is active even in the presence of caveolin 1. This could represent further evidence of host cell endocytic mechanisms acting independently of clathrin and caveolin.

Other examples of viruses which have been shown to enter via more than one mechanism include Adenoviruses 2 and 5 (AdV2/5), Coxsackie B group viruses and Influenza A. AdV 2/5 have been shown to enter via clathrin-mediated endocytosis and then stimulate macropinocytosis leading to increased viral uptake (Meier et al 2002). Coxsackie B group viruses which have been shown to enter via a mechanism dependent on caveolin 1 and some macropinocytic proteins in Caco-2 cells (Coyne et al 2007) enter via a clathrin and caveolin- independent mechanism in HeLa cells (Patel et al 2009). Moreover, Influenza A virus, which has classically been described to enter via clathrin-mediated endocytosis (Yoshimura et al 1982) has also been shown to enter cells in the absence of clathrin-mediated endocytosis (Sieczkarski et al 2002). More recently Influenza A has been shown to enter via a caveolar mechanism in MDCK cells (Nunes-Correia et al 2004), while yet another paper implicates macropinocytosis as an alternative entry mechanism for Influenza A (de Vries et al 2011).

Indeed, many viruses have evolved mechanisms to manipulate macropinocytosis to promote their own internalisation. Vaccinia virus is thought to enter host cells via a mechanism known as ‘apoptotic mimicry’ (Schmidt et al 2011). The viral envelope contains phosphatidylserine, which mimics cellular apoptotic material and results in internalisation of the virus by macrophages.

Some viruses can also stimulate macropinocytosis by directly engaging will cellular receptors; for example, binding of Coxsackie virus to its receptor OCLN in tight junctions induces uptake of the virus by a pathway that resembles macropinocytosis (Coyne et al 2007). In addition, inhibiting macropinocytosis reduces HIV infection rates, but it is unclear whether the virus induces macropinocytosis or how this effect is mediated (Marechal et al 2001, Liu et al 2002).

Moreover, different endocytic mechanisms may be used by a virus in different cell types. For example, although there is some evidence for macropinocytic uptake of HIV into endothelial cells and macrophages (Marechal et al 2001, Liu et al 2002), the virus is still able to enter and infect cells that are unable to form macropinosomes, ostensibly by an alternative endocytic pathway (Vidricaire and Tremblay 2007). For a full review of viral entry mechanisms, see Thorley et al 2010.

HCV is an enveloped virus. Infection with an enveloped virus requires the fusion of the viral envelope with a cellular membrane. In some cases, this can occur at the plasma membrane, as reported for HIV, where binding to plasma membrane-expressed forms of CD4 and chemokine receptors induce changes in the viral envelope glycoprotein that are thought to mediate membrane fusion under neutral pH conditions. Fusion of other enveloped viruses occurs within the low pH environment of an acidic endosomal compartment. Enveloped viruses typically reach the endosomal compartment via trafficking in clathrin-coated vesicles, although

caveolar routes of entry have been reported for some enveloped viruses, including human coronavirus 229E (Nomura et al 2004, Kawase et al 2009). Enveloped viruses have also been shown to enter cells via macropinocytosis where fusion is also thought to occur within the low pH environment of an endosomal (or analogous) compartment. Indeed, AdV2/5 is thought to stimulate macropinocytosis to escape from endosomes following a clathrin-mediated entry mechanism, although the mechanism by which this occurs remains somewhat unclear (Meier et al 2002).

1.4. HCV Entry

1.4.1 HCV receptors and viral tropism

HCV encodes two envelope glycoproteins, E1 and E2, which play a critical role in binding host cell surface receptors and membrane fusion (Keck et al 2004, Op De Beeck et al 2004, Helle et al 2008). E1 and E2 are heavily glycosylated and form a heterodimer. While the conformation of the two glycoproteins is somewhat co-dependent, it is thought that E2 is the primary mediator of interactions with host cell receptors. Recombinant forms of HCV E2 were used to identify the host cell binding partners tetraspanin CD81 (Pileri et al 1998, Bartosch et al 2003a, Cormier et al 2004, Flint et al 2006) and scavenger receptor B type I (SRBI) (Scarselli et al 2002, Grove et al 2007, Cantanese et al 2010), shown in **Figure 1.10**. The recent development of infectious lentiviral pseudoparticles bearing HCV glycoproteins (HCVpp) (Bartosch et al 2003b, Hsu et al 2003, Drummer et al 2003), and native HCV capable of replication in cell culture (HCVcc) (Lindenbach et al 2005, Wakita et al 2005, Zhong et al 2005) have enabled studies validating the role of CD81 and SRBI in HCV entry. Following the development of these experimental systems, the

tight junction proteins claudin 1 (CLDN1) and occludin (OCLN) were reported to be essential for virus internalization (Evans et al 2007, Zheng et al 2007, Yang et al 2008, Liu et al 2009, Ploss et al 2009). Claudins -6 and -9 have also been shown to act as additional co-receptors (Zheng et al 2007).

HCVpp bearing diverse glycoproteins of all major HCV genotypes show a marked preference for infecting liver-derived cells suggesting that receptor-dependent entry events may, at least in part, define hepatotropism (Bartosch et al 2003c, McKeating et al 2004).

Hepatocytes in the liver are highly polarised with bile canaliculi surrounded by tight junctions running between adjacent cells at the apical membrane, as shown in **Figure 1.11**. HCV enters the liver via the sinusoidal blood and is likely to encounter the basolateral surface of hepatocytes, where the co-receptors SRBI, and CD81 as well as the entry factor CLDN1 are expressed (Reynolds et al 2008).

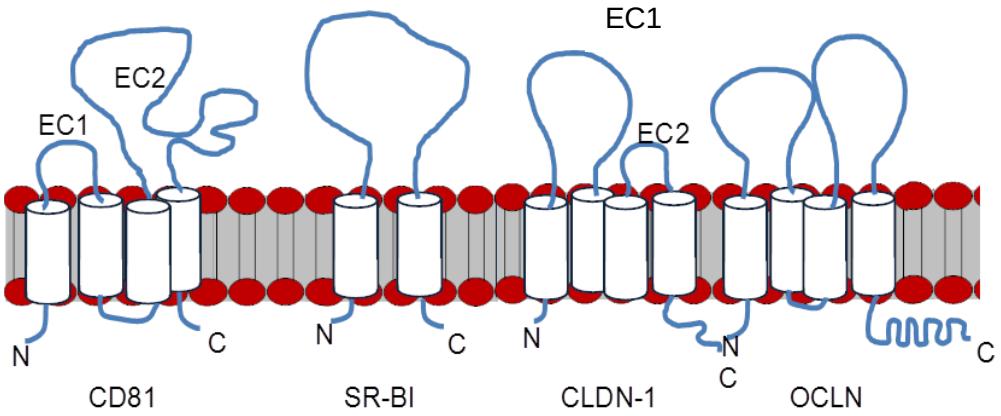

Figure 1.10: Cellular co-receptors and entry factors for HCV. The tetraspanin CD81, scavenger receptor SRBI, and the tight junction proteins claudin 1 (CLDN1) and occludin (OCLN).

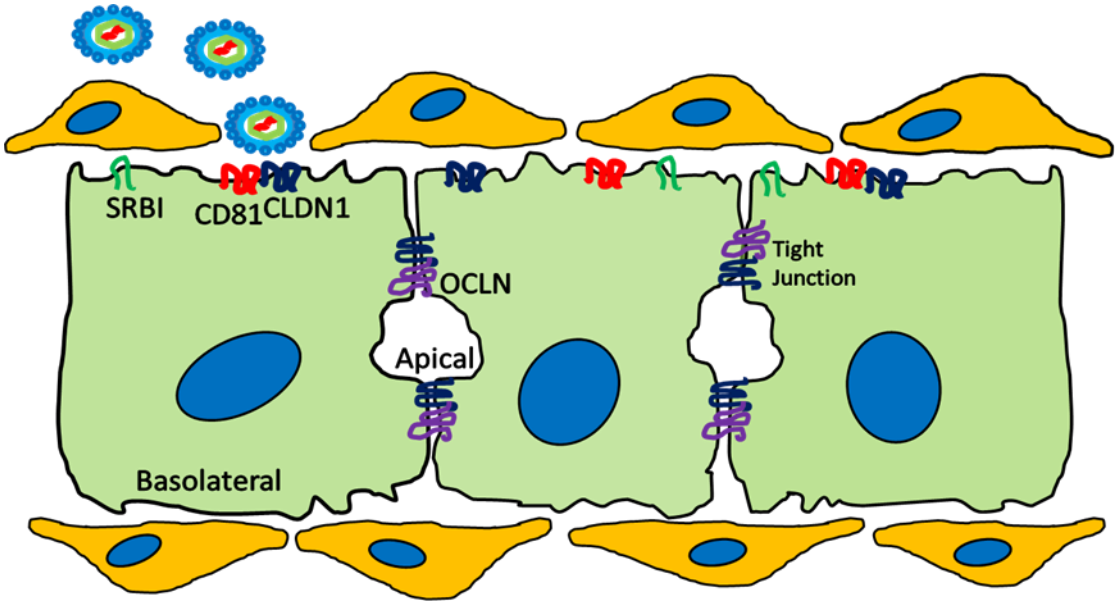

Figure 1.11: Hepatocyte polarity. Hepatocytes in the liver exhibit a complex polarity, with the basolateral surface exposed to the sinusoidal blood, while the apical membranes form bile caniliculi between adjacent cells, bound by tight junctions containing CLDN1 and OCLN.

Claudins are tight junction proteins which are able to form homo -and heterodimers with each other (Piontek et al 2008) OCLN and CD81 (Harris et al 2010), and the formation of the CD81-CLDN1 interaction is essential for HCV entry (Yang et al 2008, Qiu et al 2008, Cukierman et al 2009, Harris et al 2010, Krieger et al 2010). No direct interaction between CLDN1 and the HCV glycoproteins has to date been identified, although recent evidence suggests that CLDN1 may serve to potentiate the interaction between CD81 and E2 (Krieger et al 2010). While present in tight junctions, CLDN1 is also expressed in the basolateral membrane of polarised hepatocytes in the liver (Reynolds et al 2008).

OCLN is a tight junction protein which has been shown to internalise along with CLDN1 in caveolae and clathrin-coated vesicles (Matsuda et al 2004, Shen 2008, Stamatovic et al 2009). OCLN is necessary to confer entry into non-permissive cell

lines, and silencing of OCLN reduced infection of permissive Huh7.5 hepatoma cells (Ploss et al 2009, Liu et al 2009). OCLN is localised to tight junctions in polarised hepatocytes, which has led some to believe that viral entry must occur at tight junctions. However, as with CLDN1, there is little evidence for a direct interaction between the virus and OCLN.

More recently, the epidermal growth factor receptor (EGFR) has been identified as an entry factor for HCV, using an siRNA screen (Lupberger et al 2011). The authors also show that EGF stimulation of hepatoma Huh7.5 and Huh7.5.1 cells promotes HCV entry. Exactly how EGFR acts as an entry factor is unclear, but signalling downstream of EGFR may be important for HCV endocytosis. Moreover, as EGF stimulation results in EGFR internalisation by different pathways under different circumstances (Benmerah et al 1999, Huang et al 2004, Sigismund et al 2005, Zhu et al 2005, Orlichenko et al 2005, Roepstorff et al 2009), it is interesting to speculate that EGF may upregulate trafficking pathway(s) required for HCV entry and infection, particularly for the internalisation of HCV co-receptors and entry factors. This will be discussed in greater detail in **section 1.4.3**.

1.4.1.1 CD81 and tetraspanin-enriched microdomains

The HCV receptor CD81 is a tetraspanin. Tetraspanins are a highly conserved and broadly expressed superfamily of transmembrane proteins, which as the name suggests, span the lipid bilayer four times (Wright and Tomlinson 1994). They have short intracellular C- and N- terminal tails in addition to a small extracellular loop (SEL) and a large extracellular loop (LEL), shown in **Figure 1.10**, which are involved in mediating hetero-and homo-typic interactions.

There are 33 members of the tetraspanin superfamily expressed in humans and members of this protein family tend to form membrane signalling complexes, known as tetraspanin-enriched microdomains (TEMs) (Hemler 2005). This is mediated through their association with other membrane proteins as well as intracellular signalling and cytoskeletal components. Unsurprisingly, tetraspanins are linked to a number of physiological functions and pathologies, including diphtheria, malaria, cancer and viral infections (Wang et al 2011, Martin et al 2005).

Specific tetraspanin proteins are associated with specific viruses and appear to be involved in multiple stages of viral life cycles, from initial cellular attachment to viral budding (Martin et al 2005). As such, the relationship of tetraspanins with viruses is a particularly complex one.

Most tetraspanins possess no intrinsic enzymatic activity or signalling motifs and it is thought that they act simply by facilitating the interaction of associated proteins within TEMs. The most studied involvement of a tetraspanin in viral infection is that of CD81 in HCV entry. CD81 binds specifically to the E2 glycoprotein of HCV through its LEL and was the first HCV receptor to be identified (Pileri et al 1998, Bartosch et al 2003a, Cormier et al 2004, Flint et al 2006). E2 binds to cells of human origin but not to cell lines derived from other species such as mouse, rat, and rabbit (Flint et al 1999, Flint et al 2006). Thus, the interaction appears to be dependent on the presence of human (h)CD81 and not to require other molecules in human cells, as rat cell lines can bind E2 protein when transfected with hCD81. Other human tetraspanins are unable to compensate for the absence of hCD81.

FRET studies between overexpressed fluorescent co-receptors, revealed that CD81 and CLDN1 formed complexes within the plasma membrane of hepatoma cells

(Harris et al, 2008). When CLDN1 is prevented from interacting with CD81, HCV entry is inhibited.

1.4.1.2 The HCV co-receptor complex

As it is unclear exactly how the co-receptors come together to form a complex, whether they all interact with the virus and/or each other, and whether this requires translocation of the virus-receptor complex to the tight junctions, several models have been proposed to explain the entry mechanism of HCV. The Coxsackie B virus model is predicated on the fact that both viruses require tight junction proteins for entry. However, there is limited evidence for the direct association of HCV with the tight junction proteins CLDN1 and OCLN, and both CD81 and SRBI are localised uniformly on the plasma membrane. Therefore, the observation that CD81 and SRBI localise at basolateral hepatocellular membranes (Reynolds et al 2008) is consistent with particle attachment occurring at this site. Moreover, recent data demonstrate a role for CD81-Claudin complexes in HCV entry, and these complexes are known to form on the basolateral surface (Harris et al 2008, Harris et al 2010).

Nevertheless, the involvement of tight junction proteins has raised many questions about HCV entry. In particular, does the virus need to locate to tight junctions to internalise? Current data demonstrate that HCV E2 engagement of CD81 promotes clathrin-mediated endocytosis and there is limited evidence to support a role for CD81 induced movement of the virus to tight junctions in polarised hepatoma cells (Farquhar, personal communication). Additionally, it is thought that the virus enters the liver via the sinusoidal blood where it would encounter the basolateral surface of hepatocytes. The basolateral entry model suggests the virus enters at the

basolateral surface of the hepatocyte, which is accessible by the sinusoidal blood and that there is no role for the tight junctions in viral entry. The independence from tight junctions is supported by the fact that CD81-CLDN1 complexes, which have been shown to be essential for viral entry are entirely absent from the tight junctions of polarised hepatocytes (Harris et al 2010). In addition, reduced polarity, promoted by the addition of VEGF has been shown to increase infectivity (Mee at al 2010).

Interestingly, it has been suggested that the filopodia of hepatocytes extend through the sinusoidal membrane where they are able to make contact with T-cells, potentially mediating initial contact with the virus (Warren et al 2006). In support of this idea, HCV has been shown to initially associate with filopodia in Huh7.5 cells before being transported towards the cell body for endocytosis (Coller et al 2009). **Figure 1.12** shows the current model for HCV co-receptor complex formation on the basolateral surface of hepatocytes.

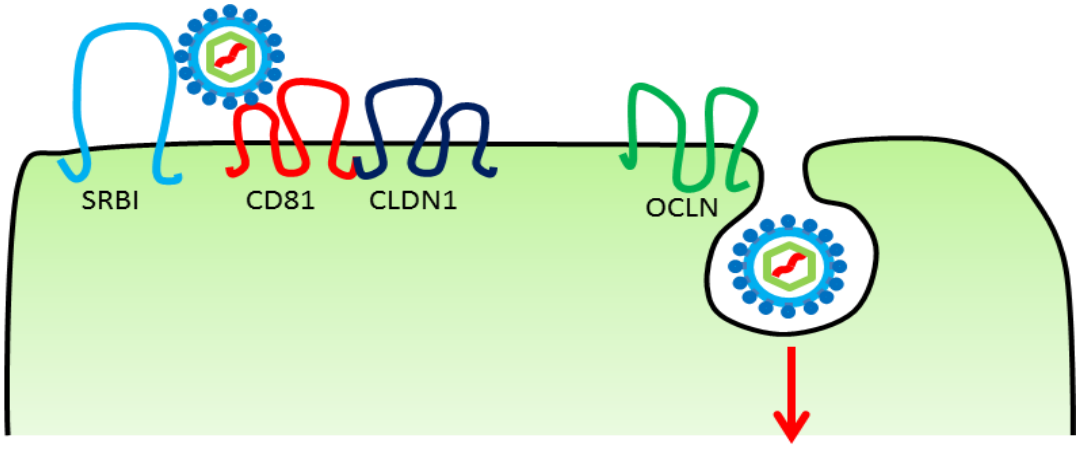

Figure 1.12: The HCV Co-Receptor Complex. SRBI and CD81 are known to form specific interactions with viral glycoproteins. While CLDN1 is not thought to interact with the virus directly, its interaction with CD81 is necessary for viral entry. There is no known interaction between tight junction protein OCLN and the virus, however OCLN is known to be an important entry factor.

1.4.2 HCV endocytosis

Soon after the development of the HCVpp and HCVcc systems, the use of drugs such as Bafilomycin A1 and concanamycin A (which inhibit the vacuolar ATPase, dissipating membrane proton gradients) demonstrated the pH-dependence of HCV entry, implicating the involvement of receptor-mediated endocytosis and fusion in an acidic endosomal compartment (Hsu 2003, Blanchard et al 2006, Tscherne et al 2006). Furthermore, the use of dominant negative constructs of Eps15 and the large GTPase dynamin suggested that HCV entry occurs via clathrin-mediated endocytosis (Meertens et al 2006). A recent siRNA study confirmed the involvement of several genes involved in clathrin-mediated endocytosis and actin polymerisation in the viral entry process and used time-lapse imaging to observe viral entry in live unpolarized liver-derived cells (Coller et al 2009). The authors demonstrated colocalisatiom between labelled HCV and clathrin, suggesting that virions bind to filopodia and traffic towards the cell body, where endocytosis occurs.

While viral internalisation via clathrin-mediated endocytosis has been confirmed using chemical inhibitors and clathrin heavy chain siRNA (Blanchard et al 2006, Codran et al 2006, Coller et al 2009), alternative entry mechanisms have not been considered in any HCV entry studies. In light of recent evidence for several viruses utilising more than one internalisation mechanism, it is becoming increasingly important that other entry mechanisms for HCV be considered as additional or alternative mechanisms in entry studies.

1.4.2.1 Caveolae in hepatocytes and hepatoma cell lines

While several studies have demonstrated that HCV can enter hepatoma cell lines in a clathrin-dependent manner, none of these studies has ruled out entry by clathrin-independent mechanisms. In particular, a potential role for caveolae in HCV infection has largely been overlooked due to a long-standing belief that the hepatoma cell lines used to study HCV infection do not express caveolin 1 or have functional caveolae (Cokakli et al 2009, Tse et al 2012). However, there is evidence both for and against the presence of caveolae in hepatoma cell lines throughout the literature (Pohl et al 2002, Botos et al 2007, Zhao et al 2009). Among the most convincing pieces of evidence for the presence of caveolae in hepatoma cell lines are electron micrographs (for example, **Figure 1.13**) of HepG2 cells, showing what appear to be caveolae (Botos et al, 2007). Moreover, several studies have noted the effects of inhibitors of caveolar endocytosis or knockdown of caveolin 1 in hepatoma cell lines (Pohl et al 2002; Zhao et al 2009). Most notably, Pohl et al demonstrate inhibition of [^{3}H]oleic acid uptake when cells were treated with filipin III, cyclodextrin and caveolin 1 antisense oligonucleotides, all of which are known to inhibit caveolar endocytosis.

However, contrary to these findings, studies have failed to detect caveolin 1 expression in hepatoma cell lines by western blot (Cokakli et al 2009, Qi et al 2010). There is mounting evidence for a pathway both morphologically and functionally similar to the caveolar pathway acting independently of caveolin 1 (Damm et al 2005). In the absence of detectable caveolin 1, it is possible that inhibitors of the caveolar pathway may be exhibiting their effects on alternative but similar or related pathways. If caveolae or related pathways exist in primary hepatocytes *in vivo*, this could represent a potential route for productive infection.

Moreover, in order to assess the role that all endocytic mechanisms play in viral entry, cell lines which express the necessary endocytic proteins and that can be shown to have active clathrin-mediated and caveolar uptake pathways should be used in infection studies. This has not been done to date.

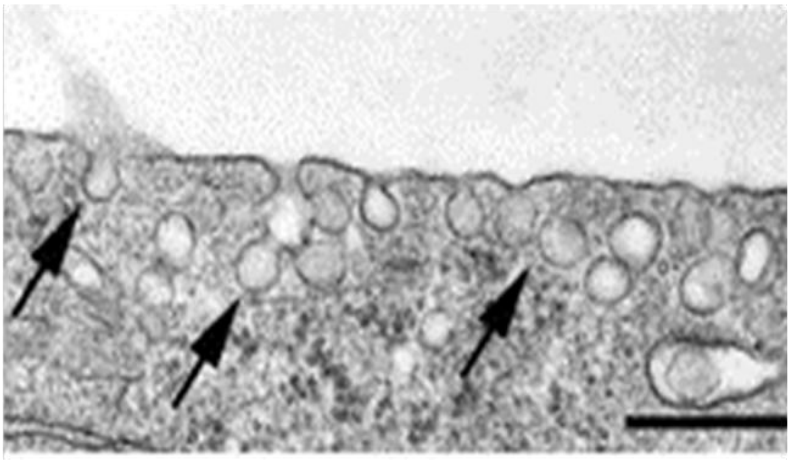

Figure 1.13: Electron micrograph of caveolae in HepG2 cells. Taken from Botos et al 2007, reprinted with permission from Springer publishing.

1.4.3 Tyrosine kinases in viral entry

Viruses co-opt host cell proteins as their receptors and utilise these to mediate their entry into the host cell. Often this is as a result of virus-binding inducing receptor complex formation and signalling cascades. Many viral receptors are tyrosine kinases, and in many cases, their kinase activity and subsequent downstream signalling is required for the viral entry process. For example, the receptor tyrosine kinase Axl has been shown to enhance internalisation of ebola Zaire virus via an indirect mechanism. The virus does not bind to Axl directly, but the interaction may be mediated by Gas6 (an Axl ligand), which has a similar role in the internalisation of other viruses (Shimojima et al 2006, Nanbo et al 2010, Saeed et al 2010, Brindley et al 2011, Morizono et al 2011).

Coxsackie virus B (CVB) requires trafficking to tight junctions for entry into host cells and uses tyrosine kinase signalling to achieve this. CVB particles initially attach to CD55 (also known as decay-accelerating factor (DAF)) on the apical cell surface. Virus binding induces clustering of this receptor, leading to the activation of Abl kinase and actin reorganisation. . This allows the virus to translocate to tight junctions where it finally binds to the coxsackie and adenovirus receptor (CAR) and is endocytosed (Cohen et al 2001, Coyne and Bergelson 2006). CD55 binding also induces caveolin 1 phosphorylation, promoting internalisation of the virus by caveolar endocytosis (Coyne and Bergelson 2006).

Influenza A virus binds to sialylated receptor tyrosine kinases, such as EGFR and c-Met, inducing their clustering and promoting tyrosine kinase and PI3K signalling, which may be important for viral entry via either clathrin-dependent or –independent pathways (Eierhoff et al 2010).

1.4.3.1. The epidermal growth factor receptor (EGFR) in HCV entry

Recent studies have identified the epidermal growth factor receptor (EGFR) as an additional entry factor for HCV, using a functional RNAi kinase screen (Lupberger et al. 2011). However, the mechanism by which EGFR promotes viral internalisation is not clear. The receptor tyrosine kinase promotes CD81-CLDN1 complex formation via unknown mechanisms, and it is thought that this effect results in increased uptake of the virus (Zona et al 2013). Blocking receptor kinase activity was shown to inhibit infection by all of the major HCV genotypes and addition of the ligands EGF and TGFα significantly stimulated viral entry and infection (Lupberger et al 2011, Diao et al 2012). The internalisation of EGFR has been shown to be required for

HCV entry (Diao et al 2012). This means that tyrosine kinase inhibitors could potentially possess substantial antiviral properties, and RTK inhibitors could be used as a new approach to prevent or treat HCV infection. However, the mechanism of action of EGFR and the involvement of downstream signalling in HCV entry is still poorly understood.

Additional recent evidence suggests the GTPase HRas, which is activated downstream of EGFR signalling, is a key host signal transducer for EGFR-mediated HCV entry (Zona et al 2013). HRas was shown to associate with membrane microdomains containing CD81 and CLDN1. Additionally, proteomic analysis revealed that HRas associates with tetraspanin CD81, CLDN1, as well as integrin β1 and Ras-related protein Rap2B in hepatic plasma membranes. HRas signalling is thought to be required for the lateral diffusion of CD81, promoting the assembly of tetraspanin receptor complexes and has also been implicated in the entry of other viruses, including influenza A (Zona et al 2013).

1.4.3.2 Signalling and trafficking of the epidermal growth factor receptor (EGFR)

There are four closely related members of the ErbB family of receptor tyrosine kinases, known as EGFR (ErbB1; HER1 in humans), ErbB2 (HER2), ErbB3 (HER3) and ErbB4 (HER4). EGFR is the prototypical member of the receptor tyrosine kinase family and is a transmembrane receptor for several extracellular protein ligands, including epidermal growth factor (EGF) (Atalay et al 2003). It is expressed on the plasma membrane and is activated by ligand binding, which is followed by dimerisation, trans-phosphorylation, clustering, endocytosis and endocytic trafficking,

and the initiation of downstream signalling cascades, as shown in **Figure 1.14**. Once in the acidic endosomal lumen, the EGFR-ligand complex dissociates. EGFR can then recycle back to the plasma membrane, allowing further rounds of receptor activation or traffic to the lysosome for degradation, leading to desensitisation.

The EGFR-binding ligands include EGF, heparin-binding EGF-like growth factor (HB-EGF), transforming growth factor-α (TGF-α), amphiregulin (AR), epiregulin (EPR), epigen, betacellulin (BTC) and neuregulins 1-4 (NRG1, NRG2, NRG3, NRG4) and recent data suggests that different ligands may promote different routes of receptor trafficking (Roepstorff et al 2009). For example, ligands which do not dissociate readily from the receptor within the acidic environment of the endosome (such as HB-EGF and BC) have been associated with increased receptor degradation over receptor recycling (Roepstorff et al 2009) Furthermore, the concentration of ligand applied can affect receptor trafficking: at low EGF concentrations EGFR primarily undergoes clathrin-mediated endocytosis (Benmerah et al 1999, Huang et al 2004), while at high EGF concentrations EGFR has been reported to undergo clathrin-independent endocytosis (Sigismund et al 2005, Zhu et al 2005, Orlichenko et al 2005).

EGFR undergoes transition upon ligand binding from an inactive monomer to an active homo- or hetero-dimer (with another member of the ErbB family of receptor tyrosine kinases) (Ferguson et al 2003). This dimerisation stimulates the intrinsic tyrosine kinase activity of EGFR, and as such, several tyrosine autophosphorylation events occur in the intracellular C-terminal domain of the receptor (Downward et al 1984). Autophosphorylation then results in downstream signalling through several

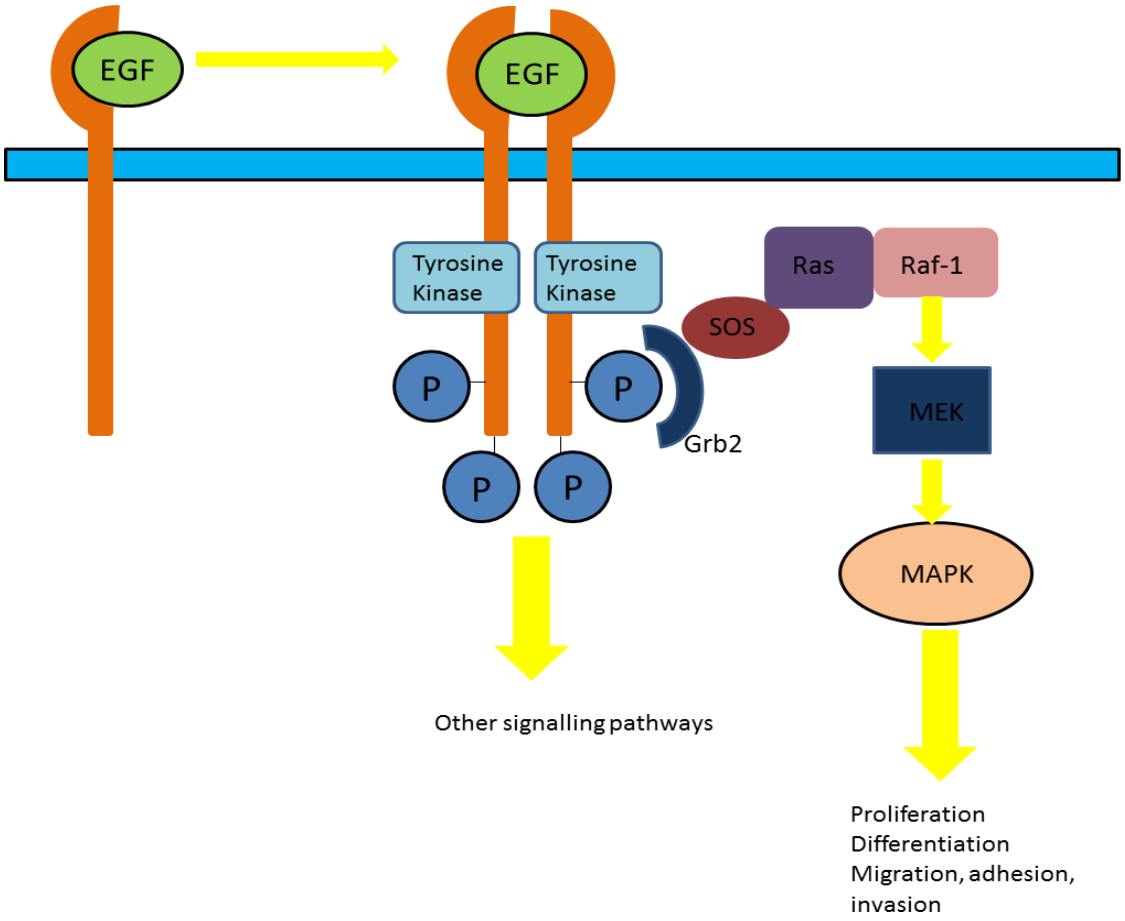

Figure 1.14: Signalling through the epidermal growth factor receptor (EGFR). Upon ligand binding, receptor dimerisation occurs, resulting in autophosphorylation. This initiates signalling cascades leading to cell proliferation, migration and invasion.

proteins, which interact with phosphorylated tyrosine residues through their SH2 domains. Several signal transduction cascades may then be activated, including the MAPK pathway, the Akt and JNK pathways (Lynch et al 2004, Oda et al 2005). These pathways modulate many important cellular processes such as, cell proliferation, cell migration and adhesion (Vermeer et al 2003).

EGFR is sometimes aberrantly activated by over-expression or mutation. Mutations that lead to upregulation of EGFR signalling have been implicated in several cancers, including lung cancer (Khazaie et al 1993, Kuan et al 2001, Arteaga 2002). As such, small molecule kinase inhibitors such as Erlotinib are often used to treat cancer (Raymond et al 2000) and can also be used in laboratory conditions (Moyer

et al 1997, Wood et al 2004, Huether et al 2005) to inhibit the kinase activity, and thus the downstream signalling of EGFR.

1.5 Imaging receptor trafficking

1.5.1 Fluorescence microscopy

The British scientist Sir George G. Stokes first described the phenomenon of fluorescence in 1852 when he observed the mineral fluorspar emitting red light when illuminated by ultraviolet (UV) light. Stokes noted that fluorescence emission always occurred at longer wavelengths (lower energy), than that of the excitation light; this is known as Stokes shift.

In fluorescence microscopy, high energy, short wavelength (for example, UV or blue) light is used to illuminate the sample. This results in the transition of the fluorescent molecules into an excited state. Vibrational energy is lost when the fluorophore returns to the ground state and, as such, lower energy, longer wavelength (eg. green or red) light is emitted. For example, excitation using UV light, invisible to the naked eye, results in the emission of visible blue fluorescence light from a label such as DAPI. This is because vibrational energy is lost when electrons relax from the excited state back to the ground state. This difference in absorption and emission wavelength is known as the ‘Stokes shift’ of a fluorophore and is shown in **Figure 1.15**. If the Stokes shift of a fluorescent molecule is great enough, the excitation and emission light can be effectively separated by a fluorescence microscope.

Fluorescence microscopy is currently one of the most powerful and versatile techniques available for biological studies. Its discovery and utilization has had a

major impact on biological research, enabling researchers to visualize cellular processes with high temporal and spatial resolution. Fluorescence microscopes range from relatively simple widefield (epi-fluorescence) systems to so called super-resolution microscopes offering novel solutions to overcome the diffraction limit of visible light, allowing us to visualise cellular structures in greater detail than ever before.

Fluorophore-labelled molecules can be very bright and readily distinguishable from other background signals making high contrast images easy to obtain. With the development of genetically encoded fluorescent proteins, such as green fluorescent protein (GFP) it has become possible to image protein expression, localisation and activity in living cells (Prendergast and Mann 1978).

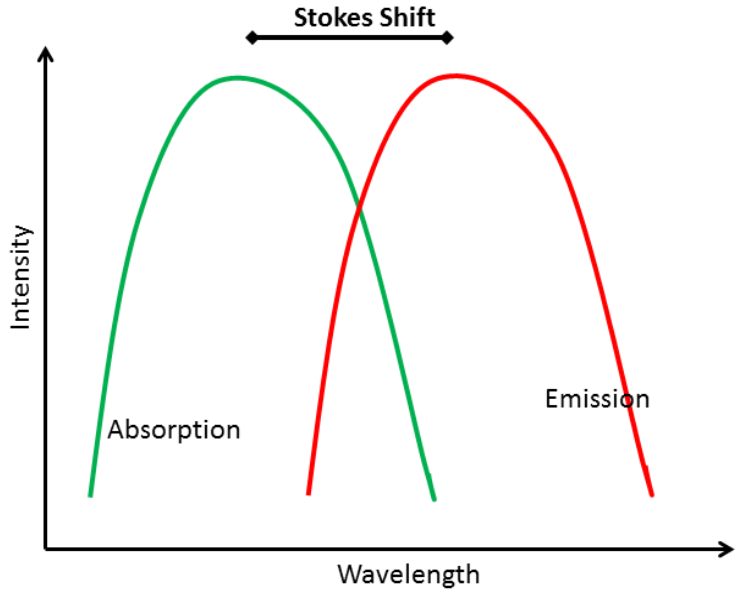

Figure 1.15: Stokes shift. The emission spectrum of a fluorophore is shifted to longer wavelengths when compared to the absorption spectrum as a result of energy loss.

1.5.2 Epifluorescence microscopy

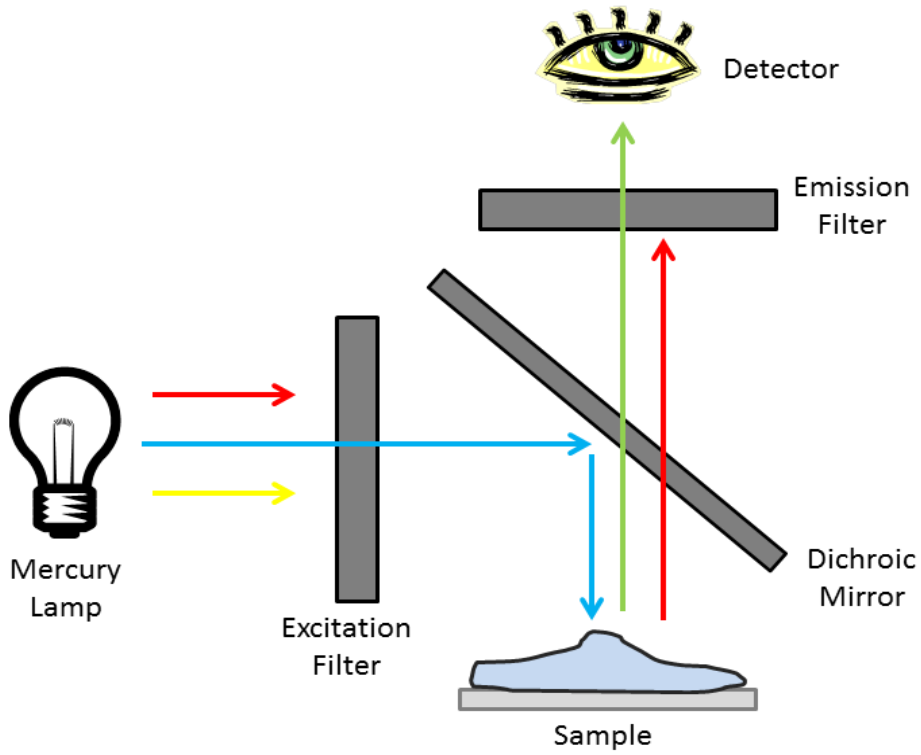

Figure 1.16: Configuration of an epi-fluorescence microscope. The excitation light is filtered to limit excitation light to one colour but is then used to illuminate the entire sample. Emission light of other wavelengths can also be filtered.

In a conventional widefield, or epi-fluorescence microscope, the entire sample is illuminated by the excitation light (e.g. from a mercury or xenon source). The light can then be collected from the whole depth of the sample and viewed by eye or detected by an image capture device (**Figure 1.16**).

The dichroic mirror is used to reflect light shorter than a certain wavelength and allow light of longer wavelengths to pass through, effectively separating the excitation and emission light paths. As the entire sample is illuminated with excitation light, as shown in **Figure 1.17**, this results in the detection of out-of-focus fluorescence emitted by the sample outside of the region of interest, which can lead to high levels

of background fluorescence in the observed image. This can be particularly problematic for specimens with a thickness greater than ~2 µm. Nevertheless, epi-fluorescence microscopy offers an overall view of the fluorescence within the sample and so represents particularly useful tool when wishing to quantify the total fluorescence of individual cells, for example when quantifying the extent to which a fluorescent molecule has been internalised by the cell (Ntziachristos 2006). As the signal-to-noise ratio in epi-fluorescence microscopy is low, a variety of techniques have been developed to reduce contamination by out-of-focus fluorescence and image a single plane of focus within the sample; these are discussed in the following sections.

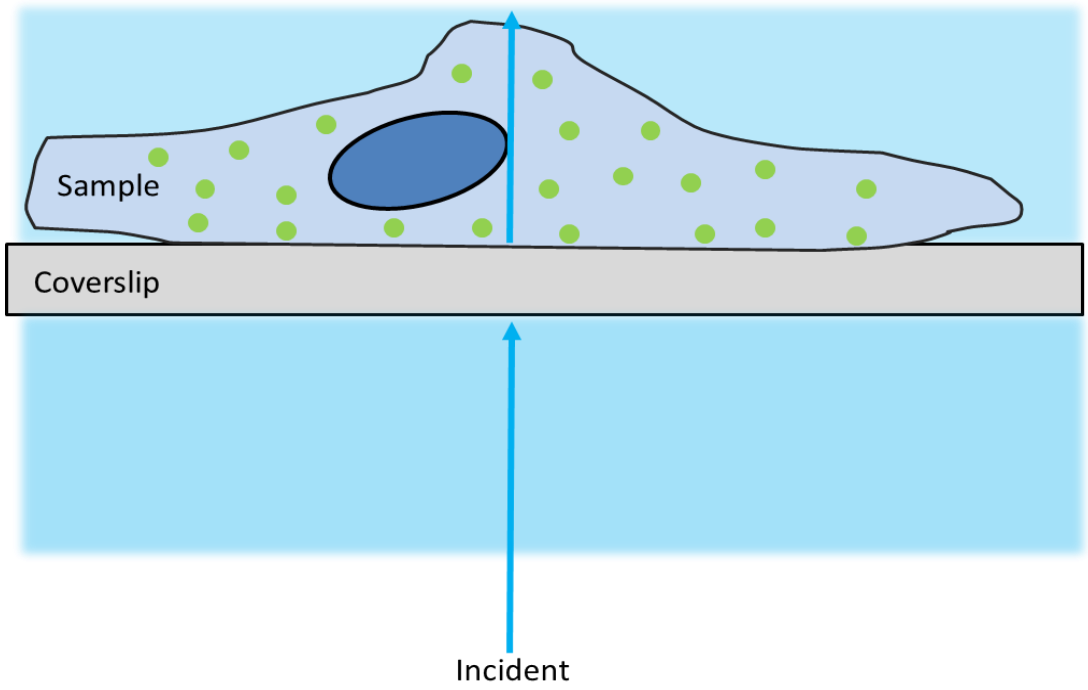

Figure 1.17: Epi-fluorescence microscopy Illumination. Excitation light of a chosen wavelength illuminated the whole sample, resulting in excitation of all fluorescent molecules within the sample.

1.5.3 Total internal reflection fluorescence (TIRF) microscopy

Various techniques are employed in fluorescence microscopy to restrict the fluorescence detected to a thin section of the sample. This is because eliminating out-of-focus fluorescence can dramatically improve signal-to-noise over widefield microscopy. Total internal reflection fluorescence (TIRF) microscopy is predicated on the fact that an induced evanescent wave can excite fluorophores within a small volume (~100 nm) above the coverslip (Mattheyses et al 2010). This is achieved by illuminating the sample at an angle greater than the critical angle (defined by Snell's Law), such that all light, as the name 'total internal reflection' suggests is reflected back without penetrating the sample.

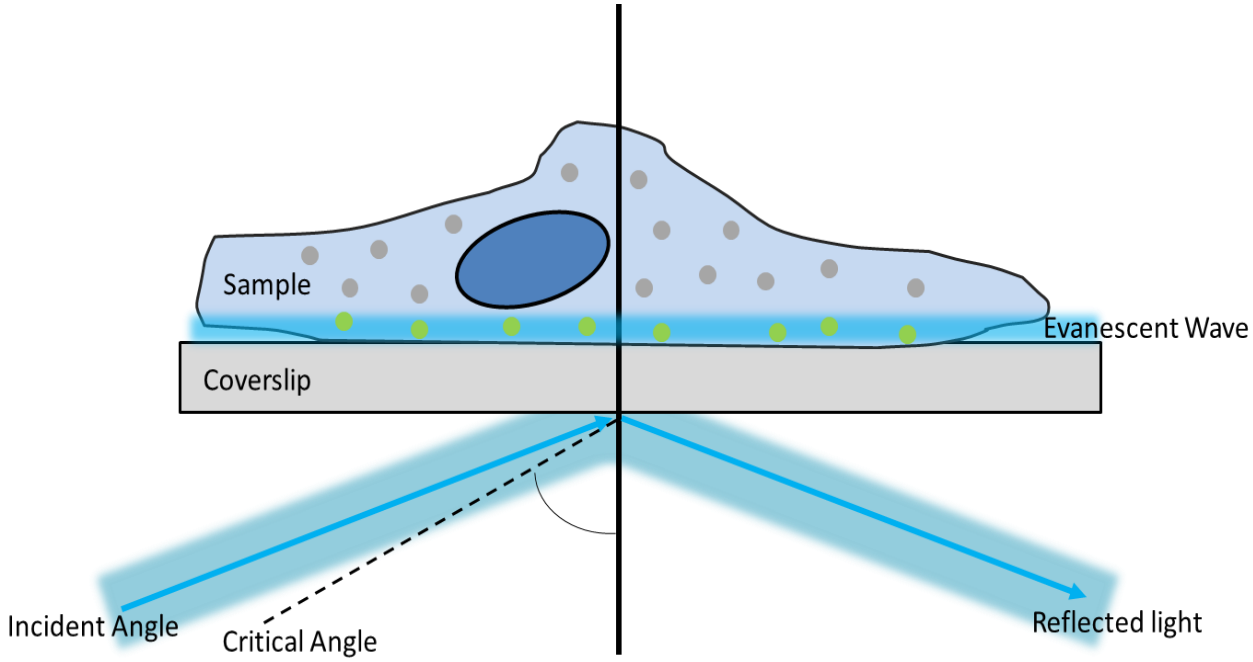

Figure 1.18: **TIRF illumination.** When the sample is illuminated at an angle greater than the critical angle, all of the incident light is reflected. However, an evanescent wave is generated, which decays exponentially with distance from the coverslip, in practice exciting fluorophores within around 100 nm of the coverslip.

Although no light propagates into the sample when it is incident at angles greater than the critical angle, the reflected light generates a highly restricted “standing” electromagnetic wave adjacent to the interface with the coverslip. This evanescent wave decays exponentially in intensity with distance from the coverslip, and as such extends only ~100 nm into the sample, as shown in **Figure 1.18**. Because of the exponential decay in intensity, the excitation of fluorophores is rest ricted to the plasma membrane and the membrane-proximal cytosol of adherent cells. As such, TIRF microscopy is an ideal experimental setup for the visualisation of events taking place in or near to the adherent plasma membrane of cells and has been of key importance to studies of membrane trafficking, endocytosis and exocytosis

(Mattheyses et al 2010).

1.5.4 Confocal microscopy

Confocal microscopy, like TIRF microscopy involves imaging a shallow depth of field by elimination of out-of-focus light. However, confocal microscopy involves imaging user-defined optical sections within the cell and allows for the collection of serial “stacks” of images from different adjacent plane in thick samples (Webb 1996). Whereas in a wide-field (e.g. epi- or TIRF) microscope, the entire field of view is illuminated, , illumination in confocal microscopy is achieved by scanning one or more focused beams of light across the sample. Diffraction-limited laser lines are used to provide the excitation light and mirrors used to scan the lasers across the sample. Light emitted by the fluorescent molecules within the sample passes through the dichroic mirror and the confocal pinhole is used to eliminate out-of-focus light, as shown in **Figure 1.19**. As the focal point of the objective lens forms an image where

the pinhole is, these are known as ‘conjugate points’. The pinhole is **con**jugate to the **focal** point of the lens, hence the term confocal.

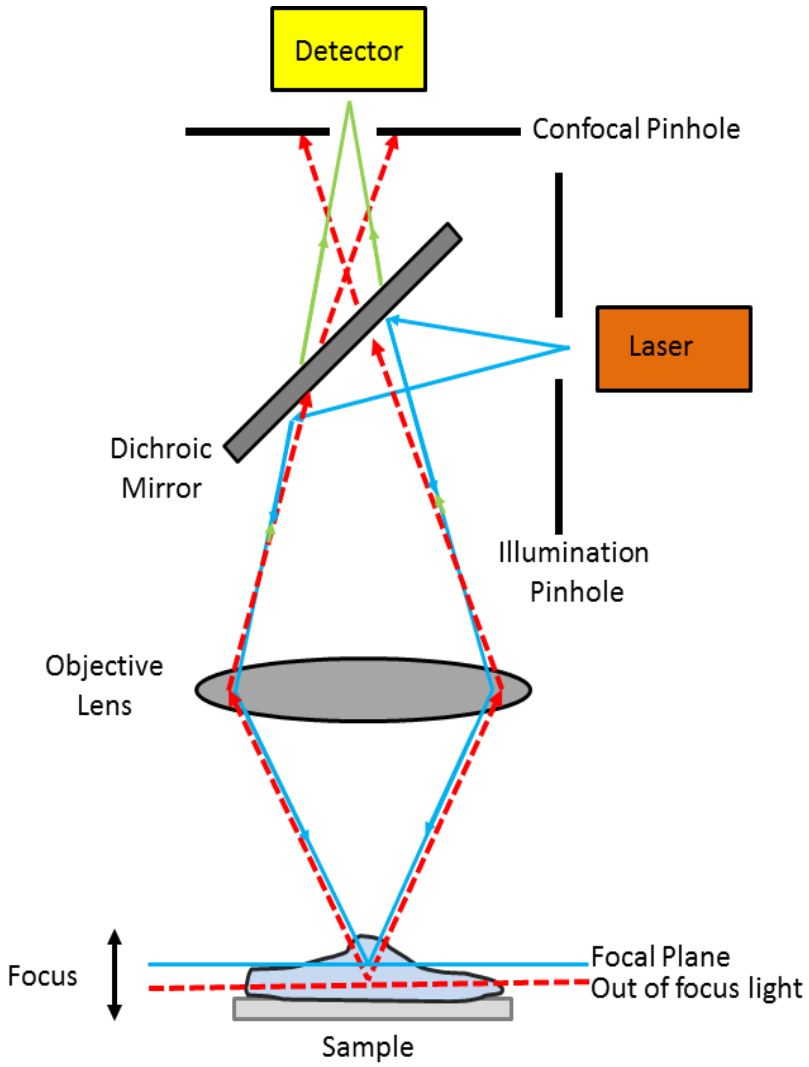

Figure 1.19: Optical configuration of a confocal microscope. A pinhole is used to exclude out-of-focus light, allowing optical sectioning of the sample.

1.5.5 Super-resolution microscopy

Optical microscopes have an inherent limitation in spatial resolution because of the wave nature of light. In light microscopy, resolution is fundamentally limited by the properties of light diffraction which were first described by Ernst Abbe in 1873. This prevents the resolution of structures smaller than approximately half the wavelength of light and as such causes sharp point-like objects to appear blurry under a microscope.

Resolution can be estimated by measuring the full-width at half maximum (FWHM) value of the point-spread function (PSF) which essentially describes how blurry a fluorescent point-like object (such as a fluorescent bead) will appear when it is diffracted through a microscope (Huang et al 2009). Importantly resolution does not refer to the ability of a microscope to detect small structures; rather it denotes the ability to distinguish adjacent objects as separate structures rather than a single object (**Figure 1.20**). However, due to the same limitations the true size of objects smaller than the PSF cannot be readily determined. As many structures in biological samples are smaller and/or closer together than the PSF, images from fluorescent microscopes do not always provide a true representation of the sample being visualised.

Practically speaking, the physical basis for the resolution limit of the light microscope depends on two main factors, the wavelength of light (λ) and the numerical aperture (NA) of the objective lens. Visible light ranges between the ultra-violet (< 400 nm) and the infrared (> 800 nm), and the NA of an objective refers to its light collecting ability. Most commercial objective lenses have a NA around 1, and the practical

upper limit for a NA is approximately 1.5. Thus applying a simplified equation based upon Abbe's work (d = λ / 2 NA), with 500 nm light and an NA of 1, gives d = 250 nm. This equation was later refined by Lord Rayleigh in 1896 to give the Rayleigh criterion, defined as the shortest distance at which two point emitters can be distinguished as separate objects: R = 0.61 λ / NA. The Rayleigh criterion is a commonly used measure of the width of the PSF, and is shown in **Figure 1.20.** Typically, this means that the effect of light diffraction limits the resolution of an optical microscope to approximately half the wavelength of the light used; this is usually around 250 nm laterally and 500 nm axially, and therefore many fine cellular structures cannot be resolved (Huang et al 2009).

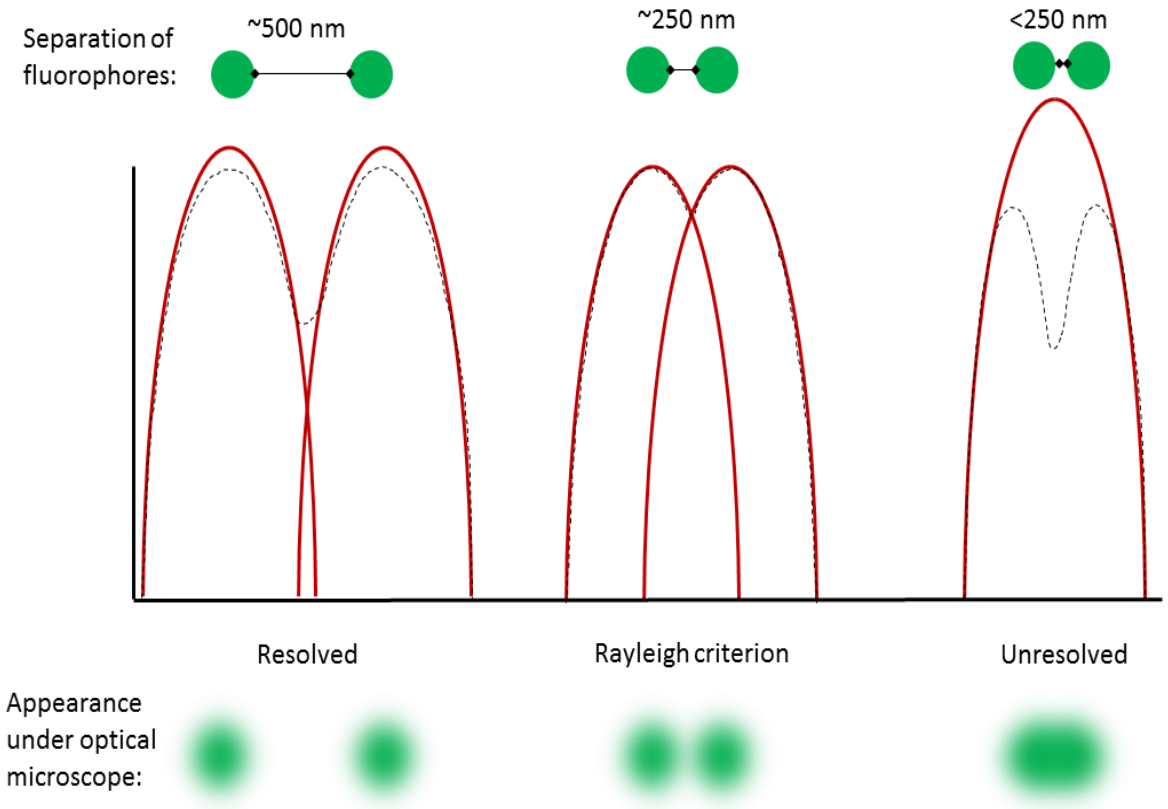

Figure 1.20: The Rayleigh criterion. The Rayleigh criterion is defined as the closest distance between two point sources for them to still be discernible as separate objects under an optical microscope. In practice this is around 250 nm.

As the de Broglie wavelength of an electron is much shorter than visible light, electron microscopy has a much higher resolution than optical microscopy and has long been relied upon to visualise cellular structures smaller and/or closer together than the 250 nm diffraction limit. However, fixation, dehydration and thin sectioning are required during sample preparation for electron microscopy, making it technically challenging, often introducing artefacts and rendering it of no use for live-cell imaging. Therefore microscopic techniques that combine the non-destructive nature of optical microscopy and the nanometer resolution of electron microscopy have been the focus of much research and development in recent years.

Recent advances in fluorescence microscopy have resulted in the development of a series of different “super-resolution” techniques for breaking the diffraction barrier inherent in light microscopy. The diffraction barrier has been broken by creating situations to which Abbe’s law does not apply, such as by switching fluorophores between bright and dark states. Super-resolution microscopy has improved optical resolution from around 250 nm to around 10 nm in the best cases. This super-resolution technology is built around conventional fluorescence microscopes equipped with lasers and sensitive cameras – equipment already in use for wide-field fluorescence imaging.

However, super-resolution microscopes are not based on one single technology, and a number of independently developed super-resolution techniques have been reported. These include structured illumination microscopy (SIM), stimulated emission depletion (STED) microscopy, photoactivation localisation microscopy (PALM) and stochastic optical reconstruction microscopy (STORM). Each of these techniques is not only predicated on a different method for overcoming the diffraction

limit but has inherent advantages and limitations when applied to different biological questions.

1.5.5.1 Single molecule localisation microscopy (SMLM)

Single molecule localization microscopy (SMLM) techniques such as photoactivation localisation microscopy (PALM) and stochastic optical reconstruction microscopy (STORM) differ from all other fluorescence imaging techniques in that an image is built up, as the name suggests, literally molecule-by-molecule.

The SMLM techniques work on the principle that although the ~250 nm limit of resolution in light microscopy prevents the separation of two objects at distances of less than 250 nm, the centres of individual objects can be determined with nanometre precision (Gelles et al 1988, Yildiz et al 2003). As discussed previously, alike objects closer together than the 250 nm diffraction limit of light microscopy cannot be distinguished as separate objects (**Figure 1.19**). However, by inhibiting the fluorescence emission of the majority of the labels at any one time, only single isolated molecules within a PSF are allowed to fluoresce at any one time. By stochastically switching on and off different single isolated molecules in subsequent camera recordings, a final image with sub-diffraction sized spatial resolution is reconstructed from the summation of individual localised spatial positions.

Cells can therefore be imaged at nanometre resolution by determining the exact location of each fluorophore one by one. All SMLM techniques rely on this temporal separation of fluorescence emission, which is be achieved either by switching between a dark and fluorescent state or by consecutive binding of individual fluorophores to the structure. This is achieved by the application of photoconvertible

or photoactivatable dyes and proteins. The emission wavelength of photoconvertible dyes or fluorescent proteins can be optically converted from one wavelength to another or fluorescence can be turned on and off in the case of photoactivatable proteins. This principle has been published by two independent groups who named the technique photoactivation localization microscopy (PALM) and stochastic optical reconstruction microscopy (STORM), respectively (Betzig et al 2006, Rust et al 2006). PALM (and fPALM (Hess et al 2006)) make use of photoactivatable fluorescent proteins to achieve the necessary bright and dark states.

As in each frame only a few fluorophores are visualised, a large number of images is required. Thus, the iterative nature of PALM means that even with a high speed electron multiplier CCD (EM CCD), it can often take several minutes to acquire all the information required to reconstruct a single image. When considering that sub-diffraction limit localisation is the goal of PALM, this introduces a significant potential for artefacts generated by even small amounts of sample drift during acquisition. For this reason, fiducial markers, such as small fluorescent beads, are often added to samples to be imaged by PALM, or other SMLM techniques, and a final image registration algorithm employed during post-acquisition processing.

Many other photoconvertible, photoactivatable, and photoswitchable fluorescent proteins have been developed. Photoactivatable FPs can be activated from a dark state to a bright state using UV light, and photoswitchable FPs such as Dronpa can be cycled between light and dark states with specific illumination wavelengths (Habuchi et al 2005).

Another SMLM method, Stochastic Optical Reconstruction Microscopy (STORM) was developed by Xiaowei Zhuang of the Howard Hughes Medical Institute (HHMI) /

Harvard University (Rust et al 2006). In theory and practice there are many similarities between PALM and STORM, however, STORM uses chemical fluorophores rather than fluorescent proteins. These fluorophores are usually photoswitchable cyanine (Cy) dyes, that are used in pairs, coupled to antibodies that bind the protein of interest. One Cy dye will act as the activator and the other as the reporter. A simplified version of this technique, known as direct STORM (dSTORM) (Heilemann et al 2008) makes use of the intrinsic 'blinking' properties of certain fluorophores, such as AlexaFluor 647, meaning that only one fluorophore is required.In the original version of the STORM technique, pairs of fluorophores are employed which can be switched on and off by the different laser lines employed. Otherwise the iterative nature of the STORM image acquisition process is quite similar to that of PALM and generally speaking microscopes that have been developed for PALM can be used for STORM, and vice versa.

These techniques are often grouped as 'single molecule techniques' and are able to localize molecules with ~20 nm resolution. In both techniques, subsets of fluorophores are switched on with a brief laser pulse, which is so weak that only a few molecules are stochastically switched on at a time, resulting in such a low density of activated molecules that overlap within diffraction limited resolution is unlikely. Imaging of the 'on' fluorophores is performed until all activated molecules are bleached and the process repeated until several hundreds of thousands of molecules are imaged. This process is summarised in **Figure 1.20**. From the positions of all molecules, an image is reconstructed, generating a 10-20 nm super-resolution image.

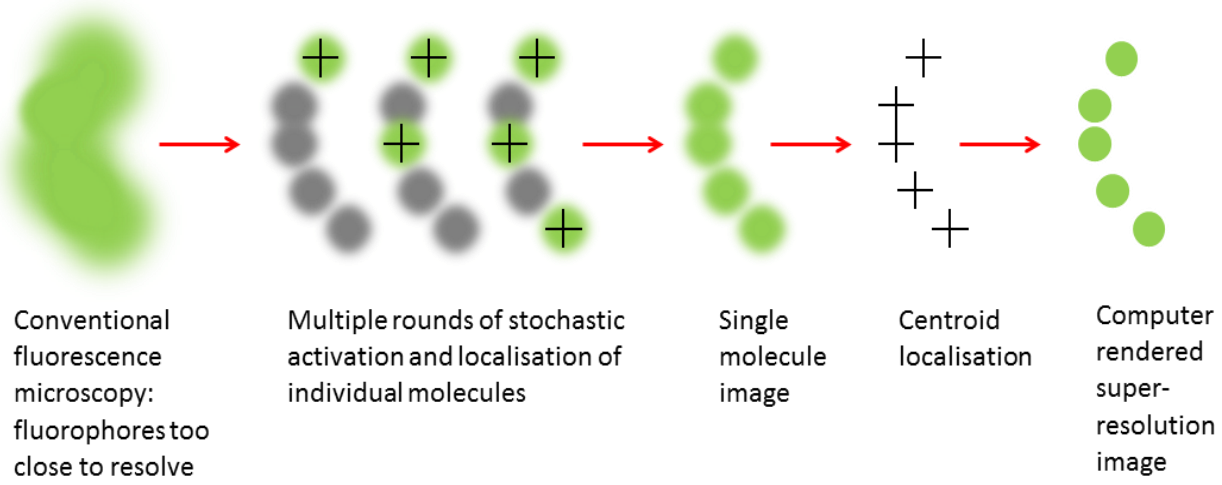

Figure 1.21: Generation of a super-resolution image by SMLM. Fluorescent molecules are stochastically switched on and off in multiple rounds of activation such that no more than one fluorescent molecule within a PSF is allowed to fluoresce at any one time. The centres of these molecules are localised to generate a computer-rendered super-resolution image.

1.5.5.1.1 Benefits and limitations of SMLM

The chemical fluorophores employed in STORM must be linked to proteins of interest post-translationally, usually through indirect methods such as immuno-cytochemistry. This introduces other potential concerns such as those regarding sample preparation, as well as issues such as the distances between the target protein and the fluorophore. Antibodies are nearly 10 nm in length, and considering in indirect immuno-fluorescence a primary antibody specific to the antigen protein of interest and a fluorophore tagged secondary antibody are employed, this can result is a relatively large distance between the fluorophore and target when compared to the compact barrel-shaped structure of most fluorescent proteins (GFP has a diameter of approximately only 4 nm). Thus, even if short peptide linkers are placed between the protein of interest and the fluorescent protein tag, STORM can potentially introduce a significant localisation error. Furthermore, the requirement of

a dual fluorophore probe for conventional STORM adds other technical concerns. However, more recently the technique of direct (dSTORM), which is generally considered to be photochemically equivalent to the phenomenon of Ground State Depletion (GSD), has been gaining prominence. In this case a single fluorophore (usually Alexa-Fluor-647) is shifted between dark and bright states, thus greatly simplifying methodological concerns.

In PALM, a cDNA construct of a chimeric fusion protein directly tagging the protein of interest must be introduced into the cell to be imaged. While fluorescent proteins are generally innocuous tags that do not affect target protein structure, function or localisation, these are potential concerns. In addition, possible over-expression artefacts much be considered, as in conventional microscopy studies.

As no two fluorophores can be in the 'on' state within a PSF at any one time, the speed of image acquisition with the SMLM techniques is limited. This makes live cell imaging with the SMLM techniques extremely challenging, as cells, and the structures within them, are likely to move during the time that is required to acquire a single super-resolution image, leading to blurring.

Additionally, as the SMLM techniques build up images literally molecule-by-molecule, the user must consider how many of these fluorescent molecules are missed or even artificially added during image acquisition. In addition, the user must decide when to stop the acquisition, by judging when a significant proportion of fluorophores are bleached, which can introduce error.

SMLM also faces the problem that if too many fluorescent molecules are missed because a low number of photons are emitted, the resulting image will be incomplete and give an incorrect image of localisation rather than simply generating a low

quality but accurate image. As such, it is not clear if localisation techniques can always be used for accurate protein quantification. In contrast, over-labelling can result in images that are improperly rendered due to the presence of partially overlapping centroids that cannot be resolved. Thus, although extremely powerful, SMLM is not suitable for all applications, and other techniques which are more rapid and/or can be used with all fluorophores have been developed.

1.5.5.1.2 SMLM data processing

As described above, once the series of sparsely populated individual frames has been acquired, techniques such as Gaussian Fitting can be applied to each in series to generate a map of fluorophore centroids, although more recently a significantly faster “wavelet” approach has also been applied (Kechkar et al 2013). Thus, when summed together these individual processed frames can provide a super-resolution image.

SMLM techniques generate images unlike those we are used to seeing as microscopists. Our eyes tend to look for patterns and to focus on the largest and brightest structures in a microscopic image. However, STORM and PALM images are generated mathematically, and the size and brightness of the ‘dots’ in the image represent user-selected parameters. There are currently two mathematical approaches to describe the distribution of molecules in two dimensions: Ripley’s K function analysis compares the actual distribution relative to a random distribution and assigns a degree of ‘non-randomness’ to each molecule to create a cluster map (Hsu and Baumgart 2011) whereas pair-correlation analysis determines the probability of finding a molecule at a given distance from another molecule compared

with the probability expected from a random distribution of molecules (Sengupta at al 2013).

1.5.5.2 Structured illumination microscopy (SIM)

Developed collaboratively between the laboratories of John Sedat at UCSF and the late Mats Gustafsson at HHMI Janelia Farms, Structured Illumination Microscopy (SIM) also relies upon computational approaches to generate a super-resolution image from a series of acquisitions. However, as the name suggests, rather than relying upon fluorophore effects, SIM utilises a structured pattern of illumination light for excitation of the whole field (Gustafsson 2000). When a high spatial frequency pattern is projected onto a sample, this generates an interference pattern known as a moiré fringe, which is simply an interference pattern created by overlaying two grids with different angles or mesh sizes (shown in **Figure 1.22**).

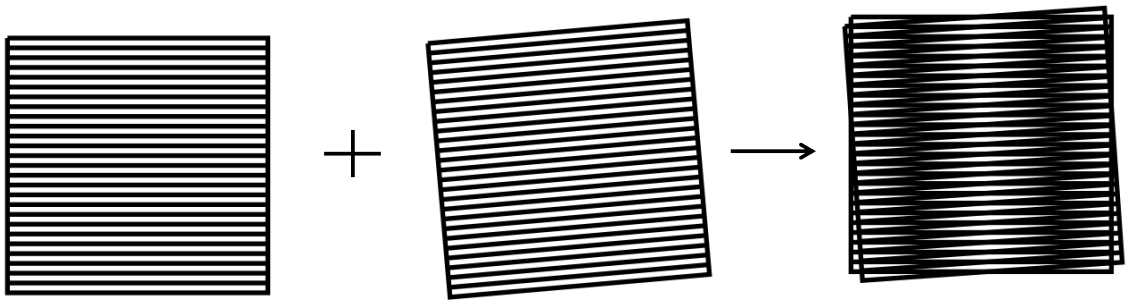

Figure 1.22: Generation of Moiré fringes. The overlay of two grids results in a Moiré pattern, from which structural information can be calculated, this effect is exploited by SIM super-resolution techniques.

If the pattern is moved across the specimen, a characteristic signal variation in the fluorescence response can be observed as a function of time and grid position. If one of the patterns is an unknown structure (the molecules in the sample being

imaged) and the other pattern is a known pattern (the grid), the moiré fringes that are generated by overlapping the two patterns will contain more information about the unknown structure than the original pattern, thus offering an improvement in spatial resolution. Multiple grid positions and rotations are required to produce several images of the same sample that have different moiré patterns (Gustafsson 2000). As the illumination pattern is a known entity, it can be mathematically removed from the moiré pattern to generate the final super-resolution image.

1.5.5.2.1 SIM data processing

To produce a super-resolution image from the generated moiré fringes, the signal variations between frames must be analysed using a Fourier transform–based algorithm (Gustafsson 2000). This algorithm requires that there are high contrast elements in the images acquired, meaning that significant levels of out-of-focus fluorescence can result in a lack of high contrast data from which to reconstruct a true super-resolution image. This issue depends on the thickness of the sample being imaged and the localisation of the molecules within the sample. However, this can represent a particular problem for over-expressed proteins tagged with fluorescent proteins such as GFP, where high levels of out of focus light are often observed.

This effect can be minimised through the utilisation of illumination via total internal reflection fluorescence (TIRF) microscopy (Mattheyses et al 2010). SMLM can also utilise TIRF illumination, and the flexibility of either TIRF or epi illumination is one of the shared benefits of these two techniques. However, in the case of SIM, if the target protein is not with 200 nm of the coverslip and is surrounded above and below

by fluorophores, proper reconstitution of a super-resolution image can be difficult to achieve.

Once generated, the super-resolution nature of a SIM image can be directly validated by visualisation of the Fourier transform. Whereas a the Fourier transform generated from a diffraction-limited image will be visualised as a circular shape, the Fourier transform of a SIM image will contain additional lobes from the extra information gained from the different grid positions and rotations used. For example, the visualisation of a Fourier transform of a SIM image generated using three grid positions and three rotations, will contain 6 lobes surrounding the central one.

Thus, while artefacts can be difficult to discern in SMLM, in SIM there are clear quantitative criteria that can be employed to determine if reconstruction was successful. However, most commercial SIM and SMLM systems provide the ability to acquire corresponding conventional non-super-resolution images which can permit direct comparisons and serve as a guide to validate that the reconstructions generated reasonable localisations.

1.5.5.2.2 Benefits and limitations of SIM

SIM is arguably one of the most user-friendly of the super-resolution techniques, particularly in terms of sample preparation, as any label used in conventional fluorescence microscopy can be applied to the technique. In addition, conventional excitation routines are applied resulting in less photobleaching than some of the other techniques (although multiple images of the same sample must be acquired to generate a super-resolution image). SIM is typically a wide-field approach, meaning that fast CCD cameras can be used. However, the imaging rate is usually slower

than conventional microscopy because of the need to acquire several images in order to generate one final image.

SIM allows resolutions of around 100 nm in *x*,*y*, and *z* when biological material is used (Schermelleh et al 2008), and as such is the least powerful super-resolution technique regarding gained resolution over conventional fluorescence microscopy. This is because, unfortunately, the spatial frequencies that can be created optically in SIM are also themselves limited by diffraction. As such SIM is limited to this factor-of-two improvement as it is still limited by the PSF of conventional microscopy (Gustafsson, 2000).

1.5.5.3 Super-resolution techniques: A comparison

Relative benefits and limitations exist within the different super-resolution microscopy techniques available (**Table 1.1**). While SMLM provides the highest spatial resolution, it also takes the longest time to acquire the necessary data, is conducted in fixed cells, and is only compatible with certain fluorophores. SIM can be used with any fluorophore and is relatively rapid, making it useful for live-cell imaging studies, but does not provide the same resolution gains as SMLM. Furthermore, SIM can be difficult to perform successfully with certain types of samples. SMLM and SIM share the benefits of being wide-field techniques compatible with both epi and TIRF illumination, but also share the limitation that image reconstruction via application of computational algorithms is required. As in some deconvolution techniques, direct image acquisition is not possible, creating a concern for potential artefacts that cannot easily be discerned.

Therefore, among the commercially available super-resolution solutions no single technique can be said to be optimal for all applications. Depending upon the specific questions being addressed and the constraints of the experimental system, the user will must decide which is best.

Modality	Resolution	Illumination	Probes	Acquisition Time	Post-Acquisition Processing	Data Size	Other Concerns
Standard fluorescence microscopy	250 nm	Epi/TIRF/ confocal	Conventional fluorescent probes				
SIM	100 nm	Wide-field (epi/TIRF)	Conventional fluorescent probes	Short (seconds)	Yes (Fourier transforms)	Small (9-15 frames)	Out of focus signal and sample thickness
PALM/fPALM	10-55 nm	Wide-field (epi/TIRF)	Photo-activatable fluorescent proteins (e.g. PA-GFP)	Long (minutes)	Yes (centroid identification)	Large (many frames)	Over/under labelling artefacts
STORM/ dSTORM	10-55 nm	Wide-field (epi/TIRF)	Photoswitchable dyes (e.g Cy3/5) Blinking fluorophores (e.g. Alexaflour-647)	Long (minutes)	Yes (centroid identification)	Large (many frames)	Over/under labelling artefacts

Table 1.1: The relative benefits and limitations of super-resolution microscopy techniques when compared to conventional fluorescence microscopy.

CHAPTER 2

MATERIALS AND METHODS

2.1 Plasmid constructs

Table 2.1: DNA constructs

Constructs were purchased from, or kindly donated by:

Plasmid	Source
Clathrin-dsRed (rat light chain a)	Prof. Thomas Kirchausen, Harvard Medical School, Boston, USA.
GFP-Clathrin	Dr Alex Benmerah, Institute Cochin, Paris, France.
pEGFP-N1	Clontech, BD Biosciences Clontech, Palo Alto, USA.
pECFP-Mem	Clontech, BD Biosciences Clontech, Palo Alto, USA.
GFP-Occludin	Prof. Tianyi Wang, Department of Infectious Diseases and Microbiology, University of Pittsburgh, USA.
AcGFP-CD81	McKeating Lab, University of Birmingham, UK.
EGFP-EGFR	Alexander Sorkin, University of Colorado Health Sciences Centre, USA.

2.2 Bacterial transformation

1 µg of the required cDNA construct (**Table 2.1**) was added to 50 µl MAX Efficiency DH5α Competent Cells (Invitrogen) on ice for 30 minutes. The MAX Efficiency DH5α cells were heat-shocked at 42ºC for 45 seconds and returned to ice for 2 minutes. 500 µl of Luria Broth (LB; **SM 1**) (Sigma) was then added, and the cells were incubated at 37ºC with agitation for 1.5 hours. 125 µl of bacterial mix was spread onto an LB agar (Sigma) 13 cm plate (**SM 2**) containing either kanamycin or ampicillin (depending on the bacterial antibiotic resistance gene encoded) using a flaming loop. Inverted plates were incubated overnight at 37ºC. For each plate, 2 well-separated colonies were picked with a pipette tip and added to 2 ml LB broth containing kanamycin (50 µg/ml) or ampicillin (100 µg/ml) in 14 ml dual -position snap cap round bottomed tubes (Falcon) and incubated at 37ºC for 6 -8 hours with agitation. 200 µl of this bacterial mix was added to 100 ml antibiotic-containing LB broth in a conical flask and incubated 37ºC for 8 hours with agitation. The flask contents were then centrifuged centrifuged at 5000 rpm at 4ºC in 50ml plastic centrifuge tubes (Falcon) using a Heraeus Labofuge 400R centrifuge (Thermo Scientific). The resulting pellets were then lysed immediately for purification with a Qiagen Plasmid Maxi Kit (Qiagen) following manufacturer's instructions. Purified DNA was dissolved in 1 ml ultrapure water and stored at -20ºC. DNA concentration was measured using a U1800 model spectrophotometer (Digilab Hitachi) prior to carrying out transfections.

2.3 Cell culture

Huh6, Huh7.5, HeLa, HepG2, 293T and CHO cells were all cultured in Dulbecco's Modified Eagle's Medium (DMEM; Lonza) with 10% FCS and 1% penicillin/streptomycin (Invitrogen) (**SM 3**). Parental SKHep1 cells were cultured in RPMI 1640 media (Gibco, Invitrogen) with 10% FCS, 1% penicillin/streptomycin. SKHep1 (SRBI+CLDN1) were cultured in RPMI 1640 media (Gibco, Invitrogen) with 10% FCS, 1% penicillin/streptomycin and under double selection with 100 µg/ml hygromycin and 700 µg/ml G418 (both Gibco, Invitrogen). HepG2-

CD81 cells were cultured in DMEM (Lonza) with 10% FCS and 1% penicillin/streptomycin under selection with zeocin (Gibco, Invitrogen). Primary human hepatocytes were a kind gift from Dr Ragai Mitry, Kings College London, UK to Garrick Wilson (McKeating lab), and were grown in Williams E growth medium. All cells were grown at 37°C with 5% CO_2.

2.4 Endocytosis assays (Tf, LDL and CTB uptake)

Cells were plated onto glass coverslips 24 hours before carrying out endocytosis assays and were 70-90% confluent when assays were carried out. Cells were pre-incubated with serum-free media (SFM) for 10 minutes at 37°C and 5% CO_2 before incubation with 1 µg/ml Alexafluor555-labelled cholera toxin B subunit (CTB-555; Invitrogen), Alexafluor-568-labelled transferrin (1:500 dilution; Invitrogen), or DiI-LDL (1:50 dilution; Invitrogen) for 5 minutes at 37°C and 5% CO_2 (unless otherwise stated). CTB-555 treated cells were then washed with room temperature SFM, and LDL and Tf-treated cells with Dulbecco's phosphate buffered saline solution (DPBS; Lonza) at pH5.5 and fixed with 4% paraformaldehyde (PFA; electron microscopy sciences) for 5 minutes at room temperature. Coverslips were mounted onto glass slides using ProLong Gold antifade reagent (Molecular probes, Invitrogen) and imaged 24 hours later. Slides were imaged using a Nikon TE300 epifluorescence microscope (Nikon) with a 60x oil immersion objective and data analysed using ImageJ 1.42q software (National Institute of Health). A student's T-test was performed to determine statistical significance.

2.5 Image analysis using Image J Software

Epifluorescence images were analysed using ImageJ 1.42q software (National Institute of Health). Per experiment 30 cells per treatment or control were circled using the 'bezier ROI' tool) and fluorescence intensity measured for each cell. Background fluorescence was subtracted by drawing a similar sized ROI in a cell-free area of the image. An average

fluorescence intensity for each treatment calculated. Results shown are the average of three repeats. A student's T-test was performed to determine statistical significance.

2.6 Preparation of cell lysates

Two confluent wells of a 6-well plate for each condition were lysed in ice cold Triton X-100 lysis buffer (**SM 5**) with added complete mini protease inhibitor cocktail tablet (Roche). Cell lysates were kept on ice for 15 minutes with vortexing every 5 minutes before clarifying by centrifugation for 15 minutes at 4°C and 14000 rpm in a bench top centrifuge (Eppendorf 5471R). Protein was quantified using the BioRad protein assay (BioRad), according to the manufacturer's instructions (**section 2.7**).

2.7 Bradford protein quantification assay

Bovine Serum Albumin (BSA) Standards were made by serial dilutions in distilled H_2O, giving BSA solutions at 25 µg/ml, 20 µg/ml, 15 µg/ml, 10 µg/ml, 5 µg/ml and 2.5 µg/ml. Bradford reagent was diluted 1:5 in distilled H_2O and 1 ml added to 10 µl of each BSA standard. Absorption at 595 nm was measured in a PU 8720 UV/Vis scanning spectrophotometer (Philips) and a standard curve of BSA concentration versus absoprtion plotted. Distilled H_2O was used as the blank control. 1 ml of diluted Bradford reagent was then added to 2 µl of cell lysate and absorption at 595 nm measured as above. Protein concentration could then be read of the standard curve.

2.8 Western blot (WB)

Western bots were performed using the Mini-Protean Tetra Electrophoresis System (BioRad). Protein lysates (35 µg) were boiled for 5 minutes in an equal volume of 3x running buffer (**SM 6**) and then separated on a 12% SDS PAGE gel (**SM9**). To each gel, 10 µl

PageRuler Plus Prestained Protein Ladder (Fermentas), was run in one lane. The gels were run at 220V for 45 minutes using a PowerPac Basic Power Supply (BioRad) in running buffer (**SM 7**). Protein was then transferred to 0.5µm Immobilon-P PVDF membrane (Millipore) in a Mini Trans-Blot Cell (BioRad) filled with transfer buffer (**SM 8**) at 4°C for 1 hour at 400 mA. The membrane was blocked for 1 hour using 5% Marvel in TBST (**SM 10**). The membrane was then incubated with primary antibody, dilutions as in table **SM table 1** in blocking solution (**SM 11**) overnight at 4°C with agitation. Primary antibody was removed by 5 10 minute washes with 20 ml TBST (**SM 9**). The membrane was probed with secondary antibody (horseradish peroxidise-conjugated donkey anti-rabbit IgG, unless otherwise stated; **SM table 2**) in blocking solution at a dilution of 1:10,000 for 1 hour at room temperature, with agitation. Protein was detected by enhanced chemiluminescence (ECL). Detection reagents 1 and 2 from ECL Western Blotting Substrate Kit (Pierce) were mixed in a 1:1 ratio, making up a total volume of 1 ml per membrane. The membrane was then incubated in ECL reagent for 60 s. The membranes were then inserted into a developing cassette; X Ray film (Scientific Laboratory Supplies) was inserted into the developing cassette and exposed to the membranes for between 10 s and 5 minutes. Exposed films were developed using a CURIX 60 XoGraph machine (AGFA).

.

2.9 Immunoprecipitation (IP)

Immunoprecipitation was carried out using rabbit polyclonal α-caveolin 1 (BD Transduction Labs) and rabbit IgG bound to protein G-sepharose beads (Sigma). Antibody coupling to G-sepharose beads was achieved by mixing 750 µl Triton X-100 lysis buffer (**SM 5**), 50 µl Protein G sepharose (50% slurry in PBS) and 2.5 µg antibody and rotating overnight at 4°C. Cell lysates were pre-cleared by adding to 20 µl protein G sepharose (50% slurry in PBS), vortexing briefly and rotating at 4°C for 30 minutes. Antibody-coupled beads were washed three times with Triton X-100 lysis buffer, vortexing for 10 s and centrifuging at 4°C at 5000

rpm for 20 s in a bench top centrifuge (5471R, eppendorf). Dry beads were then placed on ice. Cell lysates were centrifuged at maximum speed at 4°C for 1 minute to pellet the protein G sepharose. Supernatant was then added to the antibody-coupled beads, vortexed briefly and then rotated at 4°C for 90 minutes. Beads were washed four times in ice-cold Triton X-100 lysis buffer. For each wash, tubes were kept on ice, vortexing for 10 s and centrifuging at 4°C at 5000 rpm for 20 s. For the final wash, beads were transferred to new tubes to prevent protein sticking to the sides resulting in non-specific bands. Samples were eluted into 50 µl non-reducing sample buffer (**SM 6**) and stored at -20°C. Samples were boiled for 5 min and then separated on a 12% SDS PAGE gel, before western blotting for caveolin 1, as described above.

2.10 Flow cytometry

Following CTB uptake, cells were trypisined and fixed in solution with 4% PFA (electron microscopy sciences) for 5 minutes, washed with Dulbecco's phosphate buffered saline solution (DPBS) (Lonza) and then resuspended in DPBS for analysis. Flow cytometry was carried out using a BD FACScalibur flow cytometer (Becton Dickinson) and analysed using CellQuest Pro software (Tree Star, OR, USA). Appropriate unstained controls were used.

2.11 Transient DNA transfection

Cells were transfected with 4 µg DNA (**table 2.1**) and 20 µl lipofectamine 2000 transfection reagent (Invitrogen) per well of a 6-well plate, according to the manufacturer's instructions. Cells were transfected 24 hours following plating, and at 70-90% confluency. To transfect two wells of a 6-well cell culture plate, 8µg DNA was added to 500 µl serum-free cell culture media (SFM; Lonza) and 40 µl lipofectamine 2000 added to another 500 µl SFM in a separate 1.5 ml tube (eppendorf) and incubated for 5 minutes at room temperature. The DNA/SFM mix was then added to the lipofectamine 2000/SFM mix and incubated for 15

minutes at room temperature. 500 µl transfection mix was then added to each well by pipetting in a drop-wise manner. Media was changed to DMEM + 10% FCS 2 hours post-transfection.

2.12 siRNA transfection

Based upon preliminary studies and previously published work (Motley et al 2003) two rounds of transfection are usually necessary to silence expression of AP2 and caveolin 1, as they are relatively stable proteins. For transfection of one confluent well of a 6-well plate, 5 µl Lipofectamine RNAiMAX transfection reagent and 30 pmol siRNA is needed. AP2 custom siRNA (Dharmacon) and a caveolin 1 SMARTpool (dharmacon) were used (sequences in **SM 16**). A non-silencing control (ON-TARGETplus Non-trageting siRNA; Dharmacon) was used in parallel to all knockdowns. For transfection of 1 well of a 6-well plate, transfection reagent is added to 250 µl of serum-free media (SFM), and in a separate tube, siRNA is added to another 250 µl SFM. Following 5 minutes incubation at room temperature, the transfection reagent and SFM are added to the siRNA, mixed and incubated at room temperature for 15 minutes. Transfection mix is then added drop-wise to cells. The two rounds of transfection are carried out as follows: On day 1, cells are plated in a 6-well cell-culture plate to be 80-90% confluent 24 hours later. On day 2, the first round of transfection is carried out, as described above. On day 3, each well of a 6-well plate of transfected cells is split 1:2 into 2 wells of a 6-well cell culture plate. On day 4, the second round of transfection is carried out, as described above. On day 5, cells are split for lysis on day 6, or plated onto coverslips for endocytosis assays to be carried out on day 6.

2.13 Generation of HCVpp

293-T cells were plated at a density of $8x10^5$ cells per well in a 6-well cell culture plate, pre-coated with poly-L-Lysine, such that cells were 60-80% confluent 24 hours later. 24 hours

following plating, cells were transfected with virus DNA as follows: 1 hour before transfection, cell culture media was changed to DMEM containing 3% FCS with no antibiotics. For transfection of 1 well of a 6-well cell culture plate, 1.6 µg of DNA, 6 µl Fugene transfection reagent, and 100 µl Optimem serum-free media were used. The transfection mix was generated by adding the required amount of DNA to 10 µl sterile distilled water (DNAse and RNAse free). In a separate tube, 6 µl of Fugene was added to 100 µl Optimem and incubated at room temperature for 5 min. The Fugene-Optimem mix was then added to the diluted DNA, mixed and incubated at room temperature for 20 min before pipetting drop-wise onto cells. Cells were then incubated at 37°C and 5% CO_2 for 6 hours. The transfection mixture was then removed from cells and replaced with fresh media containing 3% FCS. Cells were then incubated for 72 hours at 37°C and 5% CO_2. The supernatant was then removed and clarified at 3000 rpm for 5 minutes in a bench top centrifuge (5471R, eppendorf) before storage at -80°C prior to use.

2.14 HCVpp infection assay

Target cells (SkHep1 SRBI+CLDN1 or Huh7.5) were plated at a density of $1x10^4$ cells per well in a flat bottomed 96-well cell culture plate 24 hours before infection. HCVpp and No env control particles were diluted at 1:2 in 3% media, and VSV-Gpp and MLVpp were both added at a dilution of 1:500 in 3% media. Cells were incubated at 37°C and 5% CO_2 for 8 hours. Virus was then removed, cells rinsed in 3% media, and incubated in fresh 3% media for 72 hours before carrying out a luciferase reporter assay to measure infection. Media was removed from wells and cells were lysed in Cell culture lysis buffer (Promega), 40 µl per well, incubated at 4°C for 15 min and analysed for luciferase activity using luciferase detection system (Promega E1501).

2.15 Treatment with small molecule inhibitors

Cells were plated onto glass coverslips in a 24-well cell culture plate 24 hours before carrying out endocytosis assays and were 70-90% confluent when assays were carried out. Cells were pre-incubated with 80 µM Dynasore (Sigma) in serum-free media (DMEM or RPMI) for 10 minutes at 37°C and 5% CO_2, prior to carrying out endocytosis assays, as described above. Dynasore is present throughout the endocytosis assay. As Dynsore is made up in DMSO, control wells are incubated in the corresponding volume of DMSO.

Chlorpromazine (Sigma) was added to cells in SFM at a concentration of 1 µM for 30 minutes prior to carrying out endocytosis assays as described previously and remained present throughout the endocytosis assays.

Lt-LacCer (caveolar inhibitor) and De-LacCer (inactive control) were added to cells at a concentration of 10 µM in SFM 30 minutes prior to carrying out endocytosis assays and remained present throughout endocytosis assays.

2.16 EGF stimulation of Huh7.5 cells

Huh7.5 cells were plated in glass-bottomed cell culture dishes and transfected with the indicated cDNA constructs 24 hours later. 24 hours following transfection, cells were serum starved for 10 minutes at 37°C and 5% CO_2. EGF (Bachem) was then added at 1 µg/ml unless otherwise stated for 10 minutes unless otherwise stated. In live cell imaging studies, cells were incubated in serum-free cell imaging media (CIM; **SM 12**) for 10 minutes while cells were selected and EGF added to the dish on the microscope immediately prior to beginning the live cell timelapse image acquisition. In this case 20 µl of 100 µg/ml EGF was added to a final volume of 2 ml CIM.

2.17 Live-cell confocal microscopy

Huh7.5 cells were plated into glass-bottom cell culture dishes (MatTek corp) 24-hours before transfection with constructs listed in table 2.1 using Lipofectamine 2000 transfection reagent (Invitrogen) as described previously. Cells were imaged in CIM 24 hours after transfection using a 60x oil immersion objective on a Nikon A1 confocal system (Nikon). The microscope stage was maintained at 37°C by an Okolab incubation chamber (Okolab). Images were taken every 1 minute for 60 minutes following the addition of EGF. Excitation of GFP-tagged constructs was achieved with the 488 nm line of an Argon Ion laser 457-514 nm, and excitation of pECFP-mem was achieved using a Violet Diode laser 400-405 nm. Images were acquired with a 12-bit CCD camera (Ixon 1M EMCCD camera) controlled by NIS-Elements AR version 3.2 software (Nikon).

2.18 TIRF microscopy

Huh7.5 cells were plated in glass-bottom dishes (MatTek Corp) 24-hours before transfection with clathrin-dsRed and EGFR-GFP (**table 2.1**) using Lipofectamine 2000 transfection reagent (Invitrogen) as described previously. Cells were imaged 48 hours after transfection using a Nikon A1R TIRF/confocal system (Nikon), with illumination through a 60x TIRF objective (CFL Plan Apo 60x NA 1.49, Nikon).

Single images were captured in each colour at time 0 and after 30 minutes following the addition of EGF (Bachem).

2.19 Immunocytochemistry (IC)

Huh7.5 cells were plated into glass-bottomed cell culture dishes (MatTek) and transfected 24 hours later as described in **section 2.11**. Cells were treated with EGF or PBS (control) as described in section 2.18. Cells were then washed 3 times in 2 ml

DPBS and fixed with 4% PFA for 5 minutes at room temperature. Cells were then permeabilised for 5 minutes in 2 ml permeabilisation buffer (0.1% Triton X-100) and permeabilisation buffer removed with 3 washes with 2 ml DPBS at room temperature. Cells were then incubated in BSA-GS block buffer (**SM 13**) for one hour.

Primary antibodies were diluted as stated in S.M.30 in GS -BSA block buffer and 100 µl added to the coverslip. The coverslips were incubated in a humidity chamber at room temperature in the dark for 1 hour. Primary antibodies were removed with 3 washes with DPBS at room temperature. Secondary antibodies were diluted as stated in **SM 30** in GS-BSA block buffer and 100 µl added to the coverslips for 1 hour at room temperature in a humidity chamber. Cells were then washed 3 times with 2 ml DPBS at room temperature.

2.20 Structured illumination microscopy (SIM)

Huh7.5 cells fixed and stained for CD81 by IC with and without EGF stimulation were imaged by single-colour 3D SIM at the Nikon Imaging Centre, King's College London (NIC@King's). Cells were imaged using a Ti-E inverted N-SIM super-resolution system (Nikon) through a 100x 1.49 NA oil immersion objective using an Andor Ixon camera (Andor). Images were visualised and reconstructed using NIS Elements AR with n-SIM module (Nikon).

2.21 Stochastic optical reconstruction microscopy (STORM)

Huh7.5 cells fixed and stained for CD81 by IC, using alexaflour-647 labelled secondary antibodies were imaged by dSTORM at the Nikon Imaging Centre, King's College London (NIC@King's). Cells were imaged using a Ti-E inverted N-STORM super-resolution system (Nikon), through a 100x 1.49NA oil immersion objective using an Andor Ixon camera

(Andor). Images were visualised and reconstructed using NIS Elements AR with n-STORM module (Nikon).

2.22 Analysis of SIM data (and clathrin spot data)

Images were analysed by Jeremy Pike (PSIBS doctoral training centre, University of Birmingham). A bandpass filter was used to remove noise from the images. To segment the cell boundaries in the SIM images, images were blurred using bandpass and Gaussian filtering and the resulting images thresholded to define the cell outline. Otsu thresholding with a watershed step was used to segment connected fluorescent spots.

2.23 Statistical Analyses

Data shown are the means from three independent experiments, unless otherwise indicated. Error bars represent standard error. Statistical significance was determined by Student's T-tests in all cases except where indicated. * $p<0.05$, ** $p<0.001$, *** $p<0.0001$.

CHAPTER 3

RESULTS

INVESTIGATING A ROLE FOR CAVEOLIN 1 IN HCV ENTRY

3.1 Introduction

While several studies have demonstrated that HCV can enter hepatoma cell lines in a clathrin-dependent manner, none of these studies have ruled out entry by clathrin-independent mechanisms (Blanchard et al 2006, Codran et al 2006, Coller et al 2009). In particular, any role for caveolae in HCV infection has been overlooked due to a long-standing belief that the hepatoma cell lines used to study HCV infection do not express caveolin 1, and therefore cannot form functional caveolae.

In contrast, caveolin 1 is known to be expressed in hepatocytes in the liver, where it is thought to play important roles in liver regeneration and lipid metabolism (Fernández et al 2006, Mayoral et al 2010, Fernández-Rojo et al 2013). Expression of caveolin 1 in hepatocytes is however, relatively low, and it has been reported to reside predominantly at intracellular locations rather than at the plasma membrane (Mayoral et al 2010, Woudenberg et al 2010).

The assumption then is that if HCV is able to enter and infect hepatoma cell lines which do not express caveolin 1 then this pathway plays no functional role in infection *in vivo*, even if hepatocytes in the liver express caveolin 1. However, there is evidence both for and against the presence of caveolae in hepatoma cell lines throughout the literature. Among the most convincing pieces of evidence for the presence of caveolae in hepatoma cell lines are electron micrographs (for example, **Figure 1.13**) of HepG2 cells, showing flask-shaped invaginations typical of caveolar endocytosis (Botos et al, 2007). HepG2 cells are able to develop the complex polarity exhibited by hepatocytes within the liver, and are as such, often considered to be the most physiological cell line of hepatic origin.

the pathway as an additional entry mechanism, or one which promotes infection in depolarised/non-polarised cells where caveolin 1 relocalises to the plasma membrane (Meyer et al 2013). If functional caveolae or related pathways exist in primary hepatocytes *in vivo*, this could represent a potential route for productive infection.

In order to fully assess the role that different endocytic mechanisms play in viral entry, expression of caveolin 1 in HCV-permissive cell lines must be determined and the effect of perturbation of this pathway on HCV entry and infection measured in a caveolin 1-positive, HCV-permissive cell model. This has not been done to date.

3.2 Chapter aims

While caveolin 1 is thought to be expressed by hepatocytes within the liver, the existence of a caveolar pathway in the hepatoma cell lines used to study HCV entry and infection is much debated. While it has been demonstrated that HCV can enter hepatoma cell lines via a clathrin-mediated route, clathrin-independent routes of entry have not been considered. If clathrin-independent routes of endocytosis are active in these cell lines it is possible that they offer alternative or additional routes of viral entry, which may contribute to productive HCV infection. Therefore, the aims of this chapter are:

1. **To assess caveolin 1 expression in hepatocytes, hepatoma, and HCV-permissive cell lines.**

In addition, several studies have noted the effects of inhibitors of caveolar endocytosis or silencing caveolin 1 expression, which is both necessary and sufficient for caveolar endocytosis, in hepatoma cell lines (Pohl et al 2002, Zhao et al 2009). Most notably, Pohl et al demonstrate inhibition of [^{3}H]oleic acid uptake when HepG2 cells were treated with filipin III, cyclodextrin and caveolin1 antisense oligonucleotides, all of which are known to inhibit caveolar endocytosis.

While a recent study detected low caveolin 1 mRNA and protein levels in Huh7 cells (Meyer et al 2013), several studies have failed to detect expression of caveolin 1 in hepatoma cell lines by western blot (Cokakli et al 2009, Qi et al 2010). Nevertheless, there is mounting evidence for a pathway both morphologically and functionally similar to the caveolar pathway acting independently of caveolin 1 (Damm et al 2005). In the absence of detectable caveolin 1, it is possible that inhibitors of the caveolar pathway may exert their effects on functionally similar or related pathways.

Paradoxically, while the polarised HepG2 cell line is thought to be most representative of hepatocytes within the liver, these cells are less permissive to HCV infection than their non-polarised counterparts. Moreover, evidence suggests that loss of polarisation and dedifferentiation following *in vitro* culture of primary hepatocytes results in higher expression levels of caveolin 1, particularly at the plasma membrane (Meyer et al 2013). As depolarisation and loss of tight junctions is known to promote HCV infection in cell culture (Mee et al 2009), it is important to consider the role that the concomitant relocalisation of caveolin 1 may play in promoting viral entry.

While the low level of caveolin 1 in polarised hepatocytes within the liver may limit the role that caveolae may play in viral entry *in vivo*, this does not preclude a role for

2. **To select a caveolin 1-positive HCV-permissive cell line for use in HCV entry studies.**
3. **Using the above entry model, to determine whether HCV can enter cells via caveolar endocytosis.**

3.3 Results

3.3.1 Caveolin 1 is expressed by primary human hepatocytes but not by hepatoma cell lines

Hepatoma cell lines are typically described as being devoid of caveolae and have been shown to be negative for caveolin 1 expression by western blot (Cokakli et al 2009, Qi et al 2010). However, there is some evidence to the contrary in the literature, particularly with respect to HepG2 cells, a hepatoma cell line capable of polarisation (Botos et al 2007). Therefore, it was necessary to determine whether these cell lines express caveolin 1 and have functional caveolae. Two methods were used to ascertain the presence or absence of caveolae in a panel of hepatoma, HCV-permissive and positive control cell lines (cell lines known to express caveolin 1). Firstly the expression of caveolin 1 was assessed by western blot (**Figure 3.1 A**). Utilising HeLa, SKHep1 and CHO cell lysates as positive controls, the expression of caveolin 1 was assessed in three human hepatoma cell lines frequently used in the study of HCV infection, namely: HepG2-CD81, Huh6 and Huh7.5 cells, in addition to primary human hepatocytes (PHH). While strong caveolin 1 expression was detected for HeLa, SKHep1 and CHO cells, and, notably, a lower but still detectable level of caveolin 1 in PHH, no caveolin 1 expression was detected for any of the three hepatoma cell lines studied. As caveolin 1 levels have been reported to be very low

in the liver, it is possible that caveolin 1 expression levels in hepatoma cell lines are below the threshold for detection by western blot. Therefore, immunoprecipiation (IP) with α-caveolin 1 was carried out in Huh7.5 and HepG2-CD81 cell lysates and the western blot repeated, as shown in **Figure 3.1 F**. However, IP with α-caveolin 1 did not result in detection of caveolin 1 in either HepG2-CD81 or Huh7.5 cell lysates by western blot.

To confirm this result, the presence of functional caveolae in the same cell lines was assessed by use of a frequently used model cargo for caveolar endocytosis, cholera toxin B subunit (CTB). CTB binds to the ganglioside GM1 in the plasma membrane and is internalised by caveolar endocytosis, although internalisation via other routes has been described in some cases (Torgersen et al 2001, Singh et al 2003). Use of an Alexafluor-555 labelled CTB (CTB-555) allowed detection of cells which had internalised the cargo by confocal microscopy. Uptake of the clathrin-mediated cargo transferrin (Tf) was assessed in the same cell lines as a control. As clathrin-mediated endocytosis is ubiquitous, and TfR endocytosis constitutive, Tf would be expected to be internalised by all cells. The results of CTB and Tf uptake are summarised in **Table 3.1**. HeLa, SKHep and CHO cells were all positive for CTB uptake when imaged by confocal microscopy, as expected, while HepG2-CD81 and Huh6 cells were both negative for uptake of the caveolar marker, exhibiting no fluorescence above the background level (**Figure 3.1 B-E**). Interestingly, a subpopulation of Huh7.5 cells was positive for the fluorescent marker despite lacking detectable caveolin 1 expression by western blot, as shown in **Figure 3.1 D**. The percentage of Huh7.5 cells which stained positive for the caveolar marker CTB was quantified by two methods: confocal microscopy and flow cytometry.

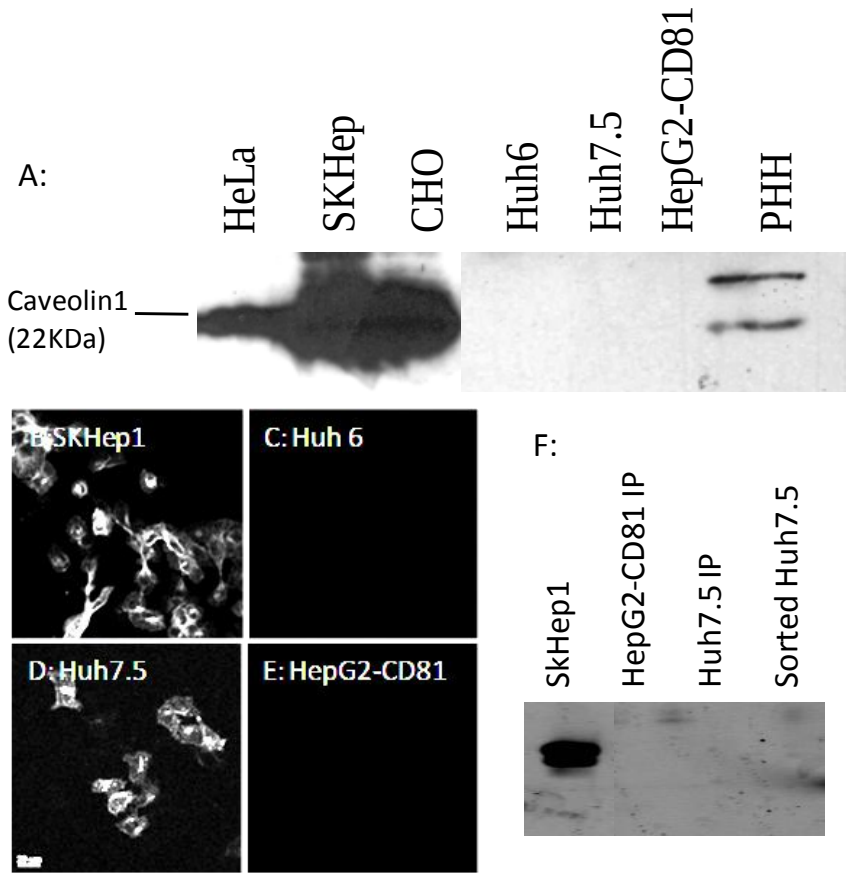

Figure 3.1: Expression of caveolin 1 in primary hepatocytes and hepatoma cell lines. Caveolin 1 levels of three positive control cell lines (HeLa, SkHep and CHO), three hepatoma cell lines and primary human hepatocytes (PHH) were measured by western blot (A). Uptake of fluorescent CTB by one positive control cell line (SkHep1) and three hepatoma cell lines (Huh6, Huh7.5. HepG2-CD81) measured by confocal imaging are shown (B-E). Scale bars = 10 μm. Immunoprecipitation with anti-caveolin 1 was carried out in HepG2 and Huh7.5 cells and lysates blotted for caveolin 1. SkHep1 cells are shown as a contol. FACS sorted CTB-positive Huh7.5 cells are shown alongside (F).

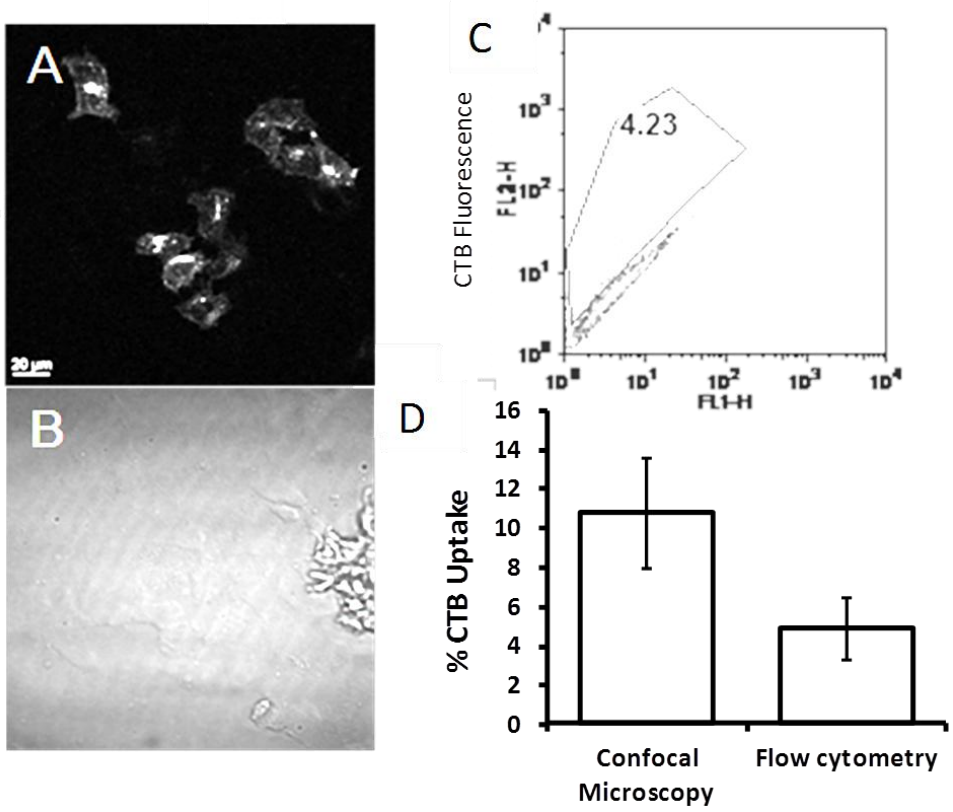

Figure 3.2: Uptake of Tf and CTB by hepatoma and control cell lines.

Representative confocal image of CTB-555 uptake in Huh7.5 cells (A) and corresponding brightfield image (B). Scale bars = 20 μm. Representative flow cytometry plot for Huh7.5 cells incubated with CTB-555, with CTB-positive cells circled (C). Quantification of CTB uptake in Huh7.5 cells by confocal microscopy and flow cytometry (D). Results are the mean of four repeats. Error bars = standard error.

By confocal microscopy, cells in a region were counted using the brightfield image and the number of fluorescent cells in each region then counted and scored as a percentage of the total number of cells. Averages are shown in **Figure 3.2 D** and a representative flow cytometry plot is shown in **Figure 3.2 C**. By flow cytometry, 4.9% of Huh7.5 cells were detected as positive for CTB and by confocal microscopy 10.8% of cells were detected as being positive for CTB. There could be several explanations for this CTB- positive subpopulation; for example, dying Huh7.5 cells may take up CTB through a permeable membrane or the CTB-positive cells could represent a contaminant from another cell line, or an Huh7.5 sub-clone, which does express caveolin 1. As a control to ensure that CTB was not leaking through the permeabilised membranes of dying cells, Huh7.5 cells were stained using Sytox green, a dead cell stain which can enter cells with permeabilsed membranes and bind to nucleic acids. Following staining with Sytox green, cells were incubated with CTB-555, fixed and imaged by confocal microscopy. As shown in **Figure 3.3**, cells which internalised CTB-555 did not stain positive for Sytox green. As a positive control, Huh7.5 cells were permeabilsed with 0.1% Triton X-100 prior to Sytox Green staining, shown in **Figure 3.3 D**. Moreover, to demonstrate that internalised CTB enters the cell via an endocytic route rather than directly penetrating the plasma membrane, SkHep and Huh7.5 cells were incubated with CTB at 4°C to prevent endocytosis from occurring. As shown in **Figure 3.3 E-F**, under these conditions, CTB binds the plasma membrane but is not internalised in both SkHep1 control cells and in Huh7.5 cells, demonstrating that CTB enters both cell lines via a receptor-mediated endocytic route. However, it is also possible that not all Huh7.5 cells contain GM1 in the plasma membrane, as not all cells are able to bind the ligand.

As other routes for CTB entry have been implicated in different cell lines (Torgersen et al 2001, Singh et al 2003), it was important to ensure that the CTB uptake observed in Huh7.5 cells was occurring via a caveolar route. To confirm this, Huh7.5 cells were transiently transfected with caveolin 1-GFP, or clathrin-GFP prior to incubation with CTB-555. Cells were then fixed and imaged by confocal microscopy. The number of red CTB punctae which were also positive for the GFP-tagged protein was scored as a percentage of the total number of CTB punctae. A negative control involving circling CTB-negative areas of the image, of similar size and similar cellular localisation to the CTB-punctae was employed to rule out colocalisation being scored as a result of the random alignment of pixels. The number of these which randomly colocalised with the GFP-tagged proteins was counted and subtracted from the percentage colocalisation. Significant colocalisation ($p<0.05$) was seen with both caveolin 1-GFP and Clathrin-GFP in transfected Huh7.5 cells, when compared to GFP-transfected control cells (significance was determined using a Student's T-test). However, as shown in **Figure 3.4,** the percentage of colocalisation of CTB with caveolin 1-GFP was significantly greater than with clathrin-GFP, with 78.6% colocalisation observed with caveolin 1-GFP and only 15.7% colocalisation observed with clathrin-GFP. As it has previously been shown

Cell Line	Tf Uptake	CTB Uptake
HeLa	+	+
SkHep1	+	+
Huh6	+	-
Huh7.5	+	4.9-10.8%
HepG2-CD81	+	-

Table 3.1: Uptake of Tf and CTB by hepatoma and control Cell Lines.

that cargo entering the cell through caveolae can traffic to early endosomes (Pelkmans et al 2004, Parton 2004) and early endosomes can contain clathrin-coated membrane domains, this colocalisation with clathrin could easily be accounted for by CTB which has trafficked to clathrin-positive early endosomes.

Therefore, we can conclude that a subpopulation of Huh7.5 cells can take up the caveolar marker CTB, are not dying cells with permeable membranes and internalised CTB in these cells may indicate the presence of caveolae, as internalised CTB colocalises with caveolin1-GFP in transiently transfected cells. However, in order to utilise these CTB-positive Huh7.5 cells for infection studies, they must be isolated so that the whole cell population is CTB-uptake positive and caveolin 1 expression shown by western blot. To achieve this, Huh7.5 cells were incubated with CTB and then FACS sorted in order to isolate the CTB-positive cells. Sorted cells were then cultured for 3 days and lysates were analysed for caveolin 1 expression by western blot (**Figure 3.1 F**). However, caveolin 1 expression was still not observed. Therefore, it is possible that the internalised CTB visible within Huh7.5 cells is internalised via a functionally and morphologically similar endocytic pathway acting independently of caveolin 1 (as described in Damm et al 2005).

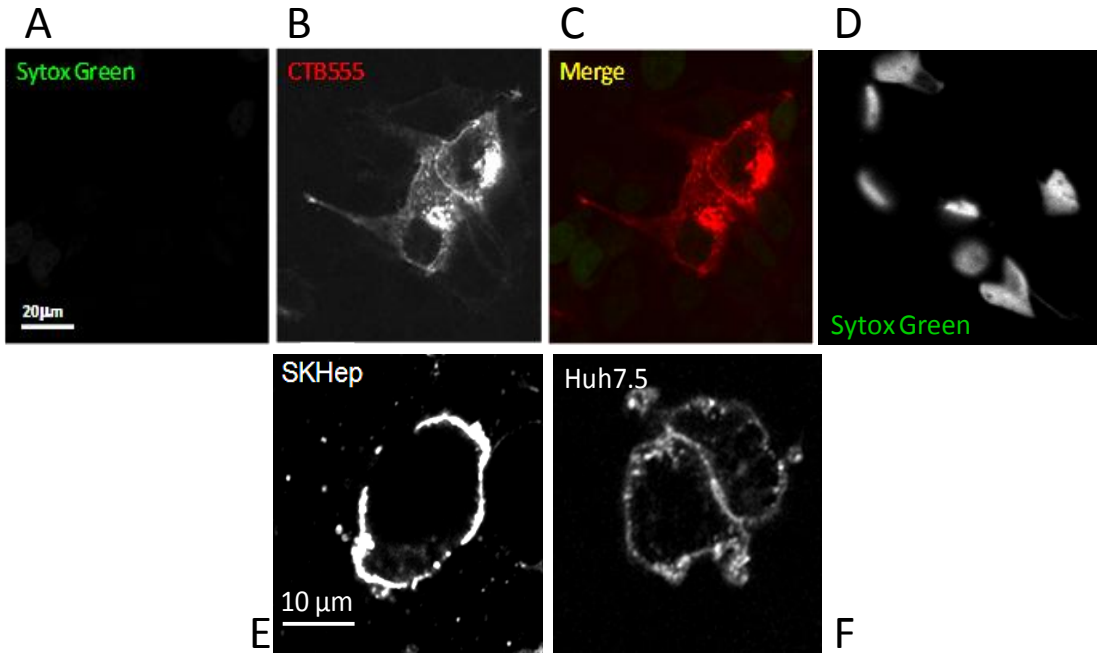

Figure 3.3: Huh7.5 cells take up CTB via endocytosis. Sytox staining (A) in Huh7.5 cells incubated with CTB-555 (B). Overlay shown in part C. Sytox staining in permeabilised cells is shown as a positive control (D). SkHep1 (E) and Huh7.5 (F) cells were incubated with CTB-555 on ice. Images are representative of three repeats.

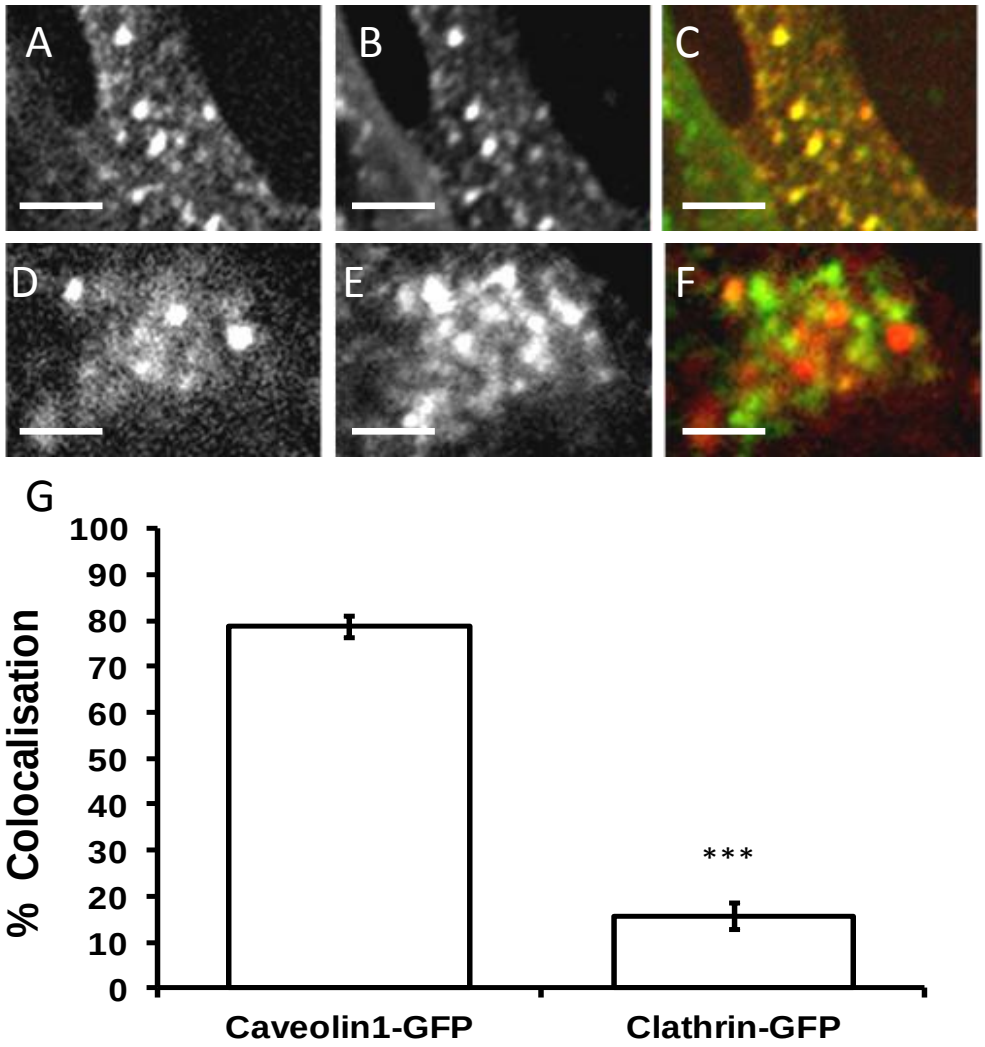

Figure 3.4: Huh7.5 cells take up CTB via caveolar endocytosis in cells transiently transfected with caveolin 1-GFP. Huh7.5 cells transfected with caveolin 1-GFP, incubated with CTB-555 and imaged by confocal microscopy (A-C). Huh7.5 cells transfected with clathrin-GFP, incubated with CTB-555 and imaged by confocal microscopy (D-F). Scale bars = 5 μm. Quantification of colocalisation between CTB and each endocytic marker is shown as a percentage in part G. Data shown are the mean of three independent experiments. Error bars = standard error.

Summary:

1. **The hepatoma cell lines Huh6, Huh7.5 and HepG2-CD81 do not express detectable caveolin 1, whereas, primary human hepatocytes and SKHep1 cells do.**
2. **A subpopulation of 4.9-10.8% of Huh7.5 cells take up the caveolar marker CTB. Internalised CTB colocalises with over-expressed caveolin 1 in Huh7.5 cells but FACS sorting of these cells does not result in caveolin 1 detection by western blot.**

3.3.2 Caveolin 1 is expressed by hepatocytes *in vivo*

As shown in **Figure 3.1 A**, primary human hepatocytes (PHH) express caveolin 1. To confirm caveolin 1 expression and observe protein localisation, PHH were grown in culture for up to three days and immunocytochemistry (IC) for caveolin 1 carried out at day 1, day 2, and day 3 post-plating. As shown in **Figure 3.5**, cultured PHH stained positive for caveolin 1, with punctate cytosolic staining at day one, with some relocalisation to the plasma membrane by day 2 and clear plasma membrane localisation at day 3. This would suggest that not only is caveolin 1 expressed in hepatocytes *in vivo* but may also be localised to the plasma membrane, where it is available for the formation of functional caveolae. In addition, IC for caveolin 1 was also carried out on human liver sections (**Figure 3.5 A**). However, while a low level of positive staining can be seen in the hepatocytes, caveolin 1 is expressed to such a high level by the liver sinusoidal endothelial cells (LSECs), the possible source of SKHep cells (see below), surrounding the hepatocytes in the liver sections that laser power and gain had to be reduced accordingly, to prevent saturation of the image. This is consistent with the expression level seen by western blot, with endothelial

cells expressing caveolin 1 at much higher levels than hepatocytes, however, the presence of endothelial cells in the liver sections makes caveolin 1 staining in the hepatocytes difficult to visualise clearly. For this reason, cultured primary human hepatocytes offer the clearest visualisation of caveolin 1 expression and localisation in liver cells. As cultured hepatocytes dedifferentiate and depolarise over time in culture, the staining observed at day 1 is likely to be most typical of that in polarised hepatocytes in the liver. Interestingly, as loss of polarisation promotes HCV infection, cultured primary hepatocytes are most permissive to HCV at days 2 and 3, when caveolin 1 is most strongly localised to the plasma membrane.

As traditional hepatoma cell lines have been shown to be negative for caveolin 1, other HCV-permissive cell lines which do express caveolin 1 must be considered for HCV infection studies.

Of the three positive control cells shown to express caveolin 1 by western blot (**Figure 3.1 A**), SkHep1 cells, are the only liver-derived cell line. SkHep1 cells were isolated from a hepatocellular carcinoma and originally believed to be of hepatocyte origin. However, there is some debate as to whether they may in fact be from an endothelial background (Heffelfinger et al 1992). Nevertheless, SkHep1 cells are HCV-permissive when transduced to express all HCV entry factors and receptors (Dreux et al 2009). They take up CTB, a commonly used marker for caveolar endocytosis and endogenously express two of the four HCV receptors/entry factors. SkHep1 cells stably transfected to express SRBI and CLDN1, known as SkHep1 (SRBI+CLDN1) cells (generated and used previously by Ke Hu, McKeating lab) therefore offer a good model cell line for infection.

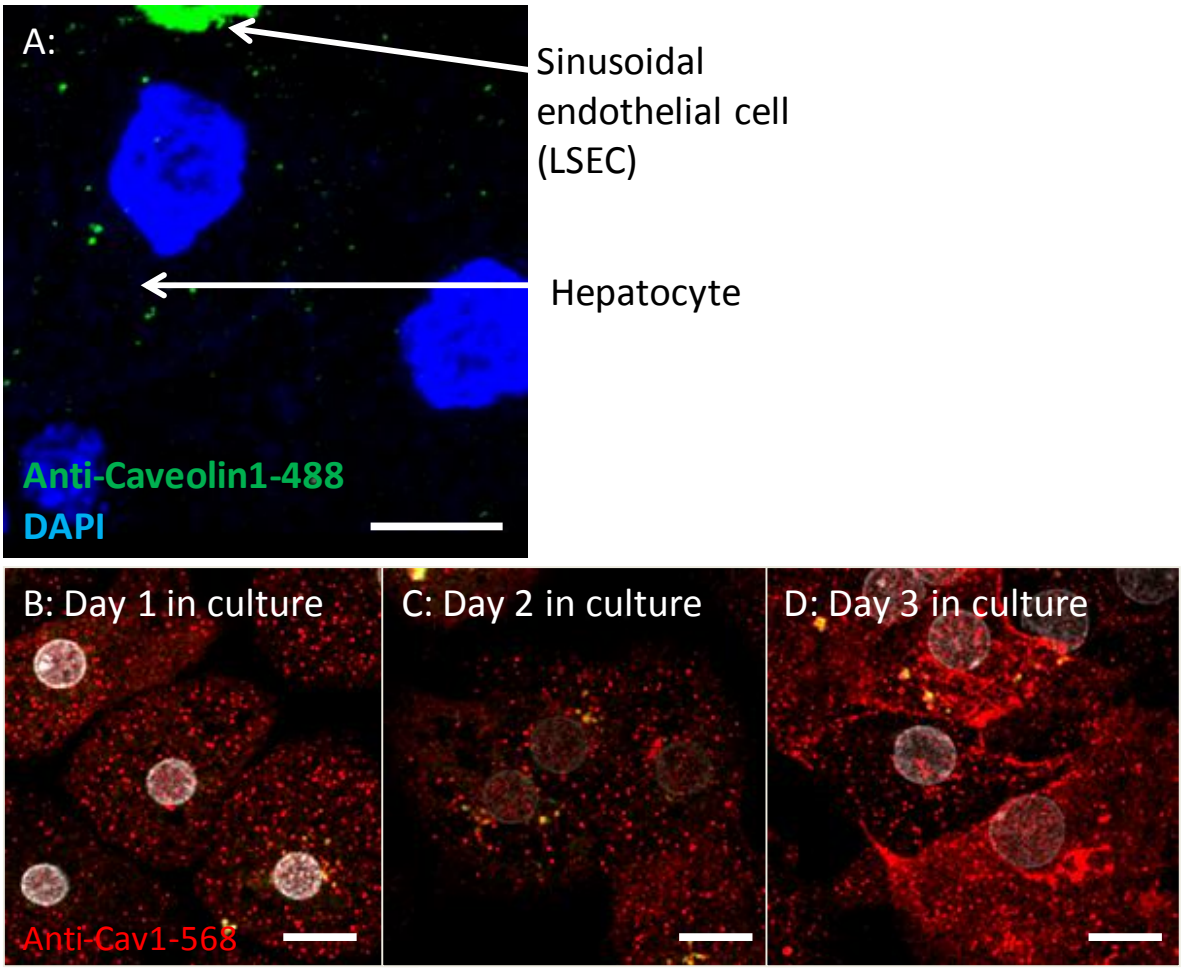

Figure 3.5: Expression of caveolin 1 in cultured primary human hepatocytes and liver sections. Caveolin 1 immunocytochemistry in human liver section containing hepatocytes with low caveolin 1 expression and liver sinusoidal endothelial cells (LSEC) with strong caveolin 1 expression (A). Caveolin 1 immunocytochemistry in primary human hepatocytes after 1 (B), 2 (C), and 3 (D) days in cell culture. Scale bars = 5 μm. Performed with help from Garrick Wilson and Helen Harris, McKeating lab, University of Birmingham, UK.

Summary:

1. **Hepatocytes within the liver express caveolin 1.**
2. **Cultured primary human hepatocytes express caveolin 1.**
3. **Plasma membrane expression of caveolin 1 increases over time in cell culture, consistent with dedifferentiation.**
4. **SkHep1 (SRBI+CLDN1) cells express caveolin 1 and are permissive to HCV, making them a suitable model for studies of HCV entry.**

3.4 Specifically inhibiting endocytic pathways in SkHep1 (SRBI+CLDN1) cells.

3.4.1 Small molecule inhibitors

Small molecule inhibitors offer an attractive means of inhibiting endocytic pathways as they exert their effects on the whole cell population and are not dependent on transfection efficiency. However, many inhibitory drugs exhibit undesired off-target effects and disrupt other endocytic pathways (Ivanov 2008). It is therefore important to use specific model cargo such as CTB and Tf to confirm the specificity of the inhibitor prior to use in viral entry experiments.

One widely used small molecule inhibitor of clathrin-mediated endocytosis is chlorpromazine (CPZ), which is thought to cause clathrin lattices to assemble on endosomal membranes, preventing clathrin-coated pits from forming at the plasma membrane (Wang et al 1993). Inhibition of viral entry by CPZ in hepatoma cells is one of the key pieces of evidence for the clathrin-mediated entry pathway for HCV (Blanchard et al 2006). However, demonstration of the effects of chlorpromazine using endocytic cargo such as Tf has not been carried out in HCV entry studies to

date, so it is uncertain if this effect is specific to the clathrin-mediated endocytic pathway. Incubation of SkHep1 (SRBI+CLDN1) cells with CPZ at 1 µM (a concentration intermediate between the two concentrations used in Blanchard et al 2006) exhibited some surprising effects on cargo uptake, unexpectedly increasing Tf uptake, and inhibiting CTB uptake, as shown in **Figure 3.6**. It is therefore clear that off-target effects of this drug in SkHep1 (SRBI+CLDN1) cells make unsuitable to take forward for use in HCV entry studies.

More recently, a lactosyl ceramide isomer, L-t-LacCer, has been shown to inhibit caveolar endocytosis (Singh et al 2003). The inhibitor is thought to work by disrupting cholesterol-rich lipid rafts. However, as both cholesterol and lipid rafts play roles in other modes of endocytosis, it is important to confirm that the effects of this drug are specific to caveolar endocytosis. In SkHep1 (CLDN1+SRBI) cells, at a concentration of 10 µM, L-t-LacCer significantly inhibited uptake of CTB, whereas, the inactive control D-e-Lac-Cer had no significant effect, as expected (**Figure 3.6**). However, both Lac-Cer isomers inhibited Tf uptake and therefore do not act specifically on the caveolar pathway in this cell line. This is shown in **Figure 3.6 K-N**. Again, it is clear that off-target effects of this inhibitor may be an issue, as with CPZ.

Dynasore is a small molecule inhibitor of both dynamin I and dynamin II and has been shown to act specifically on dynamin (Macia et al 2006). As both the clathrin-mediated and caveolar pathways are dependent on dynamin II, treatment with Dynasore should inhibit uptake of CTB and LDL. As shown in **Figure 3.7**, a 30 minute pre-incubation with 80 µM Dynasore is sufficient to inhibit CTB uptake by 46% and LDL uptake by 32% in SkHep1 (SRBI+CLDN1) cells. Dynasore is therefore the only small molecule inhibitor tested which is suitable for use in HCV entry studies.

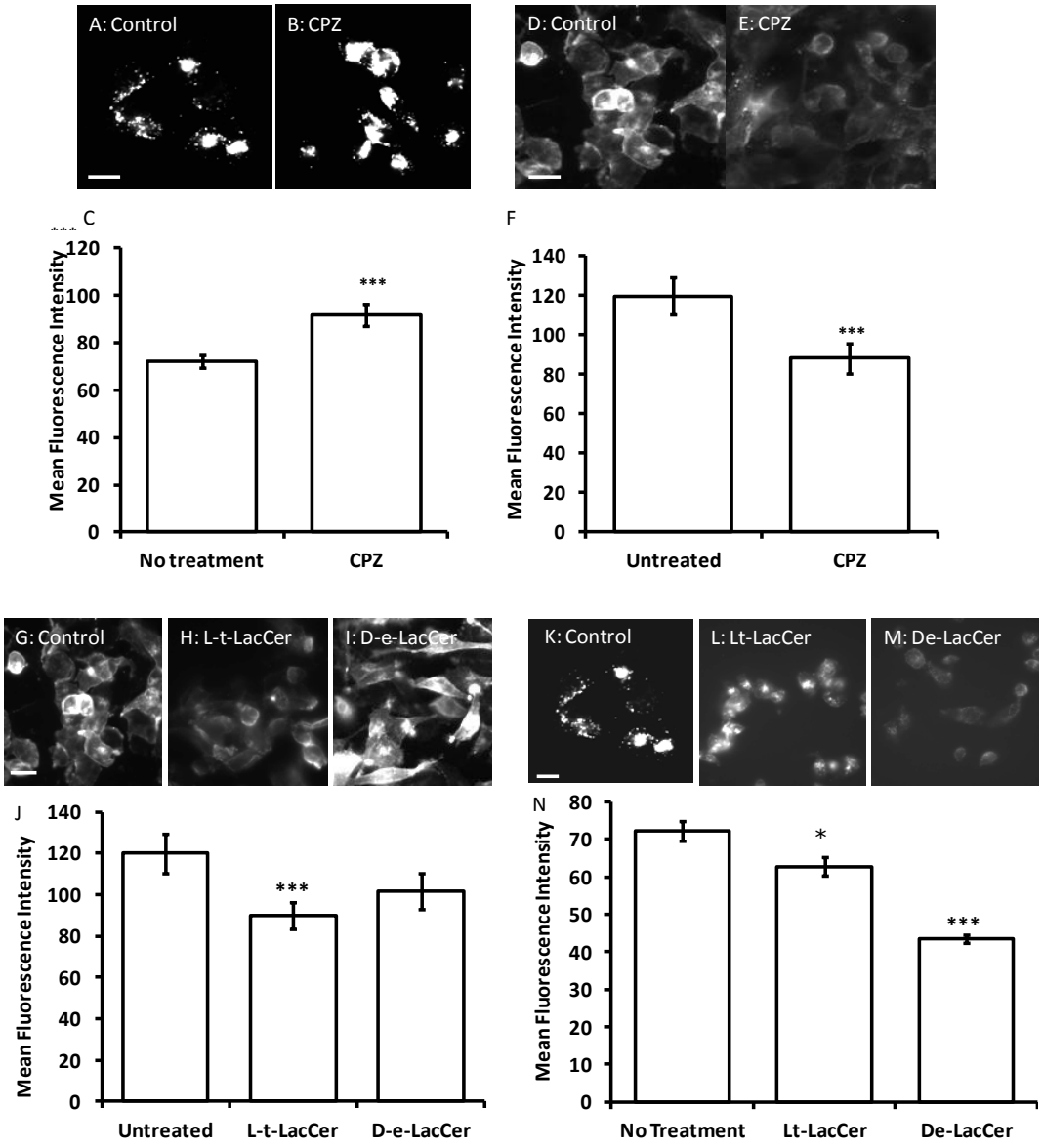

Figure 3.6: Effect of small molecule endocytosis inhibitors on uptake of model cargo in SkHep1 (SRBI+CLDN1). Uptake of a clathrin marker transferrin is shown in control cells (A) and chlorpromazine treated cells (B). Quantification of Tf uptake is shown in (C). CTB uptake in control (D) and chlorpromazine-treated cells (E). Quantification of CTB uptake is shown in (F). CTB uptake in control (G), L-t-LacCer treated (H) and De-LacCer (I) treated cells. Quantification is shown in (J). Tf uptake in control (K), L-t-LacCer (L) and De-LacCer (M) treated cells is shown. Scale bars = 10 μm. Quantification is shown in (N). 90 cells per group were quantified from three repeats. Error bars = standard error.

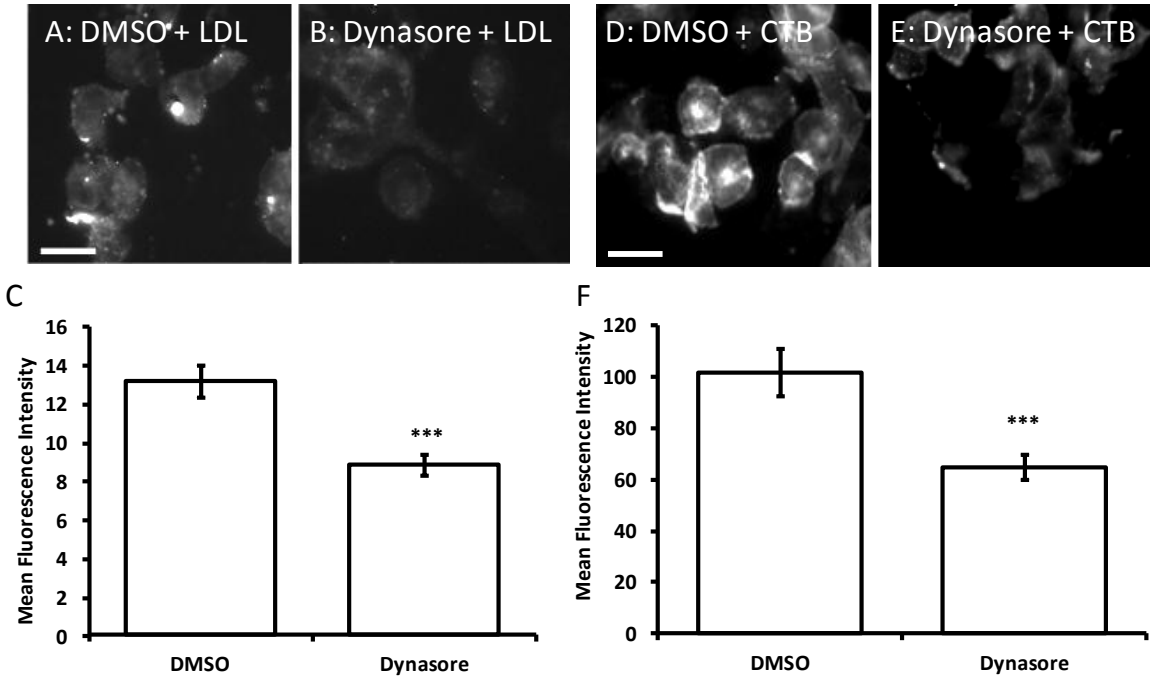

Figure 3.7: Dyanasore inhibits LDL and CTB entry in SkHep1 (SRBI+CLDN1) cells. LDL uptake in DMSO treated control cells (A) and Dynasore-treated cells (B). LDL uptake is quantified in (C). CTB uptake in DMSO treated control cells (D) and Dynasore-treated cells (E). Quantification of CTB uptake is shown in (F). Scale bars = 20 μm. 90 cells were imaged and analysed per group from three independent repeats. Error bars = standard error.

Summary:

1. **Dynasore significantly inhibits both clathrin-mediated and caveolar endocytosis.**
2. **Chlorpromazine does not inhibit Tf uptake but does inhibit CTB uptake at the concentration used and is therefore not useful for infection studies.**
3. **Lt-LacCer inhibits CTB uptake but also inhibits Tf uptake and is therefore not suitable for infection studies.**

3.4.2 HCVpp infection is Inhibited by Dynasore

As shown in **Figure 3.7**, treatment with 80 μM Dynasore for 30 minutes inhibited endocytosis of CTB by 46% and LDL by 32%. Therefore a significant inhibition of HCVpp infection is expected in Dynasore-treated cells. When carrying out HCVpp infection assays, murine leukaemia virus pseudoparticles (MLVpp) and vesicular stomatitis virus G pseudoparticles (VSV-Gpp) are used as controls. MLV is thought to be internalised by caveolar endocytosis (Beer et al 2005) and VSV is thought to be internalised exclusively by clathrin-mediated endocytosis (Cureton et al 2009), so both controls should also be significantly inhibited by Dynasore. SkHep1 (CLDN1+SRBI) cells and Huh7.5 cells were pre-treated with 80 μM Dynasore for 30 minutes prior to addition of viral pseudoparticles, and was present throughout pseudoparticle incubation (8 hours). Luciferase reporter activity of infected cells was then assayed 72 hours later.

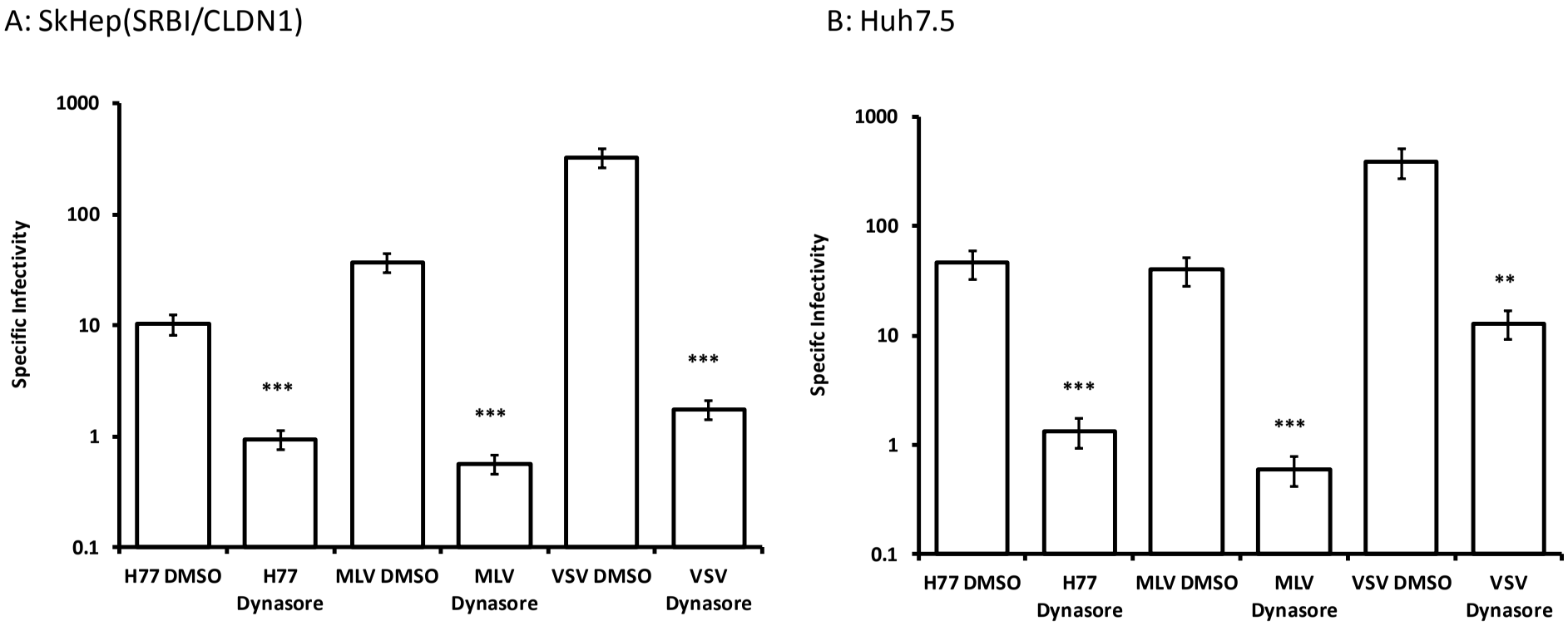

Figure 3.8: Dyanasore Inhibits HCVpp Infection in SkHep1 (SRBI+CLDN1) and Huh7.5 Cells. Dynasore treatment inhibits HCVpp (H77), MLV and VSV-Gpp entry in SkHep1 (SRBI+CLDN1) cells (A) and in Huh7.5 cells (B). Results are means of three independent repeats. Error bars = standard error.

As shown in **Figure3.8**, HCVpp infection (H77 strain) is markedly inhibited in Dynasore-treated cells when compared to the DMSO control. Moreover, this result is comparable to that seen in Huh7.5 cells, demonstrating a strong dependency of HCVpp entry on dynamin in both cell lines. MLVpp and VSV-Gpp infections also showed a strong dynamin-dependency in both cell lines, as predicted, consistent with a vital role for dynamin in viral endocytosis by both endocytic pathways.

Summary:

1. **Dynasore significantly inhibits endocytosis of HCVpp (H77) indicating a dynamin-dependent entry route.**
2. **Dynasore also significantly inhibited endocytosis of control viruses MLVpp and VSV-Gpp.**

3.4.3 Inhibition of endocytic pathways by siRNA

Silencing the expression of protein components within endocytic pathways using small interfering RNAs (siRNAs) can offer the most specific means of inhibiting endocytosis. As clathrin is involved in cellular processes other than endocytosis, siRNA against the α-adaptin subunit of the adaptor protein 2 (AP2) complex, which links the clathrin coat to cargo and the plasma membrane (Huang and Sorkin 2004), has been used alongside a pool of commercially available caveolin 1 siRNAs (Dharmacon) (Auciello et al 2013). In each case a non-targeting siRNA sequence has been used as the non-silencing control (NSC). As viral infections must take place over a 72 hour period, silencing was assayed 72 hours post-transfection with the siRNAs. **Figure 3.9 A** shows the efficiency of both AP2 and caveolin 1 knockdown achieved by western blot. Two transfection reagents, Lipofectamine

2000 and Lipofectamine RNAiMAX, were tested for efficiency of protein silencing with both siRNAs. In each case, transfection with Lipofectamine RNAiMAX resulted in the greatest reduction in protein expression (data not shown).

To ascertain specificity of protein silencing, endocytosis assays using model cargo were carried out alongside using CTB-555 and LDL-568. Over three repeats, consistent and significant inhibition of each pathway was observed, as shown in **Figure 3.9**. In each case, specificity was tested by observing the effects of silencing on the other pathway. Transfection with caveolin 1 siRNA resulted in a 58% reduction in CTB uptake, while having no significant effect on LDL uptake. AP2 knockdown inhibited LDL uptake by 46%, and had no significant effect on CTB uptake. These results demonstrate that the siRNAs used are potent and highly specific means of inhibiting endocytic pathways and are suitable for use in HCVpp infection assays.

Summary:

1. **Transfection of caveolin 1 and AP2 siRNA with Lipofectamine RNAiMAX results in efficient protein knockdown in SkHep1 (SRBI+CLDN1) cells.**
2. **Knockdown of caveolin 1 significantly inhibits CTB uptake but has no significant effect on uptake of Tf or LDL, demonstrating specificity.**
3. **Knockdown of AP2 significantly inhibits LDL uptake but has no significant effect on CTB, demonstrating specificity.**

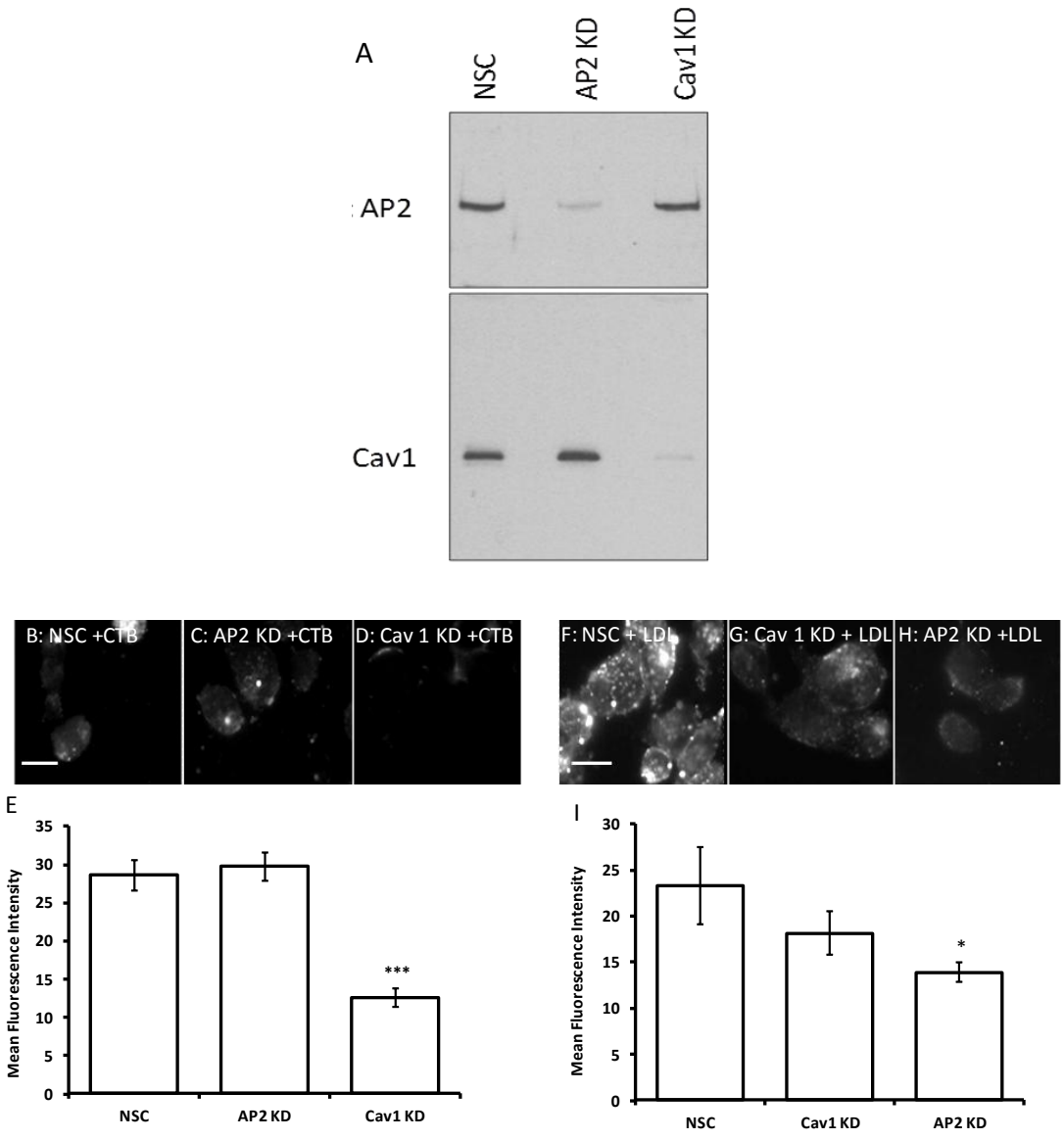

Figure 3.9: Knockdown of AP2 and caveolin 1 in SkHep1 (SRBI+CLDN1) cells. Knockdown of AP2 and caveolin 1 shown by western blot (A). CTB uptake in cells transfected with a non-silencing control (NSC) (B), AP2 siRNA (C) and caveolin 1 siRNA (D). Quantification of internalised CTB is shown in (E). LDL uptake in NSC (F), caveolin 1 knockdown (G) and AP2 knockdown (H) cells is shown. Scale bars = 20 μm. Quantification of internalised LDL is shown in (I). 60 cells were imaged and analysed per group, from three independent experiments. Error bars = standard error.

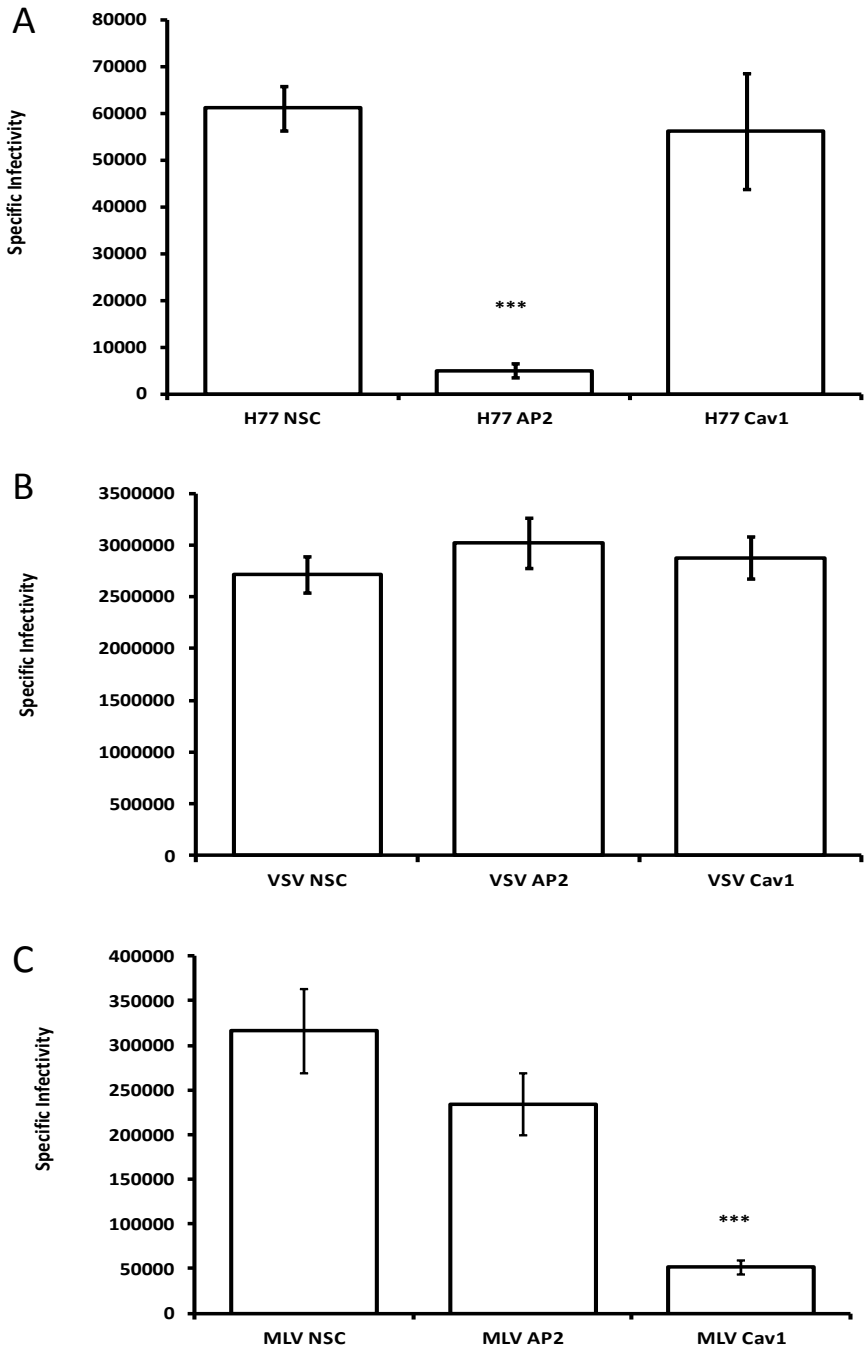

Figure 3.10: Knockdown of AP2 but not caveolin 1 inhibits HCVpp infection in SkHep1 (SRBI+CLDN1) cells. HCV (H77) infection in non-silenced control (NSC), AP2 knockdown and caveolin 1 knockdown cells (A). VSV-Gpp infection in NSC, AP2 knockdown and caveolin 1 knockdown cells (B). MLVpp infection in NSC, AP2 knockdown and caveolin 1 knockdown cells (C). Results are means of three independent experiments. Error bars = standard error.

3.4.4 HCVpp entry is inhibited by AP2 siRNA but not caveolin 1 siRNA

As mentioned previously, one of the most specific and effective ways to inhibit an endocytic pathway is to knock down proteins involved using siRNA. However, clathrin is involved in other cellular processes besides endocytosis from the plasma membrane, so siRNA targeting clathrin heavy chain could result in off-target effects. The adaptor protein 2 complex is exclusively involved in clathrin-mediated endocytosis and therefore presents an ideal target for siRNA knockdown. As shown in section 3.4.3, efficient and specific knockdown of both AP2 and caveolin 1 protein levels was achieved.

A HCVpp infection assay was then carried out in SkHep1 (CLDN1+SRBI) cells transfected with AP2 or caveolin 1 siRNA, using MLVpp and VSV-Gpp as controls. Cells were incubated with viral pseudoparticles for 8 hours and luciferase reporter activity assayed 72 hours later.

As shown in **Figure 3.10**, AP2 knockdown resulted in almost complete abrogation of HCVpp entry compared to the non-silencing control (NSC). In contrast, caveolin 1 knockdown exhibited no discernible effect on HCVpp entry. This demonstrates that HCV does not utilise caveolae as an entry mechanism, even when the protein is expressed to high levels.

Interestingly, AP2 knockdown had little effect on VSV-Gpp entry, suggesting that VSV entry is not dependent on AP2 as would be expected for a virus thought to have a clathrin-dependent entry mechanism (Cureton et al 2009). However, it is possible that VSV pseudoparticles enter via a clathrin-dependent but AP2 independent mechanism SkHep1 (CLDN1+SRBI) cells (Motley et al 2003).

Additionally, caveolin 1 knockdown significantly inhibited uptake of MLVpp in these cells, confirming effective knockdown in this case. Therefore, it is clear that even when caveolin 1 is expressed, as is the case in hepatocytes *in vivo*, HCV does not utilise caveolar endocytosis as an additional or alternative entry mechanism to clathrin-mediated endocytosis. The almost complete abrogation of HCVpp infection seen in AP2-silenced cells would suggest only one AP2-dependent pathway exists for HCV infection.

Summary:

1. **AP2 knockdown abrogates HCVpp entry but has little effect on VSV-Gpp.**
2. **Caveolin 1 knockdown does not inhibit HCVpp entry and therefore caveolin 1 is not required for HCV entry in SkHep1 (SRBI+CLDN1) cells.**

3.5 Discussion

While hepatocytes within the liver are known to express caveolin 1, there is a long-standing belief that the hepatoma cell lines used to study HCV entry *in vitro*, do not. The fact that inhibition of clathrin-mediated endocytosis by small molecule inhibitors such as chlorpromazine and silencing of clathrin heavy chain abrogate HCV entry in hepatoma models substantiates a clathrin-mediated route of entry for the virus (Blanchard et al 2006, Codran et al 2006, Coller et al 2009). However, the lack of caveolin 1 expression in hepatoma cell lines has resulted in any role this pathway may play in *in vivo* infection being ignored. With increasing numbers of viruses

exhibiting altered routes of entry across multiple cell lines, or even utilising more than one pathway within the same cell line, it is important to address any potential role caveolin 1 may play in HCV infection both *in vivo* and *in vitro*.

To confirm current understanding about caveolin 1 expression in human hepatocytes and hepatoma cell lines, caveolin 1 expression was assayed in a panel of hepatoma cell lines, as well as in primary human hepatocytes (PHH) (shown in **Figure 3.1 A**). As in the literature (Cokakli et al 2009), low levels of caveolin 1 expression were detectable in primary human hepatocytes and no detectable caveolin 1 expression seen for the hepatoma cell lines studied, even when caveolin 1 IP was carried out. Uptake assays using a common caveolar marker CTB largely confirmed these results, with no observable uptake in two of the three hepatoma cell lines investigated. However, interestingly, CTB uptake was observed in some Huh7.5 cells. This population when assayed by flow cytometry and confocal microscopy was found to represent 4.9-10.8% of the cell population. However, when these cells were isolated by FACS, they still did not test positive for caveolin 1 expression by western blot. As there is mounting evidence for (a) pathway(s) functionally similar to caveolae but acting independently of caveolin 1, it is possible that this is the pathway utilised by the caveolar marker in this instance (Damm et al 2005). When caveolin 1-GFP was over-expressed in this cell line it colocalised with internalised CTB. However, caveolin 1 expression did not result in CTB uptake in a higher proportion of the cell population, suggesting that CTB is taken up by a caveolin 1-independent mechanism in these cells. Moreover, staining with a dead cell stain revealed that CTB was not simply passing through the permeabilised membranes of dying cells, and the membrane staining with CTB on ice shown in **Figure 3.3 E and F** is consistent with an endocytic route of entry for the marker. However, as caveolin 1 expression was

still not demonstrable in isolated CTB-positive Huh7.5 cells, another HCV-permissive caveolin 1-positive cell line was needed in order to be able to test the functional significance of caveolin 1 expression in hepatocytes.

In initial caveolin 1 western blots, SkHep1 cells were used as a positive control cell line, and were shown to express high levels of the protein. SkHep1 cells transduced to express the non-endogenously expressed receptors (SRBI and CLDN1) are highly permissive for HCV infection (Cureton et al 2009) and so represent an ideal infection model for investigating the role of caveolin 1 in HCV infection.

Means of inhibiting endocytic pathways in this cell line were then tested for their specificity before being carried forward for use in infection studies. It is important to test inhibitory methods using model endocytic cargo prior to use in infection studies, as endocytic trafficking pathways are often interconnected and perturbation of one pathway can often result in altered traffic by another. In particular, small molecule inhibitors are renowned for exhibiting off-target effects. However, they offer an attractive means of pathway inhibition as they exert their effects on the whole cell population and as such are not transfection efficiency-dependent. Additionally, inhibition of HCV entry by the clathrin inhibitor chlorpromazine (CPZ) is one of the key pieces of data suggesting a clathrin-mediated route of entry for HCV (Blanchard et al 2006), and its specificity was not demonstrated in this study. When CPZ was applied to SkHep1 (SRBI+CLDN1) cells at a concentration of 1 μM, a concentration intermediate to the two concentrations used in Blanchard et al 2006, it exhibited some surprising results on the uptake of model endocytic cargo Tf and CTB. Not only did CPZ inhibit uptake of the caveolar marker, CTB, thus not acting specifically upon clathrin-mediated endocytosis, but it also promoted Tf uptake in these cells. While it is possible that these effects are cell line-dependent, it is clear that CPZ can

have undesired off-target effects and cannot be solely relied upon in studies of endocytosis. Moreover, these results highlight the need to test inhibitors using model endocytic cargo before drawing conclusions based on their use.

More recently, an isomer of lactosyl ceramide has been shown to affect caveolar endocytosis. This inhibitor, L-t-LacCer, is thought to exert its effect on the lipid-raft nature of caveolae. However, as multiple endocytic mechanisms require cholesterol and lipid rafts, perturbation of the composition of the plasma membrane is likely to result in multiple pathways being affected. When assayed in SkHep1 (SRBI+CLDN1) cells, the inhibitory isomer did markedly and specifically inhibit CTB uptake, exerting no effect on the clathrin-mediated endocytic cargo, Tf. Nevertheless, the inactive isomer intended for use as a control also inhibited CTB uptake, as well as Tf uptake in this cell line. Therefore neither of these small molecule inhibitors was suitable for use in infection studies.

The small molecule inhibitor of dynamin, Dynasore, has been shown to act specifically on dynamin in a variety of endocytosis studies (Macia et al 2006, Kirchhausen et al 2008). As dynamin is implicated in both clathrin-mediated and caveolar endocytosis, it will not distinguish between the two pathways but will be able to confirm the dynamin-dependency of HCV uptake shown by previous hepatoma cell line studies in this cell line (Farquhar et al 2012). Dynasore effectively inhibited uptake of both Tf and CTB in SkHep1 (SRBI+CLDN1) cells. In HCVpp infection studies, Dynasore abrogated HCV infection in both SkHep1 (SRBI+CLDN1) cells as well as in Huh7.5 cells (the cells used initially to show dynamin-dependency of HCV entry). As the virus was unable to enter via dynamin-independent mechanisms this both confirms previous results and suggests that even if clathrin-independent mechanisms of entry can be exploited by the virus, these must also be

dynamin-dependent. Dynasore treatment also inhibited uptake of VSV-Gpp and MLVpp which were employed as controls and are thought to internalise via clathrin-mediated endocytosis and caveolar endocytosis, respectively (Beer et al 2005, Cureton et al 2009).

As the other endocytosis inhibitors tested exhibited off-target effects when the uptake of model cargo was assayed, a more specific approach to inhibiting clathrin-mediated and caveolar endocytosis was adopted. siRNA offers one of the most specific means of inhibiting endocytic pathways, and well transfection efficiency-dependent, higher transfection efficiency can be achieved with siRNA than with DNA. To implement this approach, a custom AP2 siRNA was used to specifically inhibit clathrin-mediated endocytosis. As clathrin coated vesicles play roles in trafficking besides endocytosis from the plasma membrane, for example, transport from the trans-Golgi network, silencing of clathrin can have off-target effects. Therefore inhibition of components of the clathrin-mediated endocytic machinery is generally thought to offer a more specific means of inhibition. The AP2 complex is involved in connecting the clathrin lattice to phosphoinositides in the plasma membrane and serving as a cargo adaptor, and silencing of this protein has been shown to specifically inhibit clathrin-mediated endocytosis (Boucrot et al 2010). Additionally, a commercially available pool of siRNAs targeted to caveolin 1 was also employed (Dharmacon). Both siRNAs were compared to a non-targeting siRNA (non-silencing control; NSC). In assays of model cargo uptake, both siRNAs exhibited high specificity to their respective pathways and so were carried forward to HCVpp infection studies. As HCVpp infections must be carried out over 72 hours for measurable infection, it was important to ascertain that silencing is maintained throughout the assay. As such, cells were lysed 72 hours following transfection with

either AP2 or caveolin 1 siRNA and protein levels detected by western blot. This specificity was confirmed by endocytosis assays, as with Dynasore, and significant and specific inhibition was observed in each case. In pseudoparticle infections, HCVpp entry was markedly inhibited by AP2 silencing but unaffected by caveolin 1 silencing. This suggests that even in the presence of caveolin 1, HCV enters cells strictly via clathrin-mediated endocytosis. The effectiveness of caveolin 1 silencing is demonstrated by the inhibition of MLVpp infection and confirmed by western blot.

Interestingly, VSV-Gpp infection was not significantly inhibited by AP2 knockdown, consistent across three independent repeats. As there is some, albeit limited evidence for a clathrin-mediated pathway functioning independently of AP2 and/or accessory proteins such as Eps15 (Motley et al 2003, Hinrichsen et al 2003, Boucrot et al 2010), it is interesting to speculate that this pathway is operational in SkHep1 cells and that VSV is internalised via this mechanism. Nevertheless, if this pathway exists, it is certainly not exploited by HCVpp which shows strong AP2-dependency. Additionally, it is thought that due to size constraints, VSV is not internalised via vesicles that resemble those involved in the clathrin-mediated endocytosis of Tf or LDL, rather VSV internalises in vesicles which are only partially coated in clathrin (Cureton et al 2009). While internalisation of these partially coated vesicles is thought to be dependent on AP2 (Cureton et al 2009), it is possible that these VSVpp internalisation relies on alternative adaptor proteins in this cell line.

Therefore, the results of this chapter show that caveolin 1 plays no functional role in HCV entry in this *in vitro* model, where high levels of caveolin 1 are expressed. It is therefore is unlikely to play a role in HCV entry *in vivo*, where caveolin 1 levels are lower and localisation not enriched at the plasma membrane. This means that the increased caveolin 1 levels reported in depolarised cells, while correlating with

increased permissivity to infection, are not likely to be responsible for this change. The reason for the discrepancy between caveolin 1 expression in hepatocytes within the liver and the hepatoma cell lines used to study HCV infection remains unclear; however, it does not seem to be relevant to studies of HCV entry.

There are reports of caveolin 1 playing a role in hepatocellular carcinoma tumourigenesis and metastasis (Cokakli et al 2009, Tse et al 2012), which would seem to contradict the loss of caveolin 1 in hepatoma cells in culture. Here, caveolin 1 expression correlated with increased invasiveness, where over-expression of caveolin 1 in HepG2 and Huh7.5 cells promoted a more invasive phenotype (Tse et al 2012). This is thought to be a result of the role caveolin 1 plays in regulating the internalisation and signalling of cellular receptors such as growth factor receptors (Labrecque et al 2003, Pike et al 2005, Galvagni et al 2007). As caveolin 1 is known to play a role in liver regeneration and response to partial hepatectomy in mice (Fernández et al 2006), its role in hepatocarcinogenesis is perhaps unsurprising.

3.6 Key chapter findings

1. While hepatocytes within the liver express caveolin 1, the hepatoma cell lines used to study HCV infection in vitro do not.
2. When a caveolin 1-positive HCV-permissive cell line, SkHep1(SRBI+CLDN1) are used in infection studies, infection is inhibited by Dynasore, a small molecule inhibitor of dynamin, and AP2 siRNA, but not caveolin 1 siRNA.
3. Caveolin 1 is not required for HCV entry in caveolin 1-expressing HCV-permissive cells.

3.7 Conclusions

Data from this chapter take a systematic approach to the detection of caveolin 1 expression in human liver, cultured PHH and hepatoma cell lines, and are consistent with the majority of disparate published studies on the subject.

SkHep1 (SRBI+CLDN1) cells were identified as a HCV-permissive caveolin 1-positive cell line for use in studies of the functional role of caveolin 1 in HCV entry.

Consistent, efficient and specific knockdown of AP2 and caveolin 1 was demonstrated in this cell line and used to show definitively for the first time that caveolin 1 is not required for HCV entry, nor are caveolae utilised as an additional or alternative entry mechanism.

CHAPTER 4

RESULTS

CELLULAR EFFECTS OF EGF STIMULATION ON HUH7.5 CELLS

4.1 Introduction

The epidermal growth factor receptor (EGFR) is a member of the ErbB family of receptor tyrosine kinases and is known to control a range of physiological processes including cell proliferation, migration and differentiation (Lynch et al 2004, Oda et al 2005). EGFR is highly expressed in the liver (Lockhart and Berlin 2005) and was recently implicated as an entry factor for HCV (Lupberger et al 2011). Lupberger et al demonstrated through an RNAi kinase screen that silencing of EGFR inhibited HCVpp infection of both Huh7.5 and Huh7.5.1 hepatoma cells. Treatment with receptor tyrosine kinase inhibitors such as Erlotinib and Dasatinib also inhibited HCV entry, demonstrating that EGFR activity is necessary for HCV entry. In addition, stimulation of Huh7.5 cells with EGF was shown to promote viral entry. Following on from this, it has been shown that the internalisation of activated EGFR is required for HCV entry (Diao et al 2012).

Regulation of EGFR activity is controlled by endocytosis and endocytic trafficking (Chung et al 2012). Upon stimulation with ligand, activated growth factor receptors undergo endocytosis. Endocytic trafficking controls the duration and intensity of growth factor receptor signalling as the balance between EGFR recycling and degradation serves to modulate levels of receptor signalling. EGFR is involved in signalling through multiple pathways, including MAPK, PI-3K and Src. Internalisation of activated receptor into multivesicular bodies terminates the signal (Lynch et al 2004, Oda et al 2005). Conversely, growth factor receptor activation can cause modifications in trafficking pathways. EGF stimulation is known to exhibit effects on a number of endocytic pathways. Research has shown that at low physiological concentrations of EGF, the receptor internalises primarily via clathrin-mediated endocytosis (Benmerah et al 1999, Huang et al 2004), while at higher ligand

concentrations (which may be less physiologically relevant), clathrin-independent endocytosis may be employed for EGFR as the clathrin-mediated pathway becomes saturated with stimulated receptor (Sigismund et al 2005, Zhu et al 2005, Orlichenko et al 2006). Moreover, macropinocytosis is promoted in many cell types as a result of EGF stimulation and is typically described as a growth factor-dependent process (Bryant et al 2007). Therefore, it is possible that the increase in HCV entry shown by Lupberger et al occurs as a result of upregulation of one or more endocytic pathways following receptor activation, resulting in an increase in viral uptake in a receptor-dependent or receptor-independent manner.

There is growing interest in macropinocytosis as a route of viral entry and it has been shown to be the exclusive route of entry of some viruses in addition to a growing number of publications highlighting macropinocytosis as an alternative infection pathway for a wide variety of viruses with established receptor-mediated entry mechanisms (reviewed in Mercer and Helenius 2012). Some viruses bind to tyrosine kinases in order to initiate signalling events required for viral entry. For example, vaccinia virus has been shown to exhibit ‘apoptotic mimicry’, a mechanism by which exposed phosphatidyl serine in the viral envelope mimics apoptotic cells and binds to the tyrosine kinase Axl, stimulating macropinocytosis and consequent viral internalisation (Mercer and Helenius 2008, Mercer and Helenius 2010, Sandgren et al 2010, Schmidt et al 2011, Morizono et al 2011).

Additionally, macropinocytosis is associated with increased filopodia formation, where filopodia fold back and fuse with the plasma membrane, encapsulating the extracellular fluid and membrane proteins and lipids contained within in nascent macropinosomes (Ridley 2006). Filopodia have been implicated in HCV entry, where they are thought to penetrate the sinusoidal membrane where they are able to

interact with T-lymphocytes and viral particles circulating in the sinusoidal blood, perhaps mediating the first contact with the virus (Warren et al 2006). Live cell imaging of DiD-labelled HCV particles in Huh7.5 cells expressing CD81-GFP showed that viral particles bind to CD81 in filopodia and 'surf' towards the cell body where endocytosis can occur (Coller et al 2009). Many different viruses associate with the microvilli of polarized epithelia as well as the filopodia of nonpolarized cells, including MLV and VSV-G, which enter cells via different endocytic mechanisms (Helenius et al 1980, Duus et al 2004, Smith and Helenius 2004, Lehmann et al 2005). Virus particles surfing along filopodia are thought to exploit the inherent ability of filopodia to transport ligands towards the cell body and represents another example of viruses hijacking host cell machinery in order to achieve efficient infection (Lehmann et al 2005). Therefore it is important to consider macropinocytosis and filopodial extension as potential HCV entry-promoting effects of EGF stimulation of Huh7.5 cells.

Nevertheless, the established entry mechanism of HCV is clathrin-mediated endocytosis (Blanchard et al 2006) and it is thought that virus binding induces association of CD81 and CLDN1 and their internalisation by clathrin-mediated endocytosis (Harris et al 2008, Farquhar et al 2012). However, the host-virus interactions that govern HCV internalisation are still not well understood.

As EGFR internalization is thought to be critical for HCV entry (Diao et al 2012), determining the mechanism of internalisation of the receptor is of critical importance in understanding HCV entry. Under physiological concentrations of EGF, EGFR typically internalises via clathrin-mediated endocytosis (Benmerah et al 1999, Huang et al 2004). As such, the effects of EGF stimulation on clathrin-mediated endocytosis must be considered as a potential mechanism for increased viral entry.

As EGF stimulation is known to induce multiple cellular effects, depending on the concentration, ligand and cell type, it is important to determine the effects of EGF stimulation on endocytic pathways in Huh7.5 cells that may contribute to EGF-promoted HCV entry.

4.2. Chapter Aims

The epidermal growth factor receptor (EGFR) has recently been implicated as an entry factor for HCV and EGF stimulation has been shown to promote HCV entry into Huh7.5 cells (Lupberger et al 2011). This stimulation of virus entry could be the result of promotion of the established clathrin-mediated route of virus entry as well as via EGF-mediated stimulation of other routes of internalisation such as macropinocytosis. The aims of this chapter are therefore to delineate the effects of EGF stimulation on endocytic pathways in Huh7.5 cells, with particular respect to the established viral entry route, clathrin-mediated endocytosis, as well as the growth factor-stimulated process of macropinocytosis, and associated filopodial formation and extension.

4.3 Results

4.3.1 EGF Stimulation Promotes Macropinocytosis in Huh7.5 Cells

To observe the broad effects of EGF stimulation on hepatoma cell morphology, Huh7.5 cells were transiently transfected with CFP-mem (**Table 2.1**), a construct encoding a CFP-tagged farnesylated fluorescent protein which inserts into the plasma membrane, allowing movements of the plasma membrane to be imaged in real time by live-cell confocal microscopy. A single *z*-plane in the centre of cells, where the plasma membrane was most clearly visible was selected and confocal images acquired at this focal plane in multiple *x,y* positions every minute for 60 minutes. The most apparent effects of EGF stimulation were a visibly dramatic increase in plasma membrane ruffling, lamellipodia and filopodia formation, and membrane blebbing, all of which are indicative of macropinocytosis. This is shown in **Figure 4.1**, with yellow arrows highlighting endocytic vacuoles which appear to be macropinosomes. The effects of EGF stimulation on ruffling and blebbing in Huh7.5 cells also appear to be dose-dependent, with a concentration of 20 ng/ml, a concentration typically used in studies of EGFR signalling events (e.g. Wang et al 2002, Ren et al 2011), inducing a modest but noticeable amount of plasma membrane ruffling, and the appearance of some visible large endocytic vacuoles, possibly macropinosomes even from early timepoints of stimulation, as indicated by the yellow arrows (**Figure 4.1 A**). Similar, but more pronounced effects were seen with stimulation with a slightly higher concentration of 100 ng/ml EGF, a concentration typically used in studies of EGFR trafficking (e.g. Rappoport and Simon 2009, Sousa et al 2011) (**Figure 4.1 B**). However, much more dramatic effects were observed at a high concentration of 1 µg/ml EGF (the concentration

used by Lupberger et al 2011 to promote viral entry), and large membrane-bound vacuoles which resemble macropinosomes are clearly visible within stimulated cells, as indicated by the yellow arrows (**Figure 4.1 C**). The formation of blebs and macropinosomes in cells treated with 1 µg/ml EGF can be more clearly seen in **Supplementary Video 1 B**. While this is an extremely high concentration of EGF compared to the majority of published work on EGFR signalling and trafficking, the effects can be seen, albeit to a lesser extent, in cells stimulated with the more physiological concentrations shown in **Figure 4.1 A and B**. Therefore, we expect these effects to be physiologically relevant. Additionally, as this is the concentration shown to promote viral entry by Lupberger et al, these effects are potentially relevant to the associated increase in viral entry; therefore this is the concentration of EGF used for all further investigations into the EGF-stimulation of Huh7.5 cells, unless otherwise stated.

Internalisation of CFPmem under stimulation with 1 µg/ml EGF was quantified in **Figure 4.2** to determine if EGF stimulation resulted in bulk membrane uptake, as would be expected for macropinocytosis. To achieve this, Huh7.5 cells transiently transfected with CFPmem were imaged every 1 minute for 60 minutes in a single central plane of focus by confocal microscopy both with and without EGF stimulation (**Supplementary Video 1 A and B**, respectively). Regions of interest (ROIs) were then drawn around the plasma membrane and the intracellular area within the plasma membrane and fluorescence intensity measured at timepoints at 5 minute intervals. Background fluorescence was subtracted from each frame, and data normalised to the fluorescence intensity of the ROI at time 0. Without EGF stimulation, both plasma membrane fluorescence and intracellular CFP fluorescence remained fairly constant throughout the confocal timelapse with little internalisation

or photobleaching apparent, as shown in **Figure 4.2**. In contrast, stimulation with 1 µg/ml EGF resulted in a drop in plasma membrane CFP fluorescence throughout the timelapse. By the 60 minute timepoint, plasma membrane fluorescence was reduced to 67.5% of that of unstimulated cells. As photobleaching is not observed in the control (unstimulated) cells, this decrease is likely to be due to internalisation of areas of the plasma membrane rather than photobleaching. Correspondingly, EGF stimulation results in an increase in internal fluorescence signal throughout the timelapse, consistent with bulk internalisation of large areas of the plasma membrane.

To confirm that EGF stimulation promotes macropinocytosis, a dextran uptake assay was carried out. 10 kDa dextran is a fluid phase marker, which, due to its size is largely internalised by macropinocytosis (although a low level of basal internalisation does occur in the absence of stimulation with EGF). As demonstrated by **Figure 4.3**, EGF stimulation results in a substantial increase in dextran uptake in Huh7.5 cells, with the fluorescence intensity of dextran-568 within cells stimulated with 1 µg/ml EGF for 30 minutes 3.89 times the basal level fluorescence observed in unstimulated cells. This corroborates the increase in macropinocytosis seen by live-cell imaging of CFPmem-transfected cells in response to EGF treatment.

As macropinocytosis occurs in response to EGF stimulation, resulting in internalisation of both areas of the plasma membrane and extracellular fluid, it is possible that this effect of EGF stimulation contributes to the EGF-induced promotion of viral entry demonstrated by Lupberger et al. However, macropinocytosis is typically thought to be a relatively non-specific internalisation mechanism, with bulk uptake of areas of the plasma membrane and the extracellular fluid contained within. As such, although HCV may be internalised by EGF-induced macropinocytosis, this

route of entry may be receptor-independent and non-specific for HCV. Additionally, as the intracellular trafficking of macropinosomes is poorly understood, it is not clear whether macropinocytic viral uptake would result in productive HCV infection.

Summary:

1. **EGF stimulation of Huh7.5 cells promotes a dose-dependent increase in plasma membrane ruffling, lamellipodia formation and blebbing, indicative of macropinocytosis.**
2. **EGF stimulation results in bulk plasma membrane internalisation, suggesting macropinocytosis.**
3. **EGF stimulation promotes dextran uptake in Huh7.5 cells, confirming EGF-dependent stimulation of macropinocytosis.**

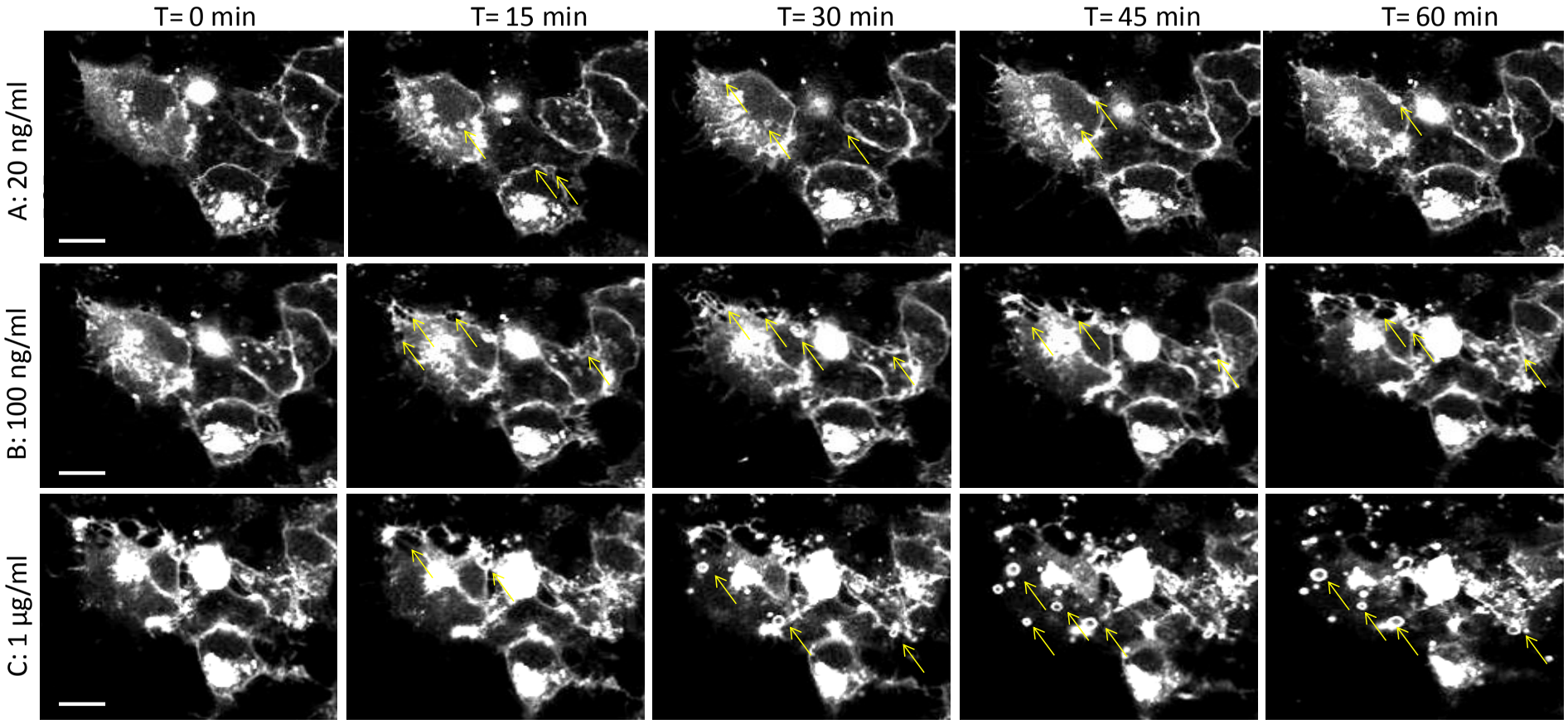

Figure 4.1: Dose -dependent stimulation of macropinocytosis by EGF. Huh7.5 cells were transfected with CFPmem to mark the plasma membrane and then stimulated with A: 20 ng/ml EGF, B: 100 ng/ml EGF or C: 1 µg/ml EGF for one hour. Ruffling, blebbing and macropinosome formation (yellow arrows) can be seen after 15 minutes stimulation. Scale bar= 10 µm.

4.3.2 EGF Stimulation promotes filopodia formation and elongation in Huh7.5 cells

Hepatocytes and hepatoma cells have been shown to be rich in filopodia protruding from the cell body (Warren et al 2006, Amy Barnes M.Res thesis). It has been suggested that the filopodia of hepatocytes extend through the sinusoidal membrane where they are able to make contact with T-cells, suggesting a role for filopodia in mediating first contact with the virus (Warren et al 2006).

Many viruses have been observed in association with the microvilli of polarised epithelial cells, as well as with filopodia of non-polarised cells (Helenius et al1980, Duus et al 2004, Smith and Helenius 2004, Lehmann et al 2005). Recently, some of these, including MLV and VSV-G have been shown to bind to receptors in the filopodia membrane and exploit the intrinsic ability of filopodia to transport receptors to the cell body for internalisation, in an actin and myosin II- dependent manner (Lehmann et al 2005).

HCV has been shown to initially associate with filopodia in Huh7.5 cells before 'surfing' towards the cell body for endocytosis (Coller et al 2009) and, in support of this, the inhibitor of actin polymerisation, Cytochalasin D markedly inhibits HCV entry (Codran et al 2006, Coller et al 2009). The HCV receptor CD81 is highly expressed within filopodia (Coller et al 2009) and is known to interact directly with viral particles (Pileri et al 1998, Zhang et al 2004). Thus, Coller et al propose a mechanism whereby viral particles bind to CD81 in filopodia before surfing towards the cell body where other viral receptors, entry factors and endocytic proteins are localised and viral entry can occur. EGF stimulation is known to induce WAVE- and Arp2/3-dependent ruffling, resulting in both lamellipodia and filopodia formation, in association with macropinocytosis. As results from **section 4.3.1** demonstrate that

macropinocytosis is significantly upregulated in Huh7.5 cells in response to EGF stimulation, and increased ruffling, lamellipodia and filopodia are clearly visible in **Figure 4.1**, this effect could be relevant to viral entry, aiding virus attachment and binding in both *in vitro* and *in vivo* settings.

To observe filopodia formation and/or elongation in response to EGF treatment, Huh7.5 cells overexpressing CD81-GFP were imaged by confocal microscopy at the plane of focus with the highest number of filopodia (close to the adherent plasma membrane) every minute for 30 minutes following stimulation with 1 µg/ml EGF. As shown in **Figure 4.4**, the average number of filopodia per µm showed a modest but significant increase following 30 minutes of stimulation with EGF. This could potentially increase the likelihood of viral particles coming into contact with target cells. Interestingly, filopodia visible throughout the timelapse also increased significantly in length during the course of the EGF stimulation, from an average of 1.86 µm to 2.71 µm (a 31.4% average increase). To take both effects into consideration, a metric called the 'filopodial index' was calculated (filopodial index= length x number/area). The filopodial index saw a marked and statistically significant increase in response to EGF treatment.

It is possible that this effect of EGF stimulation is responsible for increased viral entry, where *in vitro* more and longer filopodia would be able to increase virus binding and *in vivo*, where longer filopodia would be able to extend further through the sinusoidal membrane, aiding virus attachment.

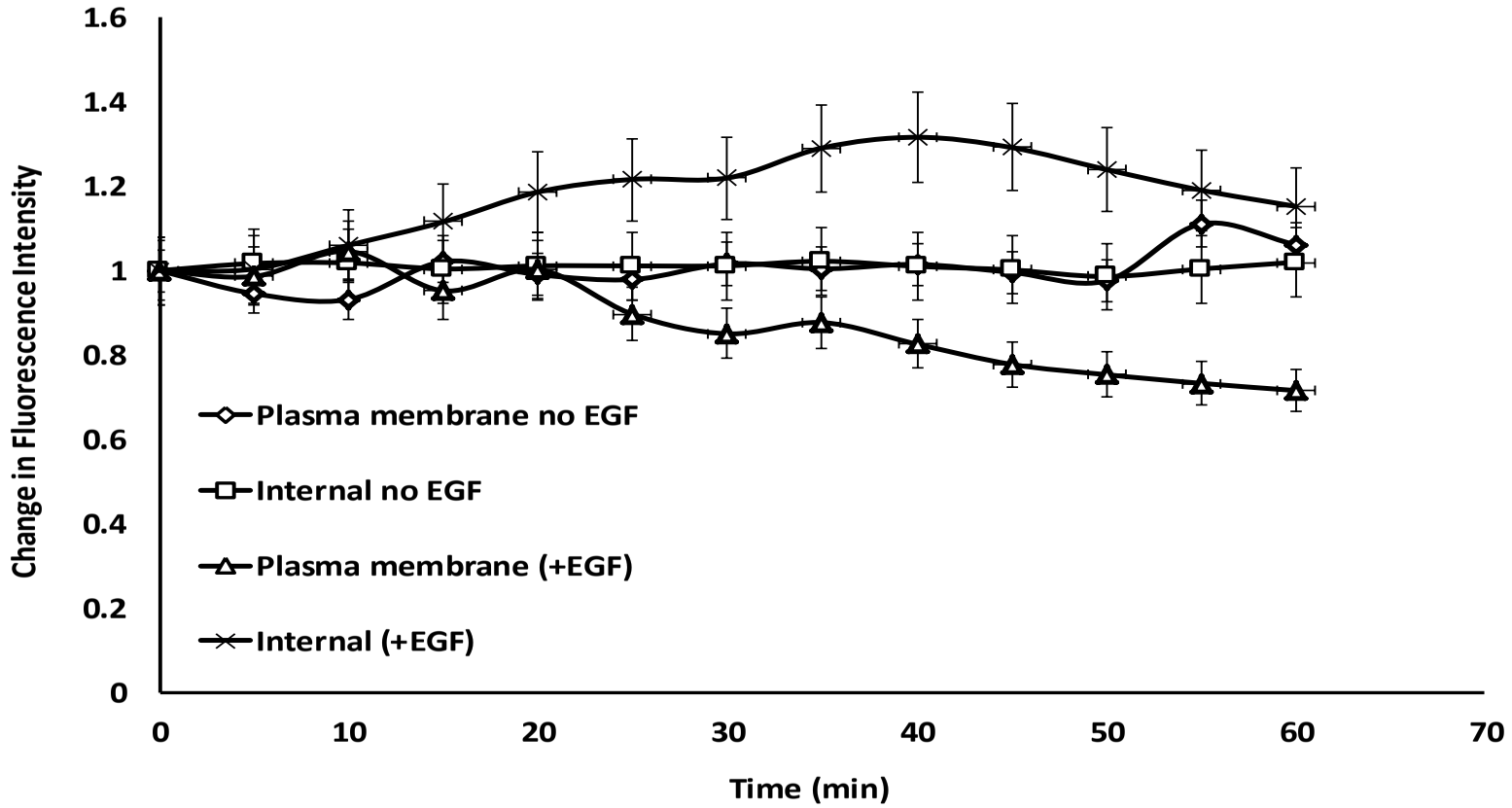

Figure 4.2: Bulk membrane uptake is stimulated by EGF treatment. Huh7.5 cells were transfected with CFPmem to mark the plasma membrane and then imaged by live cell confocal microscopy with and without stimulation with 1 µg/ml EGF for one hour. Intracellular and plasma membrane fluorescence were measured and plotted against time. 9 cells were imaged and analysed per condition. Error bars = standard error.

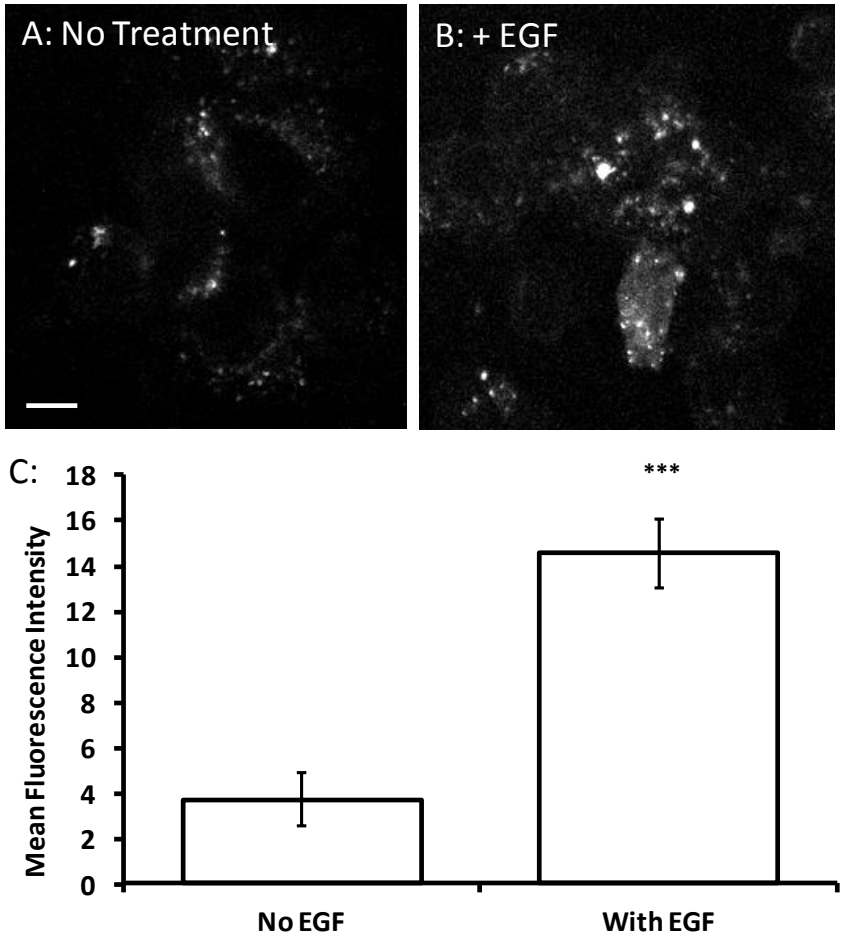

Figure 4.3: Dextran uptake in response to EGF stimulation. Huh7.5 cells incubated with fluorescent 10 kDa dextran without EGF stimulation (A) or with stimulation with 1 µg/ml EGF (B) and imaged by confocal microscopy . Scale bars = 10 µm. 60 cells were analysed per group, data shown are the mean from three independent experiments. Error bars = standard error.

4.3.3 CD81 is not enriched in filopodia following EGF stimulation

As shown in **Section 4.3.2**, filopodia formation and elongation are promoted in response to EGF stimulation of Huh7.5 cells. Filopodia have been implicated in HCV entry (Codran et al 2006, Coller et al 2009). As such, this effect of EGF stimulation may be relevant to the increase in viral entry seen in response to EGF stimulation. CD81 is highly expressed in filopodia and is thought to mediate binding of the virus to filopodia and its translocation towards the cell body (Coller et al 2009). Previous work has shown that CD81 is enriched within filopodia, and the diffusion coefficient of CD81 within filopodia is significantly higher than that at the plasma membrane (Amy Barnes M.Res thesis). However, the expression of CD81 within filopodia following EGF treatment has not been investigated to date.

Therefore, we investigated whether CD81 was enriched in filopodia following EGF stimulation. Huh7.5 cells overexpressing CD81-GFP were imaged by live-cell confocal microscopy, with images acquired every five minutes for 1 hour in the plane of focus containing the most visible filopodia. A 2 pixel x 2 pixel ROI was drawn within filopodia at time zero and after 30 minutes EGF stimulation and fluorescence intensity measured. As shown in **Figure 4.5**, there was no significant difference in the CD81-GFP fluorescence intensity within filopodia between EGF-treated and untreated cells.

Summary:

1. **EGF stimulation promotes filopodia formation in Huh7.5 cells, resulting in increased numbers of filopodia following 30 minutes of stimulation at 1 µg/ml.**

2. **EGF stimulation results in elongation of filopodia.**
3. **Filopodia may play a role in HCV infection by binding to virus and allowing it to translocate towards the cell body for internalisation.**
4. **Localisation of HCV co-receptor CD81 within filopodia is not enriched by EGF stimulation.**

4.3.4 EGF Stimulation Promotes Clathrin-Mediated Endocytosis in Huh7.5 Cells

Although macropinocytosis is a growth factor-dependent process, EGF stimulation is known to exert effects on other endocytic pathways, depending on the cell line and concentration used. High concentrations of EGF stimulation, such as that used by Lupberger et al to promote HCV entry, are thought to induce uptake of activated EGFR by caveolar endocytosis (Sigismund et al 2005, Zhu et al 2005, Orlichenko et al 2006). However, as we have already demonstrated that Huh7.5 cells do not express caveolin 1 (**Figure 3.1A**), this pathway can be excluded from our analysis. At physiological concentrations, EGF stimulation has been shown to promote clathrin-mediated endocytosis, resulting in internalisation of activated EGFR via this route (Benmerah et al 1999, Huang et al 2004). As the established route of entry for HCV and receptor CD81 is by clathrin-mediated endocytosis, it is important to consider the effects EGF stimulation has on this pathway in Huh7.5 cells.

To investigate the possibility that clathrin-mediated endocytosis is upregulated in response to EGF treatment, Huh7.5 cells were transiently transfected with Clathrin-dsRed (Table 2.1) and the same cells imaged by total internal reflection fluorescence microscopy (TIRF) microscopy both before EGF stimulation and after 30 minutes stimulation with 1 μg/ml EGF to observe clathrin-coated pit formation on the adherent plasma membrane.

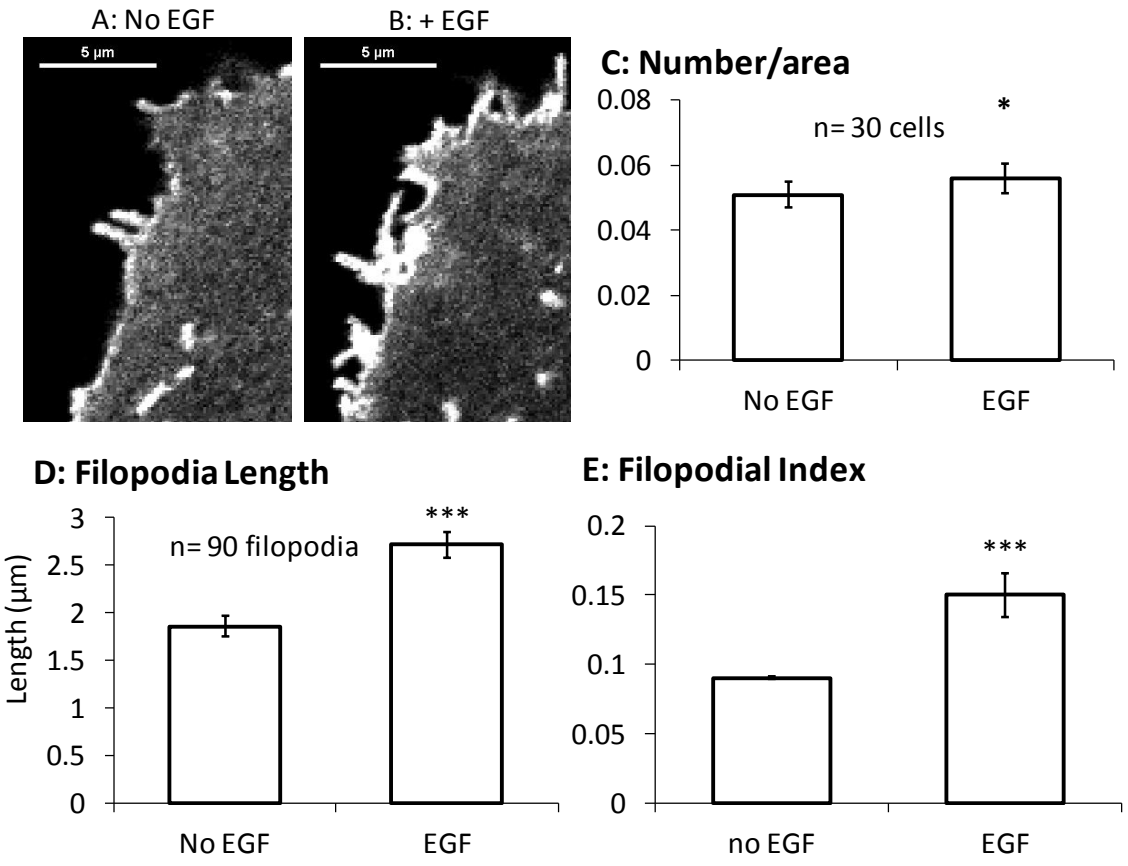

Figure 4.4: EGF stimulation promotes filopodia formation. Huh7.5 cells transiently transfected with CD81-GFP to label the filopodia and imaged by TIRF microscopy prior to EGF treatment (A) and following 30 min EGF stimulation at 1 µg/ml (B). Quantification of the number of filopodia per unit area is shown in (C), quantification of filopodia length is shown in (D) and filopodial index quantification is shown in (E). Data shown are the means of three repeats. Error bars = standard error.

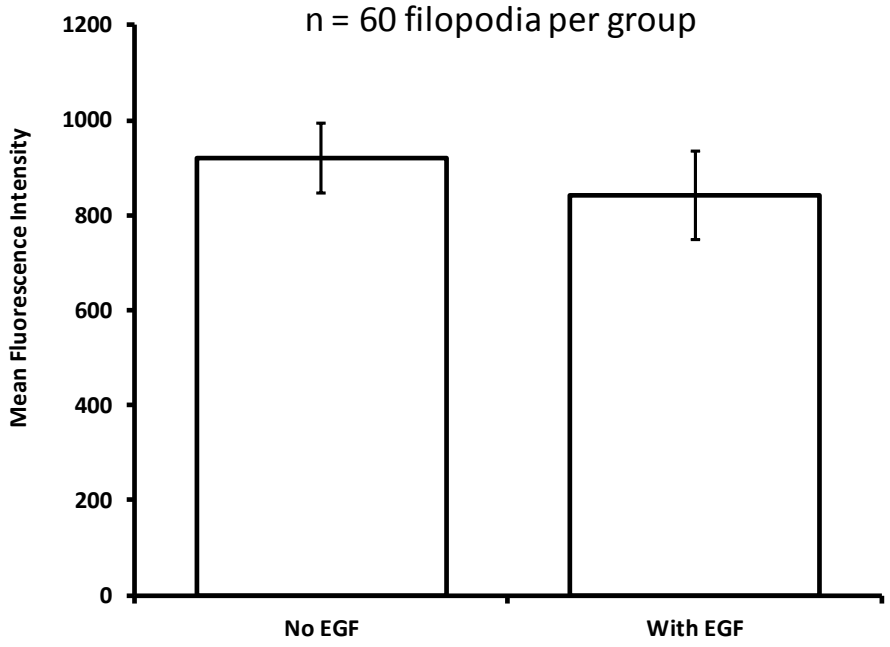

Figure 4.5: CD81 is not enriched in filopodia upon EGF stimulation. Huh7.5 cells overexpressing CD81-GFP were imaged by confocal microscopy with and without stimulation with 1 µg/ml EGF for 30 minutes, and CD81 fluorescence intensity within filopodia measured. Data shown are the mean of three independent experiments. 60 filopodia per group were analysed. Error bars = standard error.

Using an automatic analysis approach generated by Jeremy Pike (Rappoport lab), CD81 cluster density in the adherent plasma membrane was measured with and without EGF stimulation. As shown in **Figure 4.6**, 30 minutes EGF stimulation results in an average 17.71% increase in the 'structure density' of clathrin punctae in the adherent plasma membrane, demonstrating that more clathrin-coated pits are being formed under conditions of EGF stimulation. This indicates that clathrin-mediated endocytosis is upregulated in response to EGF treatment.

To observe whether activated EGFR internalises via clathrin-mediated endocytosis, Huh7.5 cells were transiently transfected with EGFR-GFP and Clathrin-dsRed (**Table 2.1**) and imaged by TIRF microscopy with and without EGF stimulation in order to observe the clustering and colocalisation of the proteins on the adherent plasma membrane. As shown in **Figure 4.7**, prior to addition of EGF, clathrin punctae were observable on the adherent plasma membrane but EGFR expression was more diffuse throughout the plasma membrane, with little observable receptor clustering. Following 30 minutes EGF stimulation, clusters of EGFR become visible and these clearly co-localise to a high degree with clathrin punctae, indicating a clathrin-mediated entry route for the activated receptor. Therefore, we can conclude that EGF stimulation promotes clathrin-coated pit formation in Huh7.5 cells, resulting in clathrin-mediated endocytosis of the activated receptor.

As HCV is known to internalise via clathrin-mediated endocytosis in Huh7.5 cells, this effect of EGF stimulation is likely to be relevant to the EGF-stimulated promotion of viral entry. Additionally, the internalisation of EGFR has been shown to be necessary for HCV entry (Diao et al), therefore this effect is of EGF stimulation is of key relevance to HCV entry.

However, it is unclear whether HCV and its receptors internalise along with EGFR. Therefore, it will be necessary to determine whether viral receptors and entry factors colocalise and internalise with EGFR following EGF treatment.

Summary:

1. **EGF stimulation promotes clathrin-coated pit formation in Huh7.5 cells.**
2. **EGF stimulation results in clustering of EGFR on the plasma membrane, and clustered EGFR colocalises with clathrin, suggesting a clathrin-mediated route of entry for the activated receptor.**

4.3.5 Knockdown of PAK1 and AP2 in Huh7.5 cells

Results from this chapter clearly demonstrate that two endocytic pathways are upregulated in response to EGF stimulation of Huh7.5 cells, which could offer a mechanism for the EGF-induced increase in viral entry in these cells. The clathrin-mediated pathway, which is the classical entry route for HCV is stimulated, as well as macropinocytosis, which is being shown to be involved in the entry of an increasing number of viruses (Mercer and Helenius 2008). In order to delineate the effects of each pathway on EGF-stimulated HCV entry, inhibition of each pathway must be achieved, as in **Chapter 3**. As AP2 is involved exclusively in clathrin-mediated endocytosis and was successfully knocked down in SkHep1 (SRBI+CLDN1) cells (**Figure 3.9**), the same siRNA sequence was transfected into Huh7.5 cells and a western blot for AP2 carried out.

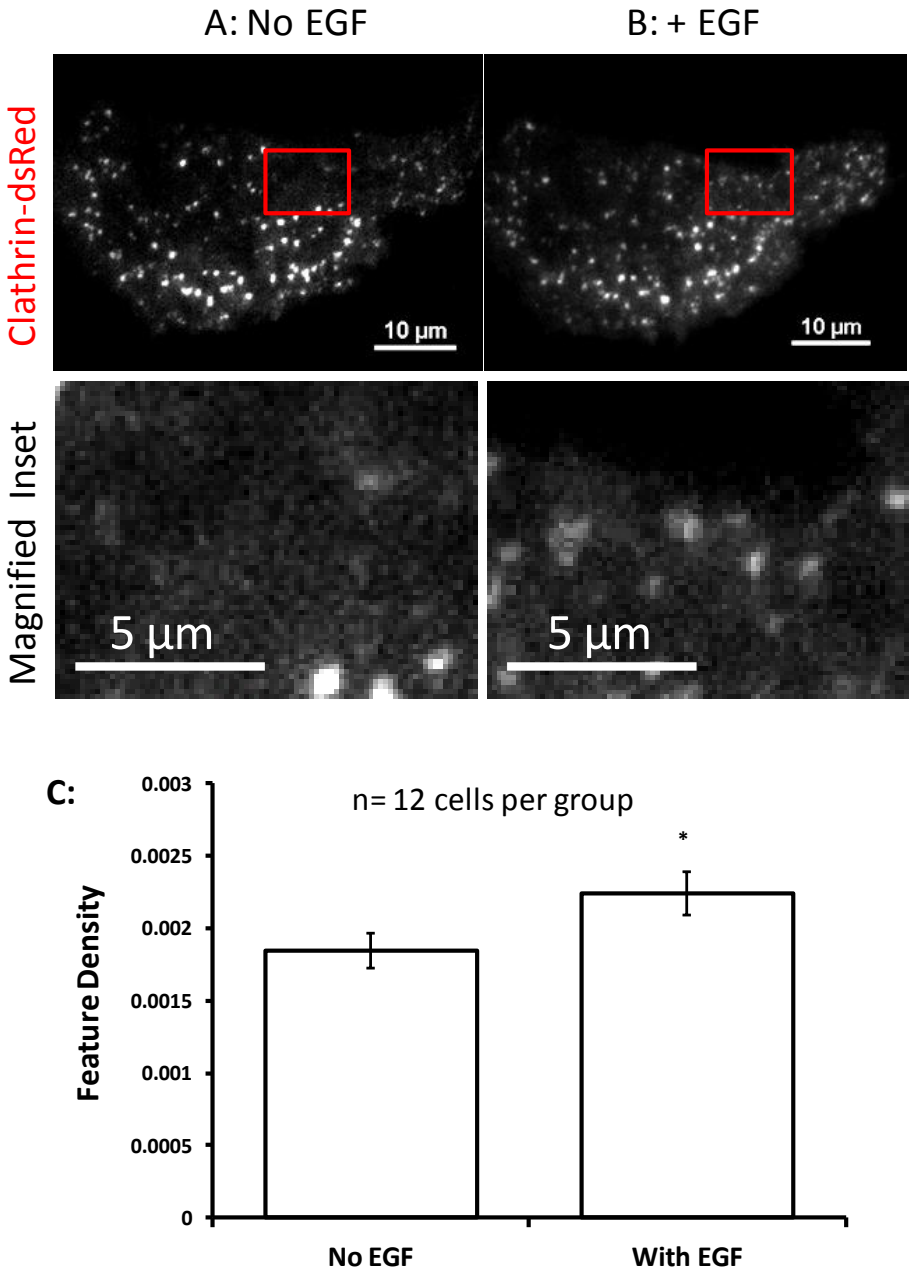

Figure 4.6: EGF stimulates clathrin-coated pit formation. Huh7.5 cells transiently transfected with clathrin-dsRed and imaged by TIRF microscopy prior to EGF treatment (A) and following 30 min EGF stimulation at 1 µg/ml (B). Quantification of the number of clathrin coated pits is shown in (C). Feature density analysis was performed by Jeremy Pike, PSIBS doctoral training centre, Univeristy of Birmingham, UK. 12 cells per group were analysed and means are shown. Error bars = standard error.

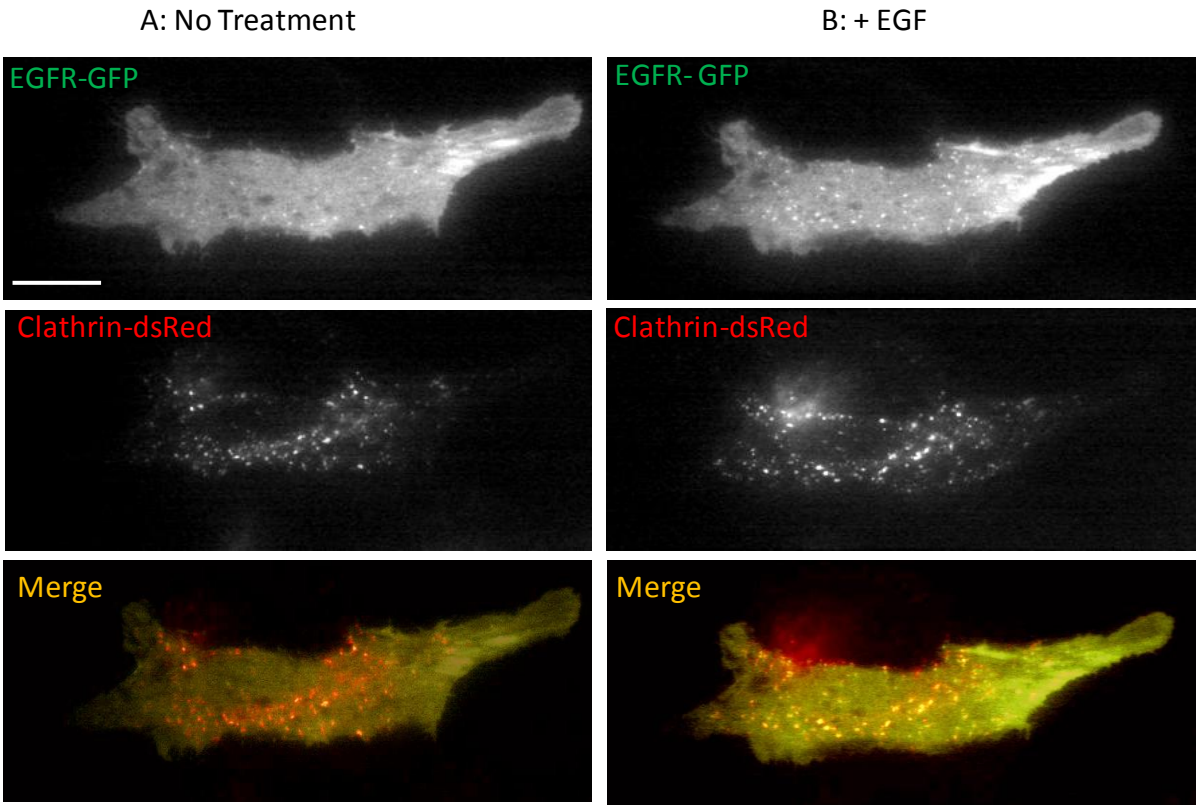

Figure 4.7: EGFR colocalises with clathrin upon EGF stimulation. Huh7.5 cells overexpressing EGFR-GFP and Clathrin-dsRed were imaged by TIRF microscopy prior to EGF stimulation (A) and after 30 minutes stimulation with 1 µg/ml EGF. Scale bar= 5 µm.

As shown in **Figure 4.8 B**, successful knockdown of AP2 was achieved, and this was confirmed by a Tf uptake assay (**Figure 4.8 D**). PAK1 has been shown to be important for all stages of macropinocytosis, including macropinosomes formation and closure, and inhibition of PAK1 has been shown to inhibit macropinocytosis in other cell lines, without affecting other endocytic pathways (Dharmawardhane et al 2000, Parrini et al 2005, Liberali et al 2008). Therefore, a PAK1 siRNA sequence (Dharmacon) was transfected into Huh7.5 cells and a western blot carried out to assay protein levels. As shown in **Figure 4.8 A**, PAK1 protein levels in siRNA-transfected cells are visibly lower than in those transfected with a non-silencing control (NSC). The functionality of this knockdown was confirmed by a dextran uptake assay. As shown in **Figure 4.8 C**, dextran uptake was significantly inhibited in PAK1 knockdown cells when compared to NSC-transfected cells. This preliminary work will allow for the contribution of each endocytic pathway to EGF-stimulated HCV entry to be determined in future HCVpp infection assays.

4.4 Discussion

The epidermal growth factor receptor (EGFR) has recently been identified as an entry factor for HCV (Lupberger et al 2011). Lupberger et al show that silencing of EGFR and inhibition with kinase inhibitors reduces HCV infection. Additionally, the authors show that stimulation of Huh7.5 cells with a high concentration (1 µg/ml) of EGF promotes viral entry in Huh7.5 cells. EGFR activation is known to affect endocytic trafficking and could therefore promote viral entry by stimulating viral endocytosis by one or more endocytic mechanisms in a receptor-dependent or -independent manner. Therefore, the aim of this chapter was to characterise the effects that EGF stimulation has on endocytic pathways in Huh7.5 cells.

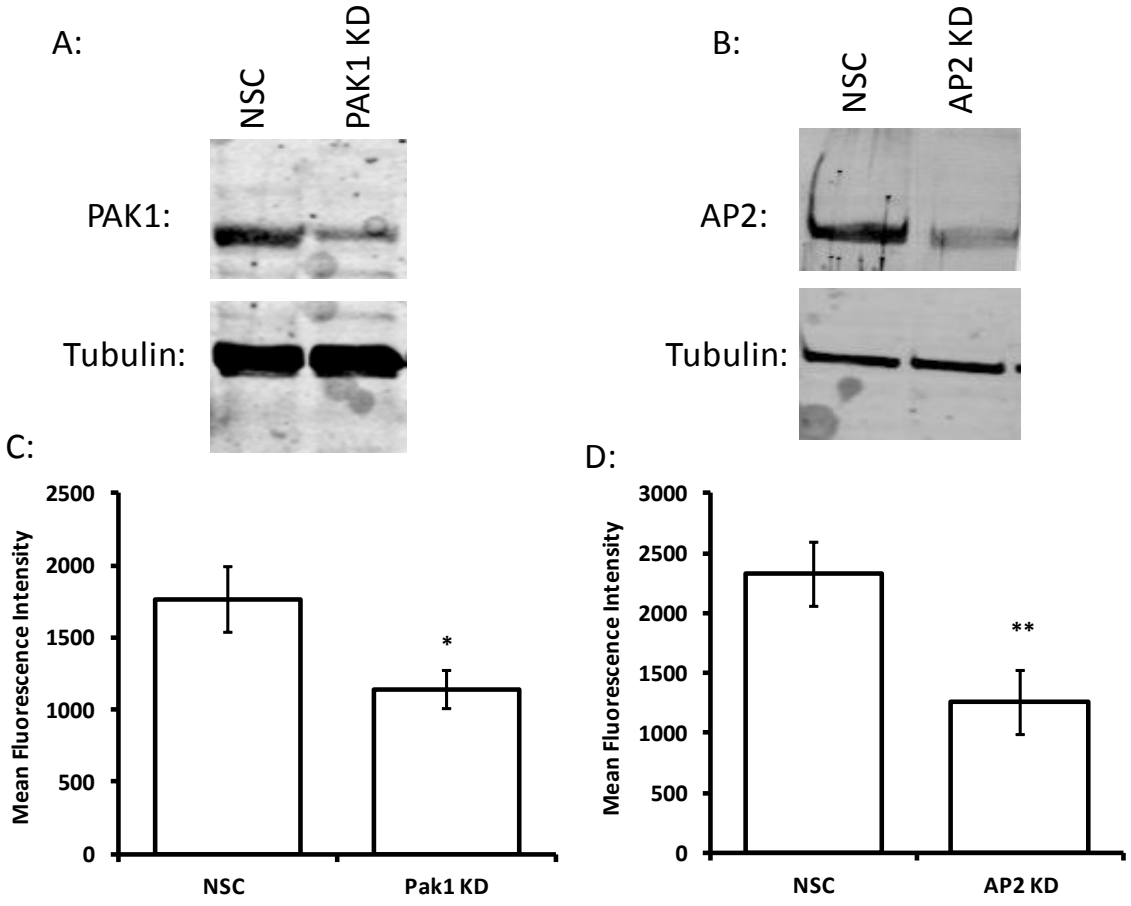

Figure 4.8: Knockdown of AP2 and PAK1 in Huh7.5 cells. Western blots showing knockdown of PAK1 and AP2 in Huh7.5 cells (A & B). Quantification of internalised dextran in Huh7.5 cells transfected with a non-silencing control (NSC) or with PAK1 siRNA (C). Quantification of internalised Tf fluorescence in Huh7.5 cells transfected with a non-silencing control (NSC) or with AP2 siRNA (D). 60 cells per condition were analysed and means are shown. Error bars = standard error.

To observe the effects of EGF stimulation, Huh7.5 cells were transiently transfected with CFPmem to label the plasma membrane and cells imaged by live-cell confocal microscopy at increasing EGF concentrations. The concentration used by Lupberger et al to promote HCV entry (1 µg/ml) is an extremely high concentration to treat cells with so multiple EGF concentrations were initially tested to observe their effects on Huh7.5 cells. Firstly, cells were treated with 20 ng/ml EGF, a concentration typically used in studies of EGFR signalling (e.g. Wang et al 2002, Ren et al 2011). This led to modest but observable ruffling of the plasma membrane, as well as the appearance of large intracellular membrane-bound vacuoles, indicative of macropinocytosis. These same effects were seen to a greater extent when the EGF concentration was increased to 100 ng/ml, a concentration typically used in studies of the endocytic trafficking of EGFR (e.g. Rappoport and Simon 2009, Sousa et al 2011). Finally, the EGF concentration was increased to 1µg/ml as this was the concentration used in Lupberger et al 2011 to promote HCV entry. Treatment with this concentration led to significant cell-wide plasma membrane ruffling, lamellipodia and filopodia formation and membrane blebbing, all of which are indicative of macropinocytosis (**Figure 4.1**). This is an extremely high concentration of EGF; however these same effects are visible at lower concentrations, as indicated by the yellow arrows, even at early timepoints. As these effects increase in a dose-dependent manner, and are most prominent at the concentration used by Lupberger et al, they may be relevant to the EGF-induced increase in HCV entry. As the effects are most apparent at 1 µg/ml, and this is the concentration at which HCV entry has been shown to be promoted, this was the concentration used for further investigations into the effects of EGF stimulation. This was also the concentration used to quantify the bulk membrane internalisation seen upon EGF stimulation

(shown in **Supplementary Video 1**). Quantification of plasma membrane fluorescence during 60 minutes EGF stimulation revealed that the plasma membrane fluorescence of EGF-treated cells decreased to around 60% of that of untreated cells by the 60 minute timepoint (**Figure 4.2**). Correspondingly, intracellular fluorescence increased in response to EGF stimulation, demonstrating that EGF stimulation promotes bulk plasma membrane internalisation, indicative of macropinocytosis. To confirm induction of macropinocytosis, uptake of the fluid-phase marker 10kDa dextran was measured in untreated and EGF-treated cells. As shown in **Figure 4.3**, dextran uptake was significantly upregulated in response to EGF treatment, confirming that EGF stimulation promotes macropinocytosis in Huh7.5 cells. Therefore, the promotion of HCV entry by EGF stimulation of Huh7.5 cells may be due to fluid-phase uptake of viral particles in the surrounding extracellular fluid. However, macropinocytosis is thought to be a relatively non-specific process, resulting in bulk uptake of the plasma membrane and the extracellular fluid contained within. Therefore, both receptor-bound and unbound virus could be internalised non-specifically via this mechanism. It has been shown that EGF treatment promotes pseudoparticle infection not only of HCV in Huh7.5 cells, but also of influenza A, VSV, and endogenous feline leukaemia virus (RD114). Treatment with protein kinase inhibitors Erlotinib and Dasatinib also reduced infection of these viruses in Huh7.5 cells, whereas EGF and kinase inhibitors exhibited no effect on measles virus entry into these cells (Lupberger et al 2011).Therefore, it seems that the effects of EGF stimulation on Huh7.5 cells are not specific to HCV, however, they do not promote infection of all viruses.

Influenza viruses and VSV are thought to be typically internalised via clathrin-mediated endocytosis (Lakadamyali et al 2004, Cureton et al 2009), whereas

measles virus and RD114 are thought to fuse directly with the plasma membrane in a pH-independent manner (Sandrin et al 2002). Therefore, macropinocytosis could offer an explanation for the internalisation of viruses with multiple entry pathways in response to EGF stimulation.

However, as endocytic trafficking following macropinocytosis is poorly understood, it is unclear if viral particles entering via this pathway would traffic through the same compartments as particles internalised via clathrin-mediated endocytosis. As HCV infection is pH and Rab5 -dependent, it is thought that fusion occurs within the early endosome; therefore traffic through this compartment is crucial for productive infection to occur.

However, more recently evidence has come to light that macropinocytosis operates some sorting capacity with different growth factors stimulating internalisation of some receptors over others (Schmees et al 2012). Therefore, EGF-induced macropinocytosis may operate in a receptor-dependent manner, with internalisation of some receptors promoted over that of others. Whether the internalisation of HCV receptors and entry factors is promoted by EGF stimulation is something that must therefore be determined.

However, as HCV is thought to internalise via clathrin mediated endocytosis in Huh7.5 cells, it was important to ascertain the effects of EGF stimulation on this pathway (Blanchard et al 2006). Therefore, clathrin-dsRed transfected cells were imaged via TIRF microscopy before and after EGF stimulation and clathrin coated pit density in the plasma membrane measured. EGF stimulation increased the density of clathrin punctae in the plasma membrane, demonstrating that EGF stimulation promotes clathrin-mediated endocytosis in Huh7.5 cells in addition to

macropinocytosis (**Figure 4.6**). Additionally, EGFR was shown to cluster on the cell surface in response to EGF stimulation and colocalise with these clathrin punctate, indicating that EGF stimulation promotes EGFR internalisation via clathrin-mediated endocytosis (**Figure 4.7**). EGFR endocytosis has been shown to be important for HCV entry as the requirement for kinase activation can be bypassed by treatment with EGFR antibodies that block both ligand-induced EGFR activation but still induce EGFR internalisation (Diao et al 2012). EGFR has been shown to internalise via different mechanisms, depending on the concentration of applied ligand, primarily internalising via clathrin-mediated endocytosis at physiological concentrations (Benmerah et al 1999, Huang et al 2004) and via clathrin-independent mechanisms when concentrations are increased and conventional internalisation routes become saturated (Sigismund et al 2005, Zhu et al 2005, Orlichenko et al 2006). As the concentrations of EGF applied in HCV entry studies (Lupberger et al 2011, Diao et al 2012) are extremely high, the demonstration of EGFR internalisation via clathrin-mediated endocytosis under these conditions is of key relevance to HCV entry.

It remains to be determined, however, whether HCV and HCV receptors internalise with EGFR. It will therefore be interesting to investigate whether HCV receptors colocalise with and internalise with activated EGFR in this manner following EGF stimulation.

As both pathways are upregulated in response to EGF stimulation, it is unclear whether one or both pathways contribute to the EGF-induced increase in HCV entry. Infection of several viral pseudoparticles with different entry mechanisms is upregulated in Huh7.5 cells in response to EGF stimulation, including VSV and influenza A which internalise via clathrin-mediated endocytosis under normal circumstances (Cureton et al 2009, Lakadamyali et al 2004). As EGFR is also

internalised via a clathrin-mediated endocytic mechanism in response to stimulation with 1 µg/ml EGF in Huh7.5 cells, this is suggestive of the upregulation of clathrin-mediated endocytosis being responsible for increased infection of viruses with established clathrin-mediated entry routes such as HCV.

Macropinocytosis however, may offer an explanation for the EGF-induced increase in entry of viruses with direct fusion entry mechanisms. These viruses are not dependent on pH-mediated fusion within intracellular compartments and so would not be dependent on trafficking through the endosomal system for fusion and productive infection to occur.

One way to delineate between the effects of the two upregulated endocytic pathways on HCV entry would be to knock down components of each pathway, as shown for caveolin 1 in **Chapter 3**. As AP2 is required for clathrin-mediated endocytosis and was knocked down successfully in SkHep1 (SRBI+CLDN1) cells, the same sequence was used with success in Huh7.5 cells (**Figure 4.8 B and D**). PAK1 has been shown to be crucial to all stages of macropinocytosis (Dharmawardhane et al 2000, Parrini et al 2005, Liberali et al 2008) and expression of a PAK1 autoinhibitory domain or dominant negative PAK1 in NIH-3t3 cells has been shown to dramatically inhibit the rate of macropinocytosis stimulated by activated PDGFR (Dharmawardhane et al 2000) without any effect on other endocytic processes such as clathrin-mediated endocytosis. Therefore, PAK1 siRNA was used to inhibit macropinocytosis in Huh7.5 cells (**Figure 4.8 A and C**). Both siRNAs reduced levels of the relevant protein and inhibited dextran and transferrin uptake respectively. Future work will involve applying these knockdowns to HCV infection assays to determine the contributions of each pathway to EGF-stimulated infection.

Nevertheless, one common result of growth factor-stimulated macropinocytosis is an increase in filopodia formation. During macropinocytosis, filopodia protruding from the plasma membrane can fold back, fusing with the plasma membrane and internalising the extracellular fluid and membrane proteins and lipids contained within into a nascent macropinosomes (Ridley 2006). Although many viruses are known to interact with actin-rich structures such as microvilli and filopodia, the role that these associations have in viral entry has been unclear (Helenius et al 1980, Duus et al 2004, Smith and Helenius 2004, Lehmann et al 2005). There is some evidence that virus binding to filopodia induces “surfing” of the virus and bound receptors towards the cell body ina process that is dependent on the actin cytoskeleton and myosin II (Lehmann et al 2005, Coller et al 2009). Liver-derived cells are rich in filopodia and these structures have recently been implicated in HCV attachment and surfing towards the cell body for internalisation (Coller et al 2009). *In vivo*, filopodia are thought to extend through the sinusoidal membrane where they mediate the first interactions between hepatocytes and viral particles (Warren et al 2006). As EGF-stimulation results in macropinocytosis and filopodia may play an important role in mediated virus contact with target cells, the effects of EGF stimulation on filopodia formation and growth were investigated. As CD81 is highly expressed in filopodia (**Figure 4.4 A and B**), CD81-GFP was used as a fluorescent marker for filopodia, and both number per unit area and length of filopodia assayed by live cell confocal microscopy. Both number of filopodia and the length of filopodia present throughout the duration of the timelapse increased significantly following EGF stimulation, compared to cells prior to addition of EGF. This corroborates the evidence for EGF-stimulated macropinocytosis in Huh7.5 cells and also offers an alternative mechanism by which infection could be promoted by EGF treatment. The observed

effects on filopodia formation and elongation were combined to describe the effects on both the *de novo* formation of filopodia and elongation of existing filopodia into the 'filopodial index', which also increases significantly upon EGF stimulation. Filopodial growth as a result of increased macropinocytosis could promote HCV infection by increasing hepatoma cell surface area, aiding virus attachment and binding and bringing greater numbers of viral particles towards the cell body for internalisation, or could promote internalisation through their role in macropinocytosis.

As CD81 is highly expressed in filopodia and is known to directly interact with the E2 envelope glycoprotein of HCV, its expression levels within filopodia were assayed prior to EGF addition and following 30 minutes stimulation with EGF. Previous work has shown that the diffusion coefficient of CD81 within filopodia is significantly higher than within the plasma membrane at the cell body, and this significantly increased in response to addition of soluble E1E2 (Amy Barnes M.Res thesis). However, there was no significant change in the fluorescence intensity of CD81-GFP within filopodia upon EGF stimulation, demonstrating that CD81 does not relocalise to these structures as a result of EGFR activation, nor does any resultant retrograde trafficking of proteins within filopodia result in a decrease in CD81 localisation within filopodia.

Therefore, EGF stimulation exhibits three non-mutually exclusive effects on Huh7.5 cells which may contribute to an EGF-stimulated increase in HCV entry. These include an increase in clathrin-mediated endocytosis, the established entry mechanism for HCV, an increase in macropinocytosis, which could promote viral uptake in a non-specific or receptor-dependent manner, and a corresponding increase in filopodial index, which could promote both virus particle attachment and internalisation.

Efficient knockdown of components of each pathway has been shown, and future work should apply this to infection assays to determine the contribution of each pathway to EGF-stimulated HCV infection.

4.5 Key Chapter Findings

1. **EGF stimulation promotes clathrin-coated pit formation and the clustering of activated EGFR in CCPs.**
2. **EGF stimulation promotes membrane ruffling and blebbing, bulk membrane uptake and fluid-phase uptake, indicative of macropinocytosis in Huh7.5 cells.**
3. **EGF stimulation promotes filopodia formation and elongation in Huh7.5 cells, which may aid virus attachment and binding as well as contributing to macropinocytic uptake.**

4.6 Conclusions

These results demonstrate that EGF stimulation exhibits multiple effects on Huh7.5, which may contribute to the associated promotion of HCV entry and provide novel insights into the possible mechanism of action of EGF stimulation in HCV entry and the role of EGFR in mediating HCV entry. The established entry route of HCV in Huh7.5 cells, clathrin-mediated endocytosis is upregulated in response to EGF stimulation and is the route of entry of the activated EGFR. However,

macropinocytosis is also upregulated in Huh7.5 cells in response to EGF stimulation, resulting in bulk membrane internalisation, which may contribute to the EGF-dependent increase in HCV entry. Additionally, filopodia formation and elongation are promoted in response to EGF stimulation, as is typical of macropinocytosis. As filopodia have been implicated in HCV attachment and ‘surfing’ towards the cell body for internalisation, this could be relevant to the increase in HCV entry following EGF stimulation. As endocytic trafficking is altered in response to EGF stimulation, it will be important to study the localisation and trafficking of HCV receptors in response to EGF stimulation.

CHAPTER 5

RESULTS

EFFECTS OF EGF STIMULATION ON EGFR AND CD81 LOCALISATION AND TRAFFICKING IN HUH7.5 CELLS

5.1 Introduction

The receptor tyrosine kinase EGFR was recently shown to be an important entry factor for HCV (Lupberger et al 2011). Lupberger et al demonstrated that knockdown of EGFR and treatment with tyrosine kinase inhibitors inhibited HCVpp infection and that stimulation with EGF promotes viral entry in Huh7.5 and Huh7.5.1 hepatoma cells. While the authors demonstrate that EGFR ligands can increase HCV entry, the exact molecular mechanisms of EGF-stimulated HCV entry still remain unclear.

The productive entry of HCV is a complex multi-step process dependent on multiple receptors and entry factors, the functional and physical interplay between which is still poorly understood. Current knowledge of HCV co-receptor interactions suggests that CD81 and CLDN1 associations are prompted by virus binding, leading to internalisation of the two co-receptors via clathrin-mediated endocytosis (Harris et al 2008, Farquhar et al 2012).

EGFR is highly expressed in the liver (Lockhart and Berlin 2005) and is thought to influence HCV entry by mediating CD81-CLDN1 co-receptor associations, as siRNA targeted against EGFR and Erlotinib treatment reduced fluorescence resonance energy transfer (FRET) between the two co-receptors (Lupberger et al 2011). Following on from this work, CD81 has been shown to colocalise intracellularly with EGFR upon TGFα stimulation by confocal microscopy, leading the authors to suggest that the two receptors/entry factors internalise together (Diao et al 2012). However, as colocalisation was visualised by confocal microscopy after 15 minutes stimulation it is not clear whether the two receptors internalised together or simply traffic to the same intracellular compartment. The authors also show that CD81-mediated virus binding is required for EGFR activation, suggesting a functional as well as physical association between the two proteins (Diao et al 2012).

Tetraspanins regulate lateral clustering of membrane proteins through their role as structural organisers of tetraspanin-enriched microdomains (TEMs) and, consequently regulate signalling from a variety of membrane proteins including growth factor receptors (Odintsova et al 2000, Odintsova et al 2003, Murayama et al 2008, Sadej et al 2010). In addition to their purely structural function as organisers of partner proteins within TEMs, tetraspanins have also recently been shown to regulate various aspects of intracellular trafficking as well as biosynthetic transport of tetraspanin-interacting membrane proteins and receptors (reviewed in Berditchevski and Odintsova 2007). The tetraspanin CD82 is well known to associate with receptor tyrosine kinases of the ErbB family and (Odintsova et al 2000, Odintsova et al 2003) increased expression of this tetraspanin in mammary epithelial cells results in increased ligand-induced internalisation of EGFR (Odintsova et al 2000).

CD9, the most closely related tetraspanin to CD81 has also been shown to physically and functionally associate with EGFR in cancer cells, including HepG2-CD9 cells of hepatocyte origin, although this interaction has been much less extensively studied than the interaction of EGFR with CD82. Here CD9 is thought to be involved in regulating EGF-induced signalling (Murayama et al 2008).

The HCV co-receptor tetraspanin CD81 interacts directly with the E2 envelope glycoprotein of HCV (Pileri et al 1999, Zhang et al 2004, Brazzoli et al 2008) and has been shown to internalise via clathrin-mediated endocytosis in response to binding of a cross-linking antibody 2s66, as well as in response to virus binding (Farquhar et al 2012). However, it has been shown that EGF stimulation does not promote the internalisation of CD81 treated with a crosslinking antibody (which has been shown to induce CD81 internalisation independently of EGF) (Zona et al 2013). Although tetraspanins are involved in interactions with a variety of membrane proteins though

TEMs, and other tetraspanins have been shown to affect growth factor localisation and trafficking, no association between CD81 and EGFR on the cell surface has been demonstrated to date.

Multiple viruses are known to induce intracellular signalling events which are critical for various stages of the viral life cycle, including entry into host cells. The interaction between HCV and CD81 has been demonstrated to activate multiple downstream signalling pathways, including Rho GTPases, Cdc42, MAPKs, and ezrin-radixin-moesin (ERM) proteins (Brazzoli et al 2008, Coffey et al 2009, Farquhar et al 2011). In addition, CD81 binding to HCV primes the E1-E2 glycoprotein complex for pH-dependent fusion in the early endosome (Sharma et al 2011). All of these data suggest that HCV activates multiple intracellular signalling pathways and that CD81, in particular, may be important in regulating these. Therefore, study of the localisation, clustering and trafficking of HCV receptors and entry factors under EGF stimulation will provide important insight into the mechanism of EGF-promoted viral entry.

5.2. Chapter Aims

EGF mediated activation of EGFR results in an increase in HCV entry into Huh7.5 cells. This effect is thought to be as a result of EGFR-mediated association between CD81 and CLDN1 (Lupberger et al 2011) and further evidence suggests that following EGF treatment EGFR and CD81 colocalise (Diao et al 2012). The aims of this chapter are therefore to determine the effect of EGF-stimulation on EGFR and CD81 localisation and trafficking in Huh7.5 cells and to investigate a possible association between CD81 and EGFR.

5.3 Results

5.3.1 EGF Stimulation Promotes EGFR Internalisation

HCV entry is dependent on four co-receptors or entry factors: the tetraspanin CD81, the scavenger receptor SR-BI, and tight junction proteins CLDN1 and OCLN, in addition to the recently identified EGFR. Data from **Chapter 4** demonstrate that both clathrin-mediated endocytosis and macropinocytosis are stimulated in response to EGF treatment of Huh7.5 cells; however, it is not clear how EGF treatment affects EGFR localisation and trafficking. Internalisation of EGFR has been shown to be crucial for ligand-induced HCV entry (Diao et al 2012) and data from **Chapter 4** revealed that EGFR localises to clathrin-coated pits on the cell surface under EGF stimulation. Therefore, the internalisation of EGFR in response to EGF stimulation was confirmed by live cell confocal microscopy. Huh7.5 cells were transiently transfected with EGFR-GFP (**Table 2.1**) and imaged by timelapse confocal imaging for 60 min at intervals of 1 min at a single central plane of focus both with and without EGF stimulation. As shown in **Figure 5.1 A and C**, when plasma membrane and intracellular EGFR-GFP fluorescence were quantified with no EGF stimulation, little change in total cellular fluorescence can be seen throughout the timelapse. However, EGF stimulation results in the formation of membrane ruffles and blebs as shown in CFPmem-labelled cells (**Figure 4.1**), which contain EGFR, as indicated by yellow arrows (**Figure 5.1**), suggestive of macropinocytic uptake of the receptor. The decrease in plasma membrane fluorescence was measured by drawing a region of interest around the plasma membrane and quantifying the fluorescence in this region of interest over time. A region of interest was also drawn within the plasma membrane in order to quantify the intracellular fluorescence. Quantification of

plasma membrane fluorescence following EGF stimulation revealed that stimulation with 1 µg/ml EGF resulted in a decrease in plasma membrane EGFR, resulting in a level of 59.18% of unstimulated fluorescence intensity by the 60 minute time point. However, in contrast to

quantification of CFPmem fluorescence (**Figure 4.1**), intracellular levels of EGFR-GFP decrease over time. This is indicative of receptor degradation at longer time points of stimulation, which is typical of EGF-induced EGFR internalisation, where signalling from the activated receptor is terminated by lysosomal degradation of activated receptor (Roepstorff et al 2009).

5.3.2 CD81 internalisation and degradation are promoted by EGF stimulation

CD81 plays an important role in virus binding by interacting directly with the viral glycoprotein E2. CD81 has also been shown to interact with the HCV entry factor CLDN1 upon virus binding, and the HCV-receptor complex is thought to internalise via clathrin-mediated endocytosis (Farquhar et al 2012). EGF stimulation has been shown to promote the formation of CD81-CLDN1 complexes by FRET (Lupberger et al 2011). The tetraspanin has also been shown to colocalise in early endosomes with EGFR following activation by ligand binding suggesting a possible physical and/or functional association between the two proteins (Diao et al 2012). Therefore, evidence suggests that CD81 may play a role in EGF-stimulated HCV entry.

To investigate the internalisation of CD81 in response to EGF treatment, Huh7.5 cells overexpressing CD81-GFP were imaged by live cell timelapse confocal microscopy for 60 minutes both with and without EGF treatment, with image acquisition every 5 minutes. The plasma membrane and intracellular fluorescence

were quantified by drawing regions of interest around the plasma membrane and within the plasma membrane and measuring mean fluorescence in these regions of interest over time, in the same way as for CFPmem. Similarly to EGFR-GFP, in untreated control cells, both plasma membrane and intracellular CD81-GFP fluorescence remain fairly constant throughout the timelapse with little internalisation or photobleaching apparent, as shown in **Figure 5.2 A and C**. In contrast, under EGF stimulation, CD81-GFP appears to internalise rapidly, with plasma membrane fluorescence visibly decreasing within 30 minutes of EGF addition (**Figure 5.2 B**).

It also appears that internalised CD81 localises to large internalised vacuoles resembling macropinosomes following EGF stimulation, as indicated by the yellow arrows, consistent with the increase in macropinocytosis demonstrated in **Section 4.3.1**. Interestingly, intracellular CD81-GFP fluorescence also visibly decreases indicating that CD81 is targeted for degradation upon internalisation.

When quantified in the same manner as EGFR-GFP in **Section 5.3.1**, CD81-GFP fluorescence, both in the plasma membrane and intracellularly, remains constant with no significant photobleaching in untreated cells. However, following EGF stimulation, CD81-GFP fluorescence in the plasma membrane is seen to decrease significantly, dropping to around 53.76% of the plasma membrane fluorescence intensity of unstimulated cells by the 60 minute timepoint. Additionally, intracellular CD81-GFP fluorescence intensity decreases throughout the EGF stimulation timelapse, with similar but delayed kinetics to CD81 internalisation. This suggests that CD81 is rapidly degraded upon internalisation, and is not recycled back to the plasma membrane, consistent with the images shown in **Figure 5.2 B**.

It is unclear whether this EGF-stimulated CD81 internalisation and degradation is a result of the bulk membrane uptake demonstrated in **Section 4.3.1**, or whether this occurs via clathrin-mediated endocytosis as is the established entry mechanism for HCV in Huh7.5 cells. It is clear that CD81-GFP is present in large membrane-bound intracellular vacuoles, which are likely to be macropinosomes, however, clathrin-mediated endocytosis has also been shown to be upregulated in response to EGF stimulation and CD81 is known to internalise via this pathway in response to HCV binding. As both CD81 and EGFR internalise in response to EGF stimulation, it is possible that the receptor and entry factor internalise and traffic together.

If receptors are internalising together, they should be seen to cluster and localise together on the plasma membrane following stimulation and prior to their internalisation. Therefore TIRF imaging and cell surface receptor localisation may offer the best means to study receptor internalisation.

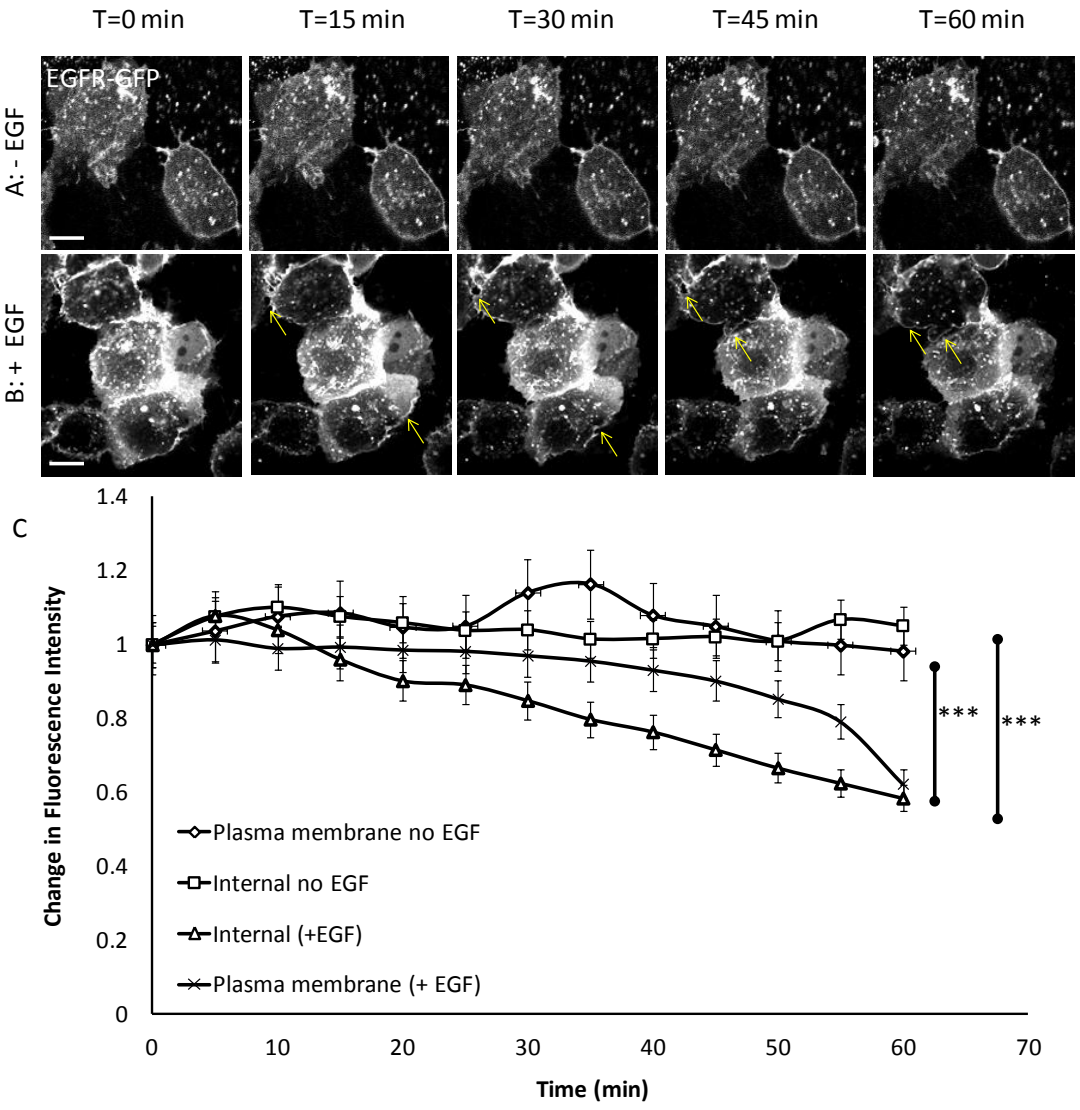

Figure 5.1 Stimulation of EGFR internalisation by EGF. Huh7.5 cells overexpressing EGFR-GFP were imaged by confocal microscopy for one hour without EGF stimulation (A) and with one hour stimulation with 1µg/ml EGF (B). Yellow arrows indicate forming macropinosomes. Scale bar = 20 µm. Plasma membrane and intracellular fluorescence were quantified and

5.3.3 EGFR and CD81 partially colocalise on the cell surface upon EGF stimulation

EGFR is known to cluster upon stimulation, localising to clathrin-coated pits on the plasma membrane (**Figure 4.7**). Tetraspanins such as CD81, through their homo- and hetero-typic interactions with membrane proteins act as structural organisers of areas of the plasma membrane known as TEMs. Other members of the highly conserved tetraspanin superfamily have been shown to interact with EGFR, and mediate signalling events, including the closely related CD9 (Murayama et al 2008). Evidence suggests that EGFR and CD81 colocalise within early endosomes following EGF stimulation (Diao et al 2012). However, this was carried out by confocal microscopy; it is therefore possible that the two receptors simply colocalise in an intracellular compartment following endocytosis rather than internalising together. To investigate whether this colocalisation was the result of the two receptors internalising together or of them simply trafficking to the same intracellular compartment, Huh7.5 cells transiently transfected with EGFR-GFP were stimulated with EGF, fixed and CD81 immunocytochemistry (IC) carried out. As cells were fixed for IC, live cell timelapses could not be carried out. Therefore unstimulated cells were compared to cells that had been stimulated with EGF for a short (5 min) and long (30 min) duration were compared and two EGF concentrations were used (1 µg/ml and 100 ng/ml). Cells were imaged by both total internal reflection fluorescence (TIRF) microscopy to view clustering and localisation in the plasma membrane and confocal microscopy, to view the localisation of internalised receptors within the cell. As shown in **Figure 5.3**, when imaged by TIRF microscopy, some colocalisation is visible between the two proteins after just 5 minutes stimulation with 1 µg/ml EGF (and with 100 ng/ml, data not shown). The degree of colocalisation was

quantified by identifying CD81-positive structures and scoring the proportion of these which were also positive for EGFR-GFP. This is plotted as percentage colocalisation in **Figure 5.3 C**. Significant colocalisation between CD81 and EGFR was observed at the five minute timepoint at both EGF concentrations. This is indicative of the receptors clustering together rapidly upon EGF stimulation, and colocalisation within 5 minutes is consistent with the rapid internalisation of both proteins upon EGF treatment shown in **Figures 5.1** and **5.2**. This is the first evidence for an association between CD81 and EGFR on the cell surface and is suggestive of the two proteins internalising together. Interestingly, by the 30 minute time-point, significant colocalisation of the two receptors was still observed, but to a lesser extent, suggesting activation and colocalisation and internalisation of the receptors occurs rapidly, again consistent with the rapid internalisation observed by live-cell confocal microscopy.

The same samples were then imaged by confocal microscopy, selecting a focal plane in the centre of the cell, where the plasma membrane and endocytic vesicles were clearly visible. To quantify colocalisation at both timepoints and concentrations, an ROI was drawn around the intracellular area of each cell (the area within the plasma membrane) and the Pearson's correlation coefficient for the ROI measured using NIS Elements software (Nikon).

C

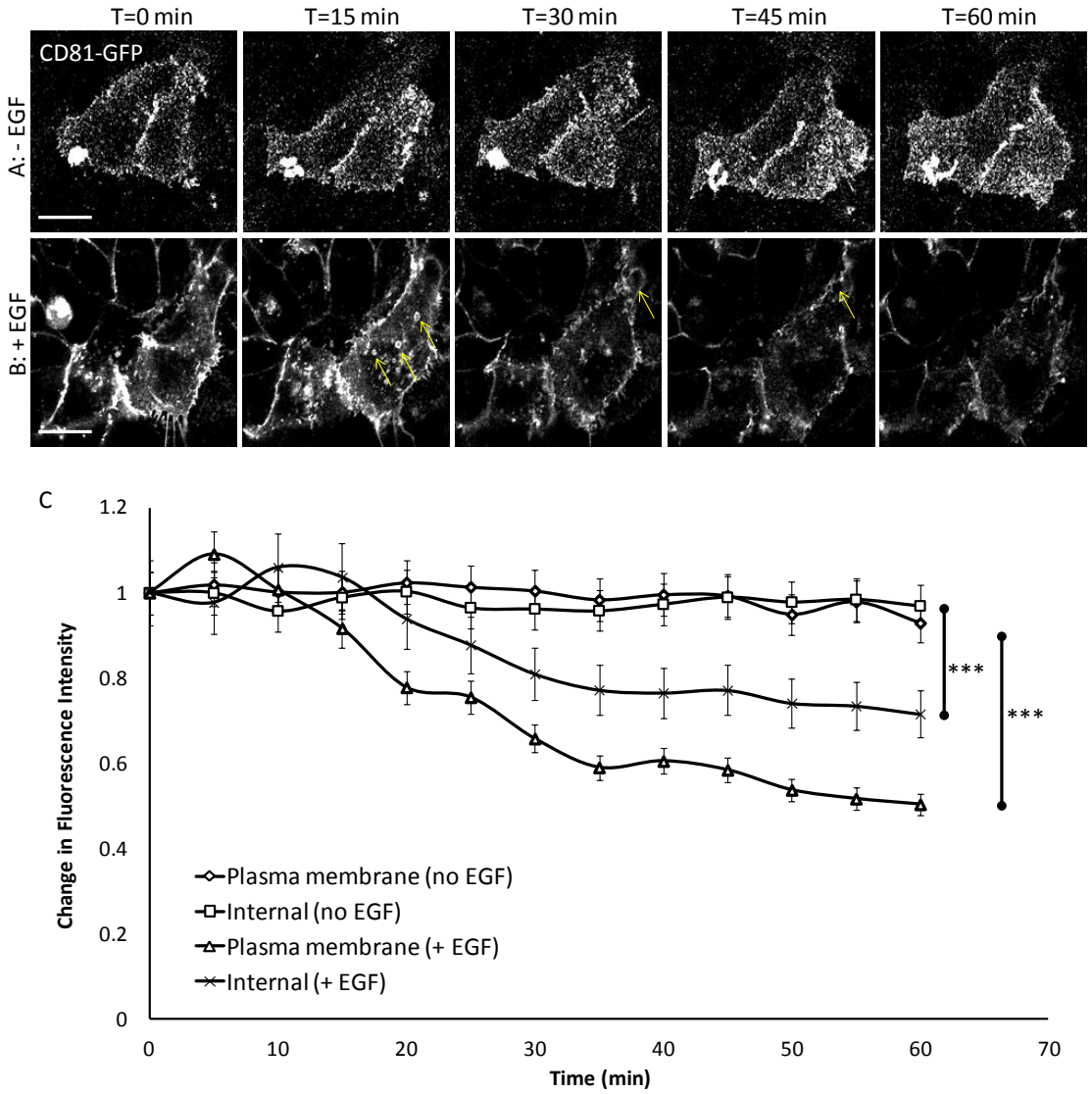

Figure 5.2: Stimulation of CD81 internalisation by EGF. Huh7.5 cells overexpressing CD81-GFP were imaged by confocal microscopy for one hour without EGF stimulation (A) and for one hour with stimulation with 1ug/ml EGF (B). Quantification of plasma membrane and intracellular CD81 fluorescence over time is shown in part C. Scale bar= 20 μm. Data shown are the mean of three independent experiments. Error bars = standard error.

As shown in **Figure 5.4 C**, significant colocalisation of EGFR and CD81 was only observed at 100 ng/ml EGF at the 5 minute time-point; representative images of this are shown in **Figure 5.4.B**). Again, this corroborates a rapid internalisation of both proteins in response to EGF stimulation and is suggestive of the two proteins internalising together. However, the lack of colocalisation in cells stimulated with 1 µg/ml EGF contradicts data shown in Diao et al, where the two proteins were shown to colocalise within EEA1-positive endocytic compartments following EGFR activation (Diao et al 2012). However, the authors used TGFα to activate EGFR. Stimulation with different ligands has been shown to induce differential trafficking of EGFR (Roepstorff et al 2009), which may account for the differences in intracellular colocalisation seen here.

As live-cell imaging demonstrates receptor degradation (**Figures 5.1 and 5.2**), particularly of C81, even at early time points, this could also account for the lack of colocalisation seen intracellularly at later time points. Additionally, trafficking of EGFR and CD81 to different endocytic compartments would be consistent with the observation that while CD81 and EGFR are both seen to internalise rapidly upon EGF stimulation, CD81 begins to degrade at much earlier time points than EGFR (**Figures 5.1** and **5.2**, respectively).

As the majority of plasma membrane colocalisation occurs within 5 minutes of EGF addition, it is probable that receptor activation, clustering and internalisation occur rapidly upon ligand addition, accounting for internal colocalisation at 5 minutes with a low EGF concentration. However, lack of colocalisation visible at the higher EGF concentration (1 µg/ml) and longer times of stimulation, mean that the majority of intracellular CD81 and EGFR do not localise to the same intracellular compartments.

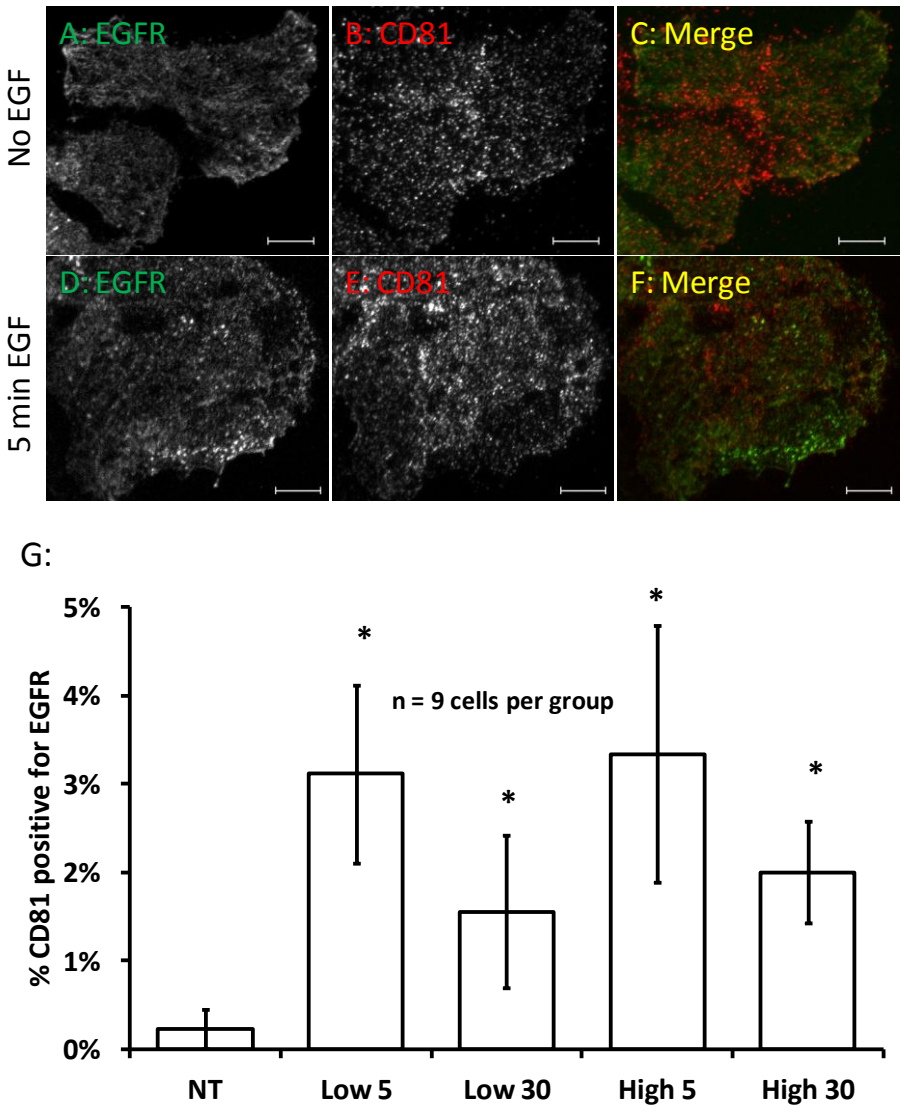

Figure 5.3: CD81 partially colocalises with EGFR on the cell surface following EGF stimulation. EGFR-GFP transfected Huh7.5 cells immunostained for CD81 with no EGF treatment (A-C) and with 5 min EGF treatment (D-F). Scale bars = 5 μm. Quantification of percentage colocalisation between CD81 and EGFR is shown in G. Error bars = standard error. NT= no treatment. Low 5 = treatment with 100 ng/ml EGF, Low 30 = treatment with 100 ng/ml EGF for 30 minutes, High 5 = treatment with 1 μg/ml EGF for 5 minutes, High 30 = treatment with 1 μg/ml EGF for 30 minutes. 9 cells were imaged and quantified per group.

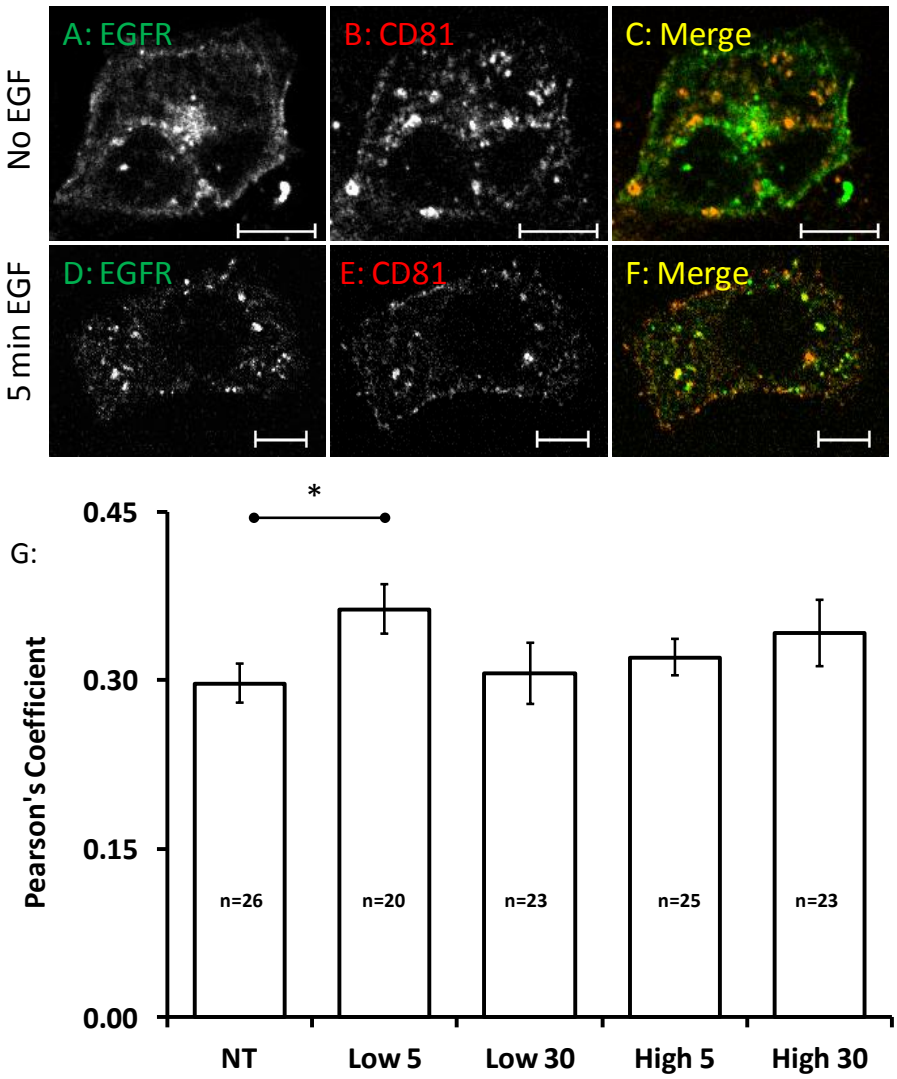

Figure 5.4: CD81 partially colocalises with EGFR in intracellular compartments at 5 minutes stimulation with EGF. EGFR-GFP transfected Huh7.5 cells immunostained for CD81 with no EGF treatment (A-C) and with 5 min EGF treatment (D-F). Scale bars = 10 µm. Pearson's correlation coefficient as a measure of colocalisation between CD81 and EGFR is shown in G. Data shown are the mean of three independent experiments. N = number of cells analysed per condition. Data shown are the mean of three independent experiments. Error bars = standard error. NT= no treatment. Low 5 = treatment with 100 ng/ml EGF, Low 30 = treatment with 100 ng/ml EGF for 30 minutes, High 5 = treatment with 1 µg/ml EGF for 5 minutes, High 30 = treatment with 1 µg/ml EGF for 30 minutes. 9 cells were imaged and quantified per group.

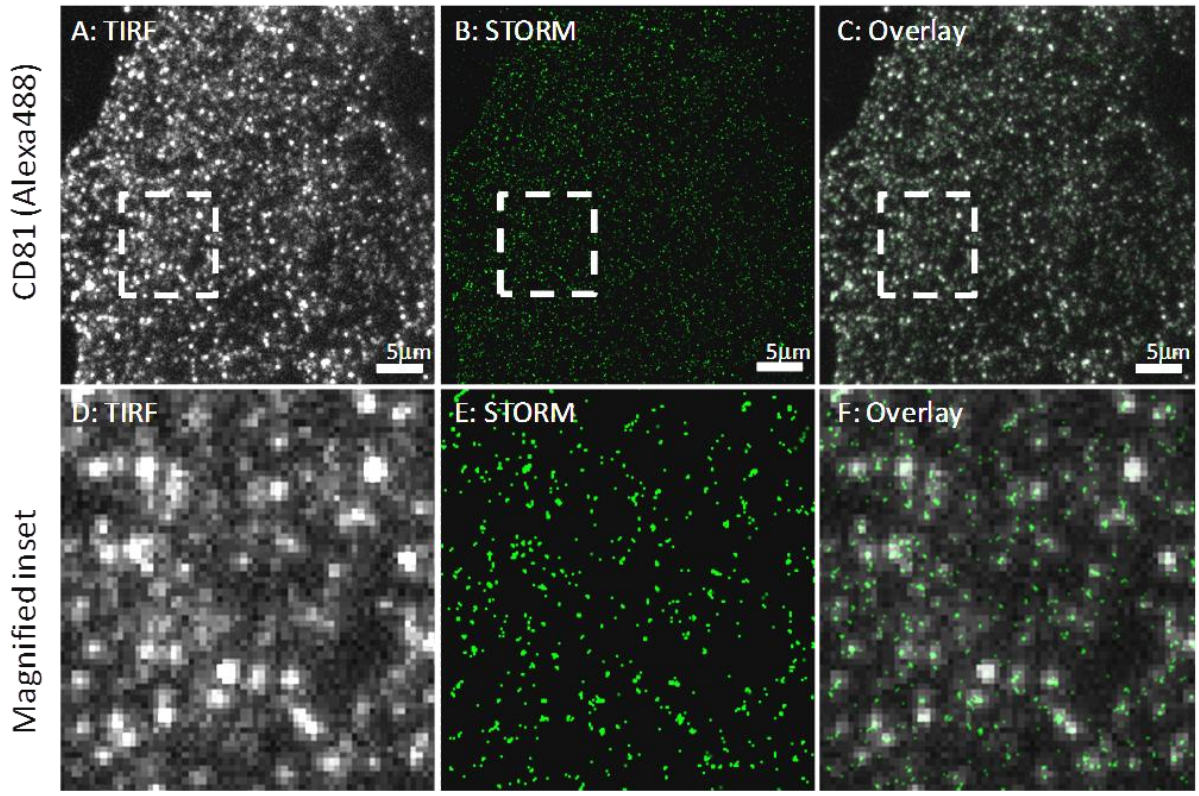

Figure 5.5: STORM imaging of CD81. Huh7.5 cells immunostained for CD81 with no EGF treatment imaged via diffraction-limited TIRF microscopy (A+D) and STORM (B+E) . Overlay is shown in (C+F). Magnified regions are shown in D-E. Scale bars = 5 µm.

5.3.4 Super-resolution imaging of CD81 localisation in response to EGF stimulation

Tetraspanins like the HCV co-receptor CD81 tend to form membrane signalling complexes, known as tetraspanin-enriched microdomains (TEMs). This is mediated through their association with other membrane proteins as well as intracellular signalling and cytoskeletal proteins. Tetraspanins possess no intrinsic enzymatic activity or signalling motifs and it is thought that they act by facilitating the interaction of associated proteins within TEMs. FRET studies between overexpressed fluorescent co-receptors, revealed that CD81 and CLDN1 formed complexes within the plasma membrane of hepatoma cells (Harris et al, 2008). In addition, data from **Figure 5.2** demonstrate that CD81 internalisation is significantly upregulated in response to EGF stimulation of Huh7.5 cells and colocalises with EGFR on the cell surface following EGF stimulation, as shown in **Figure 5.3**. Therefore, it is likely that CD81 is involved in EGFR-mediated HCV infection. EGFR clusters in response to EGF stimulation, concentrating within clathrin-positive structures on the plasma membrane (**Figure 4.7**). As CD81 appears to internalise with EGFR and it is therefore likely that it clusters with EGFR within clathrin coated pits prior to internalisation following EGF treatment.

To investigate CD81 clustering in response to EGF stimulation, Huh7.5 cells were either treated with 1 µg/ml EGF for 30 minutes or left untreated and CD81 IC carried out. As CD81 is highly expressed within the plasma membrane of liver-derived cells, clusters of CD81 in the membrane of Huh7.5 cells are densely labelled and not easily distinguishable from each other. Therefore, two super-resolution microscopy techniques were tested at the Nikon Imaging Centre, King's College London (NIC@King's): structured illumination microscopy (SIM) and (direct) stochastic

optical reconstruction microscopy (dSTORM). dSTORM relies on the intrinsic blinking properties of certain fluorophores, such as alexafluor-647. Therefore, an alexfluor-647-labelled secondary antibody was used for IC of dSTORM samples. However, poor labelling efficiency meant that, although there are centroids fitted for most fluorescent punctate detected by TIRF microscopy, the brighter structures visible in the corresponding TIRF images don't appear to have more blinking events recorded in the STORM image than less bright structures (**Figure 5.5**). Additionally, while dSTORM images do show blinking events associated with most of the CD81-positive structures in the corresponding TIRF images, many blinking events were also detected in background regions which were not positive for CD81 in the corresponding diffraction-limited TIRF images. Therefore, SIM was explored as a super-resolution alternative.

SIM can be applied to conventionally labelled fluorophores and so is not subject to the same labelling constraints and issues as dSTORM. However, SIM offers the least improvement in gained resolution over diffraction limited optical microscopy. Therefore, SIM images were compared to conventional epi-fluorescence images of CD81 acquired on the same system. As shown in **Figure 5.6**, SIM images of labelled CD81 offer a considerable improvement in resolution, allowing the analysis of CD81 structure density to be carried out. Additionally, the generation of Fourier transforms that contain six additional lobes (over a diffraction-limited image) confirms correct reconstruction from the nine recorded frames (representative of three grid positions and three rotations), as shown in **Figure 5.7**, demonstrating that true super resolution has been achieved.

Therefore, SIM images, while offering less of an improvement in resolution over diffraction-limited techniques, seem to give the most accurate picture of CD81

localisation and clustering and were therefore used for analysis of structure density following EGF treatment. Representative SIM images of CD81-labelled Huh7.5 cells treated with EGF for 30 minutes (**B**) or left untreated (**A**) are shown in **Figure 5.7**. Analysis of CD81 cluster density is shown in **Figure 5.7 C**.

Data shown are the average of three independent experiments; three cells were imaged and analysed per repeat. Analysis of feature density revealed that numbers of CD81 clusters decrease following 30 minutes EGF stimulation by 16.67 %. This is consistent with the rapid internalisation of CD81 observed by live cell confocal microscopy (**Figure 5.2**), in which considerable CD81 endocytosis occurs within 30 minutes of treatment and corroborates the colocalisation of CD81 with EGFR on the cell surface after 5 minutes of EGF stimulation (**Figure 5.3**).

While internalised receptor may recycle back to the cell surface to undergo further rounds of internalisation, live cell imaging suggests CD81 internalised in response to EGF treatment is rapidly degraded upon endocytosis, which is consistent with the reduced numbers of CD81-positive structures seen after 30 minutes EGF stimulation observed by SIM. Taken together, these data support a rapid internalisation of both CD81 and EGFR in response to EGF stimulation, with a least a significant proportion residing within the same endocytic structures, followed by trafficking down the degradative pathway.

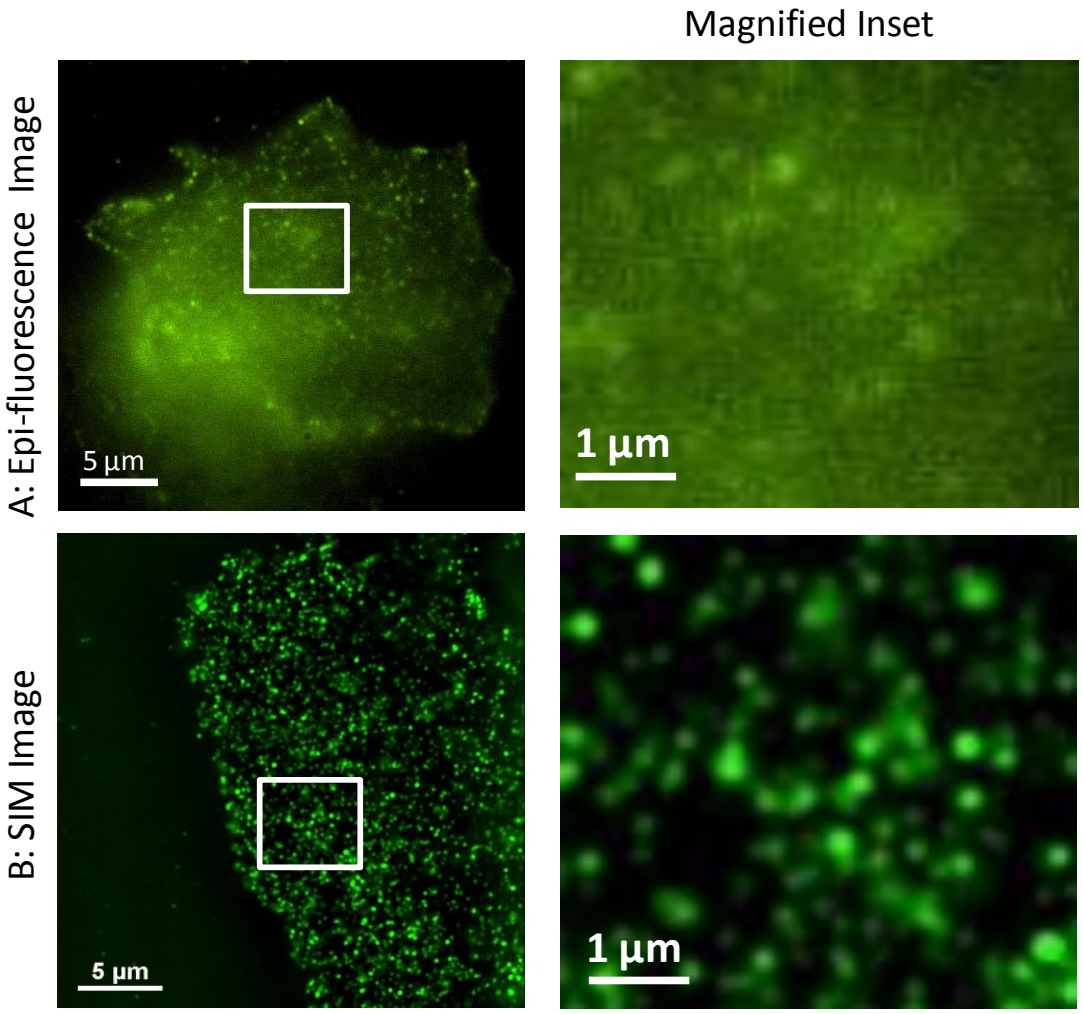

Figure 5.6: SIM imaging of CD81 allows separation of clusters.

Huh7.5 cells immunostained for CD81 with no EGF treatment imaged by epi-fluorescence microsopy and magnified inset (A). A different region of the same sample imaged by structured illumination microscopy and magnified inset (B).

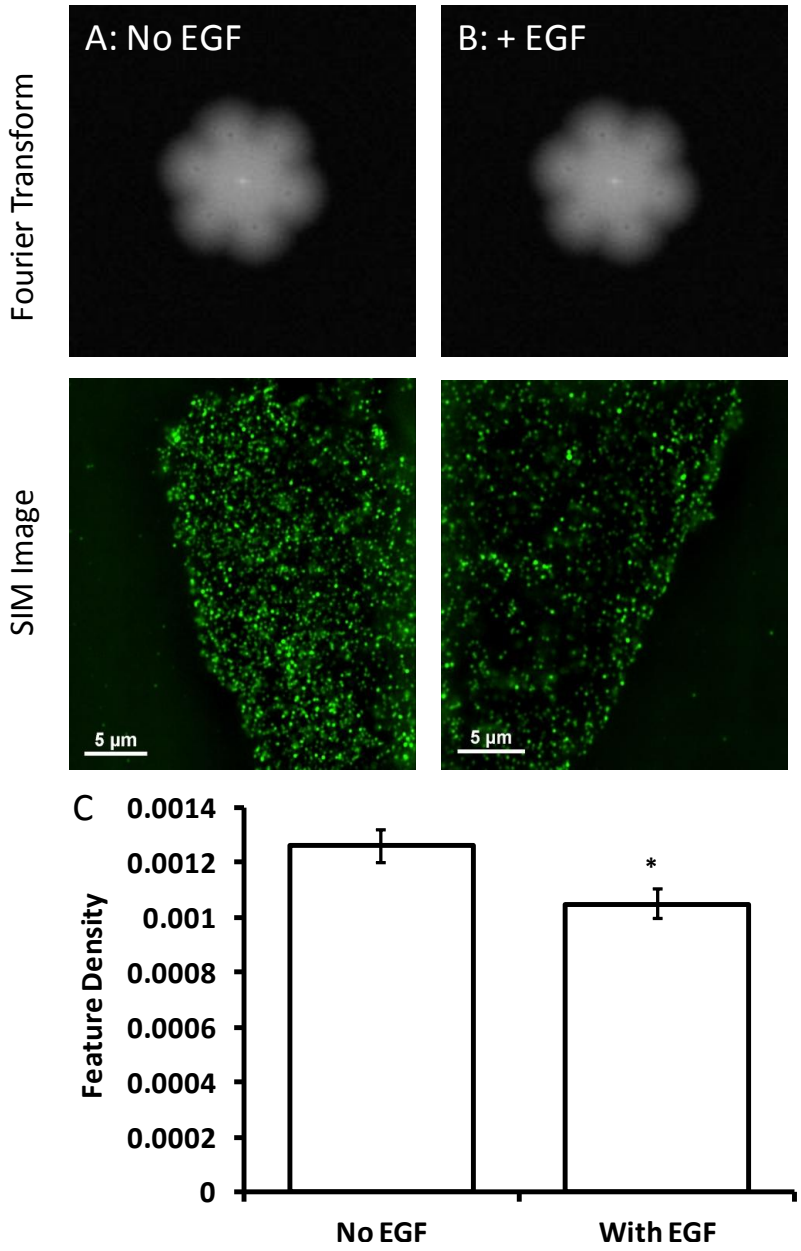

Figure 5.7: EGF stimulation results in fewer CD81 clusters in the plasma membrane. Huh7.5 cells immunostained for CD81 with no EGF treatment (A) and with 30 min EGF treatment (B) imaged by structured illumination microscopy (SIM). The corresponding Fourier transforms confirm proper reconstruction of a super-resolution image from the recorded frames. Quantification of feature density (a measure of the number of clusters per unit area; carried out by Jeremy Pike, PSIBS doctoral training centre) is shown in (C). Error bars= standard error. Scale bars = 5 µm. Data shown are the mean of 9 cells per group from 3 independent experiments. Error bars = standard error.

5.4 Discussion

EGFR has been shown to be an important factor in HCV entry (Lupberger et al 2011). Activation of the growth factor receptor by stimulation with the ligand EGF has been shown to promote viral entry. Additional evidence suggests that EGFR and the HCV co-receptor CD81 colocalise in intracellular compartments following EGF-induced internalisation (Diao et al 2012). CD81 can associate laterally with other membrane proteins via hetero- and homo-typic interactions within tetraspanin-enriched microdomains (TEMs). There is evidence that other tetraspanins affect growth factor localisation and trafficking through their organisation of TEMs (Odintsova et al 2000, Odintsova et al 2003, Murayama et al 20008), however, no association between CD81 and EGFR on the cell surface has been demonstrated to date.

While HCV entry is known to rely on multiple co-receptors and entry factors in a complex multi-step entry process, the interaction between HCV and CD81 in particular is thought to be crucial in mediating the activation of multiple downstream signalling pathways involved in viral entry, including Rho GTPases, Cdc42, MAPKs, and ezrin-radixin-moesin (ERM) proteins (Brazzoli et al 2008, Coffey et al 2009, Farquhar et al 2012). Therefore, the localisation, clustering and internalisation of EGFR and CD81 under EGF stimulation were the focus of this chapter.

Firstly, internalisation of EGFR and CD81 was assessed in Huh7.5 cells both with and without EGF stimulation by live cell confocal timelapse microscopy. Results from **Chapter 4** demonstrate that EGFR localises to clathrin-coated pits (CCPs) on the plasma membrane following addition of EGF, indicating internalisation of the activated receptor via clathrin-mediated endocytosis. To confirm internalisation of EGFR following EGF treatment, Huh7.5 cells were transiently transfected with

EGFR-GFP and imaged by live cell confocal microscopy both with and without EGF stimulation. Little internalisation of EGFR or photobleaching was observed in untreated cells over a 1 hour timelapse. In contrast, loss of EGFR from the plasma membrane was observed upon EGF addition. Intracellular levels of EGFR remained relatively constant at early timepoints but also began to drop towards the end of the timelapse, in contrast to CFPmem levels seen in Figure 4.1. This is indicative of degradation of internalised EGFR, which is consistent with EGF-mediated activation of EGFR targeting the receptor for lysosomal degradation over recycling back to the plasma membrane.

As CD81 has been shown to colocalise with EGFR in endosomal compartments following TGFα-mediated EGFR activation (Diao et al 2012), internalisation of CD81 was assessed in the same manner in Huh7.5 cells overexpressing CD81-GFP. Again, little photobleaching or CD81 internalisation is visible in untreated cells (**Figure 5.2 A and C**). In contrast, a visible decrease in CD81 fluorescence in the plasma membrane occurs upon EGF addition (**Figure 5.2 B**), which is confirmed by quantification (**Figure 5.2 C**). While this was initially followed by a corresponding rise in intracellular fluorescence, intracellular fluorescence also decreased throughout the timelapse, suggestive of degradation of internalised CD81 over recycling back to the plasma membrane (**Figure 5.2 C**).

CD81 and EGFR both internalise rapidly in Huh7.5 cells in response to EGF treatment, and have been shown to colocalise in early endosomes following TGFα-induced EGFR activation (Diao et al 2012). EGFR clusters on the cell surface in response to EGF treatment and colocalises with clathrin (**Chapter 4**). Therefore, a possible association between the two proteins on the cell surface was investigated both with and without EGF stimulation.

Huh7.5 cells transiently transfected with EGFR and labelled for CD81 by IC were imaged by TIRF microscopy to visualise localisation on the adherent plasma membrane at early (5 min) and later (30 min) timepoints with two concentrations of EGF (100 ng/ml and 1 µg/ml). As shown in **Figure 5.3**, CD81 and EGFR colocalise on the plasma membrane within five minutes of EGF stimulation at both high and low EGF concentrations. This is indicative of the two receptors internalising together and is consistent with published observations of the two proteins colocalising within intracellular compartments following ligand-induced internalisation (Diao et al 2012). This colocalisation, while still significantly greater than in untreated cells, was reduced after 30 minutes EGF stimulation, corroborating the rapid effects of EGF treatment seen by live cell confocal imaging.

However, when colocalisation was measured in the same samples imaged by confocal microscopy in order to observe intracellular colocalisation, EGFR and CD81 were only seen to colocalise after 5 minutes stimulation with a lower concentration (100 ng/ml) of EGF. No significant colocalisation was observed with 1 µg/ml EGF stimulation, even at the early 5 minute time point. This contradicts evidence that EGFR and CD81 colocalise within early endosomes (Diao et al 2012). However, these images were taken in cells where internalisation of EGFR had been stimulated with TGFα rather than with EGF. Several ligands are known to bind to and activate EGFR, however not all of these target EGFR trafficking down the lysosomal pathway; TGFα has been shown to target internalised receptor for recycling whereas EGF is known to target EGFR for lysosomal degradation (Roepstorff et al 2009).This may account for the difference in levels of colocalisation observed.

Nevertheless, the fact that colocalisation is observed on the cell surface at both time points and with both EGF concentrations demonstrates that the two receptors do

internalise together. Therefore, while recently internalised receptors may colocalise within the cell, the large numbers of intracellular structures visible where the two proteins do not colocalise mean that significant colocalisation is not seen at most timepoints and concentrations. Trafficking of EGFR and CD81 to different endocytic compartments is consistent with the observation that while CD81 and EGFR are both seen to internalise rapidly upon EGF stimulation, CD81 begins to degrade at much earlier timepoints than EGFR (**Figures 5.1** and **5.2**, respectively). Our data indicate that EGFR and CD81 do not traffic together once internalised and are rapidly trafficked to different intracellular compartments.

Taken together, these data demonstrate an EGF-dependent colocalisation of CD81 and EGFR on the cell surface, followed by rapid internalisation of the two proteins. While other tetraspanins have been shown to associate with EGFR and influence its signalling and trafficking, this is the first evidence for an association between CD81 and EGFR on the plasma membrane. This is also the first evidence that CD81 and EGFR internalise together in response to EGF stimulation and could be of key relevance to the role of EGFR in HCV entry, particularly as EGFR internalisation is thought to be of key importance to HCV entry.

EGFR was shown in **Chapter 4** to cluster on the cell surface following EGF stimulation and to localise to CCPs, the formation of which is also promoted by EGF stimulation. The colocalisation of CD81 with EGFR on the cell surface would suggest it too localises to CCPs and internalises via clathrin-mediated endocytosis along with EGFR following EGF treatment. As CD81 has no endocytic targeting sequence, and EGFR is typically internalised via clathrin-mediated endocytosis, it is possible that association with EGFR, potentially through TEMs mediates the internalisation of

CD81 through this pathway and offers a potential mechanism for the role of EGFR in HCV entry.

As CD81 and EGFR colocalise on the cell surface, and EGFR clusters in response to EGF treatment, the clustering of CD81 in response to EGF stimulation was investigated. As CD81 labelling on the cell surface is dense, and separate clusters or putative microdomains not easily distinguished by diffraction-limited microscopy, two super-resolution techniques were tested: (direct) stochastic optical reconstruction microscopy (dSTORM) and structured illumination microscopy (SIM). While SIM offers the least improvement of the two techniques in terms of resolution, it can be carried out using the same fluorescent labels as conventional fluorescence microscopy techniques, so the same IC protocol used for the colocalisation experiment could be used. dSTORM offers a greater improvement in resolution but is reliant on the inherent blinking properties of certain fluorophores such as Alexafluor-647, so an Alexafluor-647-labelled secondary antibody was used for IC. As dSTORM presented issues with labelling density, SIM images were used for analysis of CD81 clustering. Interestingly, analysis of SIM images revealed that after 30 minutes stimulation with EGF, the ‘feature density’ of CD81 punctae decreased. If CD81 localises with EGFR to clathrin-coated pits, an increase in clustering of the protein in the plasma membrane would perhaps be expected, however, as live-cell imaging and colocalisation experiments show a rapid internalisation of CD81 and colocalisation of CD81 with EGFR within 5 minutes of stimulation, this decrease in CD81 clustering at 30 minutes of EGF stimulation is consistent with CD81 having internalised and been targeted for lysosomal degradation within this time period.

Taken together, these data suggest that upon EGF stimulation, EGFR activation results in upregulation of clathrin-mediated endocytosis, localisation of EGFR to

clathrin-coated pits and the rapid internalisation of both EGFR and CD81 together. This offers a putative mechanism for the upregulation of viral entry by EGF treatment of Huh7.5 cells and for the action of EGFR in viral entry.

5.5 Key Chapter Findings

1. **EGF stimulation promotes rapid CD81 and EGFR internalisation and degradation.**
2. **CD81 and EGFR colocalisation on the cell surface increases from 0.2% to 3% following EGF stimulation but colocalisation is lost following receptor internalisation.**
3. **Super-resolution imaging of CD81 by SIM demonstrates that the density of CD81 clusters decreases following EGF stimulation, supporting the rapid internalisation and degradation seen by live-cell confocal imaging.**

5.6 Conclusions

These results demonstrate that EGF stimulation exhibits multiple effects on viral co-receptor localisation and trafficking in Huh7.5 cells, which may be relevant to HCV entry. Data in this chapter demonstrate that EGFR and CD81 are both rapidly internalised in response to EGF treatment, resulting in co-receptor degradation. Dual colour TIRF imaging revealed that the two proteins colocalise on the cell surface within 5 minutes of EGF treatment, suggesting that they internalise together following ligand stimulation. This is the first evidence to date of an association between CD81

and EGFR in the plasma membrane. SIM imaging allowed CD81 localisation to be seen in more detail than standard diffraction limited techniques. Analysis of SIM images with and without EGF stimulation revealed fewer CD81 clusters in the plasma membrane following 30 minutes EGF stimulation. This corroborates the rapid internalisation and degradation of the receptor in response to EGF stimulation seen by live cell imaging, as well as the rapid colocalisation of CD81 with EGFR on the cell surface. Therefore, these results provide novel insights into the effects of EGF stimulation on HCV receptor internalisation and trafficking and provide possible mechanisms by which EGFR may act in the viral entry process.

CHAPTER 6

FURTHER DISCUSSION AND FUTURE DIRECTIONS

6.1 Further Discussion

Viruses are obligate intracellular pathogens and viral entry is the first and crucial step in the viral life cycle, making it a key potential therapeutic target. HCV entry is a complex and multi-step process dependent on a number of attachment and entry factors and co-receptors, followed by endocytosis and pH-dependent fusion in the early endosome. Many aspects of HCV entry remain poorly understood despite extensive efforts to understand the process. Indeed, an increasing number of important cellular factors required for HCV entry are still being identified, including the epidermal growth factor receptor (EGFR) (Lupberger et al 2011), which has been the focus of much of this doctoral thesis. HCV entry is dependent on two co-receptors, the tetraspanin CD81 and the scavenger receptor SR-BI, as well as entry factors which include the tight junction proteins CLDN1 and OCLN, as well as the recently identified EGFR. However, the precise manner in which members of the HCV co-receptor complex interact with each other and the virus and internalise is yet to be elucidated.

Therefore, the focus of this doctoral thesis has been the endocytosis of HCV and its cellular receptors, including investigating a role for caveolae in HCV entry and the potential mechanisms of EGF-stimulated HCV entry.

Caveolae have long been overlooked in studies of HCV endocytosis due to a belief that the hepatoma cell lines used to study HCV entry and infection do not express caveolin 1. However, evidence suggested that hepatocytes *in vivo* do express caveolin 1, and evidence for the expression of caveolin 1 in hepatoma cell lines is mixed (Botos et al 2006, Cokakli et al 2009, Pohl et al 2002, Zhao et al 2009). Therefore, caveolin 1 expression was assayed in primary human hepatocytes and human liver sections, as well as in a panel of hepatoma cell lines. Western blot

showed that hepatocytes *in vivo* express caveolin 1 and this was confirmed by IC of human liver sections (**Figures 3.1A and 3.5**). However, no caveolin 1 was detected by western blot or cargo uptake assays for any of the hepatoma cell lines tested (**Figure 3.1 B-E**). As hepatoma cell lines do not express caveolin 1 and hepatocytes within the liver do, it was possible that caveolae offer a route for productive infection *in vivo* which had been overlooked by *in vitro* studies. Therefore, the role of caveolin 1 in HCV endocytosis was assayed in a HCV-permissive cell line which expresses caveolin 1, SkHep1 (SRBI+CLDN1). Clathrin-mediated endocytosis, the established HCV entry mechanism, and caveolar endocytosis were inhibited by silencing of AP2 and caveolin 1 using siRNA, respectively. Inhibition of clathrin-mediated endocytosis abrogated HCVpp infection of SkHep1 (SRBI+CLDN1) cells, whereas silencing of caveolin 1 had no significant effect. Therefore, although there is a discrepancy between the expression of caveolin 1 between the hepatoma cell lines used to study HCV infection and hepatocytes within the liver, caveolae play no functional role in HCV endocytosis. The reason for loss of caveolin 1 in hepatoma cell lines is unclear; however, caveolin 1 is thought to play a role in liver repair and regeneration *in vivo*. Additionally, caveolin 1 expression is associated with poor prognosis in HCC, and overexpression of caveolin 1 in HepG2 and Huh7.5 cells results in increased migration and invasion (Cokakli et al 2009, Tse et al 2012, Hsu et al 2013).

The epidermal growth factor receptor, EGFR, has recently been shown to be required for HCV entry, and stimulation of Huh7.5 cells with EGF was shown to promote HCV entry (Lupberger et al 2011). EGFR can traffic via clathrin-mediated endocytosis, as well as growth factor-stimulated macropinocytosis. Upregulation of one or more endocytic pathways by activation of EGFR may influence the internalisation of bound or extracellular virus. Therefore the effects of EGF treatment

on endocytosis and trafficking pathways were investigated. Live-cell confocal imaging of Huh7.5 cells treated with EGF revealed that membrane ruffling, lamellipodia and filopodia formation and membrane blebbing were induced in a dose-dependent response to EGF, all of which are indicative of macropinocytosis (**Figure 4.1**). Furthermore, uptake of dextran, a cargo internalised primarily via macropinocytosis, was promoted in response to EGF treatment, confirming that macropinocytosis is upregulated in Huh7.5 cells by ligand-induced EGFR activation (**Figure 4.3**). Growth factor-dependent macropinocytosis is the focus of growing numbers of publications on viral entry, most notably in the internalisation of influenza A and vaccinia virus (Eierhoff et al 2010, Marsh and Eppstein 1987, Mercer and Helenius 2008). Stimulation of HeLa cells with EGF has been shown to induce macropinocytic uptake of fluorescent-labelled vaccinia virus. Additionally, the non-receptor tyrosine kinase Axl has been implicated in vaccinia virus entry, and the virus is thought to mimic growth factor treatment, by activating the tyrosine kinase, resulting in macropinocytosis (Mercer and Helenius 2008, Morizono et al 2011). However, macropinocytosis is traditionally associated with a bulk internalisation of plasma membrane and encapsulated extracellular fluid, as demonstrated by live-cell imaging of CFPmem-transfected Huh7.5 cells under EGF treatment (**Figure 4.2**). This would likely result in a relatively non-specific uptake of virus, which may occur in a receptor-independent manner. It has been shown that EGF stimulation of Huh7.5 cells results in increased uptake of several different viral pseudoparticles, including influenza A, VSV and endogenous feline leukaemia virus RD114 (Lupberger et al 2011). Both influenza A and VSV have been demonstrated to enter cells via clathrin-dependent mechanisms (Lakadamyali et al 2004, Cureton et al 2009), as with HCV, however there is also evidence for macropinocytic uptake of influenza A (de Vries et

al 2011). However, RD114 has been shown to enter cells by directly penetrating the plasma membrane in a pH-independent manner. As uptake of viruses with multiple endocytic mechanisms is promoted by EGF stimulation, macropinocytosis could offer a mechanism for this effect. Nevertheless, trafficking of macropinosomes is poorly understood and the trafficking of viruses internalised via clathrin-mediated endocytosis requires trafficking through the endosomal system for pH-mediated fusion, and productive infection to occur. It is therefore unclear whether macropinocytosis would offer a route for productive infection of viruses which require a pH-mediated endosomal fusion step, such as HCV.

However, HCV has been shown to internalise exclusively via clathrin-mediated endocytosis under normal circumstances. Additionally, EGFR internalisation has been shown to be important for HCV entry and, under physiological concentrations, EGFR is thought to internalise via clathrin-mediated endocytosis (Sigismund et al 2008). TIRF imaging revealed that formation of clathrin-coated pits on the plasma membrane is promoted by EGF stimulation in Huh7.5 cells and that activated EGFR localises to these CCPs (**Figures 4.6 and 4.7**).

Therefore, two endocytic pathways are upregulated in response to EGFR activation in Huh7.5, which may be relevant for the concomitant increase in HCV entry in EGF-treated cells. It will be necessary to distinguish between the effects of the upregulation of each pathway on HCV entry. Therefore, knockdown of PAK1, a protein involved in macropinocytosis, and AP2 was carried out using siRNA in Huh7.5 cells and strong knockdown was achieved in both cases. Future work should include applying these knockdowns to HCV infection studies to distinguish between the contributions of each pathway to the EGF-induced increase in HCV entry (see **6.2 Future Directions**).

Internalisation of the HCV co-receptor CD81 with entry factor CLDN1 has been shown to be stimulated by virus binding and is thought to occur via clathrin-mediated endocytosis (Harris et al 2008, Farquhar et al 2012). As EGF stimulation has been shown to promote clathrin-mediated endocytosis (**Figure 4.6**), the effects of EGF stimulation on internalisation and trafficking of CD81 and EGFR were investigated in further detail. Live-cell confocal imaging of Huh7.5 cells with and without EGF stimulation revealed that both membrane proteins are internalised rapidly and degraded in response to EGFR activation (**Figures 5.1 and 5.2**, respectively). The two receptors colocalise on the cell surface within 5 minutes of EGF addition and the degree of colocalisation decreases over time (**Figure 5.3**). This points to a possible mechanism for CD81 internalisation alongside the growth factor receptor and offers the first observation of the two proteins colocalising on the cell surface. However, there is little intracellular colocalisation between the two proteins (**Figure 5.4**), suggesting that internalisation occurs rapidly, followed by trafficking through different endocytic compartments, consistent with the differing kinetics of degradation seen. This was confirmed by super-resolution imaging of CD81 clustering with and without EGF stimulation. Analysis revealed that there are less clusters of CD81 on the cell surface after 30 minutes stimulation, corroborating a rapid internalisation of the tetraspanin in response to EGF stimulation (**Figure 5.7**). This evidence highlights possible mechanisms by which EGF stimulation may mechanistically promote HCV internalisation. Firstly, virus may be internalised as a result of fluid-phase uptake, resulting in entry of extracellular or receptor-bound virus into the cell. Secondly, upregulation of clathrin-mediated endocytosis may result in increased viral uptake through its established internalisation mechanism.

Tetraspanins have long been known to regulate the signalling and trafficking of growth factor receptors (Murayama et al 2008, Sadej et al 2010). CD82 associates with ErbB family receptor tyrosine kinases, and its increased expression in mammary epithelial cells significantly increased ligand-induced internalisation of EGFR (Odintsova et al 2003). Additionally, CD9, the most closely related tetraspanin to CD81 has been shown to physically and functionally associate with EGFR in cancer cells, including HepG2-CD9 cells, regulating EGF-induced signalling (Murayama et al 2008). Therefore, while it is unclear whether there is a direct interaction between CD81 and EGFR in Huh.7 cells, a functional interplay between the two membrane proteins within tetraspanin microdomains may play a role in mediating the EGF-stimulated increase in HCV entry.

Filopodia formation and growth were also interestingly shown to be promoted in response to EGF stimulation (**Figure 4.4**). Filopodia are thought to play a role in mediating first contact with viral particles *in vivo* (Warren et al 2006), and increasing filopodial length and number would increase the chances of virus binding, and therefore entry. Interestingly, filopodia have been shown to sense EGF and to respond by inducing retrograde transport of activated EGFRs towards the cell body for internalisation (Lidke et al 2005). Evidence has suggested that HCV particles bind to CD81 in filopodia, where it is highly expressed and to traffic towards the cell body for internalisation (Coller et al 2009). It would therefore be interesting to investigate the localisation and lateral movement of CD81 and EGFR in filopodia in response to EGF stimulation. While evidence from this thesis suggests that CD81 localisation is not enriched, or depleted in filopodia (as would be expected if CD81 had been transported to the cell body) (**Figure 4.5**), this was carried out with overexpressed CD81, which results in such high expression within the plasma membrane and

filopodia that individual clusters of CD81 are not easily distinguishable. Therefore, future work looking at CD81 localisation in filopodia should be carried out using IC to label CD81 and super-resolution techniques used to be able to visualise clusters of CD81 more readily.

Several other viruses have been shown to activate growth factor receptor signalling, thus mimicking the action of growth factors on the cells they infect, including Influenza A virus (Monick et al 2005, Eierhoff et al 2010). Evidence suggests that HCV may act in the same manner (Diao et al 2012), and as such, could be responsible for inducing the effects seen in **Chapters 4 and 5**, independently of EGF. Therefore, it is interesting to speculate that HCV could instigate its own entry by promoting endocytic pathways and the internalisation and trafficking of its own receptors, as well as promoting virus attachment through filopodial extension. Future work should investigate whether HCV-infected cells have increased membrane ruffles and blebs or have increased numbers of, or longer filopodia.

6.2 Future Directions

In summary, results in this thesis demonstrate that EGF stimulation of Huh7.5 cells promotes clathrin-mediated endocytosis, colocalisation of CD81 with EGFR and EGFR localisation to clathrin-coated pits, resulting in increased internalisation of CD81 and EGFR, all of which offer potential mechanisms of EGF-induced HCV endocytosis. Tetraspanins have been shown to interact with and influence growth factor receptor signalling and trafficking through their association in TEMs. However, it remains to be determined whether the two receptors interact directly. Additionally, this thesis demonstrates that two endocytic pathways are stimulated by EGF

treatment, which could contribute to the EGF-induced promotion in viral entry observed by Lupberger et al (Lupberger et al 2011). While the colocalisation of activated EGFR with clathrin in the plasma membrane suggests that EGFR and CD81 internalise via clathrin-mediated endocytosis, the functional role for macropinocytosis in viral entry remains to be assessed.

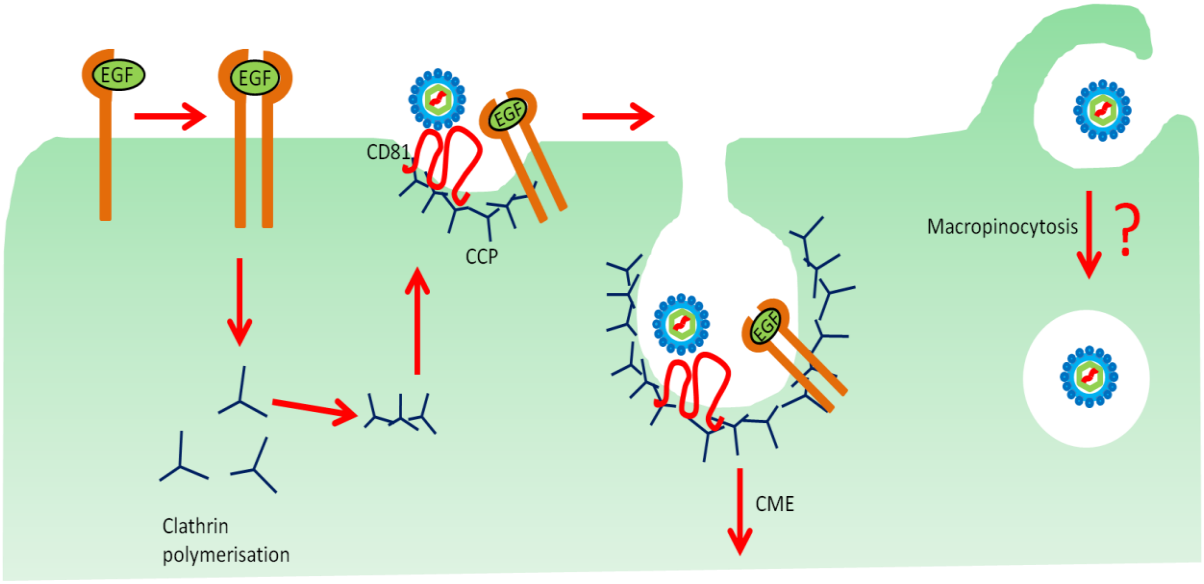

Figure 6.1: Possible mechanisms for EGF-induced HCV entry. EGF promotes the formation of clathrin-coated pits (CCPs) and macropinocytosis in Huh7.5 cells. Activated EGFR localises to clathrin-coated pits and colocalises with CD81 on the cell surface, suggesting they internalise together via clathrin-mediated endocytosis (CME).

This is summarised in **Figure 6.1**. Preliminary work in this direction has shown that PAK1, a protein required for all stages of macropinocytosis can be efficiently silenced in Huh7.5 cells by siRNA transfection, and that this reduces dextran uptake. AP2, which is required for clathrin-mediated endocytosis was also efficiently knocked

down (**Figure 4.8**). Future work should investigate the effects of these knockdowns on HCV entry using HCVpp infection assays.

Additionally, as CD81 localisation in filopodia was measured in cells overexpressing CD81-GFP, this should be further investigated with endogenous protein, and the localisation and trafficking of EGFR within filopodia should be investigated alongside, to determine whether EGF stimulation promotes retrograde traffic of the two receptors towards the cell body.

Finally, it is possible that HCV mimics EGF stimulation by activating EGFR independently of EGF (Diao et al 2012), as has been shown for other viruses (Monick et al 2005, Eierhoff et al 2010), stimulating its own internalisation. Therefore, the internalisation of receptors, upregulation of endocytic pathways and filopodial extension should be studied in HCV-infected cells.

CHAPTER 7

REFERENCES

Aboulaich N, Vainonen JP, Strålfors P, Vener AV. Vectorial proteomics reveal targeting, phosphorylation and specific fragmentation of polymerase I and transcript release factor (PTRF) at the surface of caveolae in human adipocytes. Biochem J. 383(2), 237-48 (2004).

Adam R, McMaster P, O'Grady JG et al. Evolution of liver transplantation in Europe. Report of the European Liver Transplant Registry. Liver Transplantation. 9(12),1231–1243 (2003).

Agnello V, Abel G, Elfahal M, Knight GB and Zhang QX. Hepatitis C virus and other flaviviridae viruses enter cells via low density lipoprotein receptor. Proc. Natl Acad. Sci. USA. 96, 12766–12771 (1999).

Amyere M, Payrastre B, Krause U, Van Der Smissen P, Veithen A, Courtoy PJ. Constitutive macropinocytosis in oncogene-transformed fibroblasts depends on sequential permanent activation of phosphoinositide 3-kinase and phospholipase C. Mol. Biol. Cell. 11(10), 3453-67 (2000).

Anderson HA et al. Bound simian virus 40 translocates to caveolin-enriched membrane domains, and its entry is inhibited by drugs that selectively disrupt caveolae. Mol. Biol. Cell 7 (11), 1825-34 (1996).

André P, Komurian-Pradel F, Deforges S, Perret M, Berland JL, Sodoyer M, Pol S, Bréchot C, Paranhos-Baccalà G, Lotteau V. Characterization of low- and very-low-density hepatitis C virus RNA-containing particles. J. Virol. 76(14), 6919-28 (2002).

Alpuche-Aranda CM et al. Salmonella stimulate macrophage macropinocytosis and persist within spacious phagosomes. J. Exp. Med. 179, 601-608 (1994).

Arteaga CL. Overview of epidermal growth factor receptor biology and its role as a therapeutic target in human neoplasia. Semin. Oncol. 29(5 Suppl 14), 3-9 (2002).

Ashfaq UA, Javed T, Rehman S, Nawaz Z, Riazuddin S. An overview of HCV molecular biology, replication and immune responses. Virol. J. 8, 161 (2011).

Atalay G, Cardoso F, Awada A, Piccart MJ. Novel therapeutic strategies targeting the epidermal growth factor receptor (EGFR) family and its downstream effectors in breast cancer. Ann. Oncol. 14(9), 1346-63 (2003).

Auciello G, Cunningham DL, Tatar T, Heath JK and Rappoport JZ. Regulation of fibroblast growth factor receptor signalling and trafficking by Src and Eps8. J. Cell Sci. 126(2), 613-24 (2013).

Auger KR et al. PDGF-dependent tyrosine phosphorylation stimulates production of novel phosphoinositides in intact cells. Cell 57, 167-175 (1989).

Barnes A. Hepatitis C virus entry receptor dynamics. M. Res. Thesis, University of Birmingham, Uk (2011).

Bar-Sagi D et al. Induction of membrane ruffling and fluid-phase pinocytosis in quiescent fibroblasts by Ras proteins. Science 233, 1061-1068 (1986).

Bartenschlager et al. Replication of Hepatitis C Virus. Baillieres Best Pract. Res. Clin. Gastroenterol. 14, 241-54 (2000).

Bartenschlager et al. Replication of hepatitis C virus in cell culture. Antiviral Res. 60, 91-102 (2003).

Barth H, Schafer C, Adah MI, Zhang F, Linhardt RJ et al. Cellular binding of hepatitis C virus envelope glycoprotein E2 requires cell surface heparan sulfate. J. Biol. Chem. 278, 41003–41012 (2003).

Bartosch B et al. Cell entry of hepatitis C virus requires a set of co-receptors that include the CD81 tetraspanin and the SR-B1 scavenger receptor. J. Biol. Chem. 278, 41624-41630 (2003a).

Bartosch B et al. Infectious hepatitis C virus pseudo-particles containing functional E1-E2 envelope protein complexes. J. Exp. Med. 197(5), 633-642 (2003b).

Bartosch B et al. In vitro assay for neutralizing antibody to hepatitis C virus: evidence for broadly conserved neutralization epitopes. Proc. Natl Acad. Sci. USA 100(24), 14199-14204 (2003c).

Bartosch B and Cosset FL. Cell Entry of hepatitis C. Virology 348(1), 1-12 (2006).

Beer C, Andersen DS, Rojek A and Pedersen L. Caveola-dependent endocytic entry of amphotropic murine leukemia virus. J. Virol. 79(16), 10776-87 (2005).

Benedicto I et al. The tight junction-associated protein occludin is required for a postbinding step in hepatitis C virus entry and infection. J Virol. 83(16), 8012-20 (2009).

Benmerah A, Bayrou M, Cerf-Bensussan N and Dautry-Varsat A. Inhibition of clathrin-coated pit assembly by an Eps15 mutant. J. Cell Sci. 112(9), 1303-11 (1999).

Berditchevski F and Odintsova E. Tetraspanins as regulators of protein trafficking. Traffic 8(2), 89-96 (2007).

Bergelson JM et al. Isolation of a common receptor for coxsackie B viruses and adenoviruses 2 and 5. Science 275(5304), 1320 (1997).

Betzig E, Patterson GH, Sougrat R, Lindwasser OW, Olenych S et al. Imaging intracellular fluorescent proteins at nanometer resolution. Science. 313(5793),1642-5 (2006).

Blanchard E et al. Hepatitis C virus entry depends on clathrin-mediated endocytosis. J. Virol. 80(14), 6964-6972 (2006).

Botos E et al. Regulatory role of kinases and phosphatases on the internalisation of caveolae in HepG2 cells. Micron. 38(3), 313-20 (2007).

Boucrot E, Saffarian S, Zhang R, Kirchhausen T. Roles of AP-2 in clathrin-mediated endocytosis. PLoS ONE 5(5), e10597 (2010).

Brazzoli M, Bianchi A, Filippini S, Weiner A, Zhu Q et al. CD81 is a central regulator of cellular events required for hepatitis C virus infection of human hepatocytes. J Virol. 82(17), 8316-29 (2008).

Bretscher A, Reczek D and Berryman M. Ezrin: a protein requiring conformational activation to link microfilaments to the plasma membrane in the assembly of cell surface structures. J Cell Sci. 110 (24), 3011-8 (1997).

Brindley MA, Hunt CL, Kondratowicz AS, Bowman J, Sinn PL et al. Tyrosine kinase receptor Axl enhances entry of Zaire ebolavirus without direct interactions with the viral glycoprotein. Virology 415(2), 83-94 (2011).

Bryant D et al. EGF induces macropinocytosis and SNX1-modulated recycling of E-cadherin. J. Cell Sci. 120, 1818-1828 (2007).

Buccione R, Orth JD and McNiven MA. Foot and mouth: podosomes, invadopodia and circular dorsal ruffles. Nat. Rev. Mol. Cell Biol. 5(8), 647-57 (2004).

Burgdorf S and Kurts C. Endocytosis mechanisms and the cell biology of antigen presentation. Curr. Opin. Immunol. 20(1), 89-95 (2008).

Cao H, Chen J, Awoniyi M, Henley JR and McNiven MA. Dynamin 2 mediates fluid-phase micropinocytosis in epithelial cells. J. Cell Sci.120(23):4167-77 (2007).

Carpentier JL, Lew DP, Paccaud JP, Gil R, Iacopetta B et al. Internalization pathway of C3b receptors in human neutrophils and its transmodulation by chemoattractant receptors stimulation. Cell Regul. 2(1):41-55 (1991).

Caswell PT and Norman JC. Integrin trafficking and the control of cell migration. Traffic 7(1):14-21 (2006).

Catanese MT et al. Role of scavenger receptor class B type I in hepatitis C virus entry: kinetics and molecular determinants. J. Virol. 84, 34-43 (2010).

Chang MP, Mallet WG, Mostov KE and Brodsky FM. Adaptor self-aggregation, adaptor-receptor recognition and binding of alpha-adaptin subunits to the plasma membrane contribute to recruitment of adaptor (AP2) components of clathrin-coated pits. EMBO J. 12(5), 2169-80 (1993).

Charras GT, Hu CK, Coughlin M and Mitchison TJ. Reassembly of contractile actin cortex in cell blebs. J. Cell Biol. 175(3), 477-90 (2006).

Choo Q et al. Isolation of a cDNA clone derived from a blood-borne non-A, non-B viral hepatitis genome. Science 244(4902), 359–62 (1989).

Chung CK, Ge W. Epidermal growth factor differentially regulates activin subunits in the zebrafish ovarian follicle cells via diverse signaling pathways. Mol. Cell Endocrinol. 361(1-2), 133-42 (2012).

Clotet B , Bellos N, Molina JM, Cooper D, Goffard JC et al. Efficacy and safety of darunavir-ritonavir at week 48 in treatment-experienced patients with HIV-1 infection in POWER 1 and 2: a pooled subgroup analysis of data from two randomised trials. Lancet 369,1169–1178 (2007).

Codran A, Royer C, Jaeck D, Bastien-Valle M, Baumert TF et al. Entry of hepatitis C virus pseudotypes into primary human hepatocytes by clathrin-dependent endocytosis. J. Gen. Virol. 87(9), 2583-93 (2006).

Coffey GP, Rajapaksa R, Liu R, Sharpe O, Kuo CC, et al. Engagement of CD81 induces ezrin tyrosine phosphorylation and its cellular redistribution with filamentous actin. J. Cell Sci. 122(17), 3137-44 (2009).

Cohen FS, Akabas MH, Zimmerberg J and Finkelstein A. Parameters affecting the fusion of unilamellar phospholipid vesicles with planar bilayer membranes. J. Cell Biol. 98(3),1054-62 (1984).

Cokakli M, Erdal E, Nart D, Yilmaz F, Sagol O, et al. Differential expression of Caveolin-1 in hepatocellular carcinoma: correlation with differentiation state, motility and invasion. BMC Cancer. 24:9, 65 (2009).

Coller KE, Berger KL, Heaton NS, Cooper JD, Yoon R, et al. RNA interference and single particle tracking analysis of hepatitis C virus endocytosis. PLoS Pathogens 5(12), e1000702 (2009).

Cormier EG, Tsamis F, Kajumo F, Durso RJ, Gardner JP, et al. CD81 is an entry coreceptor for hepatitis C virus. Proc. Natl Acad. Sci. USA 101, 7270-7274 (2004).

Couet J, Sargiacomo M and Lisanti MP. Interaction of a receptor tyrosine kinase, EGF-R, with caveolins. Caveolin binding negatively regulates tyrosine and serine/threonine kinase activities. J. Biol. Chem. 272, 30429 (1997).

Coyne CB et al. Coxsackie virus entry across epithelial tight junctions requires occludin and the small GTPases Rab34 and Rab5. Cell Host Microbe 2,181-192 (2007).

Coyne CB and Bergelson JM. Virus-induced Abl and Fyn kinase signals permit coxsackievirus entry through epithelial tight junctions. Cell 124(1),119-31 (2006).

Cukierman L, Meertens L, Bertaux C, Kajumo F and Dragic T. Residues in a highly conserved claudin-1 motif are required for hepatitis C virus entry and mediate the formation of cell-cell contacts. J. Virol. 83(11), 5477-84 (2009).

Cureton DK, Massol RH, Saffarian S, Kirchhausen TL and Whelan SP. Vesicular stomatitis virus enters cells through vesicles incompletely coated with clathrin that depend upon actin for internalization.PLoS Pathog.5(4),e1000394 (2009).

Daecke J, Fackler OT, Dittmar MT, Kräusslich HG. Involvement of Clathrin-Mediated Endocytosis in Human Immunodeficiency Virus Type 1 Entry. J. Virol. 79(3),1581-1594 (2005).

Damm E-M, Pelkmans L, Kartenbeck J, Mezzacasa A, Kurzchalia T, et al. clathrin and caveolin-1- independent endocytosis: entry of simian virus 40 into cells devoid of caveolae. J. Cell Biol. 168(3), 477-488 (2005)..

Dangoria NS, Breau WC, Anderson HA, Cishek DM and Norkin LC. Extracellular Simian Virus 40 Induces and ERK/MAP Kinase-Independent Signalling Pathway that Activates Primary Response Genes and Promotes Virus Entry. J. Gen. Virol. 77, 2173-2182 (1996).

de Vries E, Tscherne DM, Wienholts MJ, Cobos-Jiménez V, Scholte F, et al. Dissection of the influenza A virus endocytic routes reveals macropinocytosis as an alternative entry pathway. PLoS Pathog. 7(3), e1001329 (2011).

Dharmawardhane S, Schürmann A, Sells MA, Chernoff J, Schmid SL and Bokoch GM. Regulation of macropinocytosis by p21-activated kinase-1. Mol. Biol. Cell 11(10), 3341-3352 (2000).

Diao J, Pantua H, Ngu H, Komuves L, Diehl L, Schaefer G and Kapadia SB. Hepatitis C virus induces epidermal growth factor receptor activation via CD81 binding for viral internalization and entry. J. Virol. 86(20):10935-49 (2012).

Doherty GJ and McMahon HT. Mechanisms of endocytosis. Annu. Rev. Biochem. 78, 857-902 (2009).

Donepudi M and Resh MD. c-Src trafficking and co-localization with the EGF receptor promotes EGF ligand-independent EGF receptor activation and signaling. Cell Signal. 20(7),1359-67 (2008).

Downes CP, Gray A and Lucocq JM. Probing phosphoinositide functions in signalling and membrane trafficking. Trends Cell Biol.15, 259-268 (2005).

Downward J, Parker P and Waterfield MD. Autophosphorylation sites on the epidermal growth factor receptor. Nature 311(5985), 483–5 (1984).

Dowrick P, Kenworthy P, McCann B and Warn R. Circular ruffle formation and closure lead to macropinocytosis in hepatocyte growth factor/scatter factor-treated cells. Eur. J. Cell Biol. 61(1), 44-53 (1993).

Dreux M, Dao Thi VL, Fresquet J, Guérin M, Julia Z, Verney G, Durantel D, Zoulim F, Lavillette D, Cosset FL and Bartosch B. Receptor complementation and mutagenesis reveal SR-BI as an essential HCV entry factor and functionally imply its intra- and extra-cellular domains. PLoS Pathog. 5(2), e1000310 (2009).

D'Souza-Schorey C and Chavrier P. ARF Proteins: Roles in Membrane Traffic and Beyond. Nat. Rev. Mol. Cell Biol. 7(5), 347-58 (2006).

Duus KM, Lentchitsky V, Wagenaar T, Grose C and Webster-Cyriaque J. Wild-type Kaposi's sarcoma-associated herpesvirus isolated from the oropharynx of

immune-competent individuals has tropism for cultured oral epithelial cells. J. Virol. 78(8), 4074-84 (2004).

Eierhoff T, Hrincius ER, Rescher U, Ludwig S and Ehrhardt C. The epidermal growth factor receptor (EGFR) promotes uptake of influenza A viruses (IAV) into host cells. PLoS Pathog. 6(9), e1001099 (2010).

Evans MJ von Hahn T, Tscherne DM, Syder AJ, Panis M, Wölk B, et al. Claudin-1 is a hepatitis C virus co-receptor required for a late step in entry. Nature 446, 801-805 (2007).

Farquhar MJ, Hu K, Harris HJ, Davis C, Brimacombe CL, Fletcher SJ, Baumert TF, Rappoport JZ, Balfe P and Mceating JA. Hepatitis C virus induces CD81 and claudin-1 endocytosis. J Virol. 86(8), 4305-16 (2012).

Feinstone, SM, Kapikian, AZ, Purcell, RH, Alter, HJ and Holland, PV. Transfusion-associated hepatitis not due to viral hepatitis type A or B. N. Engl. J. Med. 292, 767–770 (1975).

Ferguson KM, Berger MB, Mendrola JM, Cho HS, Leahy DJ and Lemmon MA. EGF activates its receptor by removing interactions that autoinhibit ectodomain dimerization. Mol. Cell 11 (2), 507–517 (2003).

Fernández MA, Albor C, Ingelmo-Torres M, Nixon SJ, Ferguson C, Kurzchalia T, Tebar F, Enrich C, Parton RG and Pol A. Caveolin-1 is essential for liver regeneration.Science 313(5793), 1628-32 (2006).

Fletcher NF, Wilson GK, Murray J, Hu K, Lewis A, et al. Hepatitis C virus infects the endothelial cells of the blood-brain barrier. Gastroenterology 142(3):634-643 (2012).

Fletcher SJ and Rappoport JZ. The Role of Vesicle Trafficking in Epithelial Cell Motility. Biochem. Soc. Trans. 37(5), 1072-6 (2009).

Flint M, Maidens C, Loomis-Price LD, Shotton C, Dubuisson J, et al. Characterisation of Hepatitis C Virus E2 Glycoprotein Interaction with a Putative Cellular Receptor, CD81. J. Virol. 73(80), 6235-44 (1999).

Flint M, von Hahn T, Zhang J, Farquhar M, Jones CT, et al. Diverse CD81 proteins support hepatitis C virus infection. J. Virol. 80, 11331-11342 (2006).

Ford MG, Mills IG, Peter BJ, Vallis Y, Praefcke GJ, et al. Curvature of clathrin-coated pits driven by epsin. Nature 419, 361–66 (2002).

Francis CL, Ryan TA, Jones BD, Smith SJ and Falkow S. Ruffles induced by salmonella and other stimuli direct macropinocytosis of bacteria. Nature 364, 639-642 (1993).

Frank C, Mohamed MK, Strickland GT, Lavanchy D, Arthur RR, et al. The role of parenteral antischistosomal therapy in the spread of hepatitis C virus in Egypt. Lancet 355, 887–91 (2000).

Frick M, Bright NA, Riento K, Bray A, Merrified C and Nichols BJ. Coassembly of flotillins induces formation of membrane microdomains, membrane curvature, and vesicle budding. Curr. Biol. 7(13), 1151-6 (2007).

Forgac M. Vacuolar ATPases: rotary proton pumps in physiology and pathophysiology. Nat. Rev. Mol. Cell Biol. 8(11), 917-29 (2007).

Galvagni F, Anselmi F, Salameh A, Orlandini M, Rocchigiani M and Oliviero S. Vascular endothelial growth factor receptor-3 activity is modulated by its association with caveolin-1 on endothelial membrane. Biochemistry 46(13), 3998-4005 (2007).

Gelles J, Schnapp BJ and Sheetz MP. Tracking kinesin-driven movements with nanometre-scale precision. Nature 331(6155), 450-3 (1988).

Glebov OO Bright NA and Nichols BJ. Flotillin-1 defines a clathrin-independent endocytic pathway in mammalian cells. Nat. Cell Biol. 8(1),46-54 (2006).

Grewe C, Beck A and Gelderblom HR. HIV: early virus-cell interactions. J. Acquir. Immune Defic. Syndr. 3(10), 965-74 (1990).

Grimmer S, van Deurs B, Sandvig K. Membrane ruffling and macropinocytosis in A431 cells require cholesterol. J. Cell Sci. 115, 2953-2962 (2002).

Grove J, Huby T, Stamataki Z, Vanwolleghem T, Meuleman P, et al. Scavenger receptor BI and BII expression levels modulate hepatitis C virus infectivity. J. Virol. 81, 3162-3169 (2007).

Grove J and Marsh M. The cell biology of receptor-mediated virus entry. J. Cell Biol.195(7), 1071-82 (2011).

Gruenberg J and van der Goot FG. Mechanisms of pathogen entry through the endosomal compartments. Nat. Rev. Mol. Cell Biol. 7(7), 495-504 (2006).

Guo Q, Ho HT, Dicker I, Fan L, Zhou N, Friborg J, et al. Biochemical and genetic characterizations of a novel human immunodeficiency virus type 1 inhibitor that blocks gp120-CD4 interactions. J. Virol. 77, 10528–36 (2003).

Gustafsson MG. Surpassing the lateral resolution limit by a factor of two using structured illumination microscopy. J. Microsc. 198(2), 82-7 (2000).

Gustafsson MG. Super-resolution light microscopy goes live. Nat. Methods 5(5), 385-7 (2008).

Habuchi S, Ando R, Dedecker P, Verheijen W, Mizuno H, et al. Reversible single-molecule photoswitching in the GFP-like fluorescent protein Dronpa. Proc. Natl Acad. Sci. U S A 102(27), 9511-6 (2005).

Harris HJ, Farquhar MJ, Mee CJ, Davis C, Reynolds GM, et al. CD81 and claudin 1 coreceptor association: role in hepatitis C virus entry. J. Virol. 82(10), 5007-20 (2008).

Harris HJ, Davis C, Mullins JG, Hu K, Goodall M, et al. Claudin association with CD81 defines hepatitis C virus entry. J. Biol. Chem. 285(27), 21092-102 (2010).

Heffelfinger SC, Hawkins HH, Barrish J, Taylor L and Darlington GJ. Sk Hep-1: a cell line of endothelial origin. In Vitro Cell Dev. Biol. 28A(2),136-42 (1992).

Helle F and Dubuisson J. Hepatitis C virus entry into host cells. Cell. Mol. Life Sci. 65(1):100-12 (2008).

Heilemann M, van de Linde S, Schüttpelz M, Kasper R, Seefeldt B, Mukherjee A, Tinnefeld P and Sauer M. Subdiffraction-resolution fluorescence imaging with conventional fluorescent probes. Angew Chem. Int. Ed. Engl. 47(33), 6172-6 (2008).

Helenius A, Kartenbeck J, Simons K and Fries E. On the entry of Semliki forest virus into BHK-21 cells. J. Cell Biol. 84(2), 404-20 (1980).

Heller-Harrison RA, Morin M, Guilherme A and Czech MP. Insulin-mediated targeting of phosphatidylinositol 3-kinase to GLUT4-containing vesicles. J. Biol. Chem. 271, 10200-10204 (1996).

Hemler ME. Tetraspanin functions and associated microdomains. Nat. Rev. Mol. Cell Biol. 6(10), 801-11 (2005).

Henley JR, Krueger EW, Oswald BJ and McNiven MA. Dynamin-mediated internalization of caveolae. J. Cell Biol. 141(1), 85-99 (1998).

Hess ST, Girirajan TP and Mason MD. Ultra-high resolution imaging by fluorescence photoactivation localization microscopy. Biophys. J. 91(11), 4258-72 (2006).

Hewlett LJ Prescott AR and Watts C. The coated pit and macropinocytic pathways serve distinct endosome populations. J. Cell Biol. 124, 689-703 (1994).

Hicks CB Cahn P, Cooper DA, Walmsley SL, Katlama C, et al. Durable efficacy of tipranavir-ritonavir in combination with an optimised background regimen of antiretroviral drugs for treatment-experienced HIV-1-infected patients at 48 weeks in the Randomized Evaluation of Strategic Intervention in multi-drug reSistant patients with Tipranavir (RESIST) studies: an analysis of combined data from two randomised open-label trials. Lancet 368, 466–75 (2006).

Hijikata M, Kato N, Ootsuyama Y, Nakagawa M and Shimotohno K. Gene mapping of the putative structural region of the hepatitis C virus genome by in vitro processing analysis. Proc. Natl Acad. Sci. USA 88, 5547–5551 (1991).

Hinners I and Tooze SA. Changing directions: clathrin-mediated transport between the Golgi and endosomes. J Cell Sci. 116(5), 763-71 (2003).

Hinrichsen L, Harborth J, Andrees L, Weber K and Ungewickell EJ. Effect of clathrin heavy chain- and alpha-adaptin-specific small inhibitory RNAs on endocytic accessory proteins and receptor trafficking in HeLa cells. J Biol Chem 278(46), 45160-70 (2003).

Hinshaw and Schmid. Dynamin self-assembles into rings suggesting a mechanism for coated vesicle budding. Nature 374(6518), 190-2 (1995).

Hirsch E , Katanaev VL, Garlanda C, Azzolino O, Pirola L, et al. Central role for G protein-coupled phosphoinositide 3-kinase gamma in inflammation. Science 287, 1049-1053 (2000).

Holt MR and Koffer A. Cell motility: proline-rich proteins promote protrusions. Trends Cell Biol. 11(1), 38-46 (2001).

Hsu CJ and Baumgart T. Spatial association of signaling proteins and F-actin effects on cluster assembly analyzed via photoactivation localization microscopy in T cells. PLoS ONE 6(8), e23586 (2011).

Huang F, Khvorova A, Marshall W and Sorkin A. Analysis of clathrin-mediated endocytosis of epidermal growth factor receptor by RNA interference. J. Biol. Chem. 279(16), 16657-61 (2004).

Huang B, Bates M and Zhuang X. Super-resolution fluorescence microscopy. Ann. Rev. Biochem.78, 993-1016 (2009).

Huether A, Höpfner M, Sutter AP, Schuppan D and Scherübl H. Erlotinib induces cell cycle arrest and apoptosis in hepatocellular cancer cells and enhances chemosensitivity towards cytostatics. J. Hepatol. 43(4), 661-9 (2005).

Huotari J and Helenius A. Endosome maturation. EMBO J. 30(17), 3481-500 (2011).

Ivanov AI. Pharmacological inhibition of endocytic pathways: is it specific enough to be useful? Methods Mol. Biol. 440,15-33 (2008).

Jones CT, Murray CL, Eastman DK, Tassello J and Rice CM. Hepatitis C virus p7 and NS2 proteins are essential for production of infectious virus. J. Virol. 81, 8374–8383 (2007).

Jovic M, Sharma M, Rahajeng J and Caplan S. The early endosome: a busy sorting station for proteins at the crossroads. Histol. Histopathol. 25(1), 99-112 (2010).

Kane GC, Lam CF, O'Cochlain F, Hodgson DM, Reyes S, Liu XK, Miki T, Seino S, Katusic ZS and Terzic A. Gene knockout of the KCNJ8-encoded Kir6.1 K(ATP) channel imparts fatal susceptibility to endotoxemia. FASEB J. 20(13), 2271-80 (2006).

Kasahara K, Nakayama Y, Sato I, Ikeda K, Hoshino M, Endo T and Yamaguchi N. Role of Src-family kinases in formation and trafficking of macropinosomes. J. Cell Physiol. 211(1), 220-32 (2007).

Kawase M, Shirato K, Matsuyama S and Taguchi F. Protease-mediated entry via the endosome of human coronavirus 229E. J. Virol. 83(2), 712-21 (2009).

Kechkar A, Nair D, Heilemann M, Choquet D and Sibarita JB. Real-time analysis and visualization for single-molecule based super-resolution microscopy. PLoS ONE 8(4), e62918 (2013).

Keck ZY, Sung VM, Perkins S, Rowe J, Paul S, et al.. Human Monoclonal Antibody to Hepatitis C Virus E1 Glycoprotein that Blocks Virus Attachment and Viral Infectivity. J. Virol. 78(13), 7257-63 (2004).

Keller HU. Diacylglycerols and PMA are particularly effective stimulators of fluid pinocytosis in human neutrophils. J. Cell Physiol.145(3), 465-71 (1990).

Kerr MC, Lindsay MR, Luetterforst R, Hamilton N, Simpson F, et al. Visualisation of macropinosome maturation by recruitment of sorting nexins. J Cell Sci. 119, 3967-3980 (2006).

Khazaie K, Schirrmacher V and Lichtner RB. EGF receptor in neoplasia and metastasis. Cancer Metastasis Rev. 12(3-4), 255-74 (1993).

Kirchhausen T, Macia E and Pelish HE. Use of dynasore, the small molecule inhibitor of dynamin, in the regulation of endocytosis. Methods Enzymol. 438, 77-93 (2008).

Kirkham M and Parton RG. Clathrin-independent endocytosis: new insights into caveolae and non-caveolar lipid raft carriers. Biochim. Biophys. Acta. 1745(3), 273-86 (2005).

Kirkham M, Fujita A, Chadda R, Nixon SJ, Kurzchalia TV, et al. Ultrastructural identification of uncoated caveolin-independent early endocytic vehicles. J. Cell Biol. 168, 465–76 (2005).

Kiser JJ, Burton JR, Anderson PL and Everson GT. Review and management of drug interactions with boceprevir and telaprevir.Hepatology 55(5),1620-1628 (2012).

Kolykhalov AA, Agapov EV, Blight KJ, Mihalik K, Feinstone, SM and Rice CM. Transmission of hepatitis C by intrahepatic inoculation with transcribed RNA. Science 277, 570–574 (1997).

Koike K. Hepatitis C virus contributes to hepatocarcinogenesis by modulating metabolic and intracellular signaling pathways. J. Gastroenterol. Hepatol. 22, S108–11 (2007).

Koivusalo , Welch C, Hayashi H, Scott CC, Kim M, et al. Amiloride inhibits macropinocytosis by lowering submembranous pH and preventing Rac1 and Cdc42 signaling. J. Cell Biol. 188(4), 547–563 (2010).

Koutsoudakis G, Kaul A, Steinmann E, Kallis S, Lohmann V, Pietschmann T and Bartenschlager R. Characterization of the early steps of hepatitis C virus infection by using luciferase reporter viruses. J. Virol. 80, 5308–5320 (2006).

Krieger SE, Zeisel MB, Davis C, Thumann C, Harris HJ, et al. Inhibition of hepatitis C virus infection by anti-claudin-1 antibodies is mediated by

neutralization of E2-CD81-claudin-1 associations. Hepatol. 51(4), 1144-57 (2010).

Kuan CT, Wikstrand CJ and Bigner DD. EGF mutant receptor vIII as a molecular target in cancer therapy. Endocr. Relat. Cancer 8(2), 83–96 (2001).

Kuiken C and Simmonds P. Nomenclature and numbering of the hepatitis C virus. Methods Mol. Biol. 510, 33-53 (2009).

Kuo G, Choo QL, Alter HJ, Gitnick GL, Redeker AG, et al. An assay for circulating antibodies to a major etiologic virus of human non-A, non-B hepatitis. Science 244(4902), 362–4 (1989).

Kuritzkes DR, Jacobson J, Powderly WG, Godofsky E, DeJesus E, et al. Antiretroviral activity of the anti-CD4 monoclonal antibody TNX-355 in patients infected with human immunodeficiency virus type 1. J. Infect. Dis. 189, 286–91 (2004).

Labrecque L, Royal I, Surprenant DS, Patterson C, Gingras D and Béliveau R. Regulation of vascular endothelial growth factor receptor-2 activity by caveolin-1 and plasma membrane cholesterol. Mol. Biol. Cell 14(1), 334-47 (2003).

Lajoie P and Nabi IR. Lipid rafts, caveolae, and their endocytosis. Int. Rev. Cell Mol. Biol. 282, 135-63 (2010).

Lalezari JP, Henry K, O'Hearn M, Montaner JS, Piliero PJ, et al. Enfuvirtide, an HIV-1 fusion inhibitor, for drug-resistant HIV infection in North and South America. N. Engl. J. Med. 348, 2175–85 (2003).

Lakadamyali M, Rust MJ and Zhuang X. Endocytosis of influenza viruses. Microbes Infect. 6(10), 929-36 (2004).

Lanzetti L, Palamidessi A, Areces L, Scita G and Di Fiore PP. Rab5 is a signalling GTPase involved in actin remodelling by receptor tyrosine kinases. Nature 429, 309-314 (2004).

Lauer GM and Walker BD. Hepatitis C virus infection. N. Engl. J. Med. 345(1), 41-52 (2001).

Lavoie JN, Hickey E, Weber LA and Landry J. Modulation of actin microfilament dynamics and fluid phase pinocytosis by phosphorylation of heat shock protein 27. J. Biol. Chem. 268(32), 24210-4 (1993).

Lavillette D, Bartosch B, Nourrisson D, Verney G, Cosset FL, Penin F and Pécheur EI. Hepatitis C virus glycoproteins mediate low pH-dependent membrane fusion with liposomes. J. Biol. Chem. 281(7), 3909-17 (2006).

Lehmann MJ, Sherer NM, Marks CB, Pypaert M and Mothes W. Actin- and myosin-driven movement of viruses along filopodia precedes their entry into cells. J. Cell Biol.170(2), 317-25 (2005).

Lewis WH. Pinocytosis. John Hopkins Hosp Bull 49, 17-27 (1931).

Li X, Jeffers LJ, Shao L, Reddy KR, de Medina M, Scheffel J, Moore B and Schiff ER. Identification of Hepatitis C Virus by Immunoelectron Microscopy. J. Viral Hepat. 2(5), 227-34 (1995).

Liberali P, Kakkonen E, Turacchio G, Valente C, Spaar A, et al. The closure of Pak1-dependent macropinosomes requires the phosphorylation of CtBP1/BARS. Embo J. 27, 970-981 (2008).

Lidke DS, Lidke KA, Rieger B, Jovin TM and Arndt-Jovin DJ. Reaching out for signals: filopodia sense EGF and respond by directed retrograde transport of activated receptors. J. Cell Biol. 170(4), 619-26 (2005).

Lim JP, Wang JT, Kerr MC, Teasdale RD and Gleeson PA. A role for SNX5 in the regulation of macropinocytosis. BMC Cell Biol. 9, 58 (2008).

Lin C, Prágai BM, Grakoui A, Xu J and Rice CM. Hepatitis C virus NS3 serine proteinase: trans-cleavage requirements and processing kinetics. J. Virol. 68(12), 8147-57 (1994).

Lin PF, Blair W, Wang T, Spicer T, Guo Q, et al. A small molecule HIV-1 inhibitor that targets the HIV-1 envelope and inhibits CD4 receptor binding. Proc. Natl Acad. Sci. USA 100, 11013–18 (2003).

Lindenbach BD, Evans MJ, Syder AJ, Wölk B, Tellinghuisen TL, et al. Complete replication of hepatitis C virus in cell culture. Science 309(5734), 623-6 (2005).

Lipardi C Mora R, Colomer V, Paladino S, Nitsch L, Rodriguez-Boulan E and Zurzolo C. Caveolin transfection results in caveolae formation but not apical sorting of glycosylphosphatidylinositol (GPI)-anchored proteins in epithelial cells. J. Cell Biol. 140, 617–26 (1998).

Liu L and Pilch PF. A critical role of cavin (polymerase I and transcript release factor) in caveolae formation and organization. J. Biol. Chem. 283(7), 4314-22 (2008).

Liu NQ, Lossinsky AS, Popik W, Li X, Gujuluva C, et al. Human Immunodeficiency virus type 1 enters brain microvascular endothelia by macropinocytosis dependent on lipid rafts and the mitogen-activated protein kinase signalling pathway. J. Virol. 76, 6689-6700 (2000).

Liu YW, Surka MC, Schroeter T, Lukiyanchuk V and Schmid SL. Isoform and splice-variant specific functions of dynamin-2 revealed by analysis of conditional knock-out cells. Mol. Biol. Cell. 19(12), 5347-59 (2008).

Liu S, Yang W, Shen L, Turner JR, Coyne CB and Wang T. Tight junction proteins claudin-1 and occludin control hepatitis C virus entry and are downregulated during infection to prevent superinfection. J. Virol. 83, 2011-2014 (2009).

Lockhart AC and Berlin JD. The epidermal growth factor receptor as a target for colorectal cancer therapy. Semin, Oncol. 32(1), 52-60 2005

Lupberger J, Zeisel MB, Xiao F, Thumann C, Fofana I, et al. EGFR and EphA2 are host factors for hepatitis C virus entry and possible targets for antiviral therapy. Nat. Med. 17(5), 589-95 (2011).

Lynch TJ, Bell DW, Sordella R, Gurubhagavatula S, Okimoto RA, et al. Activating mutations in the epidermal growth factor receptor underlying responsiveness of non-small-cell lung cancer to gefitinib. N. Engl. J. Med. 350(21), 2129–39 (2004).

Macia E, Ehrlich M, Massol R, Boucrot E, Brunner C and Kirchhausen T. Dynasore, a cell-permeable inhibitor of dynamin. Dev. Cell 10(6), 839-50 (2006).

Manes S, Ana Lacalle R, Gómez-Moutón C and Martínez-A C. From rafts to crafts: membrane asymmetry in moving cells. Trends Immunol. 24, 320-326 (2003).

Maniak M. Conserved features of endocytosis in Dictyostelium. Int. Rev. Cytol. 221, 257-287 (2002).

Martin F, Roth DM, Jans DA, Pouton CW, Partridge LJ, Monk PN and Moseley GW. Tetraspanins in viral infections: a fundamental role in viral biology? J. Virol. 79, 10839–10851 (2005).

Mellman I. Membranes and sorting. Curr Opin Cell Biol. 8(4), 497-8 (1996).

Marechal, Prevost MC, Petit C, Perret E, Heard JM and Schwartz O. Human immunodeficiency virus type1 entry into macrophages is mediated by macropinocytosis. J. Virol. 75, 11166-11177 (2001).

Marsh YV and Eppstein DA. Vaccinia virus and the EGF receptor: a portal for infectivity? J. Cell Biochem. 34(4), 239-45 (1987).

Matsuda M, Kubo A, Furuse M and Tsukita S. A peculiar internalization of claudins, tight junction-specific adhesion molecules, during the intercellular movement of epithelial cells. J. Cell Sci. 117(7), 1247-57 (2004).

Mattheyses AL, Simon SM and Rappoport JZ. Imaging with total internal reflection fluorescence microscopy for the cell biologist. J. Cell Sci. 123(21), 3621-8 (2010).

Mayor S and Pagano RE. Pathways of clathrin-independent endocytosis. Nat. Rev. Mol. Cell Biol. 8, 603–12 (2007).

McMahon HT and Boucrot E. Molecular mechanism and physiological functions of clathrin-mediated endocytosis. Nat .Rev. Mol. Cell Biol. 12(8), 517-33 (2011).

McKeating JA, Zhang LQ, Logvinoff C, Flint M, Zhang J, et al. Diverse hepatitis C virus glycoproteins mediate viral infection in a CD81-dependent manner. J. Virol. 78(16), 8496-505 (2004).

Mee CJ, Farquhar MJ, Harris HJ, Hu K, Ramma W, Ahmed A, Maurel P, Bicknell R, Balfe P and McKeating JA. Hepatitis C virus infection reduces hepatocellular

polarity in a vascular endothelial growth factor-dependent manner. Gastroenterology 138(3), 1134-42 (2010).

Meertens L, Bertaux C and Dragic T. Hepatitis C virus entry requires a critical postinternalization step and delivery to early endosomes via clathrin-coated vesicles. J. Virol. 80(23), 11571-1157 (2006).

Meertens L, Bertaux C, Cukierman L, Cormier E, Lavillette D, Cosset FL and Dragic T. The tight junction proteins claudin-1, -6, and -9 are entry cofactors for hepatitis C virus. J. Virol. 82, 3555-3560 (2008).

Meier O, Boucke K, Hammer SV, Keller S, Stidwill RP, Hemmi S and Greber UF.

Adenovirus triggers macropinocytosis and endosomal leakage together with its clathrin-mediated uptake. J. Cell Biol. 158(6), 1119-31 (2002).

Mercer J and Helenius A. Vaccinia virus uses macropinocytosis and apoptotic mimicry to enter host cells. Science 320, 531-535 (2008).

Mercer J and Helenius A. Virus entry by macropinocytosis. Nat. Cell Biol. 11(5), 510-20 (2009).

Mercer J and Helenius A. Apoptotic mimicry: phosphatidylserine-mediated macropinocytosis of vaccinia virus. Ann. NY Acad. Sci. 1209, 49-55 (2010).

Mercer J and Helenius A. Gulping rather than sipping: macropinocytosis as a way of virus entry. Curr. Opin. Microbiol.15(4), 490-9 (2012).

Miyanari Y, Atsuzawa K, Usuda N, Watashi K, Hishiki T, Zayas M, Bartenschlager R, Wakita, T, Hijikata M and Shimotohno K. The lipid droplet is an important organelle for hepatitis C virus production. Nat. Cell Biol. 9, 1089–1097 (2007).

Miyauchi K, Kim Y, Latinovic O, Morozov V and Melikyan GB. HIV Enters cells via endocytosis and dynamin-dependent fusion with endosomes. Cell 137, 433-444 (2009).

Molina S, Castet V, Fournier-Wirth C, Pichard-Garcia L, Avner R, Harats D, Roitelman J, Barbaras R, Graber P, Ghersa P et al. The low-density lipoprotein receptor plays a role in the infection of primary human hepatocytes by hepatitis C virus. J. Hepatol. 46, 411–419 (2007).

Monazahian M, Böhme I, Bonk S, Koch A, Scholz C, Grethe S and Thomssen R. Low Density Lipoprotein Receptor as a Candidate Receptor for Hepatitis C Virus. J. Med. Virol. 57(3), 223-9 (1999).

Monick MM, Cameron K, Staber J, Powers LS, Yarovinsky TO, Koland JG and Hunninghake GW. Activation of the epidermal growth factor receptor by respiratory syncytial virus results in increased inflammation and delayed apoptosis. J. Biol. Chem. 280(3), 2147-58 (2005).

Moriyama T, Marquez JP, Wakatsuki T and Sorokin A. Caveolar Endocytosis is critical for BK virus infection of human renal proximal tubular epithelial cells. J. Virol. 81(16), 8552-8562 (2007).

Morizono K, Xie Y, Olafsen T, Lee B, Dasgupta A, Wu AM and Chen IS. The soluble serum protein Gas6 bridges virion envelope phosphatidylserine to the TAM receptor tyrosine kinase Axl to mediate viral entry. Cell Host Microbe. 9(4), 286-98 (2011).

Motley A, Bright NA, Seaman MN, Robinson MS. Clathrin-mediated endocytosis in AP-2-depleted cells. J. Cell Biol. 162(5), 909-18 (2003).

Moyer JD, Barbacci EG, Iwata KK, Arnold L, Boman B, et al. Induction of apoptosis and cell cycle arrest by CP-358,774, an inhibitor of epidermal growth factor receptor tyrosine kinase. Cancer Res. 57(21), 4838-48 (1997).

Murayama Y, Shinomura Y, Oritani K, Miyagawa J, Yoshida H, et al. The tetraspanin CD9 modulates epidermal growth factor receptor signaling in cancer cells. J Cell Physiol. 216(1), 135-43 (2008).

Nanbo A, Imai M, Watanabe S, Noda T, Takahashi K, Neumann G, Halfmann P and Kawaoka Y. Ebolavirus is internalized into host cells via macropinocytosis in a viral glycoprotein-dependent manner. PLoS Pathog. 6(9), e1001121 (2010).

Ntziachristos V. Fluorescence molecular imaging. Annu. Rev. Biomed. Eng. 8, 1-33 (2006).

Nielsen SU, Bassendine MF, Martin C, Lowther D, Purcell PJ, King BJ, Neely D and Toms GL. Characterization of hepatitis C RNA-containing particles from human liver by density and size. J. Gen. Virol. 89(10), 2507-17 (2008).

Nomura R, Kiyota A, Suzaki E, Kataoka K, Ohe Y, Miyamoto K, Senda T and Fujimoto T. Human coronavirus 229E binds to CD13 in rafts and enters the cell through caveolae. J. Virol. 78(16), 8701-8 (2004).

Norkin LC, Anderson HA, Wolfrom SA and Oppenheim A. Caveolar endocytosis of simian virus 40 is followed by brefeldin a- sensitive transport to the endoplasmic reticulum, where the virus disassembles. J. Virol. 76(10), 5156-5166 (2002).

Nunes-Correia I, Eulálio A, Nir S and Pedroso de Lima MC. Caveolae as an Additional Route for Influenza Virus Endocytosis in MDCK Cells. Cell. Mol. Biol. Lett. 9(1), 47-60 (2004).

Oda K, Matsuoka Y, Funahashi A and Kitano H. A comprehensive pathway map of epidermal growth factor receptor signaling. Mol. Syst. Biol. 1(1), 2005.0010 (2005).

Odintsova E, Sugiura T and Berditchevski F. Attenuation of EGF receptor signaling by a metastasis suppressor, the tetraspanin CD82/KAI-1. Curr. Biol.10(16), 1009-12 (2000).

Odintsova E, Voortman J, Gilbert E and Berditchevski F. Tetraspanin CD82 regulates compartmentalisation and ligand-induced dimerization of EGFR. J Cell Sci. 116(22), 4557-66 (2003).

Oh P, McIntosh DP and Schnitzer JE. Dynamin at the neck of caveolae mediates their budding to form transport vesicles by GTP-driven fission from the plasma membrane of endothelium. J. Cell Biol. 141(1), 101-14 (1998).

Okada T, Hazeki O, Ui M and Katada T. Synergistic activation of PtdIns 3-kinase by tyrosine-phosphorylated peptide and beta gamma-subunits of GTP-binding proteins. Biochem. J. 317, 475-480 (1996).

Op De Beeck A, Voisset C, Bartosch B, Ciczora Y, Cocquerel L, Keck Z, Foung S, Cosset FL and Dubuisson J. Characterisation of Functional Hepatitis C Virus Envelope Glycoproteins. J. Virol. 78(6), 2994-3002 (2004).

Orlandi PA and Fishman PH. Filipin-dependent inhibition of cholera toxin: evidence for toxin internalization and activation through caveolae-like domains. J. Cell Biol. 141(4), 905-15 (1998).

Orlichenko L Huang B, Krueger E and McNiven MA. Epithelial growth factor-induced phosphorylation of caveolin 1 at tyrosine 14 stimulates caveolae formation in epithelial cells. J. Biol. Chem. 281(8), 4570-9 (2005).

Owen DJ and Evans PR. A structural explanation for the recognition of tyrosine-based endocytotic signals. Science. 282(5392), 1327-32 (1998).

Parrini MC, Matsuda M and de Gunzburg J. Spatiotemporal regulation of the Pak1 kinase. Biochem Soc Trans. 33(4), 646-8 (2005).

Parton RG and Simons K. The multiple faces of caveolae. Nat. Rev. Mol. Cell Biol. 8(3), 185-94 (2007).

Patel KP, Coyne CB and Bergelson JM. Dynamin- and lipid raft-dependent entry of decay-accelerating factor (DAF)-binding and non-DAF-binding coxsackieviruses into nonpolarized cells. J Virol. 83(21), 11064-77 (2009).

Pike LJ. Growth factor receptors, lipid rafts and caveolae: an evolving story. Biochim Biophys Acta. 1746(3), 260-73 (2005).

Pauza CD and Price TM. Human immunodeficiency virus infection of T cells and monocytes proceeds via receptor-mediated endocytosis. J. Cell. Biol 107(3), 959-68 (1988).

Pelkmans L, Kartenbeck J and Helenius A. Caveolar endocytosis of Simian Virus 40 reveals a new two-step vesicular-transport pathway to the ER. Nat. Cell Biol. 3, 473-483 (2001).

Pelkmans L, Püntener D and Helenius A. Local actin polymerization and dynamin recruitment in SV40-Induced internalization of caveolae. Science 296, 535-538 (2002).

Pelkmans L Bürli T, Zerial M and Helenius A. Caveolin-stabilized membrane domains as multifunctional transport and sorting devices in endocytic membrane traffic. Cell 118(6), 767-80 (2004).

Pelkmans L and Zerial M. Kinase-regulated quantal assemblies and kiss-and-run recycling of caveolae. Nature 436, 128–33 (2005).

Phuong LU Guay G, Altschuler Y and Nabi IR. Caveolin-1 Is a negative regulator of caveolae-mediated endocytosis to the endoplasmic reticulum. J. Biol. Chem. 277, 3371-9 (2001).

Pileri P Uematsu Y, Campagnoli S, Galli G, Falugi F, Petracca R, Weiner AJ, Houghton M, Rosa D, Grandi G and Abrignani S. Binding of Hepatitis C Virus to CD81. Science 282, 938-941 (1998).

Piontek J, Winkler L, Wolburg H, Müller SL, Zuleger N et al. Formation of tight junction: determinants of homophilic interaction between classic claudins. FASEB J. 22(1):146-58 (2008).

Platek A, Mettlen M, Camby I, Kiss R, Amyere M and Courtoy PJ. v-Src accelerates spontaneous motility via phosphoinositide 3-kinase, phospholipase C and phospholipase D, but abrogates chemotaxis in Rat-1 and MDCK cells. J. Cell Sci. 117(20), 4849-61 (2004).

Platek A, Vassilev VS, de Diesbach P, Tyteca D, Mettlen M and Courtoy PJ. Constitutive diffuse activation of phosphoinositide 3-kinase at the plasma membrane by v-Src suppresses the chemotactic response to PDGF by abrogating the polarity of PDGF receptor signalling. Exp. Cell Res. 313(6), 1090-105 (2007).

Ploss A, Evans MJ, Gaysinskaya VA, Panis M, You H, de Jong YP and Rice CM. Human occludin is a hepatitis C virus entry factor required for infection of mouse cells. Nature 457, 882-886 (2009).

Pohl J, Ring A and Stremmel W. Uptake of long-chain fatty acids in HepG2 cells involves caveolae: analysis of a novel pathway. J. Lipid Res. 43, 1390-1399 (2002).

Prendergast FG and Mann KG. Chemical and physical properties of aequorin and the green fluorescent protein isolated from Aequorea forskålea. Biochemistry. 17(17), 3448-53 (1978).

Pu Y and Zhang X. Mouse hepatitis virus type 2 enters cells through a clathrin-mediated endocytic pathway independent of Eps15. J. Virol. 82(16), 8112-23 (2003).

Qi R Mullen DG, Baker JR and Holl MM. The mechanism of polyplex internalization into cells: testing the GM1/caveolin-1 lipid raft mediated endocytosis pathway. Mol. Pharm. 7(1), 267-79 (2010).

Racoosin EL and Swanson JA. Macropinosome maturation and fusion with tubular lysosomes in macrophages. J. Cell Biol. 121, 1011-1020 (1993).

Rappoport JZ and Simon SM. Endocytic trafficking of activated EGFR is AP-2 dependent and occurs through preformed clathrin spots. J. Cell Sci. 122(9), 1301-5 (2009).

Raymond E, Faivre S and Armand JP. Epidermal growth factor receptor tyrosine kinase as a target for anticancer therapy. Drugs 60 Suppl 1, 15-23; discussion 41-2 (2000).

Reiter JL and Maihle NJ. Characterization and expression of novel 60-kDa and 110-kDa EGFR isoforms in human placenta. Ann. NY Acad. Sci. 995, 39-47 (2003).

Ren Y, Yin H, Tian R, Cui L, Zhu Y, Lin W, Tang XD, Gui Y and Zheng XL. Different effects of epidermal growth factor on smooth muscle cells derived from human myometrium and from leiomyoma. Fertil. Steril. 96(4), 1015-20 (2011).

Reynolds GM, Harris HJ, Jennings A, Hu K, Grove J, Lalor PF, Adams DH, Balfe P, Hübscher SG and McKeating JA. Hepatitis C virus receptor expression in normal and diseased liver tissue. Hepatology 47(2), 418-27 (2008).

Ridley AJ Paterson HF, Johnston CL, Diekmann D and Hall A. The small GTP-binding protein rac regulates growth factor-induced membrane ruffling. Cell 70, 401-410 (1992).

Rodal SK Skretting G, Garred O, Vilhardt F, van Deurs B and Sandvig K. Extraction of cholesterol with methyl-beta-cyclodextrin perturbs formation of clathrin-coated endocytic vesicles. Mol. Biol. Cell 10(4), 961-74 (1999).

Roepstorff K, Grandal MV, Henriksen L, Knudsen SL, Lerdrup M, Grøvdal L, Willumsen BM and van Deurs B. Differential effects of EGFR ligands on endocytic sorting of the receptor. Traffic 10(8), 1115-27 (2009).

Rothberg KG, Heuser JE, Donzell WC, Ying YS, Glenney JR and Anderson RG. Caveolin, a protein component of caveolae membrane coats. Cell 68, 673–82 (1992).

Royle SK. The cellular functions of clathrin. Cell Mol. Life Sci. 63(16), 1823-32 (2006).

Ruderman NB Kapeller R, White MF and Cantley LC. Activation of phosphatidylinositol 3-kinase by insulin. Proc. Natl Acad. Sci. USA 87, 1411-1415 (1990).

Rust MJ, Bates M and Zhuang X. Sub-diffraction-limit imaging by stochastic optical reconstruction microscopy (STORM). Nat. Methods 3(10), 793-5 (2006).

Rustgi VK. The epidemiology of hepatitis C infection in the United States. J. Gastroenterology 42, 513-521 (2007).

Sadej R, Romanska H, Kavanagh D, Baldwin G, Takahashi T, Kalia N and Berditchevski F. Tetraspanin CD151 regulates transforming growth factor beta signaling: implication in tumor metastasis. Cancer Res. 70(14), 6059-70 (2010).

Saeed MF, Kolokoltsov AA, Albrecht T and Davey RA. Cellular entry of ebola virus involves uptake by a macropinocytosis-like mechanism and subsequent trafficking through early and late endosomes. PLoS Pathog. 6(9), e1001110 (2010).

Sakai A, Claire MS, Faulk K, Govindarajan S, Emerson SU, Purcell RH and Bukh J. The p7 polypeptide of hepatitis C virus is critical for infectivity and contains functionally important genotype-specific sequences. Proc. Natl Acad. Sci. USA 100, 11646–11651 (2003).

Sallusto F, Cella M, Danieli C and Lanzavecchia A. Dendritic cells use macropinocytosis and the mannose receptor to concentrate macromolecules in the major histocompatibility complex class II compartment: downregulation by cytokines and bacterial products. J Exp Med. 182(2), 389-400 (1995).

Sandgren KJ, Wilkinson J, Miranda-Saksena M, McInerney GM, Byth-Wilson K, Robinson PJ and Cunningham AL. A differential role for macropinocytosis in mediating entry of the two forms of vaccinia virus into dendritic cells. PLoS Pathog. 6(4), e1000866 (2010).

Sandilands E, Cans C, Fincham VJ, Brunton VG, Mellor H, Prendergast GC, Norman JC, Superti-Furga G and Frame MC. RhoB and actin polymerization coordinate Src activation with endosome-mediated delivery to the membrane. Dev. Cell 7(6), 855-69 (2004).

Sandrin V, Boson B, Salmon P, Gay W, Nègre D, Le Grand R, Trono D and Cosset FL. Lentiviral vectors pseudotyped with a modified RD114 envelope glycoprotein show increased stability in sera and augmented transduction of primary lymphocytes and CD34+ cells derived from human and nonhuman primates. Blood 100(3), 823-32 (2002).

Sandvig K Pust S, Skotland T and van Deurs B. Clathrin-Independent Endocytosis: Mechanisms and Functions. Curr. Opin. Cell Biol. 23(4), 413-420 (2011).

Scarselli E Ansuini H, Cerino R, Roccasecca RM, Acali S, Filocamo G, Traboni C, Nicosia A, Cortese R and Vitelli A. The human scavenger receptor class B type I is a novel candidate receptor for the hepatitis C virus. EMBO J. 21, 5017-5025 (2002).

Schaeffer E, Soros VB and Greene WC. Compensatory link between fusion and endocytosis of human immunodeficiency virus type 1 in human CD4 T lymphocytes. J. Virol. 78(3), 1375-83 (2004).

Schermelleh L, Carlton PM, Haase S, Shao L, Winoto L, et al. Subdiffraction multicolor imaging of the nuclear periphery with 3D structured illumination microscopy. Science 320(5881), 1332-6 (2008).

Schmees C, Villaseñor R, Zheng W, Ma H, Zerial M, Heldin CH and Hellberg C. Macropinocytosis of the PDGF β-receptor promotes fibroblast transformation by H-RasG12V. Mol. Biol. Cell 23(13), 2571-82 (2012).

Schlunck G, Damke H, Kiosses WB, Rusk N, Symons MH, Waterman-Storer CM, Schmid SL and Schwartz MA. Modulation of Rac localization and function by dynamin. Mol. Biol. Cell15(1), 256-67 (2004).

Schmid EM, Ford MG, Burtey A, Praefcke GJ, Peak-Chew SY, Mills IG, Benmerah A and McMahon HT. Role of the AP2 betaappendage hub in recruiting partners for clathrin-coated vesicle assembly. PLoS Biol. 4, e262 (2006).

Schmidt MH Furnari FB, Cavenee WK and Bögler O. Epidermal growth factor receptor signaling intensity determines intracellular protein interactions, ubiquitination, and internalization. Proc. Natl Acad. Sci. USA 100, 6505 (2003).

Schnatwinkel C Christoforidis S, Lindsay MR, Uttenweiler-Joseph S, Wilm M, Parton RG and Zerial M. The Rab5 effector rabankyrin-5 regulates regulates and coordinates different endocytic mechanisms. PLoS Biol. 2, E261 (2004).

Schroeder GN and Hilbi H. Molecular pathogenesis of shigella spp: controlling host cell signalling, invasion and death by type III secretion. Clin. Microbiol. Rev. 21, 134-156 (2008).

Sengupta P, Jovanovic-Talisman T and Lippincott-Schwartz J. Quantifying spatial organization in point-localization superresolution images using pair correlation analysis. Nat. Protoc. 8(2), 345-54 (2013).

Sharma NR, Mateu G, Dreux M, Grakoui A, Cosset FL and Melikyan GB. Hepatitis C virus is primed by CD81 protein for low pH-dependent fusion. J. Biol. Chem. 286(35), 30361-76 (2011).

Shen L, Weber CR and Turner JR. The tight junction protein complex undergoes rapid and continuous molecular remodeling at steady state. J. Cell Biol. 181(4), 683-95 (2008).

Shepard CW, Finelli L and Alter MJ. Global epidemiology of hepatitis C virus infection. Lancet Infect. Dis. 6, 628 (2006).

Shimojima M, Takada A, Ebihara H, Neumann G, Fujioka K, Irimura T, Jones S, Feldmann H and Kawaoka Y. Tyro3 family-mediated cell entry of Ebola and Marburg viruses. J. Virol. 80(20), 10109-16 (2006).

Sieczkarski SB and Whittaker GR. Influenza Virus Can Enter and Infect Cells in the Absence of Clathrin-Mediated Endocytosis. J. Virol. 76(20), 10455-64 (2002).

Sigismund S Woelk T, Puri C, Maspero E, Tacchetti C, Transidico P, Di Fiore PP and Polo S. Clathrin-independent endocytosis of ubiquitinated cargos. Proc. Natl Acad. Sci. USA 102(8), 2760-2765 (2005).

Singh RD, Puri V, Valiyaveettil JT, Marks DL, Bittman R and Pagano RE. Selective caveolin-1-dependent endocytosis of glycosphingolipids. Mol. Biol. Cell 14(8), 3254-65 (2003).

Smith AE and Helenius A. How viruses enter animal cells. Science 304(5668), 237-42 (2004).

Smythe E Carter LL and Schmid SL. Cytosol- and clathrin-dependent stimulation of endocytosis in vitro by purified adaptors. J. Cell Biol. 119(5), 1163-71 (1992).

Song G Yang S, Zhang W, Cao Y, Wang P, Ding N, Zhang Z, Guo Y and Li Y. Discovery of the first series of small molecule H5N1 entry inhibitors. J. Med. Chem. 52(23), 7368–7371 (2009).

Sorkin, A.. Internalization of the epidermal growth factor receptor: role in signalling. Biochem.Soc.Trans. 29(4), 480-484 (2001).

Sottile J and Chandler J. Fibronectin matrix turnover occurs through a caveolin-1–dependent process. Mol. Biol. Cell 16(2), 757-768 (2004).

Sousa V, Espírito Santo J, Silva M, Cabral T, Alarcão AM, Gomes A, Couceiro P and Carvalho L. EGFR/erB-1, HER2/erB-2, CK7, LP34, Ki67 and P53 expression in preneoplastic lesions of bronchial epithelium: an immunohistochemical and genetic study. Virchows Arch. 458(5), 571-81 (2011).

Stamatovic SM, Keep RF, Wang MM, Jankovic I and Andjelkovic AV. Caveolae-mediated internalization of occludin and claudin-5 during CCL2-induced tight junction remodeling in brain endothelial cells. J. Biol. Chem. 284(28), 19053-66 (2009).

Stein BS Gowda SD, Lifson JD, Penhallow RC, Bensch KG and Engleman EG. pH-independent HIV entry into CD4-positive T cells via virus envelope fusion to the plasma membrane. Cell 49(5), 659-68 (1987).

Steinman RM, Brodie SE and Cohn ZA. Membrane flow during pinocytosis. A stereologic analysis. J. Cell Biol. 68(3), 665-87 (1976).

Steinmann E, Penin F, Kallis S, Patel AH, Bartenschlager R and Pietschmann T. Hepatitis C virus p7 protein is crucial for assembly and release of infectious virions. PLoS Pathog. 3, e103 (2007).

Stenmark H and Olkkonen VM. The Rab GTPase family. Genome Biol. 2(5), REVIEWS3007 (2001).

Stoorvogel W Oorschot V and Geuze HJ. A novel class of clathrin-coated vesicles budding from endosomes. J. Cell Biol. 132(1-2), 21-33 (1996).

Sun P, Yamamoto H, Suetsugu S, Miki H, Takenawa T and Endo T. Small GTPase Rah/Rab34 is associated with membrane ruffles and macropinosomes and promotes macropinosome formation. J. Biol. Chem. 278(6), 4063-71 (2003).

Swanson JA and Watts C. Macropinocytosis. Trends Cell Biol. 5, 424-428 (1995).

Tacheva-Grigorova SK, Santos AJ, Boucrot E and Kirchhausen T. Clathrin-Mediated Endocytosis Persists during Unperturbed Mitosis. Cell Rep. 4(4), 659-68 (2013).

Takenawa T and Suetsugu S. The WASP-WAVE protein network: connecting the membrane to the cytoskeleton. Nat. Rev. Mol. Cell Biol. 8(1), 37-48 (2007).

Thorley JA, McKeating J and Rappoport JZ. Mechanisms of viral entry: sneaking in the front door. Protoplasma 244(1-4), 15-24 (2010).

Thorley JA, Pike J and Rappoport JZ. In Fluorescence Microscopy,1st Edition. Super-Resolution and other Novel Techniques. (Elsevier, 2014).

Tscherne DM Jones CT, Evans MJ, Lindenbach BD, McKeating JA and Rice CM. Time- and temperature-dependent activation of hepatitis C virus for low-pH-triggered entry. J. Virol. 80(4), 1734-1741 (2006).

Tse EY, Ko FC, Tung EK, Chan LK, Lee TK, Ngan ES, Man K, Wong AS, Ng IO and Yam JW. Caveolin-1 overexpression is associated with hepatocellular carcinoma tumourigenesis and metastasis. J. Pathol. 226(4), 645-53 (2012).

Torgersen ML, Skretting G, van Deurs B and Sandvig K. Internalization of cholera toxin by different endocytic mechanisms. J. Cell Sci. 114(20), 3737-47 (2001).

Van Dam EM and Stoorvogel W. Dynamin-dependent transferrin receptor recycling by endosome-derived clathrin-coated vesicles. Mol. Biol. Cell 13(1), 169-82 (2002).

Vermeer PD, Einwalter LA, Moninger TO, Rokhlina T, Kern JA, Zabner J and Welsh MJ. Segregation of receptor and ligand regulates activation of epithelial growth factor receptor. Nature 422(6929), 322-6 (2003).

Vidricaire G and tremblay MJ. A clathrin, caveolae and dynamin-independent endocytic pathway requiring free membrane cholesterol drives HIV-1 internalisation and infection in polarised trophoblastic cells. J. Mol. Biol. 368(5), 1267-1283 (2007).

Voss T, LeBlanc C, Barbercheck J, Kaplan B, Wilson R, Robert G. Peptide-based entry inhibitors for Influenza. Antiviral Res. 78(2), A18 (2008).

Wakita T Pietschmann T, Kato T, Date T, Miyamoto M, Zhao Z, Murthy K, Habermann A, Kräusslich HG, Mizokami M, Bartenschlager R and Liang TJ. Production of hepatitis C virus in tissue culture from a cloned viral genome. Nat. Med. 11(7), 791-6 (2005).

Wang LH, Rothberg KG and Anderson RGW. Mis-Assembly of Clathrin Lattices on Endosomes Reveals a Regulatory Switch for Coated Pit Formation. J. Cell Biol. 123(5), 1107-1117 (1993).

Wang XQ, Sun P and Paller AS. Ganglioside induces caveolin-1 redistribution and interaction with the epidermal growth factor receptor. J. Biol. Chem. 277(49), 47028-34 (2002).

Wang HX, Li Q, Sharma C, Knoblich K, Hemler ME. Tetraspanin protein contributions to cancer. Biochem. Soc. Trans. 39(2), 547-52. doi:10.1042/BST0390547 (2011).

Warren A, Bertolino P, Benseler V, Fraser R, McCaughan GW and Le Couteur DG. Marked changes of the hepatic sinusoid in a transgenic mouse model of acute immune-mediated hepatitis. J. Hepatol. 46(2), 239-46 (2006).

Waugh MG, Lawson D and Hsuan JJ. Epidermal growth factor receptor activation is localized within low-buoyant density, non-caveolar membrane domains. Biochem J. 337, 591 (1999).

Webb RH. Confocal optical microscopy. Rep. Prog. Phys. 59, 427–471 (1996).

West MA, Bretscher MS and Watts C. Distinct enodcytic pathways in epidermal growth factor-stimulated human carcinoma A431 cells. J. Cell Biol. 109, 2731-2739 (1989).

WHO Epidemiological Record, 2009.

Wiedłocha and Sørensen. Signaling, internalization, and intracellular activity of fibroblast growth factor. Curr. Top. Microbiol. Immunol. 286, 45-79 (2004).

Wiesner H, Sorrell M, Villamil F, International Liver Transplantation Society Expert Panel. Report of the first international liver transplantation society expert panel consensus conference on liver transplantation and hepatitis C. Liver Transpl. 9(11), S1–S9 (2003).

Wolf AA Jobling MG, Wimer-Mackin S, Ferguson-Maltzman M, Madara JL, Holmes RK and Lencer WI. Ganglioside structure dictates signal transduction by cholera toxin and association with caveolae-like membrane domains in polarized epithelia. J. Cell Biol. 141(4), 917-27 (1998).

Wood ER, Truesdale AT, McDonald OB, Yuan D, Hassell A, et al. A unique structure for epidermal growth factor receptor bound to GW572016 (Lapatinib): relationships among protein conformation, inhibitor off-rate, and receptor activity in tumor cells. Cancer Res. 64(18), 6652-9 (2004).

Wright MD and Tomlinson MG. The ins and outs of the transmembrane 4 superfamily. Immunol. Today 15(12), 588-94 (1994).

Wunschmann S, Medh JD, Klinzmann D, Schmidt WN and Stapleton JT. Characterization of hepatitis C virus (HCV) and HCV E2 interactions with CD81 and the low-density lipoprotein receptor. J. Virol. 74, 10055–10062 (2000).

Yamaya M Shinya K, Hatachi Y, Kubo H, Asada M, Yasuda H, Nishimura H and Nagatomi R. Clarithromycin inhibits type A seasonal Influenza virus infection in human airway epithelial cells. J. Pharmacol. Exp. Ther. 333(1), 81-90 (2010).

Yanagi M, Purcell RH, Emerson SU and Bukh J. Transcripts from a single full-length cDNA clone of hepatitis C virus are infectious when directly transfected into the liver of a chimpanzee. Proc. Natl Acad. Sci. USA 94, 8738–8743 (1997).

Yang W Qiu C, Biswas N, Jin J, Watkins SC, Montelaro RC, Coyne CB and Wang T. Correlation of the tight junction-like distribution of Claudin-1 to the cellular tropism of hepatitis C virus. J. Biol. Chem. 283, 8643-8653 (2008).

Yi M, Villanueva RA, Thomas DL, Wakita T and Lemon SM. Production of infectious genotype 1a hepatitis C virus (Hutchinson strain) in cultured human hepatoma cells. Proc. Natl Acad. Sci. USA 103(7), 2310-5 (2006).

Yildiz A, Forkey JN, McKinney SA, Ha T, Goldman YE and Selvin PR. Myosin V walks hand-over-hand: single fluorophore imaging with 1.5-nm localization. Science 300(5628), 2061-5 (2003).

Yoshimura A Kuroda K, Kawasaki K, Yamashina S, Maeda T and Ohnishi S. Infectious cell entry mechanism of Influenza virus. J. Virol. 43(1), 284-93 (1982).

Zeuzem Sl. Heterogeneous virological response rates to interferon-based therapy in patients with chronic hepatitis C: who responds less well? Ann. Intern. Med. 140, 370-81 (2004).

Zhang J Randall G, Higginbottom A, Monk P, Rice CM and McKeating JA. CD81 is Required for Hepatitis C Virus Glycoprotein-Mediated Viral Infection. J. Virol. 78(3), 1448-1455 (2004).

Zhao X Liu Y, Ma Q, Wang X, Jin H, Mehrpour M and Chen Q. Caveolin-1 negatively regulates TRAIL-induced apoptosis in human hepatocarcinoma cells. Biochem. Biophys. Res. Comms. 378(1), 21-26 (2009).

Zheng A Yuan F, Li Y, Zhu F, Hou P, Li J, Song X, Ding M and Deng H. Claudin-6 and claudin-9 function as additional coreceptors for hepatitis C virus. J. Virol. 81, 12465-12471 (2007).

Zhong J Gastaminza P, Cheng G, Kapadia S, Kato T, Burton DR, Wieland SF, Uprichard SL, Wakita T and Chisari FV. Robust Hepatitis C Virus Infection in vitro. Proc. Natl Acad. Sci. USA 102(26), 9294-9299 (2005).

Zhu JX, Goldoni S, Bix G, Owens RT, McQuillan DJ, Reed CC and Iozzo RV. Decorin evokes protracted internalization and degradation of the epidermal growth factor receptor via caveolar endocytosis. J. Biol. Chem. 280(37), 32468-79 (2005).

Zona L, Lupberger J, Sidahmed-Adrar N, Thumann C, Harris HJ, et al. HRas signal transduction promotes hepatitis C virus cell entry by triggering assembly of the host tetraspanin receptor complex. Cell Host Microbe 13(3), 302-13 (2013).

APPENDIX I

SUPPLEMENTARY METHODS

SM 1: LB Broth

20 g of LB Broth (Sigma) was dissolved in 1 L distilled H20 and autoclaved at 121ºC for 20 minutes.

SM 2: Pouring LB agar plates

35 g of LB Agar (Sigma) was dissolved in 1 L distilled H_20 and autoclaved at 121ºC for 20 minutes. Kanamycin or ampicillin was added to a final concentration of 50 µg/ml or 100 µg/ml respectively to cooling plates, before setting of the LB agar. In a laminar flow hood, 50 ml of the LB agar antibiotic mix was poured into 12 cm plastic dishes. Plates were stored inverted at 4ºC before use.

SM 3: Cell culture medium

500 ml Dulbecco's Modified Eagle Medium (DMEM; Lonza), or RPMI (Gibco, Invitrogen) was added to 50 ml fetal calf serum (FCS) and 5 ml Penicillin/Streptomycin (all Lonza) and sterile filtered through a 500ml Corning 0.1 µM pore Vacuum Filter System (Corning) to give a final concentration of 10% FCS and 1% penicillin/streptomycin.

SM 4: Trypsin

10X trypsin (Gibco) was aliquoted, frozen then diluted to 1X trypsin in PBS for use.

SM 5: Cell Imaging Media (CIM)

9.7 g Hanks Balanced Salt (without phenol red and sodium bicarbonate) (Sigma) and 2.38 g HEPES (Fisher Scientific) were dissolved in 1 L distilled H_20. 1 M HCl (Fisher

Scientific) was then added dropwise until pH 7.4 was reached using a Basic Denver Instrument pH meter (Denver Instruments). The media was then sterile filtered through a 500 ml Corning 0.1 µM pore Vacuum Filter System and stored at 4°C prior to use.

SM 6: 4% Paraformaldehyde (PFA)

10 ml 16% Paraformaldehyde (PFA; Electron Microscopy Sciences) was added to 30 ml PBS for a final concentration of 4% PFA.

SM 7: Permeabilisation buffer

A 0.1% Triton-X100 solution was made by adding 1 ml Triton-X100 (Sigma) to 99 ml DPBS (Lonza), vortexed thoroughly and stored at 4°C.

SM 8: GS-BSA Block buffer

2 ml normal goat serum (Gibco, Invitrogen) and 0.5 g bovine serum albumin (BSA; Sigma) were added to 20 ml DPBS (Lonza) to generate a solution of 10% goat serum and 5% BSA.

SM 9: Acrylamide gel solutions

	4% Stacking gel	**12% Main gel**
Distilled H_2O	6.8 ml	6.6 ml
0.5 M Tris-HCl (pH 6.8)	2.5 ml	-
1.5 M Tris-HCl (pH 8.8)	-	5 ml
Bis-Acrylamide (Protogel)	1.7 ml	8 ml
10% SDS	100 µl	200 µl
10% APS	100 µl	200 µl
TEMED (Fisher Scientific)	10 µl	8 µl
Total Volume*	10 ml	20 ml

* Makes enough for two gels

0.5 M pH 6.8 Tris-HCl was made as follows:

60.57 g Tris (Fisher Scientific) dissolved in 1 L distilled H_2O. 1 M HCl was added dropwise until pH 6.8 was reached, using a Basic Denver Instrument pH meter (Denver Instruments)

1.5 M pH 8.8 Tris-HCl was made as follows:

181.71 g Tris (Fisher Scientific) was dissolved in 1 L distilled H_2O. 1 M HCl was added dropwise until pH 8.8 was reached, using a Basic Denver Instrument pH meter (Denver Instruments).

10% Ammonium Persulphate (APS) was made as follows:

100 mg ammonium persuphate (APS; Sigma) was dissolved in 1 ml distilled H_2O. 10% APS was made fresh for each western blot.

10% Sodium Dodecyl Sulphate (SDS) was made as follows:

10 g sodium dodecyl sulphate (SDS; Fisher Scientific) was dissolved in 100 ml distilled H_2O and stored at room temperature.

SM 10: Running buffer

1X running buffer was made by diluting 100 ml 10X running buffer in 900 ml distilled H_2O. 10X running buffer was made by dissolving 144g glycine (Fisher Scientific), 30g Tris (Fisher Scientific) and 4g SDS (Fisher Scientific) in 1 L distilled H_2O. Running buffer was stored at room temperature.

SM 11: Transfer buffer

1X transfer buffer was made by diluting 100 ml 10X transfer buffer in 700 ml distilled H_2O and 200 ml methanol (Fisher Scientific). 10X transfer buffer was made by dissolving 144 g glycine (Fisher Scientific) and 30 g Tris in 1 L in distilled H_2O.

SM 12: TBST

1X TBST buffer was made by mixing 100 ml 10X TBS and 1 ml Tween 20 (Sigma) in 900 ml distilled H_2O. Tween 20 was added using a P1000 pipette tip with the tip end cut off and ejecting the tip into the solution and mixing for 10 minutes. 10X TBS was made by mixing 200ml 1M Tris-HCl pH 7.5, 300 ml 5M NaCl and 500 ml distilled

H_2O. 1 M pH 7.5 Tris-HCl was made by dissolving 121.14 g Tris (Fisher Scientific) in 1 L distilled H_2O. 1 M HCl was added dropwise until pH 7.5 was reached, using a Basic Denver Instrument pH meter (Denver Instruments). 5 M NaCl solution was made by dissolving 292.2 g NaCl (Fisher Scientific) 1 L distilled H_2O.

SM 13: Blocking Buffer (5% Marvel-TBST)

A 5% skimmed milk solution (Marvel) was made by dissolving 2.5 g Marvel skimmed milk powder in 50 ml TBST (**SM 14**).

SM 14: Triton-X100 Lysis Buffer

1 ml 10% Triton-X100 (Sigma) was added to 9 ml DPBS (Lonza) and stored at 4°C. One Complete mini-cocktail protease inhibitor tablet (Roche) was added immediately prior to use and the solution vortexed vigorously to dissolve.

SM 15: 3x Sample buffer

3x sample buffer was made by mixing 18.8 ml 0.5 M Tris pH 6.8 (Fisher Scientific) (as described in **SM 10**), 6 g sodium dodecyl sulphate (SDS; Sigma), 15 ml beta-mercaptoethanol (Sigma) and 30 ml glycerol in 100 ml distilled H_2O. A small spatula of bromophenol blue was added and the solution mixed thoroughly. 3x sample buffer was stored at room temperature.

SM 16: siRNA sequences

AP2: siRNA targeted to alpha-adaptin was generated using the sequence GAGCAUGUGCACGCUGGCCAdTdT (as used by Huang and Sorkin 2004) by Dharmacon RNAi, UK.

Caveolin 1: A SMARTpool of ON-TARGETplus CAV1 siRNAs was purchased from Dharmacon, UK.

SM 17: Tables of Antibodies

Table SM 1: Primary Antibodies

Antibody	**Dilution**	**Procedure**	**Company**	**Catalogue #**
2s131 (mouse α-CD81)	1:2	IC	McKeating lab	-
Rabbit α-caveolin 1	1:20,000	WB	BD Biosciences	610060
α-AP2	1:1000	WB	Santa Cruz biotechnology	sc-10761

Table SM 2: Secondary Antibodies

Antibody	Dilution	Procedure	Company	Catalogue #
Goat α-rabbit IgG horseradish peroxidase	1:10,000	WB	Thermo Fisher Scientific	31460
Sheep α-mouse IgG horseradish peroxidase	1:5000	WB	GE Healthcare	RPN4201
Donkey α-rabbit-AlexaFluor-568	1:200	IC	Invitrogen	A10042
Goat α-rabbit-AlexaFluor-488	1:200	IC	Invitrogen	A11008
Donkey α-mouse-AlexaFluor-568	1:200	IC	Invitrogen	A10037
Goat α-mouse-AlexaFluor-488	1:200	IC	Invitrogen	A11001
Donkey α-mouse-AlexaFluor-647	1:200	IC	Invitrogen	A-31571

APPENDIX II

SUPPLEMENTARY VIDEOS

Figure Legends for Supplementary Videos

Supplementary Video 1A: Huh7.5 cells transfected with CFPmem and imaged every 1 minute for 60 minutes by live-cell confocal microscopy.

https://www.youtube.com/watch?v=CNh9pb5A7wY

Supplementary Video 1B: Huh7.5 cells transfected with CFPmem and treated with 1 µg/ml EGF, imaged every 1 minute for 60 minutes by live-cell confocal microscopy.

https://www.youtube.com/watch?v=b37pO18kG1g&feature=youtu.be

APPENDIX III

PUBLISHED PAPERS

Thorley JA, McKeating JA, Rappoport JZ. Mechanisms of viral entry: sneaking in the front door. Protoplasma. 2010 Aug; 244 (1-4):15-24

Thorley JA, Pike J, Rappoport JZ. In Fluorescence Microscopy: Super-resolution and Other Novel Techniques, 1st edition (Elsevier, 2014)